ISSN 1916-6117 (online)
ISBN 978-1-4435-7405-1 (PDF)

ISSN 0826-9580 (print)
ISBN 978-1-4435-7404-4 (print)

THESE TERMS GOVERN YOUR USE OF THIS DOCUMENT

Your use of this Ontario Geological Survey document (the "Content") is governed by the terms set out on this page ("Terms of Use"). By downloading this Content, you (the "User") have accepted, and have agreed to be bound by, the Terms of Use.

Content: This Content is offered by the Province of Ontario's *Ministry of Northern Development and Mines* (MNDM) as a public service, on an "as-is" basis. Recommendations and statements of opinion expressed in the Content are those of the author or authors and are not to be construed as statement of government policy. You are solely responsible for your use of the Content. You should not rely on the Content for legal advice nor as authoritative in your particular circumstances. Users should verify the accuracy and applicability of any Content before acting on it. MNDM does not guarantee, or make any warranty express or implied, that the Content is current, accurate, complete or reliable. MNDM is not responsible for any damage however caused, which results, directly or indirectly, from your use of the Content. MNDM assumes no legal liability or responsibility for the Content whatsoever.

Links to Other Web Sites: This Content may contain links, to Web sites that are not operated by MNDM. Linked Web sites may not be available in French. MNDM neither endorses nor assumes any responsibility for the safety, accuracy or availability of linked Web sites or the information contained on them. The linked Web sites, their operation and content are the responsibility of the person or entity for which they were created or maintained (the "Owner"). Both your use of a linked Web site, and your right to use or reproduce information or materials from a linked Web site, are subject to the terms of use governing that particular Web site. Any comments or inquiries regarding a linked Web site must be directed to its Owner.

Copyright: Canadian and international intellectual property laws protect the Content. Unless otherwise indicated, copyright is held by the Queen's Printer for Ontario.

It is recommended that reference to the Content be made in the following form:

Beakhouse, G.P. 2011. The Abitibi Subprovince plutonic record: Tectonic and metallogenic implications; Ontario Geological Survey, Open File Report 6268, 161p.

Use and Reproduction of Content: The Content may be used and reproduced only in accordance with applicable intellectual property laws. *Non-commercial* use of unsubstantial excerpts of the Content is permitted provided that appropriate credit is given and Crown copyright is acknowledged. Any substantial reproduction of the Content or any *commercial* use of all or part of the Content is prohibited without the prior written permission of MNDM. Substantial reproduction includes the reproduction of any illustration or figure, such as, but not limited to graphs, charts and maps. Commercial use includes commercial distribution of the Content, the reproduction of multiple copies of the Content for any purpose whether or not commercial, use of the Content in commercial publications, and the creation of value-added products using the Content.

Contact:

FOR FURTHER INFORMATION ON	PLEASE CONTACT:	BY TELEPHONE:	BY E-MAIL:
The Reproduction of the EIP or Content	MNDM Publication Services	Local: (705) 670-5691 Toll Free: 1-888-415-9845, ext. 5691 (inside Canada, United States)	Pubsales.ndm@ontario.ca
The Purchase of MNDM Publications	MNDM Publication Sales	Local: (705) 670-5691 Toll Free: 1-888-415-9845, ext. 5691 (inside Canada, United States)	Pubsales.ndm@ontario.ca
Crown Copyright	Queen's Printer	Local: (416) 326-2678 Toll Free: 1-800-668-9938 (inside Canada, United States)	Copyright@gov.on.ca

Ontario Geological Survey
Open File Report 6268

The Abitibi Subprovince Plutonic Record: Tectonic and Metallogenic Implications

2011

ONTARIO GEOLOGICAL SURVEY

Open File Report 6268

The Abitibi Subprovince Plutonic Record: Tectonic and Metallogenic Implications

by

G.P. Beakhouse

2011

Open File Reports of the Ontario Geological Survey are available for viewing at the John B. Gammon Geoscience Library in Sudbury and at the regional Mines and Minerals office whose district includes the area covered by the report (see below).

Copies can be purchased at Publication Sales and the office whose district includes the area covered by the report. Although a particular report may not be in stock at locations other than the Publication Sales office in Sudbury, they can generally be obtained within 3 working days. All telephone, fax, mail and e-mail orders should be directed to the Publication Sales office in Sudbury. Purchases may be made using cash, debit card, VISA, MasterCard, American Express, cheque or money order. Cheques or money orders should be made payable to the *Minister of Finance.*

John B. Gammon Geoscience Library 933 Ramsey Lake Road, Level A3 Sudbury, Ontario P3E 6B5	Tel:	(705) 670-5615
Publication Sales 933 Ramsey Lake Rd., Level A3 Sudbury, Ontario P3E 6B5	Tel: Toll-free: Fax: E-mail:	(705) 670-5691 (local) 1-888-415-9845 ext. 5691 (705) 670-5770 pubsales.ndm@ontario.ca

Regional Mines and Minerals Offices:

Kenora - Suite 104, 810 Robertson St., Kenora P9N 4J2

Kirkland Lake - 10 Government Rd. E., Kirkland Lake P2N 1A8

Red Lake - Box 324, Ontario Government Building, Red Lake P0V 2M0

Sault Ste. Marie - 875 Queen St. E., Suite 6, Sault Ste. Marie P6A 6V8

Southern Ontario - P.O. Bag Service 43, 126 Old Troy Rd., Tweed K0K 3J0

Sudbury - 933 Ramsey Lake Rd., Level A3, Sudbury P3E 6B5

Thunder Bay - Suite B002, 435 James St. S., Thunder Bay P7E 6S7

Timmins - Ontario Government Complex, P.O. Bag 3060, Hwy. 101 East, South Porcupine P0N 1H0

Cette publication est disponible en anglais seulement.

Parts of this report may be quoted if credit is given. It is recommended that reference be made in the following form:

Beakhouse, G.P. 2011. The Abitibi Subprovince plutonic record: Tectonic and metallogenic implications; Ontario Geological Survey, Open File Report 6268, 161p.

Contents

FIGURES

TABLES

Miscellaneous Release—Data 285
Lithogeochemical Data for Abitibi Subprovince Intermediate to Felsic Intrusive Rocks; by G.P. Beakhouse. This digital release contains 1 Microsoft® Excel® file containing locational and whole rock geochemical data for 306 samples of intermediate to felsic intrusive rocks from the Abitibi greenstone belt in Ontario. Most of these samples were collected as part of an Ontario Geological Survey – Goldcorp Inc. collaborative project agreement. Some of these data were released previously within MRD 209, *Lithogeochemical Data for Intermediate to Felsic Intrusive Rocks Sampled in 2005*, and are re-released here with additional data that are described in a companion report (Open File Report 6268, *The Abitibi Subprovince Plutonic Record: Tectonic and Metallogenic Implications*). These results constitute a part of a long-term Ontario Geological Survey project: "Characteristics of Mineralized and Unmineralized Intermediate to Felsic Plutonic Systems".

MRD 285 is available separately from this report.

Abstract

Intermediate to felsic intrusive rocks within the Abitibi Subprovince exhibit diversity in terms of their field relationships, petrology, whole rock and mineral chemical characteristics that correlates with the relative timing of their emplacement, and are subdivided into 5 suites. The pretectonic suite is synchronous with volcanic-dominated assemblages (2750–2695 Ma), consists predominantly of units with high-Al tonalite–trondhjemite–granodiorite (TTG) petrogenetic affinity (eclogitic to mafic garnet granulitic residue), occurs predominantly in large belt-bounding batholithic complexes and is the most voluminous component of the Abitibi plutonic record. The early syntectonic suite is synchronous with "Krist" volcanism in the basal portion of the sediment-dominated Porcupine assemblage (2691–2685 Ma), consists predominantly of high-level porphyry units with high-Al TTG petrogenetic affinity (mafic garnet granulitic residue), and is widespread but volumetrically minor, with major concentrations associated with regional, east-trending faults. The syntectonic suite is approximately synchronous with the later sedimentary-dominated Porcupine assemblage (2686–2676 Ma), has a transitional sanukitoid to high-Al TTG petrogenetic affinity and occurs as moderate-sized plutons predominantly within folded Tisdale assemblage units and within large belt-bounding batholithic complexes. The late-tectonic suite is synchronous with Timiskaming assemblage volcanism and sedimentation (2680–2668 Ma), is characterized by a strongly alkalic, mantle-derived petrogenetic affinity and, although not volumetrically significant in a regional sense, is locally abundant where it is associated with east-trending regional fault systems. The posttectonic to late-tectonic suite is interpreted to originate by intracrustal melting of the pretectonic suite tonalites, and its timing is not well constrained as it occurs as a minor component within the Kenogamissi Batholith. These suites record a temporal change, similar to that recognized widely across the Superior Province, from voluminous, early melting of mafic crust at lower crustal to upper mantle depths that abruptly (at ~2685 Ma) transitions to melting of a metasomatized ultramafic (mantle) source. This process is interpreted within a modified uniformitarian tectonic model, with early magmas generated by partial melting of subducted oceanic crust and with later magmas generated by partial melting of the subduction-modified mantle wedge.

The pretectonic TTG units occur primarily in large batholithic complexes that record paleopressures of 500 to 700 MPa and structurally underlie the lower metamorphic grade (maximum paleopressures ~350 MPa) greenstone belt, resulting in an inversely density-stratified crustal configuration that persisted throughout the pretectonic stage, suggesting the crust was relatively rigid and consequently characterized by low average geothermal gradients. Heating of the crust occurred synchronously with emplacement of syntectonic plutons, and initiation of regional metamorphism at approximately 2682 ± 5 Ma modified the rheology of the crust permitting density inversion (Rayleigh–Taylor-type instabilities), which led to the juxtaposition of the more buoyant, midcrustal plutonic substrate with the greenstone belt in regional structural culminations represented by the large granitoid complexes such as the Kenogamissi and Round Lake batholiths. This process incorporated regional-scale detachment faults at the base of and within the greenstone belt and folding that is largely responsible for the observed crustal architecture of the Abitibi Subprovince. The midcrustal plutonic root was exposed in the regional structural culminations and is a major provenance component for Porcupine assemblage sedimentary units. The trigger for this range of processes is interpreted to be the introduction of hot asthenospheric mantle into the previously cool mantle wedge, resulting in late, mantle-derived intermediate to felsic magmatism and extensional orogenic collapse.

Gold-dominated mineral systems in the prolifically endowed Abitibi Subprovince are hydrothermal mineral deposits which exhibit a close spatial association with regional east-trending faults as well as late-tectonic alkaline magmatism and/or early syntectonic TTG magmatism. The latter magmatic group pre-dates mineralization, and its local spatial association with mineralization is interpreted to be a consequence of localization of enhanced, structurally controlled porosity and permeability developed in

zones of lithologically controlled contrasts in rheology. The late-tectonic alkalic plutons are interpreted to be approximately coeval with a main stage of gold introduction and are the probable source of any magmatic hydrothermal fluid component contributing to gold mineralization. In addition to their spatial and temporal association, the highly oxidized characteristic of these plutons and the mineralogy of a subset of gold deposits are consistent with a genetic linkage between magmatic hydrothermal fluids derived from late-tectonic alkalic plutons and at least some gold mineralization.

Zones of gold mineralization are likely characterized by the sequential and/or concurrent introduction of multiple fluid types. Acknowledging that more than one type of fluid may be auriferous and additional study is required, a working hypothesis is proposed wherein magmatic hydrothermal fluids exsolved from late-tectonic alkaline magmas are a major or dominant source of gold in Abitibi Subprovince gold deposits. The atypical abundance and extremely alkalic character of the late-tectonic suite contrasts with that observed more generally throughout the Superior Province. These atypical characteristics are attributed to differences in either the nature of the subduction-modified mantle or melting process at the terminal stage of mantle-derived magmatism. The hypothesis implicates a major role for high CO_2/H_2O fluids in both mantle melting and magmatic volatile phase exsolution. CO_2-enrichment may have the potential to optimize the capability of hydrothermal fluid to transport gold and consequently this hypothesis may provide a viable explanation for the significant gold endowment of this region.

The Abitibi Subprovince Plutonic Record: Tectonic and Metallogenic Implications

G.P. Beakhouse[1]
Ontario Geological Survey
Open File Report 6268
2011

---

[1]**Geoscientist, Precambrian Geoscience Section, Ontario Geological Survey, Sudbury, Ontario P3E 6B5**
gary.beakhouse@ontario.ca

Introduction

Intermediate to felsic intrusive rocks in the Abitibi greenstone belt are poorly understood relative to the more thoroughly investigated metavolcanic and metasedimentary rocks (Ayer et al. 2002). Moderately detailed investigations of intrusive rocks have been carried out in several areas where the plutons are spatially associated with mineralization (e.g., Rowins et al. 1991; Rowins et al. 1993; Pigeon 2003; MacDonald et al. 2005). General frameworks for Abitibi granitic plutonism have been developed based in part on selected units from the Ontario portion of the subprovince (Feng and Kerrich 1992a, 1992b; Sutcliffe et al. 1993). General frameworks have also been presented for the Quebec portion of the Abitibi Subprovince (Rivé et al. 1990; Chown et al. 2002).

This project was initiated as a collaborative research agreement between the Ontario Geological Survey and Placer Dome Inc. (now Goldcorp Inc.) with the objective of providing a high-quality petrologic and geochemical database for Abitibi Subprovince intermediate to felsic intrusive rocks and interpreting the tectonic and metallogenic significance of these rocks. This report describes results of this investigation of characteristics of intermediate to felsic intrusive rocks occurring within the Ontario portion of the Abitibi Subprovince of the Superior Province and is accompanied by a data release (Miscellaneous Release—Data 285 (MRD 285), available separately from this report) containing lithogeochemical data on which these interpretations are based. The work described here includes detailed petrologic and petrogenetic interpretations of individual plutons, discussion of petrogenetic suites within a temporal, tectonic and metallogenic framework and implications for regional tectonic development and gold metallogeny of the Abitibi Subprovince. The database and derived interpretations constitute part of a broader project concerned with the potential application of granite studies to predictive metallogeny (Beakhouse 2007a).

Subdivision of Abitibi Subprovince Intermediate to Felsic Plutons

Intermediate to felsic intrusive rocks associated with the Abitibi greenstone belt are diverse with respect to their field relationships, petrology, timing relative to the volcanic, sedimentary and tectonometamorphic evolution of the greenstone belt and relationships to mineralization. Plutons large enough to be displayed on 1:50 000 scale maps are provisionally broadly subdivided into 4 types (Figure 1), described separately below. Minor intrusions are in part related to the larger plutons; however, in many cases the relationships of minor intrusions to regional magmatic and tectonometamorphic processes are ambiguous and these units are discussed separately.

Synvolcanic, Pretectonic Plutons

Many of the large batholiths (e.g., Kenogamissi, Round Lake, Lake Abitibi, Groundhog River) are complex, multiphase intrusive complexes that structurally underlie the Abitibi greenstone belt. Foliated to gneissic tonalitic to granodioritic phases are a predominant or major component of these batholiths and are characteristically the oldest plutonic component. These rocks are intruded by more massive granodioritic to granitic and dioritic to quartz monzodioritic plutons as well as diverse minor intrusions.

The earlier foliated to gneissic phases are biotite ± hornblende tonalite to granodiorite. The U/Pb ages of these units are broadly comparable to that of structurally overlying metavolcanic rocks (Heather

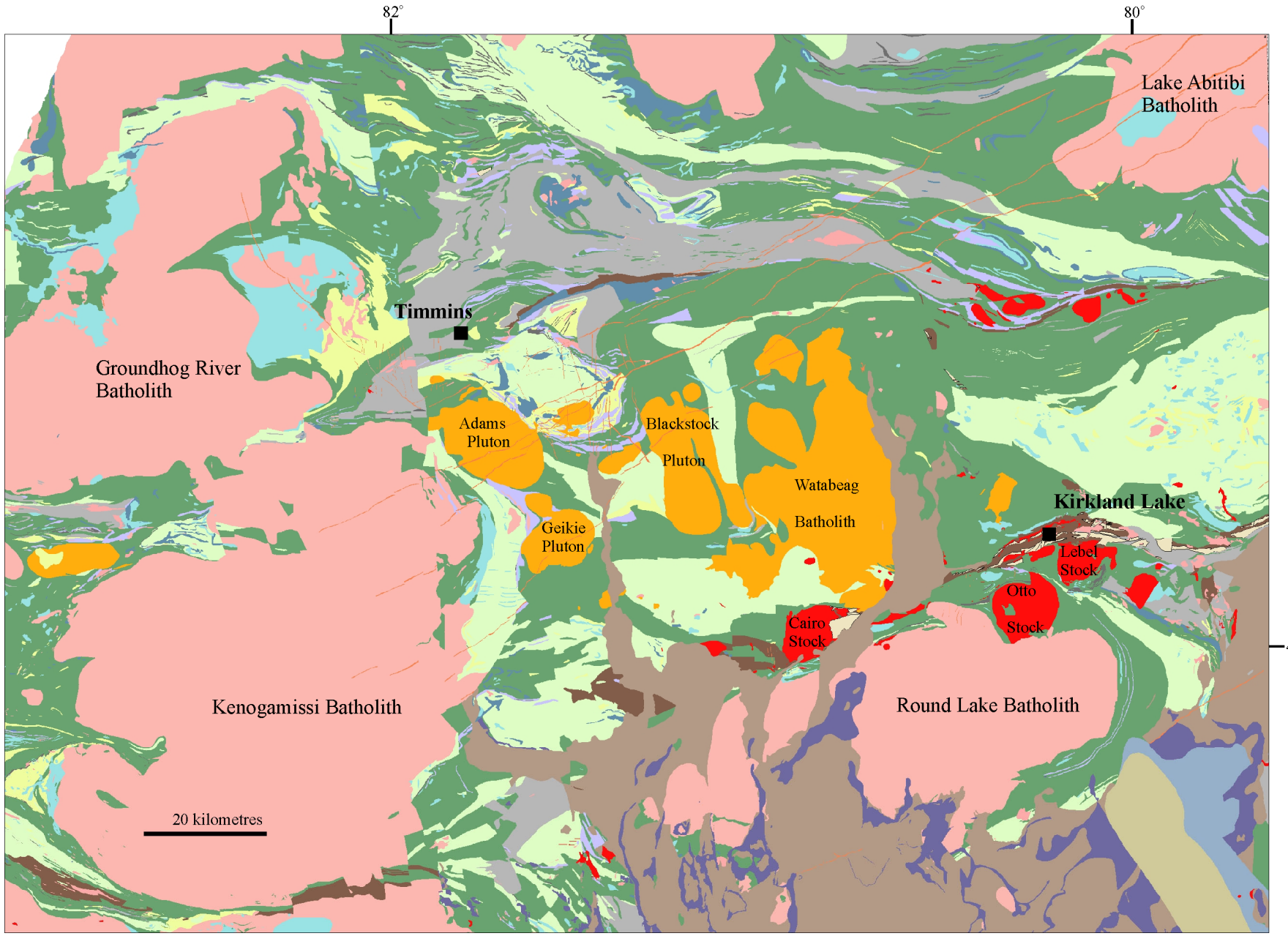

Figure 1. Generalized geological map of the Ontario portion of the Abitibi Subprovince showing the location of some of the large plutons and batholiths discussed in the text. Plutonic units in red are late-tectonic plutons and those in orange are syntectonic plutons. Units in pink are predominantly pretectonic and early syntectonic; however, syntectonic and posttectonic units also occur within the Kenogamissi and Round Lake batholiths but are not distinguished on this map.

2001; Corfu 1993). Some smaller synvolcanic plutons occurring within the greenstone belt may be related to the units occurring in the large batholithic complexes. Well-developed gneissic fabrics are commonly associated with intercalations of amphibolite, which in some cases are interpreted to represent either highly deformed mafic metavolcanic rocks or strongly transposed mafic dikes. The foliation and/or gneissosity is commonly parallel to the contacts with, and foliations within, metavolcanic country rocks and defines regional-scale structural culminations, indicating that these granitoid rocks have been folded along with overlying metavolcanic sequences. This interpretation is consistent with those of Peschler et al. (2006) who identified paleopressures of 7 to 8 kbar within the Kenogamissi Batholith and interpreted regional folding to have involved volcanics and underlying tonalitic batholiths to depths of 18 to 25 km. The ages and relationships to deformational fabrics defined by metamorphic mineral assemblages indicate that these foliated to gneissic units are synvolcanic and pretectonic.

Weakly foliated to massive plutons ranging from tonalitic to granitic (most commonly granodioritic) intrude the units discussed above and are locally observed to crosscut the foliation and/or gneissosity. The timing of their emplacement with respect to regional folding of the older tonalites is not clearly established, but based on the occurrence of some of these plutons in the cores of folds, they may be broadly synchronous with regional folding. The general character and U/Pb ages of some of these units (e.g., 2681 ± 3 Ma for the Hillary pluton and 2682 ± 3 Ma, Neville pluton: Heather 2001) are comparable to the syntectonic plutons discussed below and are interpreted here to be temporally and genetically related to this plutonic association. The Somme pluton (2662 ± 4 Ma) is interpreted to be posttectonic (Heather 2001) and may provide a minimum timing constraint on regional folding.

Compositionally distinct, relatively melanocratic hornblende diorite to quartz monzodiorite occurs locally as small, massive to weakly foliated plutons and minor intrusions. Their structural relationships are similar to that of the possibly synfolding plutons described above and they may have broadly similar timing. Somewhat similar plutons occur locally in the greenstone belt (e.g., Millie Lake pluton) and it is possible that these intrusions are part of a more widespread suite.

Minor, variously deformed dike phases are widely distributed although their abundance in outcrop is highly variable, ranging from less than 1% to up to 50% in rare cases. Pegmatitic and aplitic leucogranitic dikes are most common but there is a wide range of both composition (granitic to gabbroic) and texture.

The following section describes the characteristics of 2 of these batholiths (Round Lake and Kenogamissi) in some detail with brief discussion of some additional batholiths for which less data is available.

CHARACTERISTICS OF INDIVIDUAL PLUTONS

Round Lake Batholith

FIELD RELATIONSHIPS

The Round Lake batholith is a large, multiphase granitoid complex lying to the south of the Cadillac–Larder Lake fault. The most detailed description of the batholith is that of LaFleur (1986). At its eastern border, the batholith occupies the core of a regional anticlinal culmination and is in contact with metavolcanic rocks of the Pacaud assemblage (ca. 2745 Ma). Foliation and gneissosity in tonalitic phases

of the batholith define a geometry paralleling that defined by the stratigraphy and internal greenstone belt fabrics, indicating that the batholith has been folded along with the greenstone belt. A tonalitic phase of the Round Lake batholith is intruded by the Otto Stock (LaFleur 1986) which has a U/Pb age of 2680 ± 1 Ma (Corfu et al. 1989). Relationships elsewhere along the contact, and even the precise location of the contact, are concealed beneath Paleoproterozoic Huronian supergroup sedimentary deposits. The aerial extent of the batholith is difficult to estimate because of the presence of these cover rocks but probably extends over an area of at least 2000 km^2.

A number of individual U/Pb age determinations (~2743, 2713, 2698, 2697 Ma) for tonalitic to granodioritic phases within the batholith (Mortensen 1993; Ketchum et al. 2008) confirm that the igneous emplacement ages for the batholith span an interval of time that can be broadly correlated with that observed for the structurally overlying metavolcanic sequences.

PETROLOGY

The Round Lake batholith is a multiphase intrusive complex. The predominant lithology present within the batholith is a medium-grained, grey, moderately well-foliated to locally gneissic, biotite ± hornblende tonalite (samples 7468, 7473, 7474, 7475A, 7476, 7488, 7537, 7552, 7553, 7554, 7555, 7579, 7580; *see* Table 1). Weakly to moderately foliated to massive tonalite (samples 7467, 7471, 7472, 7477, 7489, 7556; *see* Table 1) occurs primarily in the south-central portions of the batholith and is mostly mineralogically and chemically similar to the distinctly foliated tonalite (Figure 2). Most of the aforementioned samples contain minor amounts of potassium feldspar, mostly as small interstitial grains but locally occurring as incipiently developed, anhedral to subhedral megacrysts. One sample of megacrystic granodiorite (7482) may be an extreme example of this process. Two samples (7469 and 7470) of somewhat more mafic quartz diorite from the southern portion of the batholith may also be related (either cumulate or more primitive phases) to the weakly foliated tonalite. Based on their texturally and compositionally intergradational character, together with broadly similar geochemical characteristics (discussed below), all of the aforementioned phases will be discussed together.

A number of discrete phases occupying lobes around the margins of the Round Lake batholith differ in certain respects from phases predominating within the main part of the batholith, and these are discussed separately. Two of these phases occur near the southern margin of the batholith and, although their contact relationships are partly obscured by unconformably overlying Paleoproterozoic strata, they appear to represent discrete plutons. One of these, referred to as the Hope Lake stock (samples 7524, 7525), occurs in Tudhope Township (Johns et al. 1985) whereas the other, referred to here as the Everett Lake pluton (samples 7547, 7548), occurs in Hultain Township. A single sample (7578) from a lobe occurring along the north margin of the batholith in Eby Township may also represent a discrete pluton.

GEOCHEMISTRY

This section discusses the geochemical characteristics of 27 samples representative of different components of the Round Lake batholith. Data are tabulated (Table 1), with selected geochemical variation diagrams presented in Figures 3 to 6.

Geochemical characteristics of the samples discussed above support the hypothesis that some of the discrete lobes occurring around the margins of the batholith may be distinct from the main mass of the Round Lake batholith and are also consistent with the inferred intergradational character of some of the variously foliated tonalitic phases that predominate in the main mass of the batholith. The data also suggest, however, that the tonalitic phases, regardless of their more massive versus more foliated

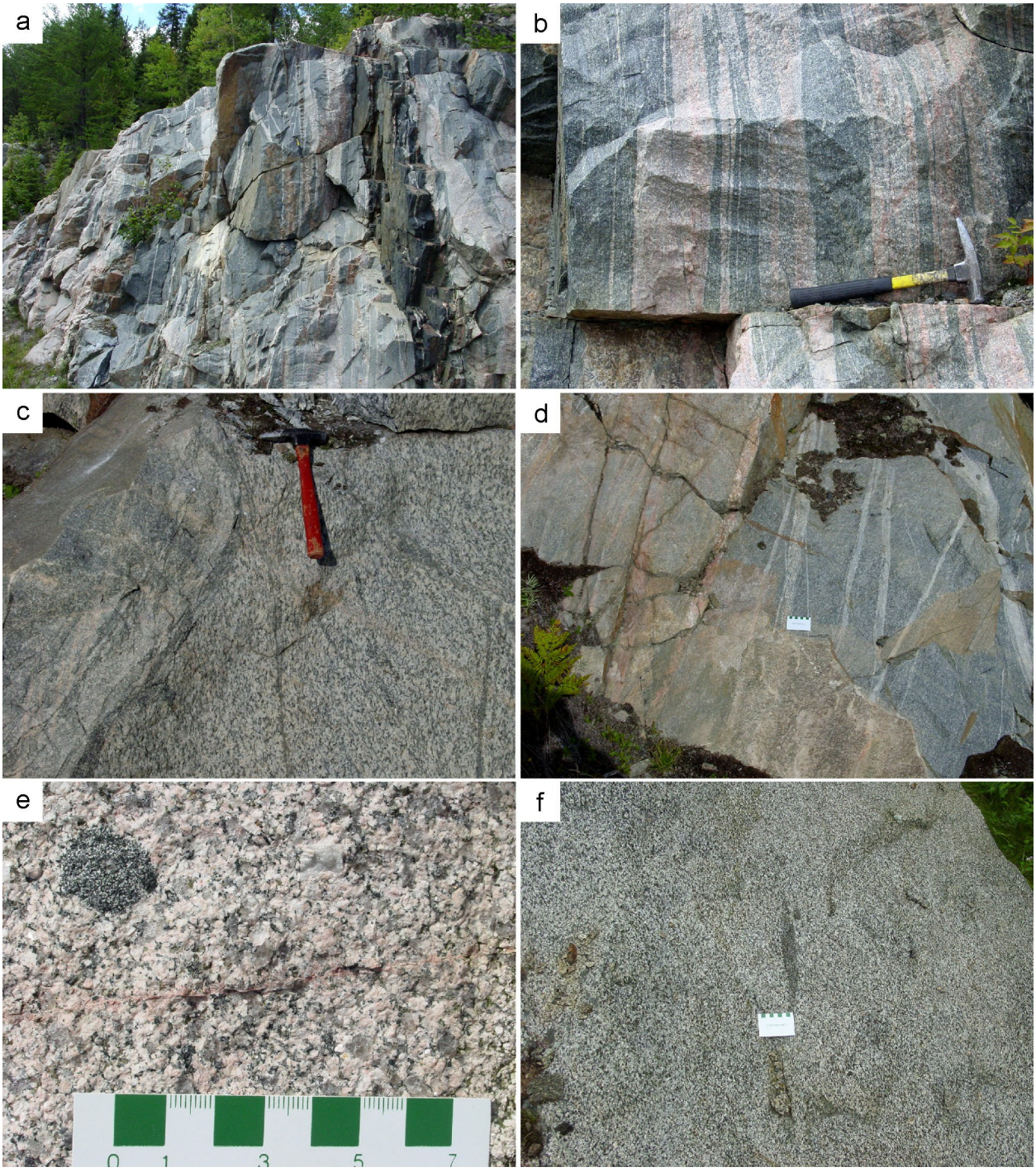

Figure 2. Field characteristics within the Round Lake batholith. Units are predominantly tonalite to granodiorite and range from well foliated to gneissic (a and b), to foliated (c, d and f) to weakly foliated (e). Variously deformed leucogranitic dikes (a, b and d) tend to be more abundant in more strongly foliated units and near the margin of the batholith. Dioritic enclaves (e and f) are most abundant in less-deformed phases concentrated near the margins of the batholith.

Table 1. Whole rock geochemical data for samples from the Round Lake batholith.

	Round L. Batholith - Type 1										Round L. Batholith - Type 2				Round L. Batholith - Type 2								Discrete Plutons				
	Foliated to Gneissic							Massive to Foliated			Foliated to Gneissic				Foliated		Massive to Foliated				Quartz Diorite		Eby	Hope Lake		Everett Lake	
Sample	7474	7475A	7476	7488	7552	7553	7554	7477	7482	7489	7468	7473	7537	7555	7579	7580	7467	7471	7472	7556	7469	7470	7578	7524	7525	7547	7548
SiO_2	72.56	70.24	70.02	70.22	70.60	72.85	72.63	71.38	70.81	71.65	65.42	68.34	69.84	65.76	67.01	67.58	66.86	65.33	68.11	65.95	62.62	64.67	68.14	67.13	68.11	64.29	62.13
Al_2O_3	15.60	17.65	16.62	16.99	16.38	16.56	16.39	16.81	16.42	16.81	17.06	16.71	17.00	17.62	16.34	18.10	16.47	17.52	16.63	17.59	18.04	17.27	15.92	15.97	16.50	15.73	16.26
MnO	0.02	0.02	0.02	0.02	0.03	0.03	0.02	0.02	0.01	0.02	0.05	0.03	0.04	0.06	0.07	0.04	0.05	0.06	0.04	0.06	0.07	0.07	0.04	0.05	0.05	0.07	0.08
FeO	1.26	0.81	0.85	0.29	1.00	0.23	0.78	0.85	0.38	0.25	2.88	1.57	0.92	1.45	2.10	1.32	1.55	2.43	1.44	2.24	2.72	2.52	1.31	1.52	1.53	2.16	2.43
Fe_2O_3	0.77	0.55	0.34	0.96	0.95	0.76	0.37	0.46	0.79	0.89	0.65	0.74	1.07	2.36	2.12	1.10	1.58	1.66	1.01	1.51	1.83	1.92	1.29	0.99	0.97	2.16	2.27
MgO	0.65	0.55	0.43	0.48	0.76	0.29	0.67	0.49	0.68	0.40	2.40	0.93	1.07	1.53	1.45	1.13	2.22	1.96	1.58	1.85	2.40	2.28	1.98	2.03	1.98	3.19	3.69
CaO	3.20	2.65	2.70	2.31	2.77	2.07	1.56	2.85	1.80	2.29	3.67	3.40	2.44	4.80	4.55	3.58	3.58	4.78	2.30	4.75	5.93	5.19	2.65	2.53	2.49	4.32	4.72
Na_2O	4.86	6.01	5.83	5.75	5.18	5.56	5.62	5.65	5.84	5.54	5.36	5.70	6.15	4.60	4.24	5.52	5.75	4.32	6.35	4.20	4.03	3.96	5.37	5.82	5.95	4.84	5.19
K_2O	1.00	1.23	1.29	1.65	1.18	2.26	2.24	1.39	1.49	1.99	1.41	1.15	1.22	0.89	1.18	1.19	1.53	1.31	1.57	1.60	1.01	1.35	2.25	2.18	2.32	2.19	2.42
TiO_2	0.22	0.16	0.14	0.13	0.22	0.11	0.14	0.16	0.13	0.12	0.40	0.32	0.24	0.40	0.49	0.26	0.35	0.43	0.31	0.39	0.47	0.51	0.30	0.31	0.30	0.46	0.47
P_2O_5	0.06	0.05	0.04	0.04	0.07	0.03	0.04	0.05	0.04	0.03	0.15	0.10	0.08	0.12	0.13	0.08	0.15	0.14	0.14	0.12	0.16	0.15	0.12	0.14	0.14	0.22	0.28
LOI	0.74	1.26	0.74	1.41	1.13	0.66	0.93	0.63	1.46	0.99	1.50	0.74	0.95	1.51	0.80	1.23	0.95	1.13	1.38	1.26	1.06	1.27	1.02	1.12	1.16	0.96	1.12
Total	101.10	101.27	99.10	100.25	100.39	101.44	101.48	100.83	99.89	101.02	101.28	99.88	101.12	101.28	100.70	101.27	101.21	101.34	101.02	101.78	100.64	101.43	100.54	99.95	101.68	100.82	101.33
Mg#	37	43	40	43	42	36	52	41	53	40	55	43	50	43	39	47	57	47	55	48	49	49	59	60	59	58	60
A/CNK	1.05	1.10	1.05	1.10	1.10	1.08	1.13	1.05	1.13	1.09	1.00	0.99	1.07	1.02	0.99	1.07	0.93	1.02	1.02	1.02	0.97	0.99	0.99	0.97	0.98	0.86	0.82
CO_2	0.09	0.3	0.06	0.48	0.08	0.01	0.08	0.04	0.4	0.13	0.21	0.01	0.05	0.18	0.04	0.03	0.01	0.08	0.05	0.01	0.01	0.09	0.01	0.03	0.19	0.05	0.31
Li	27	17	26	16	18	37	32	26	21	23	26	18	15	24	45	24	19	37	23	32	38	35	26	18	30	20	18
Cs	0.35	0.75	0.38	0.69	0.53	1.09	0.89	0.30	0.59	0.52	0.73	0.45	0.46	0.23	1.46	0.38	0.43	0.56	0.67	0.64	0.59	0.64	0.81	0.41	0.70	0.46	0.55
Rb	17	21	20	27	25	46	47	22	23	34	28	23	19	13	32	23	21	23	29	31	16	25	36	38	44	48	50
Sr	317	764	801	739	300	522	346	771	644	662	611	628	719	392	235	541	845	377	797	336	425	372	649	668	666	930	872
Ba	230	384	417	754	255	530	326	413	717	701	476	406	347	229	219	338	526	267	505	328	138	286	569	681	748	758	963
Nb	1.8	0.8	1.1	0.9	2.4	2.4	1.8	1.3	0.7	2.1	2.8	1.7	2.0	3.0	8.0	1.6	2.6	3.5	2.2	4.1	4.2	4.0	2.8	2.5	2.6	4.3	3.5
Zr	111	95	86	80	114	70	85	88	82	81	134	106	106	132	132	116	112	109	120	97	68	94	96	95	101	141	133
Hf	3.0	2.5	2.4	2.2	3.1	2.3	2.6	2.3	2.3	2.4	3.3	2.7	2.7	3.3	3.6	2.9	3.0	2.8	3.1	2.6	1.8	2.3	2.8	2.8	2.9	3.6	3.3
Th	0.78	0.83	0.69	0.47	1.56	1.68	1.01	1.24	0.81	0.88	1.82	1.13	1.80	0.23	2.49	0.47	1.61	1.62	1.83	2.12	0.80	1.43	2.56	2.98	2.77	12.78	5.56
U	0.16	0.16	0.21	0.22	0.32	0.43	0.68	0.40	0.20	0.53	0.21	0.20	0.43	0.10	0.70	0.14	0.46	0.67	0.47	0.47	0.35	0.21	0.62	0.91	0.67	2.23	1.29
Cr	16	7	11	5	2	2	4	19	14	10	61	17	13	8	26	12	66	22	25	10	37	26	52	39	34	89	89
Pb	2	5	7	5	2	7	5	7	5	6	6	7	7	2	2	6	7	5	6	5	7	2	7	39	62	17	10
Y	1.6	1.1	1.9	1.1	3.1	3.0	2.4	1.8	1.0	3.6	6.1	3.0	3.8	6.5	10.4	4.0	5.6	6.3	4.6	8.6	7.0	7.4	5.7	4.0	4.5	12.0	11.3
La	6.95	7.35	6.09	4.91	11.43	6.94	3.48	10.48	6.93	5.55	18.78	10.41	15.64	10.45	17.76	7.82	16.37	11.60	20.79	14.61	11.72	15.86	18.27	21.96	22.70	59.86	47.12
Ce	13.12	15.93	11.55	10.42	22.98	16.66	8.17	21.80	14.90	12.15	38.72	21.99	33.21	24.01	38.82	15.48	36.80	24.97	45.34	31.05	25.85	33.44	40.45	44.56	46.13	121.04	103.67
Pr	1.36	1.80	1.42	1.20	2.28	1.85	0.81	2.50	1.68	1.48	4.47	2.56	3.80	2.77	4.56	2.03	4.50	2.93	5.51	3.69	3.12	3.83	4.89	5.04	5.49	13.96	12.60
Nd	4.84	6.73	5.28	4.36	8.24	7.39	3.18	9.23	5.99	5.91	16.97	9.76	14.56	11.48	17.45	8.35	18.06	11.64	21.91	14.40	12.48	14.58	19.38	19.27	21.32	51.41	49.90
Sm	0.82	1.06	0.87	0.66	1.32	1.51	0.65	1.50	0.88	1.36	3.01	1.76	2.44	2.26	3.30	1.82	3.26	2.16	3.82	2.68	2.36	2.50	3.34	3.08	3.46	8.05	8.24
Eu	0.42	0.35	0.36	0.31	0.46	0.36	0.28	0.41	0.29	0.42	0.82	0.56	0.65	0.74	0.95	0.54	0.86	0.65	0.98	0.81	0.73	0.73	0.87	0.82	0.91	1.98	2.15
Gd	0.61	0.58	0.59	0.42	0.99	1.14	0.54	0.90	0.46	1.18	2.16	1.30	1.56	1.81	2.73	1.47	2.23	1.72	2.33	2.18	1.91	1.93	2.22	1.86	2.07	4.93	5.07
Tb	0.07	0.06	0.07	0.05	0.12	0.13	0.07	0.09	0.05	0.16	0.26	0.15	0.17	0.24	0.38	0.18	0.25	0.23	0.24	0.30	0.25	0.26	0.25	0.20	0.23	0.54	0.54
Dy	0.35	0.25	0.37	0.22	0.65	0.64	0.38	0.41	0.20	0.82	1.32	0.70	0.83	1.33	2.12	0.86	1.22	1.27	1.06	1.69	1.42	1.48	1.23	0.90	1.05	2.61	2.53
Ho	0.06	0.04	0.07	0.04	0.11	0.11	0.07	0.07	0.04	0.14	0.24	0.12	0.14	0.25	0.38	0.15	0.21	0.25	0.17	0.33	0.27	0.28	0.21	0.15	0.17	0.45	0.42
Er	0.17	0.11	0.19	0.11	0.31	0.27	0.21	0.17	0.10	0.34	0.60	0.29	0.36	0.69	1.04	0.37	0.54	0.69	0.41	0.91	0.73	0.78	0.56	0.39	0.43	1.08	1.04
Tm	0.02	0.02	0.03	0.02	0.04	0.04	0.03	0.02	0.02	0.04	0.08	0.04	0.05	0.10	0.15	0.05	0.07	0.10	0.05	0.13	0.11	0.11	0.08	0.05	0.06	0.15	0.13
Yb	0.16	0.11	0.19	0.12	0.28	0.23	0.24	0.17	0.11	0.27	0.53	0.23	0.32	0.63	0.95	0.30	0.46	0.63	0.35	0.85	0.68	0.71	0.48	0.35	0.38	0.94	0.85
Lu	0.03	0.02	0.03	0.02	0.04	0.03	0.04	0.03	0.02	0.04	0.08	0.03	0.05	0.10	0.14	0.04	0.07	0.10	0.05	0.13	0.10	0.11	0.07	0.05	0.05	0.14	0.12
Eu/Eu*	1.74	1.25	1.46	1.67	1.17	0.80	1.41	1.01	1.26	0.99	0.94	1.07	0.96	1.09	0.93	0.98	0.92	0.99	0.93	0.99	1.02	0.97	0.92	0.97	0.96	0.89	0.95
Ce_N/Yb_N	23	40	17	24	23	20	9	36	38	13	20	27	29	11	11	14	22	11	36	10	11	13	23	35	34	36	34

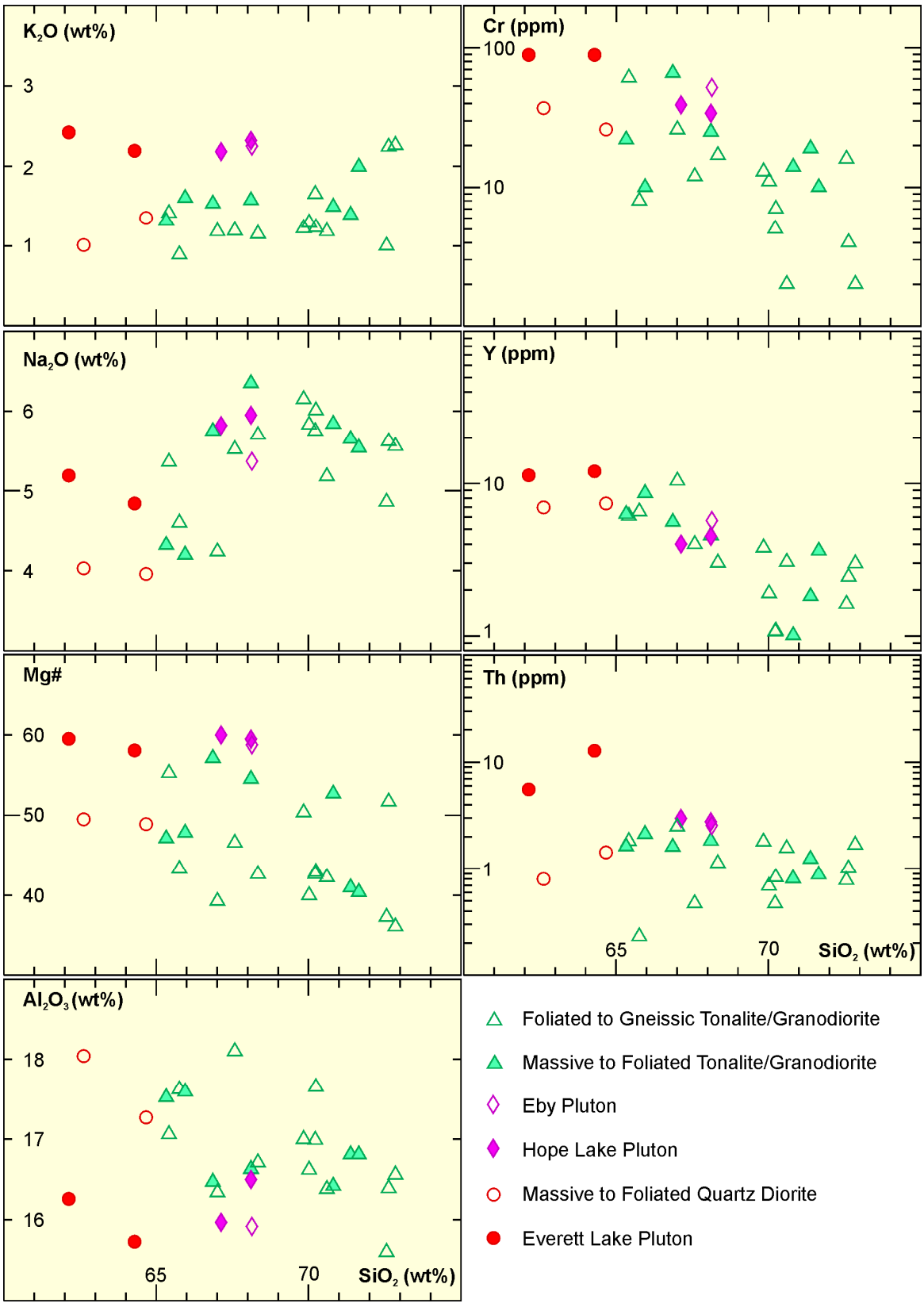

Figure 3. Harker variation diagrams for samples from the Round Lake batholith.

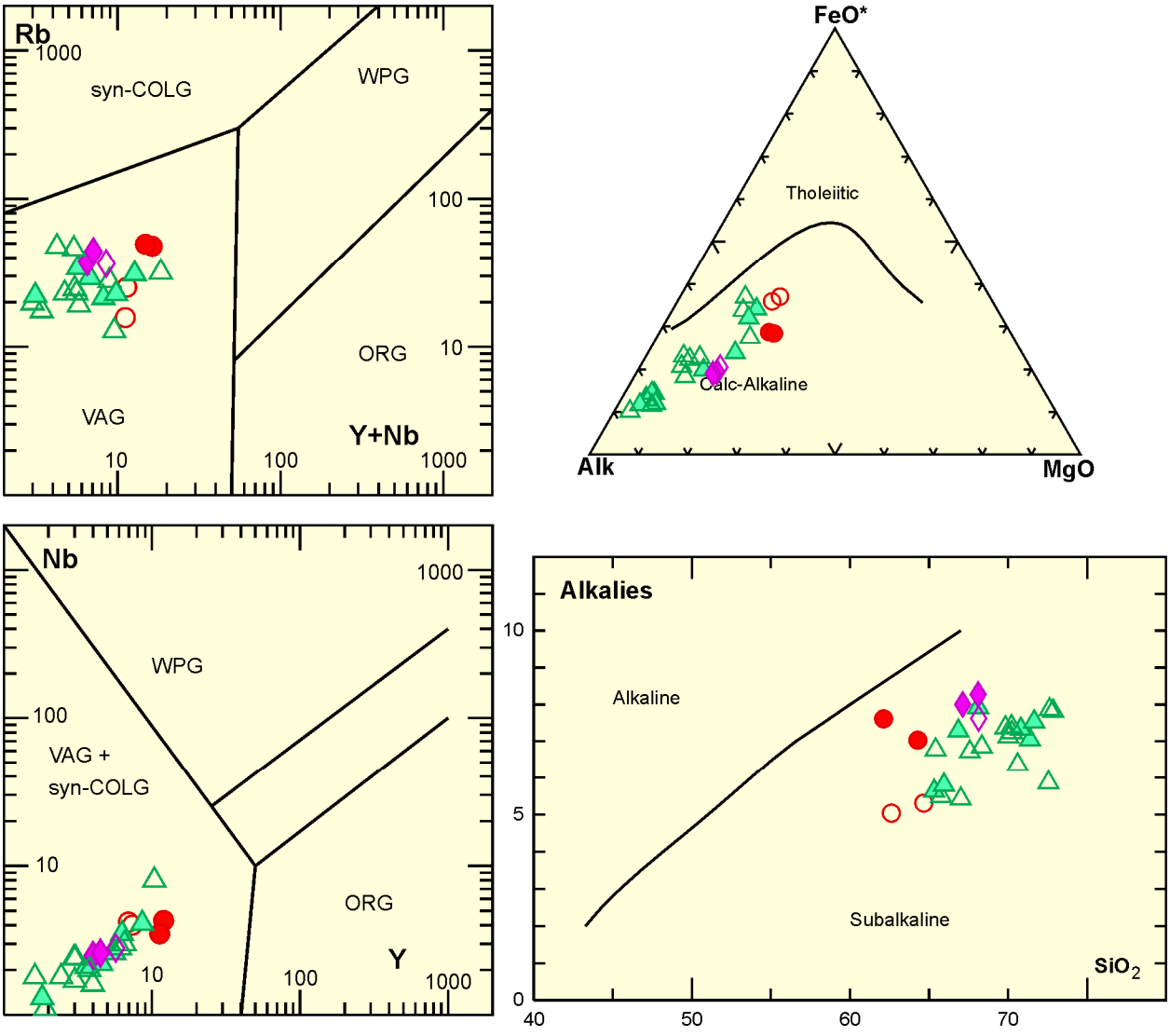

Figure 4. Tectonic discrimination diagrams for samples from the Round Lake batholith. Rb vs Y+Nb and Nb vs Y plots are after Pearce et al. (1984). AFM and alkalies vs SiO_2 plots are after Irvine and Baragar (1971). Symbols same as for Figure 3. Abbreviations: WPG, within-plate granites; ORG, ocean-ridge granites; VAG, volcanic-arc granites; syn-COLG, syncollisional granites.

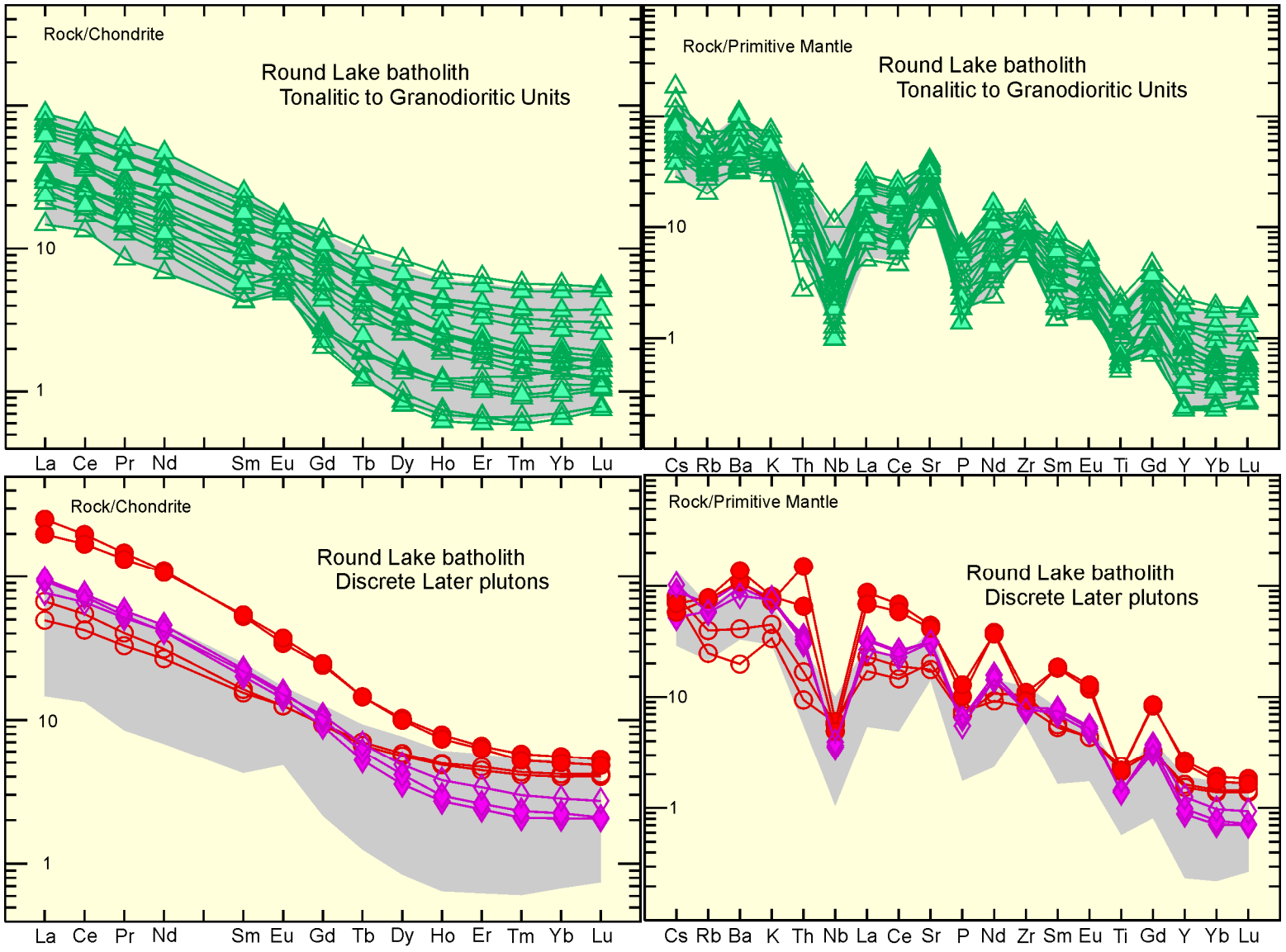

Figure 5. Chondrite and primitive mantle normalized trace element plots for samples from the Round Lake batholith. Grey shading in the upper diagrams is reproduced in the lower diagrams to facilitate comparison. Symbols same as for Figure 3.

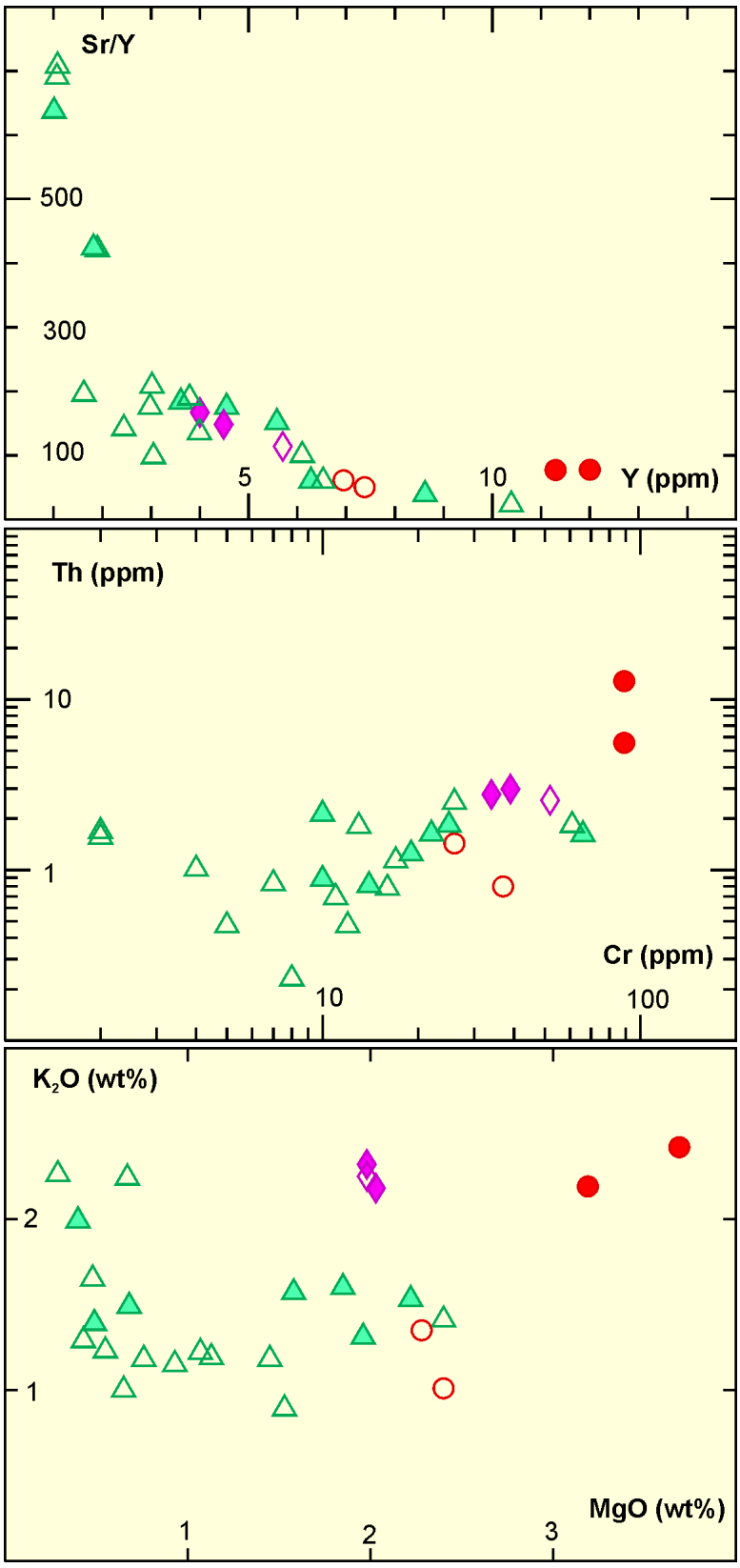

Figure 6. Sr/Y vs Y, Th vs Cr and K_2O vs MgO for samples from the Round Lake batholith. Symbols same as for Figure 3.

character, may be subdivided into 2 distinct groups on the basis of both their geographic distribution and geochemical characteristics. The first of these groups, referred to hereafter as the type 1 or eastern lobe tonalites, includes samples 7474, 7475, 7476, 7477, 7482, 7489, 7552, 7553 and 7554, which are from the eastern portion of the batholith. The second group, referred to as the type 2 tonalites, includes all of the other tonalite samples and are widely distributed throughout the remainder of the batholith.

All units associated with the Round Lake batholith are subalkaline and calc-alkalic although the type 1 tonalites lie within a slightly higher SiO_2 range than other units (*see* Figure 3) and have lower $Fe_2O_3^{total}$ and MgO, reflecting their more leucocratic character. All samples lie within the ranges for volcanic arc granites on tectonic discrimination plots (e.g., Rb vs Y+Nb, *see* Figure 4).

The geochemical characteristics of type 1 tonalites display limited variation from sample to sample. They lie within a restricted range in SiO_2 (70 to 73%), with noteworthy characteristics being relatively low abundances of both compatible and incompatible trace elements, low Mg# (mostly 37 to 42), mildly peraluminous character, and high Al_2O_3 and Sr abundances and Na/K and Sr/Y ratios (*see* Figures 3, 5 and 6). These units are also characterized by moderately fractionated rare earth element (REE) abundances with near chondritic heavy rare earth elements (HREE), with most samples having small positive Eu anomalies (*see* Figure 5). These characteristics are typical of high-Al tonalite–trondhjemite–granodiorite (TTG) plutons, which are widespread in Archean terranes worldwide.

Type 2 tonalites are similar in some respects to type 1 tonalites but do differ in a number of ways. As a consequence of their more melanocratic nature, they have higher abundances of $Fe_2O_3^{total}$ and MgO and lower SiO_2 (*see* Figure 3). Compared to type 1 tonalites, the type 2 tonalites are similarly depleted in incompatible trace elements but tend, on average, to have higher compatible trace element abundances. Strontium abundance tends to be more variable; however, abundance of Y and HREE is distinctly higher resulting in lower Sr/Y (*see* Figures 5 and 6). The type 2 tonalites are relatively enriched relative to the type 1 tonalites in all high field strength elements (HFSE) including the REE which also lack the positive Eu anomaly displayed by most of the type 1 tonalites (*see* Figure 5). Quartz dioritic units within the interior of the batholith are similar in most respects to the type 2 tonalitic units with which they are spatially associated.

Discrete plutons located around the periphery of the Round Lake batholith differ in some respects from the main tonalitic phases of the batholith although they more closely resemble the type 2 tonalites. All of these plutons (Everett Lake, Hope Lake, Eby) are characterized by high Mg# and compatible trace element abundances. The Everett Lake pluton is also characterized by a strongly meta-aluminous character and high abundances of incompatible trace elements and HFSE, especially LREE, Th and U.

PETROGENESIS

Type 1 tonalites within the Round Lake batholith have characteristics typical of many high-Al TTG units for which an origin involving high-pressure partial melting of basaltic crust is commonly inferred. The mafic bulk composition of the source is required to produce the bulk major element composition as well as the comparatively low abundances of both compatible and incompatible trace elements. Low abundance of large-ion lithophile elements (LILE), intermediate Mg#, high abundance of Sr and lack of negative Eu anomalies are inconsistent with significant contribution from felsic igneous or sedimentary crustal sources, and intermediate Mg# and low compatible trace element abundances suggest limited input from mantle sources although minor contribution from these sources cannot be ruled out. The requirement for high-pressure melting comes from geochemical characteristics suggesting that the residue contains significant garnet (extreme HREE depletion resulting in moderately fractionated REE) and no, or limited amounts of, plagioclase (high Al_2O_3, Sr and positive Eu anomalies). This implies eclogitic or

mafic garnet granulitic metamorphic conditions with melting occurring near or below the plagioclase stability field near the base of the crust or within the upper mantle.

Type 2 tonalites also classify as high-Al TTG and likely share a similar petrogenesis to that outlined above but their differences require that there be variations in detail. Lower SiO_2 and higher MgO and $Fe_2O_3^{total}$ may in part be explained by higher degrees of melting of a mafic protolith; however, LILE abundances are comparable or even slightly higher, suggesting that this is not an entirely suitable explanation. These units also have Mg# (40 to 57) and Cr abundances (10 to 65 ppm) that range from values typical of high-Al TTG to those suggestive of partial involvement or interaction with an ultramafic component.

The uniformly high Mg# and Cr abundance in discrete plutons peripheral to the batholith suggests that these rocks are derived from, or have very extensively interacted with, an ultramafic (mantle) component. High abundances of LILE and incompatible trace elements suggest that an enriched component must also be involved. Crustal contamination is an unlikely source of the enriched component given the meta-aluminous, primitive character of these units and the fact that abundance of some incompatible elements is in some cases (average Th in Everett Lake pluton is ~10 ppm) greater than that characterizing potential volumetrically significant crustal contaminants. The most plausible explanation for the abundance of LILE and incompatible trace elements is interpreted to be a mantle source modified by introduction of slab-derived, fluid mobile components and low degree partial melts.

DISCUSSION

Field relationships and petrographic, geochronological and geochemical data suggest that the Round Lake batholith is a composite intrusive complex. The batholith is broadly synvolcanic, with U/Pb ages indicating temporal linkages with the Pacaud, Kidd–Munro and Blake River assemblages although some of the younger discrete intrusive phases concentrated near the margins have not been isotopically investigated and could postdate volcanism. Tonalitic to granodioritic units that predominate within the batholith are dominantly high-Al TTG, interpreted to be derived by partial melting of mafic crust at lowermost crustal or upper mantle depths although a subset of these have geochemical characteristics suggesting that they have interacted to some degree with an ultramafic (mantle) component. The latest plutons concentrated near the periphery of the batholith also display characteristics suggesting a major involvement of a metasomatized mantle component and have possible affinity with the sanukitoid suite.

Kenogamissi Batholith

FIELD RELATIONSHIPS

Field observations indicate that the Kenogamissi Batholith is a composite intrusion composed of regionally predominant, earlier foliated to gneissic tonalite to granodiorite cut by later, massive to weakly foliated plutons having a range of compositions (hornblende granodiorite, biotite granodiorite to granite and quartz diorite to monzodiorite) (Figure 7). Pegmatitic to aplitic granitic dikes are widespread although they are generally volumetrically minor.

On a regional scale, flanking greenstone stratigraphy is parallel to the contact of the batholith and outward facing, and deformational fabrics within the batholith are locally very shallowly dipping but steepen and parallel those in the adjacent greenstone belts near the contact, indicating that the Kenogamissi Batholith occupies the core of a regional structural dome. Younger, more massive to weakly

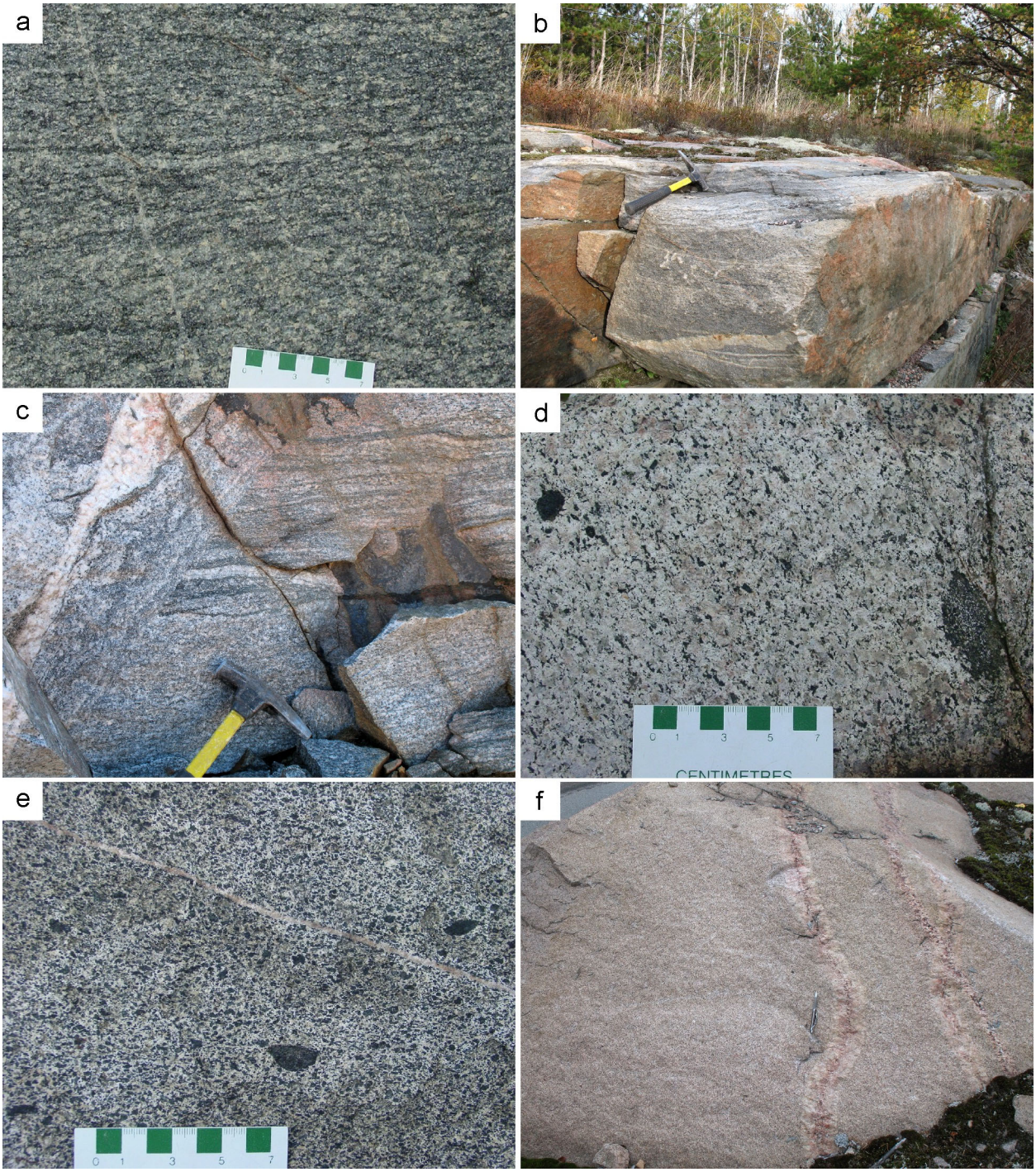

Figure 7. Field characteristics of units within the Kenogamissi Batholith. Moderately to well-foliated, locally gneissic tonalite to granodiorite with prominent heterogeneity arising from amphibolitic inclusions, mafic schlieren, variously deformed granitic dikes and heterogeneous strain predominating over large areas within the batholith (a, b and c). Very shallow dips characterize many portions of the batholith (a, b and c), particularly in the interior portions, and are locally overprinted by more steeply dipping fabrics (c). More homogeneous, weakly to moderately foliated, commonly megacrystic, granodiorite plutons (d) occur in central portions of the batholth. Late, more massive phases within the batholith range from hornblende ± clinopyroxene-bearing diorite and quartz monzodiorite with abundant mafic enclaves (e) to leucogranodiorite to leucogranite that is largely devoid of inclusions or enclaves (f).

foliated phases commonly occupy the immediate contact area but the intensity of fabric development generally increases towards the contact with the greenstone belt. In some cases (one described in detail in a subsequent section), mylonitic fabrics are developed within the later, generally more massive phases in the immediate vicinity of the contact.

U/Pb age determinations confirm the complex emplacement history for the batholith suggested by field relationships and indicate that the components of the batholith were emplaced over an interval of approximately 70 million years commencing at approximately 2747 Ma (Heather 2001; van Breemen et al. 2006; Ketchum et al. 2008). Foliated to gneissic tonalite to granodiorite emplacement (~2747, 2722, 2715, 2700, 2698 Ma) is broadly coeval with Abitibi Subprovince volcanism whereas more massive dioritic units (~2684, 2682, 2681 Ma) and granitic units (~2673, 2676 Ma) are distinctly younger. Xenocrystic zircons are present in some units and are primarily comparable in age to volcanic and plutonic units occurring elsewhere in the region but several samples have anomalously old (~2840 Ma) xenocrysts (Ketchum et al. 2008).

PETROLOGY

The Kenogamissi Batholith is characterized by considerable lithologic diversity on a regional and, in some cases, outcrop scale. Generalized descriptions of the predominant rock types follow.

The most widespread and voluminous phases of the batholith are foliated to gneissic, relatively leucocratic (color index generally 4 to 15) biotite ± hornblende tonalite to granodiorite. Other than widespread but volumetrically minor amphibolitic inclusions, these are the oldest component of the batholith. A well to weakly developed foliation is defined by alignment of biotite and hornblende as well as tabular polycrystalline quartz grains (in zones of most intense fabric development). Gneissosity, where present, is a composite fabric arising from parallel to subparallel alignment of 1) tabular amphibolite units, 2) mafic schlieren, 3) lenses of more leucocratic tonalite to granodiorite, in some cases with more mafic selvages, 4) concordant intrusive sheets of younger phases and 5) intensely transposed, discordant younger phases. Plagioclase feldspar is generally oligoclase, occasionally with albitic rims, and displays weak to moderate, patchy to zone-controlled partial alteration to a fine-grained mixture of white mica, epidote and carbonate. Microcline generally occurs as small interstitial grains where present in tonalites and may form larger discrete grains, optically continuous interstitial masses or poorly developed megacrysts in granodioritic bulk compositions. Biotite is almost always the predominant mafic mineral with subordinate hornblende being present locally. Secondary alteration of biotite to chlorite and hornblende to fibrous (actinolite?) amphibole is generally negligible to weakly developed. Primary accessory minerals include epidote, titanite, magnetite, apatite and zircon and are widespread but not abundant.

A number of relatively large areas (up to 100 km^2) within the batholith are characterized by weakly to moderately foliated, relatively homogeneous granodiorite units. Contacts with the more heterogeneous, foliated to gneissic tonalite to granodiorite discussed above may be either sharp or gradational, with fabrics in both units being similarly oriented. The difference in intensity of fabric development is attributed to the partitioning of strain into zones, with highly variable rheological properties arising because of local scale lithological complexity. These more homogeneous units are characteristically biotite ± hornblende, microcline megacrystic granodiorite containing widely distributed but volumetrically minor dioritic to quartz dioritic enclaves. Other than the consistent presence of microcline and a slightly more melanocratic (colour index (CI) ~10 to 15 vs ~2 to 10) character, the mineralogical characteristics of the more homogeneous foliated units are broadly similar to those of the more heterogeneous foliated to gneissic units.

Relatively melanocratic (CI ~15 to 30) quartz monzodiorite to diorite occur as discrete plutons underlying areas as large as 50 km^2 as well as more localized minor phases. The discrete plutons are predominantly localized near the southern and eastern contacts of the batholith, one of these being referred to as the Neville pluton (Heather 2001). The minor phases commonly have intrusive relationships indicating that they postdate the fabrics developed within the foliated to gneissic tonalite to granodiorite, and the discrete plutons have only very weakly developed foliations that in some cases are interpreted to represent magmatic flowage fabrics. An exception to this generalization, discussed in more detail in a subsequent section, occurs at the southern contact of the Neville pluton with the greenstone belt where mylonitic fabrics are developed. These relationships, together with the young U/Pb ages for some of these dioritic units summarized above, suggest that these quartz monzodioritic to dioritic units are broadly syntectonic to late tectonic.

Within the dioritic to quartz monzodioritic units, plagioclase feldspar is generally oligoclase to andesine and displays weak to moderate, patchy to zone-controlled partial alteration to a fine-grained mixture of white mica, epidote and carbonate. Microcline is generally present as small interstitial grains but locally occurs as poorly developed megacrysts. Hornblende is the predominant mafic mineral, invariably with subordinate biotite; in some cases clinopyroxene occurs as cores within hornblende. Secondary alteration of hornblende to biotite or fibrous (actinolite?) amphibole and biotite to chlorite is generally weakly developed. Primary accessory minerals include epidote, titanite, magnetite, apatite and zircon and are widespread but with all but zircon being locally relatively abundant. Dioritic enclaves (more mafic than host unit, with CI ~25 to 50) with sharp to gradational contacts, together with subordinate ultramafic clots, are commonly present. Together with irregular variation in the proportion of mafic minerals and quartz, this commonly imparts a local heterogeneity within the scale of an individual outcrop.

Relatively leucocratic granodiorite to granite is interpreted to be the youngest component of the batholith on the basis of both field relationships and U/Pb ages. A single, large, discrete, biotite leucogranodiorite to leucogranite pluton (Somme pluton, Heather 2001) occurs in the south-central portion of the batholith. Widespread, locally abundant leucogranitic to leuco alkali-feldspar granitic dikes and minor intrusions with equigranular to pegmatitic to aplitic textures are predominantly late but display a range of relationships with respect to deformational fabrics. Plagioclase is relatively sodic (albite to oligoclase) and is commonly extensively altered to white mica. Microcline occurs both as homogeneous, anhedral crystals similar in size to plagioclase and quartz and as well-formed, subhedral to euhedral, perthitic, poikilitic megacrysts with longest dimension ranging up to 5 cm. Biotite is the sole ferromagnesian silicate but is usually present in low abundance (<3%) and is commonly extensively chloritized. Primary magmatic accessory minerals (magnetite, apatite, titanite, zircon) occur in very low abundance.

GEOCHEMISTRY

This section discusses the geochemical characteristics of 43 samples representative of different components of the Kenogamissi Batholith. Data are tabulated (Table 2), with selected geochemical variation diagrams presented in Figures 8 to 13.

The geochemical data broadly correlate with the subdivisions based on structural and petrographic criteria discussed above and suggest that a range of processes are involved in the petrogenesis of the different components of the batholith. As discussed below, a couple of samples may be misclassified. All units have calc-alkalic affinity and are mostly subalkaline with the exception of some of the dioritic units which are distinctly higher in alkalies, with 2 samples lying just into the alkaline field (Figure 9). In trace element tectonic discrimination diagrams, most samples plot as volcanic arc granites, with the later granitic units overlapping the field for syncollisional granites (*see* Figure 9).

Table 2. Whole rock geochemical data for samples from the Kenogamissi Batholith.

	Foliated to Gneissic Tonalite to Granodiorite											Foliated Tonalite to Granodiorite			
Number	7272	7273A	7274	7565	7666	7667A	7667B	7682A	7682B	7687	7688	7276A	7455	7459	7460A
SiO_2	72.16	70.50	69.82	71.30	67.60	60.92	66.59	69.60	65.27	68.61	68.69	70.87	72.00	65.69	69.43
Al_2O_3	16.37	16.82	16.84	16.17	15.79	17.87	15.66	16.55	16.22	15.69	16.34	16.24	15.64	16.83	17.19
MnO	0.02	0.03	0.04	0.04	0.07	0.07	0.06	0.03	0.07	0.05	0.03	0.03	0.03	0.05	0.03
FeO	0.81	0.37	1.31	1.34	2.25	3.04	2.97	1.17	2.80	2.21	1.63	1.27	0.83	1.66	0.67
Fe_2O_3	0.55	1.29	1.10	0.91	1.87	2.24	1.87	0.86	1.82	1.59	1.01	0.70	0.72	1.81	1.99
MgO	0.63	0.79	0.93	0.70	1.14	1.83	1.38	0.80	1.86	0.86	0.85	0.80	0.52	1.31	0.93
CaO	2.12	2.52	3.82	3.60	4.02	5.29	5.15	3.40	4.68	3.93	3.64	2.35	1.79	2.79	3.31
Na_2O	5.28	5.58	5.27	4.58	5.53	5.78	4.83	5.48	4.33	4.82	5.16	4.66	4.54	4.59	4.79
K_2O	2.81	2.23	1.13	1.27	0.80	0.84	0.61	1.04	1.36	0.92	1.06	3.17	4.13	3.89	1.10
TiO2	0.20	0.27	0.32	0.31	0.32	0.73	0.43	0.27	0.56	0.29	0.34	0.30	0.24	0.65	0.32
P_2O_5	0.08	0.11	0.09	0.07	0.12	0.24	0.09	0.09	0.11	0.11	0.10	0.10	0.09	0.34	0.09
LOI	0.45	0.70	0.62	0.63	0.42	0.97	0.40	0.52	1.17	0.52	0.38	0.71	0.65	0.59	1.22
TOTAL	101.58	101.24	101.44	101.08	100.16	100.16	100.38	99.94	100.54	99.85	99.41	101.35	101.27	100.39	101.14
Mg#	46	48	42	37	34	39	35	42	43	30	37	43	39	42	40
A/CNK	1.05	1.04	1.00	1.05	0.91	0.89	0.87	1.01	0.95	0.98	1.01	1.06	1.03	1.00	1.14
Li	35	39	27	25	23.7	14	5.5	26	34.6	27	15.2	53	42	93	20
Cs	2.3	3.3	1.9	3.2	1.4	1.4	0.6	1.1	2.4	1.2	0.5	6.9	4.4	4.4	1.1
Rb	75	74	37	33	37	26	14	34	26	26	27	124	157	160	43
Sr	712	802	512	282	369	298	214	407	274	208	351	527	352	720	300
Ba	1012	952	226	364	156	188	156	368	244	284	308	861	687	1247	320
Nb	2.3	3.5	2.0	3.5	4.3	8.4	5.1	1.7	5.2	4.5	3.4	6.6	7.4	14.1	3.2
Zr	101	127	104	123	81	80	154	115	131	209	141	177	142	282	153
Hf	2.8	3.3	2.5	3.4	2.1	2.2	4.2	3.2	3.8	5.5	4.3	4.4	4.0	6.9	4.1
Th	3.07	3.57	0.84	2.50	0.58	1.56	1.05	1.85	2.63	2.61	2.21	11.12	15.47	14.17	2.70
U	0.48	1.13	0.52	0.21	0.56	0.66	0.38	0.35	1.05	0.25	0.21	1.31	1.75	1.85	0.33
Cr	27	27	30	6	19	18	16	30	42	20	17	20	13	25	13
Y	3.2	4.7	2.9	2.7	5.7	11.5	14.5	2.3	11.3	10.0	5.5	5.4	4.8	8.5	3.5
La	16.6	20.7	9.29	16.4	8.80	12.6	8.50	13.3	12.9	18.1	17.0	43.4	35.7	88.2	16.2
Ce	33.4	42.8	17.9	31.7	15.6	25.5	18.2	26.6	27.8	33.7	31.8	80.4	66.7	169.6	30.5
Pr	3.77	4.96	1.98	3.27	1.86	3.08	2.47	2.99	3.50	3.84	3.60	8.11	6.81	17.38	3.05
Nd	14.0	18.8	7.13	11.1	7.55	12.3	11.2	10.7	14.1	14.5	13.3	26.3	21.7	57.6	10.3
Sm	2.34	3.18	1.20	1.65	1.41	2.84	3.02	1.57	2.98	3.04	2.39	3.56	2.95	7.44	1.54
Eu	0.57	0.77	0.45	0.52	0.66	0.91	0.92	0.41	0.77	0.87	0.67	0.78	0.67	1.63	0.54
Gd	1.42	1.94	0.88	1.11	1.24	2.69	3.16	0.89	2.53	2.70	1.82	2.02	1.68	4.06	1.10
Tb	0.15	0.21	0.11	0.14	0.18	0.38	0.48	0.10	0.36	0.38	0.23	0.24	0.20	0.44	0.14
Dy	0.69	1.00	0.56	0.63	1.00	2.20	2.80	0.50	2.20	2.10	1.20	1.15	0.95	1.97	0.72
Ho	0.11	0.16	0.10	0.11	0.20	0.41	0.54	0.08	0.42	0.37	0.20	0.19	0.16	0.31	0.13
Er	0.29	0.43	0.29	0.27	0.60	1.10	1.50	0.22	1.19	0.99	0.53	0.51	0.42	0.75	0.35
Tm	0.04	0.06	0.04	0.04	0.08	0.15	0.21	0.03	0.17	0.13	0.07	0.07	0.06	0.10	0.05
Yb	0.26	0.38	0.27	0.22	0.59	0.93	1.34	0.20	1.10	0.83	0.43	0.46	0.41	0.61	0.32
Lu	0.04	0.06	0.04	0.04	0.09	0.14	0.19	0.03	0.15	0.11	0.06	0.07	0.06	0.08	0.05
Eu/Eu*	0.89	0.88	1.28	1.11	1.49	0.99	0.90	0.97	0.83	0.91	0.94	0.82	0.84	0.82	1.21
Ce_N/Yb_N	36	31	18	40	7	8	4	37	7	11	21	49	45	77	26

Table 2. (continued)

	Foliated Tonalite to Granodiorite					Massive to Foliated Granodiorite			Massive Granodiorite					Beemer Pluton	
Number	7665	7678	7680	7681	7683	7461	7462	7677	7269	7275	7336	7456	7686	7669	7670
SiO_2	70.42	66.90	63.25	70.77	67.73	70.43	69.06	70.87	68.10	70.67	70.12	71.00	72.12	71.41	71.51
Al_2O_3	16.07	16.12	17.60	16.50	17.38	15.88	17.01	15.15	16.32	15.74	15.94	16.09	14.48	16.45	15.86
MnO	0.03	0.10	0.06	0.02	0.04	0.05	0.03	0.03	0.04	0.04	0.02	0.03	0.03	0.01	0.02
FeO	1.08	2.61	2.43	1.34	1.68	0.41	1.59	1.10	1.27	0.92	0.63	0.46	0.75	0.42	0.50
Fe_2O_3	0.56	1.30	1.56	0.89	1.04	1.66	0.73	0.74	1.07	0.81	0.54	0.86	0.86	0.52	0.68
MgO	0.62	2.10	1.92	0.69	1.23	0.68	0.85	0.60	1.34	1.03	0.58	0.43	0.31	0.30	0.35
CaO	2.15	2.57	5.11	3.30	4.04	2.04	2.51	1.87	3.11	2.11	1.76	1.92	1.24	1.64	1.51
Na_2O	4.74	4.77	4.86	5.00	5.36	4.82	4.94	4.17	5.36	5.17	5.65	4.85	3.97	5.68	5.41
K_2O	3.42	1.93	1.23	0.99	0.92	3.40	3.10	4.23	2.89	3.63	2.66	3.56	4.97	2.99	3.52
TiO2	0.22	0.35	0.53	0.29	0.33	0.31	0.36	0.29	0.28	0.18	0.16	0.18	0.22	0.14	0.21
P_2O_5	0.08	0.09	0.18	0.07	0.11	0.11	0.15	0.11	0.14	0.09	0.06	0.06	0.06	0.06	0.09
LOI	0.61	1.58	0.63	0.47	0.35	0.64	0.66	0.55	0.61	0.98	0.72	0.67	0.37	0.49	0.50
TOTAL	100.12	100.71	99.62	100.49	100.39	100.49	101.17	99.83	100.70	101.47	98.92	100.16	99.46	100.17	100.23
Mg#	41	50	47	36	46	39	40	38	52	53	48	38	27	38	36
A/CNK	1.04	1.10	0.95	1.08	1.01	1.04	1.06	1.02	0.93	0.97	1.04	1.05	1.02	1.06	1.03
Li	57.9	33	62.2	22.6	32.9	41	42	32.2	25	5	22	46	66.5	24.6	32.9
Cs	6.4	0.8	4.3	2.7	0.8	2.7	3.1	2.7	0.7	0.6	0.7	4.9	2.9	1.9	1.1
Rb	179	72	32	37	15	179	144	139	63	78	59	160	291	63	90
Sr	387	322	439	340	495	282	507	413	938	675	824	425	161	1061	1201
Ba	833	508	175	395	306	627	924	974	1253	1051	1110	662	723	1727	1424
Nb	7.7	3.5	8.9	2.5	2.0	10.0	11.3	10.4	6.8	3.7	2.4	5.8	11.5	1.7	3.5
Zr	135	99	158	102	97	174	211	146	146	90	84	114	195	76	123
Hf	3.9	2.9	4.2	3.1	2.8	4.6	5.4	4.1	3.7	2.6	2.6	3.5	6.1	2.1	3.5
Th	12.35	1.94	1.17	1.63	0.59	16.88	13.74	12.63	5.87	6.46	2.02	11.51	26.96	1.78	3.59
U	2.31	0.77	2.23	0.29	0.27	1.22	1.52	1.69	1.11	0.66	0.94	1.47	2.85	0.69	1.03
Cr	13	28	27	19	26	12	14	18	49	48	19	4	19	9	13
Y	7.2	7.9	11.8	1.5	5.4	6.0	9.0	6.1	9.8	5.6	3.5	3.8	10.7	2.5	3.3
La	32.2	10.3	5.10	13.8	8.10	47.0	59.4	47.2	33.6	14.6	13.3	27.6	62.4	11.1	28.9
Ce	59.6	22.3	14.3	25.9	17.5	86.1	111.5	85.1	67.5	30.2	25.2	49.6	117.0	24.1	60.6
Pr	6.16	2.75	2.16	2.73	2.35	8.60	11.18	9.09	7.74	3.52	3.12	5.11	11.93	2.82	7.09
Nd	19.5	10.8	9.54	9.34	10.1	27.1	36.3	29.6	29.2	13.4	12.2	16.8	37.4	10.6	26.0
Sm	2.82	2.07	2.43	1.23	2.21	3.67	5.18	3.96	5.06	2.42	2.01	2.25	5.09	1.87	3.71
Eu	0.63	0.61	0.78	0.47	0.69	0.68	1.09	0.85	1.22	0.63	0.58	0.56	0.72	0.50	0.87
Gd	1.83	1.70	2.28	0.66	1.73	2.14	3.21	2.17	3.47	1.75	1.29	1.34	2.93	1.19	1.84
Tb	0.24	0.25	0.32	0.07	0.21	0.25	0.37	0.26	0.41	0.20	0.15	0.15	0.36	0.13	0.18
Dy	1.30	1.50	1.80	0.30	1.10	1.21	1.85	1.20	2.03	1.08	0.70	0.74	2.00	0.60	0.70
Ho	0.24	0.29	0.36	0.06	0.20	0.21	0.32	0.21	0.34	0.19	0.12	0.13	0.35	0.08	0.10
Er	0.67	0.82	1.11	0.14	0.53	0.57	0.81	0.53	0.86	0.51	0.32	0.34	0.97	0.19	0.23
Tm	0.10	0.12	0.17	0.02	0.07	0.08	0.11	0.07	0.11	0.07	0.04	0.05	0.15	0.03	0.03
Yb	0.64	0.86	1.27	0.14	0.47	0.56	0.70	0.47	0.75	0.50	0.30	0.34	0.98	0.16	0.19
Lu	0.09	0.13	0.17	0.02	0.06	0.09	0.10	0.07	0.10	0.07	0.04	0.05	0.15	0.02	0.03
Eu/Eu*	0.79	0.96	1.00	1.45	1.03	0.69	0.76	0.81	0.84	0.90	1.03	0.91	0.52	0.95	0.90
Ce_N/Yb_N	26	7	3	52	10	43	44	50	25	17	23	40	33	43	87

Table 2. (continued)

	Neville Pluton				Misc Diorite to Quartz Monzodiorite				Somme Granite				Granite Dike
Number	7661	7662	7663	7664	7276B	7460B	7564	7679	7646	7647	7684	7685	7273B
SiO_2	60.16	66.61	60.44	64.07	54.31	54.71	57.67	62.67	70.78	71.04	74.10	73.74	75.68
Al_2O_3	14.96	15.68	15.49	16.05	14.86	12.98	15.98	17.21	15.05	15.55	14.33	14.48	14.84
MnO	0.10	0.05	0.10	0.06	0.15	0.11	0.13	0.08	0.03	0.03	0.02	0.02	0.01
FeO	3.47	1.37	3.35	2.05	5.40	5.94	6.04	2.99	0.91	1.04	0.54	0.46	0.19
Fe_2O_3	1.98	1.39	2.00	1.66	3.41	2.61	1.30	1.96	0.78	0.60	0.57	0.65	0.34
MgO	3.98	1.53	3.20	2.08	5.01	9.37	5.69	2.17	0.54	0.56	0.19	0.35	0.13
CaO	5.25	3.22	5.24	4.09	8.02	8.30	6.80	5.32	1.60	2.21	1.24	0.82	1.39
Na_2O	4.20	5.44	4.71	5.43	4.14	2.81	3.20	4.31	4.25	4.79	3.91	4.07	4.48
K_2O	3.19	2.70	3.72	2.66	3.19	1.01	0.94	1.25	4.06	3.33	5.03	4.92	3.96
TiO2	0.53	0.29	0.54	0.40	1.04	1.15	0.65	0.50	0.21	0.22	0.07	0.13	0.03
P_2O_5	0.24	0.15	0.38	0.23	0.77	0.08	0.18	0.13	0.07	0.08	0.03	0.03	0.01
LOI	1.30	1.00	0.49	0.69	0.07	1.56	1.77	0.86	0.76	0.43	0.26	0.69	0.68
TOTAL	99.74	99.59	100.02	99.70	100.97	101.29	101.02	99.76	99.13	100.00	100.36	100.40	101.74
Mg#	57	51	53	51	51	67	58	45	37	39	24	37	32
A/CNK	0.75	0.88	0.73	0.83	0.60	0.62	0.86	0.95	1.05	1.00	1.01	1.07	1.05
Li	11.8	7.7	5.4	6	16	30	25	30.7	14.5	58.8	13.5	24.6	3
Cs	2.7	0.3	2.2	1.8	0.6	0.6	1.0	1.5	3.3	5.2	2.4	2.2	0.9
Rb	94	55	103	42	63	42	25	23	163	176	177	244	88
Sr	707	777	1103	979	1389	169	293	463	361	382	208	180	457
Ba	897	1001	1110	1129	1371	167	247	326	1051	797	764	561	2454
Nb	4.9	5.4	7.0	6.8	6.4	5.0	3.9	3.2	5.3	8.1	2.6	8.1	2.3
Zr	128	125	201	169	216	58	96	97	169	135	123	100	41
Hf	3.8	3.8	5.8	4.5	5.1	2.0	2.0	2.9	4.8	4.0	4.2	3.3	1.4
Th	4.37	6.52	7.94	5.56	3.15	1.47	1.49	1.23	14.54	12.67	23.56	36.09	0.38
U	1.31	1.20	1.77	1.21	0.93	1.39	0.38	0.24	1.25	2.57	1.48	1.64	0.51
Cr	194	48	74	59	106	163	212	37	10	12	9	15	25
Y	14.7	10.6	17.9	13.9	30.4	13.7	12.8	10.4	4.3	8.5	2.8	7.7	2.4
La	25.7	27.2	46.0	35.5	67.0	13.4	15.2	16.2	57.6	31.3	37.9	24.2	1.70
Ce	53.7	56.6	98.1	77.0	146.2	35.7	34.3	35.2	99.1	58.2	65.5	48.7	3.78
Pr	6.61	6.68	12.24	9.16	18.81	4.97	4.09	4.49	10.22	6.05	6.09	5.41	0.44
Nd	26.5	25.3	49.1	34.7	79.1	21.6	16.1	18.2	31.3	20.0	17.7	18.2	1.73
Sm	5.18	4.59	8.92	6.38	15.64	5.10	3.09	3.34	3.68	3.06	1.84	3.15	0.36
Eu	1.24	1.16	2.24	1.54	4.18	1.38	1.05	0.90	0.71	0.66	0.33	0.54	0.16
Gd	4.07	3.26	6.58	4.48	12.02	4.42	2.80	2.61	1.69	2.02	0.87	2.13	0.31
Tb	0.52	0.41	0.78	0.54	1.41	0.56	0.42	0.35	0.18	0.27	0.09	0.27	0.05
Dy	2.90	2.10	3.90	2.80	6.79	2.90	2.46	2.00	0.80	1.50	0.40	1.50	0.32
Ho	0.53	0.37	0.66	0.50	1.11	0.53	0.50	0.38	0.14	0.28	0.09	0.27	0.07
Er	1.46	0.99	1.69	1.34	2.69	1.34	1.42	1.10	0.40	0.78	0.28	0.72	0.25
Tm	0.20	0.14	0.23	0.18	0.34	0.18	0.21	0.15	0.06	0.11	0.05	0.10	0.05
Yb	1.32	0.91	1.47	1.17	2.11	1.18	1.38	0.97	0.45	0.74	0.38	0.72	0.35
Lu	0.20	0.14	0.20	0.17	0.29	0.17	0.21	0.14	0.08	0.11	0.07	0.11	0.06
Eu/Eu*	0.80	0.87	0.85	0.84	0.90	0.87	1.07	0.90	0.76	0.76	0.69	0.60	1.43
Ce_N/Yb_N	11	17	19	18	19	8	7	10	61	22	49	19	3

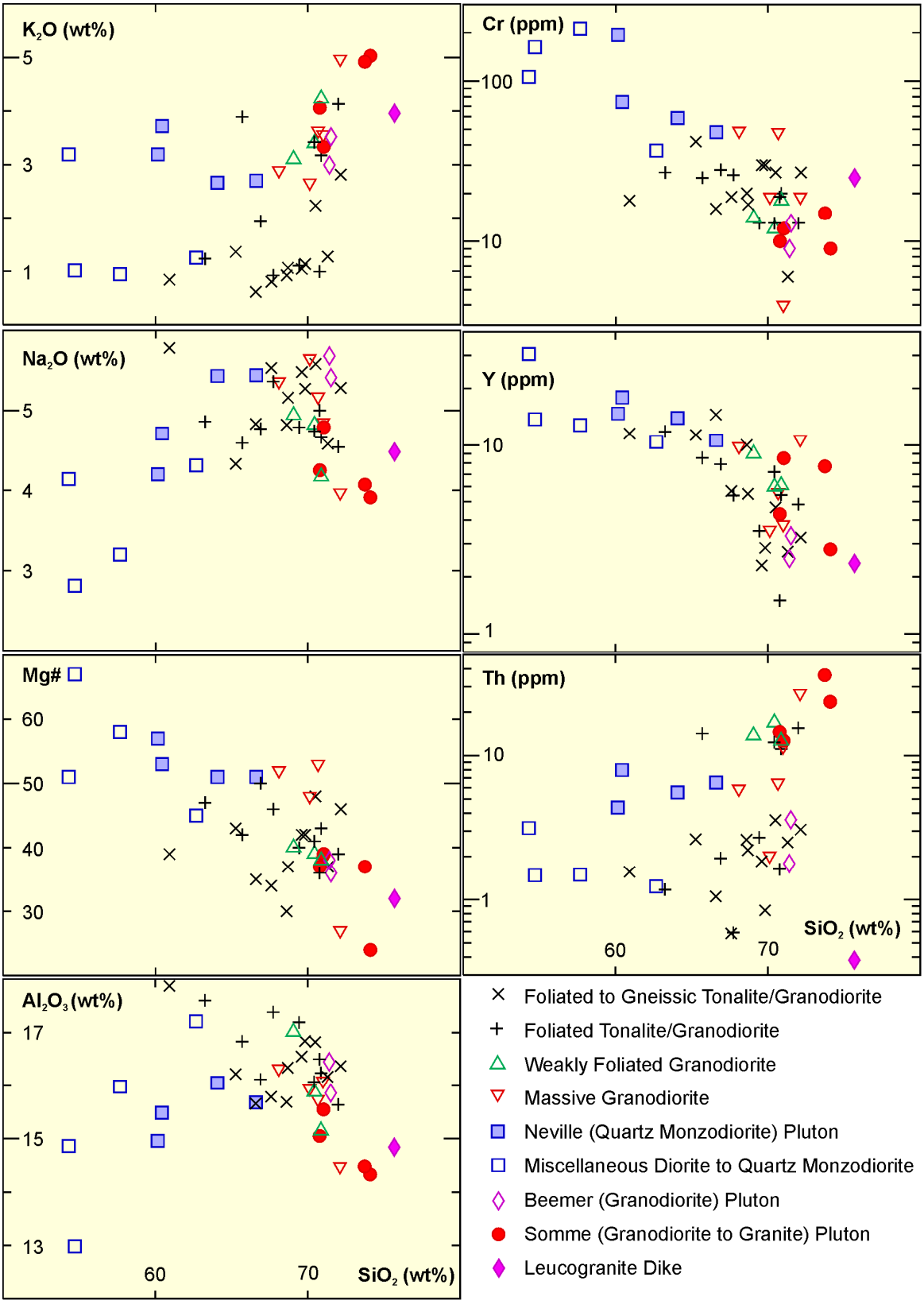

Figure 8. Harker variation diagrams for samples from the Kenogamissi Batholith.

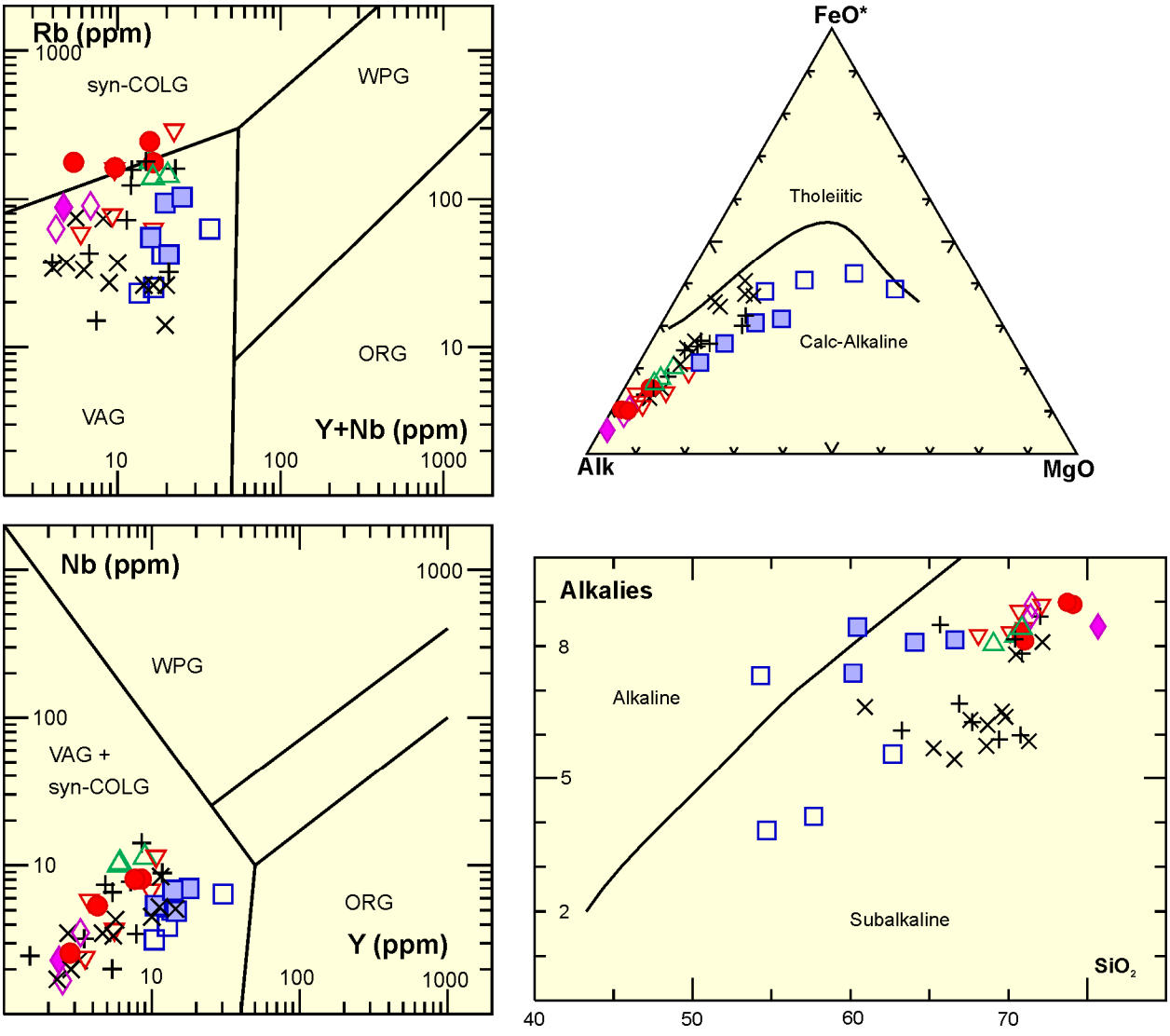

Figure 9. Tectonic discrimination diagrams for samples from the Kenogamissi Batholith. Rb vs Y+Nb and Nb vs Y plots are after Pearce et al. (1984). AFM and alkalies vs SiO_2 plots are after Irvine and Baragar (1971). Symbols same as for Figure 8; abbreviations, Figure 4.

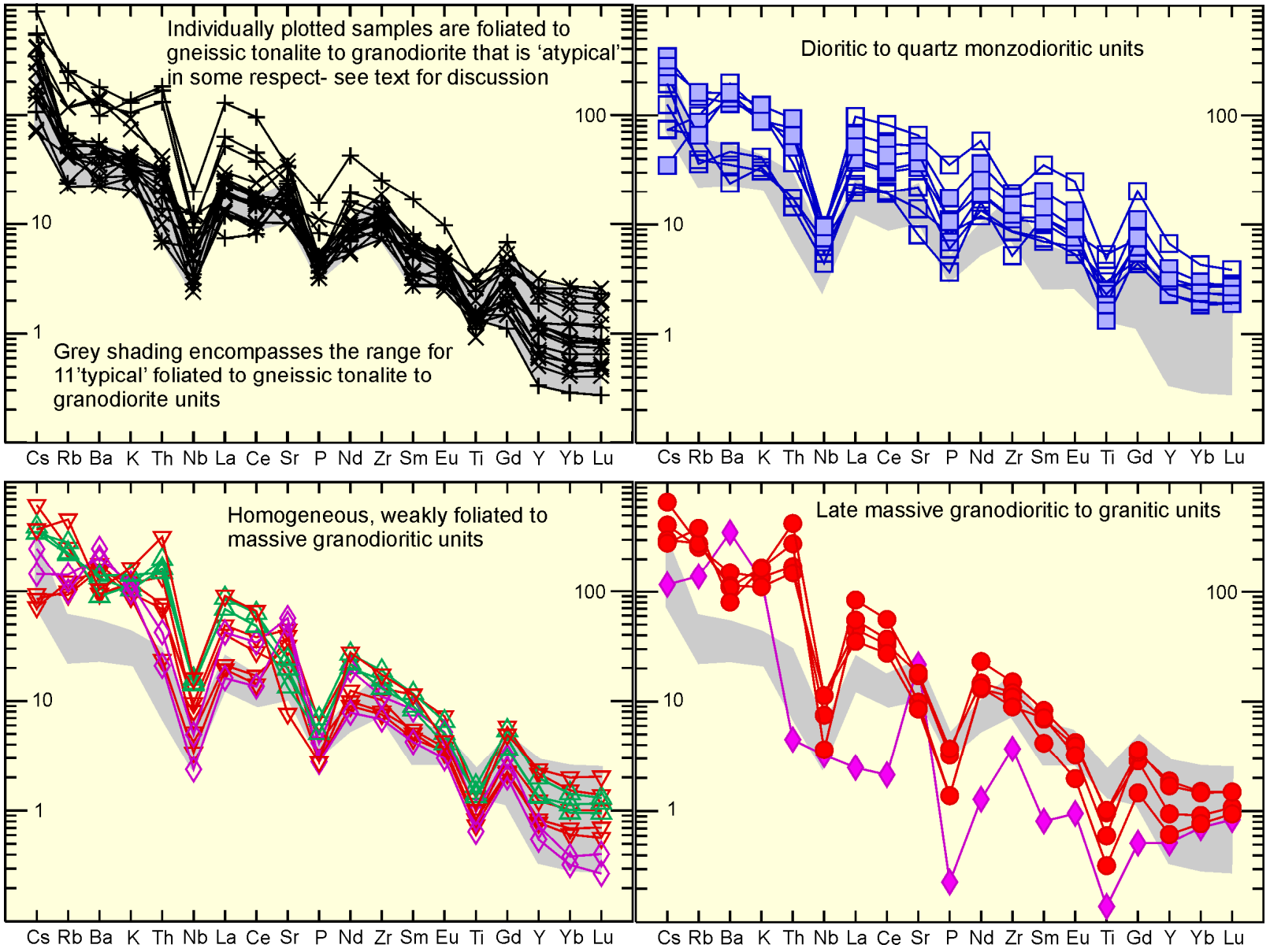

Figure 10. Primitive mantle normalized trace element plots for samples from the Kenogamissi Batholith. Grey shaded area in upper left diagram is reproduced in all other diagrams to facilitate comparison. Normalization values from Sun and McDonough (1989). Symbols same as for Figure 8.

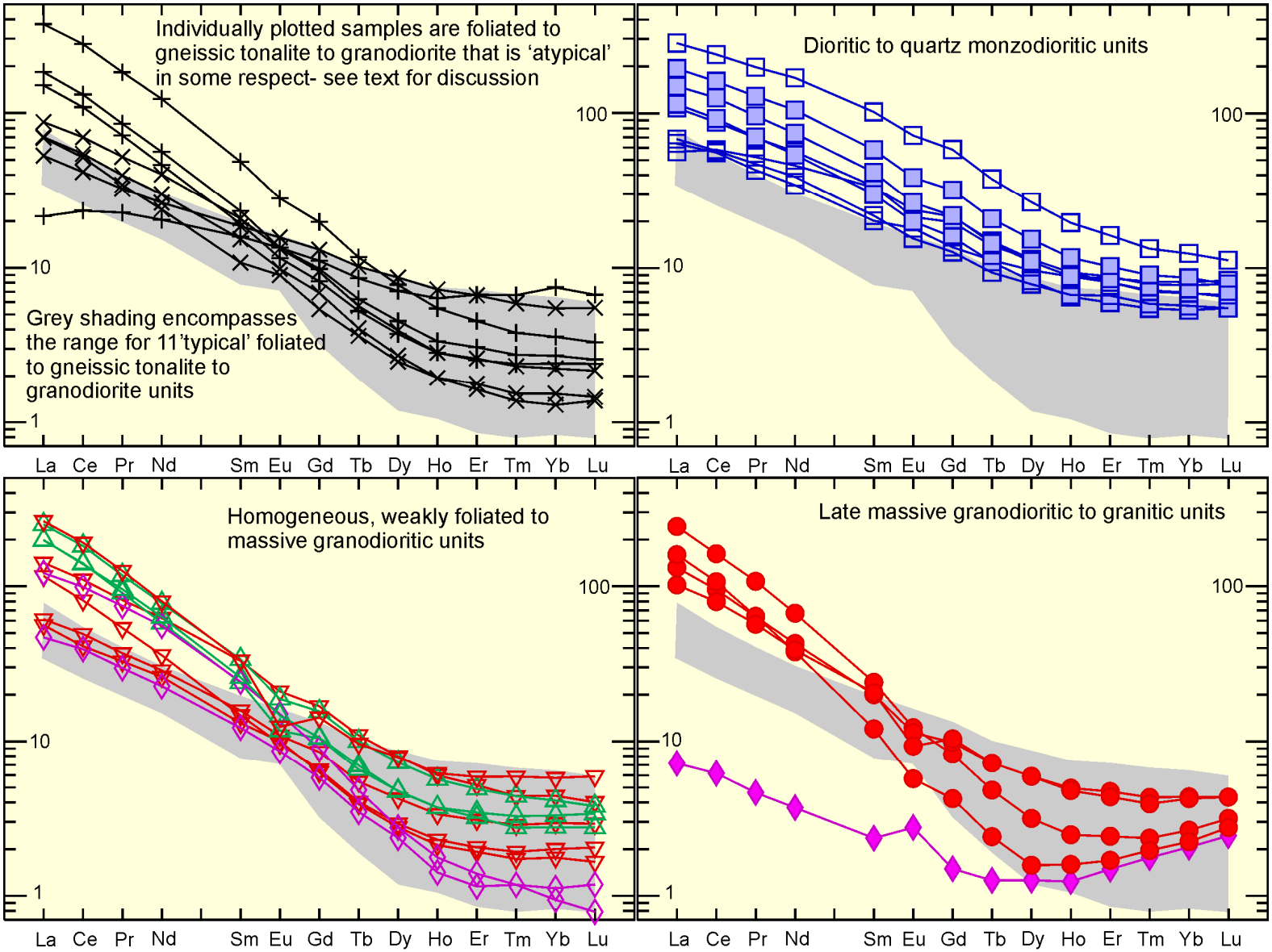

Figure 11. Chondrite normalized REE plots for samples from the Kenogamissi Batholith. Grey shaded area in upper left diagram is reproduced in all other diagrams to facilitate comparison. Normalization values from Sun and McDonough (1989). Symbols same as for Figure 8.

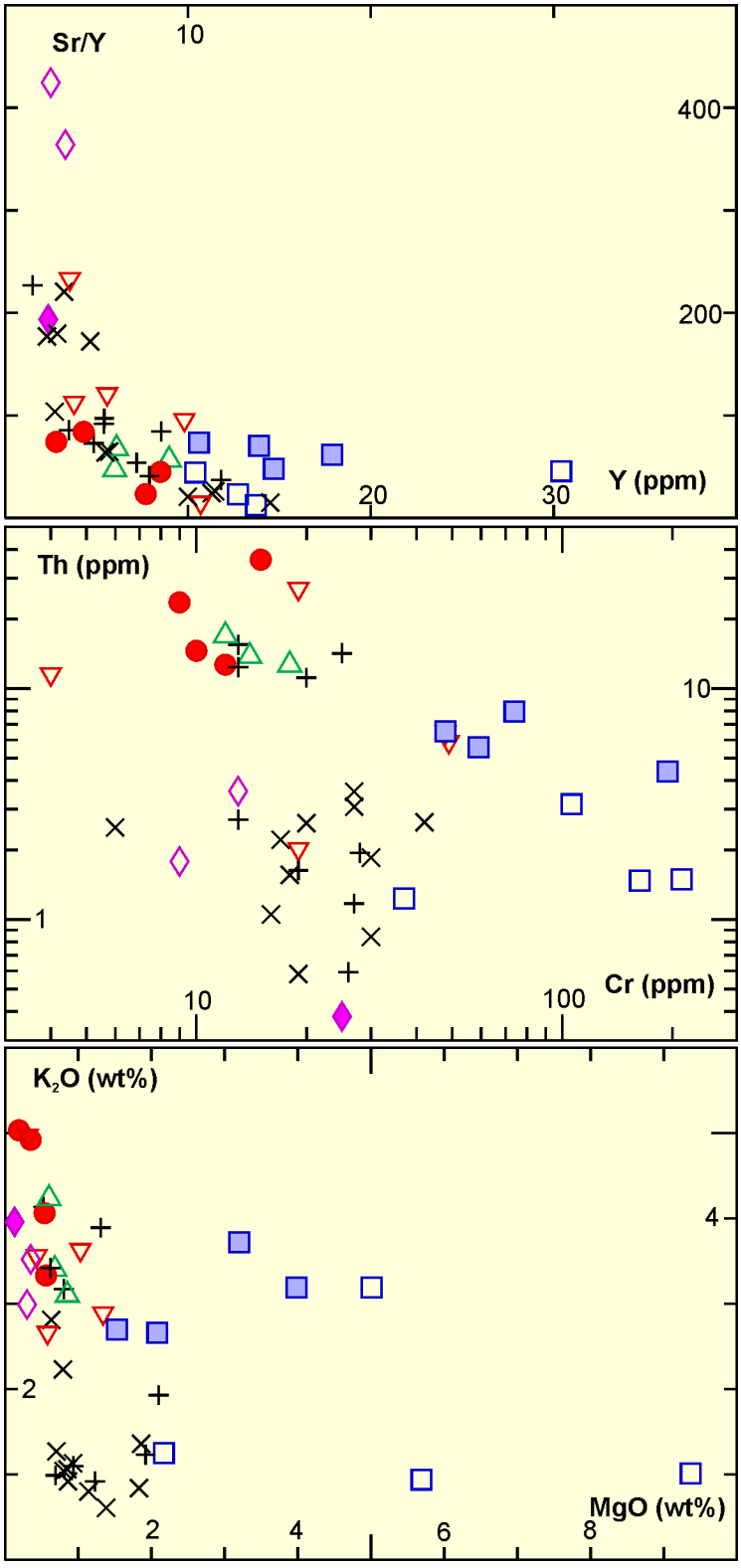

Figure 12. Sr/Y vs Y, Th vs Cr and K_2O vs MgO for samples from the Kenogamissi Batholith. Symbols same as for Figure 8.

The volumetrically predominant foliated to gneissic tonalite to granodiorite units are broadly similar to comparable units occurring in the Round Lake batholith. The majority of samples from this group are high-Al TTG characterized by relatively high abundances of Al_2O_3, Na_2O and Sr, low abundances of LILE (*see* Figure 8), moderately fractionated REE with low HREE (1 to 5 times chondrite) and negligible to slightly positive Eu/Eu*. A minority of samples from this group, though broadly similar, differ in certain respects from the "typical" high-Al TTG either by virtue of somewhat elevated LILE (samples 7272, 7273A, 7276A, 7455, 7459, 7665) or very weakly fractionated REE (sample 7680) (*see* Figures 10 and 11).

A number of massive to weakly foliated granodioritic units could not be unambiguously assigned to either the pretectonic or syntectonic to late-tectonic groupings on the basis of field relationships and are therefore considered separately. Three samples (7461, 7462 and 7677) characterized by a weakly developed, probably tectonic, fabric are similar in most respects to the LILE-enriched, "atypical" moderately to well-foliated units discussed above. Massive granodiorites display a range of characteristics, with only sample 7456 being generally comparable to the weakly foliated granodiorites discussed above. Three samples (7269, 7275 and 7336) are characterized by dual primitive (high Mg# and Cr abundance) and evolved (elevated LILE abundances) characteristics as well as high abundances of Ba and Sr. These samples, though having higher SiO_2 abundances, have many geochemical similarities to the dioritic units discussed below. Sample 7686 is interpreted to have affinity with the nearby Somme granite (discussed below) based on distinctive, shared geochemical characteristics including low Mg#, elevated LILE abundances, low Al_2O_3, CaO and Sr abundances, low Na/K and negative Eu/Eu*. Two samples from a massive granodiorite unit along the eastern contact of the batholith in Beemer Township share many of the geochemical characteristics of the LILE-enriched, "atypical" well-foliated granodiorites.

Dioritic to quartz monzodioritic units (including the Neville pluton) have lower SiO_2 and higher FeO^{total} than other components of the Kenogamissi Batholith, reflecting their more quartz-poor and more mafic character. A striking characteristic of all samples, with the exception of 7679, is elevated Mg# and Cr abundance, suggesting an overall primitive character. Many of the samples also have high abundances of LILE as well as Sr, Ba and REE^{total}. These rocks tend to be relatively enriched in alkali elements given their overall composition, with a few of the samples actually plotting as alkaline on the total alkalies vs SiO_2 plot (*see* Figure 9).

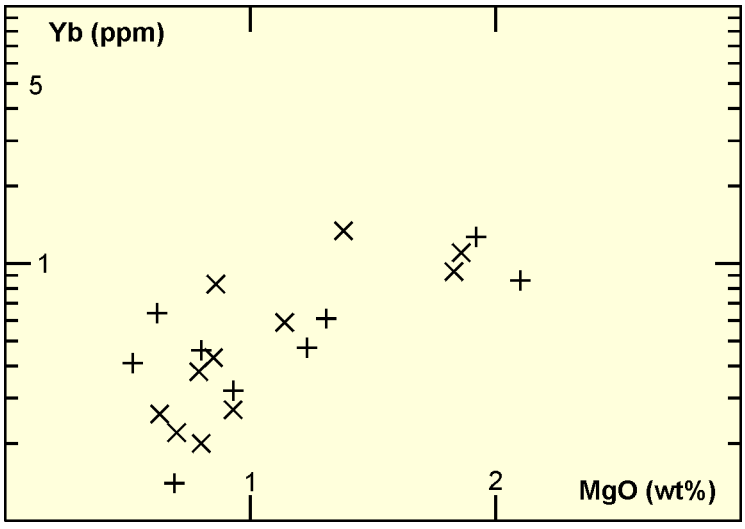

Figure 13. Yb vs MgO for foliated to gneissic tonalite to granodiorite samples from the Kenogamissi Batholith. Symbols same as for Figure 8.

The Somme granite (as well as sample 7686 discussed above) are distinct from all other major units within the Kenogamissi Batholith. Noteworthy characteristics include low abundance of CaO, Al_2O_3, Sr and Cr, high abundance of LILE, low Mg# and Na/K as well as pronounced negative Eu/Eu*. A single late granitic dike displays similar major element characteristics but has unusual abundance of certain trace elements. For example, Th is extremely low in abundance and REE are neither abundant nor strongly fractionated and display a positive Eu anomaly.

PETROGENESIS

The petrologic and geochemical characteristics discussed above are interpreted to reflect the operation and involvement of at least 3 distinct petrogenetic processes in the generation of the various components of the Kenogamissi Batholith.

The volumetrically dominant, well- to weakly foliated, locally gneissic tonalite to granodiorite units are interpreted to be high-Al TTG derived by partial melting of mafic crust at lower crustal to upper mantle depths. The range observed in HREE depletion (~1 to 10 times chondrite) and Al_2O_3, CaO, Sr and Eu/Eu* suggests considerable variation in the proportions of garnet and plagioclase in the residue. This is interpreted to indicate that melting may have occurred at a variety of depths with residual assemblages ranging from hornblende- and/or garnet-bearing mafic granulite to eclogite. The atypical high LILE abundances observed in some samples are interpreted to originate either by melting of a more complex source that included a minor sedimentary or felsic crustal component or by postcrystallization introduction of LILE. The later possibility is considered to be especially probable in the case of hetherolithic, gneissic units that have widespread, leucogranitic veining on a variety of scales.

A second distinct petrogenetic process is inferred for the dioritic to quartz monzodioritic units that are characterized by high Mg# and compatible trace element abundances, suggesting they are derived from, or extensively equilibrated with, an ultramafic (mantle) source. Elevated abundances of a wide range of LILE and HFSE, including moderately fractionated REE, suggest the mantle source was locally enriched by the introduction of metasomatic fluids or low-degree partial melts as envisaged for the sanukitoid model (Shirey and Hanson 1984).

A third distinct origin is attributed to the late granodiorite to granitic units, exemplified by the Somme granite, which are interpreted to originate by partial melting of pre-existing felsic crust. The very low Mg# and compatible trace element abundances, coupled with the high abundances of LILE, point to the evolved felsic composition of the source. Low abundance of CaO, Al_2O_3 and Sr and negative Eu anomalies further suggest an abundance of plagioclase in the residue. The most probable source is older TTG-type tonalitic crust analogous to that characterizing earlier components of the batholith.

DISCUSSION

The Kenogamissi Batholith was emplaced over a protracted interval spanning much of the development of the Abitibi Subprovince. The early components of the batholith, predominantly high-Al TTG originating by partial melting of mafic crust in the lowermost crust or upper mantle depths, are broadly synvolcanic, with available U/Pb ages ranging from 2747 to 2698 Ma suggesting temporal affinity of different components of the batholith with the Pacaud, Staughton–Roquemaure, Kidd–Munro and Blake River volcanic assemblages. The ages and field relationships indicate that these components of the batholith predate the deformation of the greenstone belt, which they structurally underlie, and were folded and otherwise deformed along with the metavolcanic-dominated greenstone assemblages.

Dioritic to quartz monzodioritic components of the batholith were emplaced at approximately 2680 to 2685 Ma, subsequent to greenstone belt volcanism. Their petrogenesis differs from the earlier components and they are interpreted to have affinity with the sanukitoid suite, being derived largely by partial melting of variously metasomatized mantle. The field relationships, timing and petrogenesis suggests that these components of the Kenogamissi Batholith may be related to discrete, syntectonic plutons intruding the greenstone belt that are discussed below.

The youngest components of the batholith are leucocratic granitic to granodioritic phases that postdate the dioritic phases by approximately 10 Ma. Their geochemical characteristics are interpreted to indicate that they originated by partial melting of pre-existing tonalitic crust comparable to the early phases of the batholith.

Groundhog River Batholith

The Groundhog River batholith defines the western limit of the main Abitibi greenstone belt to the north of the Porcupine–Destor fault. The batholith is very poorly exposed and consequently has not been investigated in detail and remains poorly understood. Most of the work carried out as part of this study pertains to 3 isolated clusters of exposures in the vicinity of Carscallen, Enid and Fortune townships. In addition, a number of possibly related intrusions lying within the greenstone belt and just to the east of the batholith contact in the Kamiskotia area were examined.

Most samples examined are relatively megascopically homogeneous biotite tonalites or, less commonly, granodiorites. Hornblende is present locally in addition to biotite, most notably in the southeastern lobe of the batholith in the vicinity of Carscallen Township. Other primary magmatic mineral phases (magnetite, apatite, titanite and zircon) are common but never conspicuously abundant. Generally, secondary alteration (chloritization of biotite and sericitization of plagioclase feldspar) is minimal, except for some of the external tonalitic units in the Kamiskotia area which are locally intensely carbonatized and chloritized.

Many of the additional components, such as those that contribute to the internal complexity of the Round Lake and Kenogamissi batholiths, were rarely encountered in the Groundhog River batholith, although this may be largely a consequence of limited and unevenly distributed exposure. Dioritic units are present in the southwestern portion of the batholith in the vicinity of Muskego Township (sample 7675). Massive, late granodioritic to granitic plutons were not encountered although minor dike phases are noted in the Enid Township area (samples 7311B and 7312). Complexly deformed, heterogeneous, gneissic tonalite units were not encountered.

The geochemical characteristics (summarized in Table 3 and Figures 14 to 16) of the predominant tonalitic to granodioritic components of the Groundhog River batholith differ in certain respects from similar rock types occurring in the Round Lake and Kenogamissi batholiths. Tonalite from the Carscallen and Enid Township areas are broadly similar to high-Al TTG tonalites from the other batholiths. Noteworthy characteristics include high abundance of Al_2O_3, Na_2O and Sr, low LILE abundances and fractionated REE with near chondritic HREE and negligible Eu anomalies. In contrast, one of the Fortune Township area samples and all of the Kamiskotia area samples are distinctive, with low abundances of Al_2O_3, CaO and Sr, elevated abundance of HFSE, including the HREE, resulting in high, but relatively modestly fractioned REE. These samples are also characterized by prominent negative Eu anomalies and very low compatible element abundances. The geochemical characteristics described above are similar to those described for low-Al TTG (Galley 2003) and F3 felsic volcanics (Lesher et al. 1986), both of which exhibit a close spatial, temporal and probably genetic association with volcanogenic massive sulphide (VMS) mineralization.

Table 3. Whole rock geochemical data for samples from the Groundhog River, Lake Abitibi, Case and Ramsey–Algoma batholiths.

	Groundhog River Batholith															
	Carscallen Tp area						Enid Tp area				Fortune Tp area		Kamiskotia area (external to batholith)			
Sample	7265A	7266	7267	7271	7265B	7268	7311A	7313	7312	7311B	7315	7314	7310	7572	7573	7571
SiO_2	67.35	67.54	67.54	69.91	67.91	69	69.93	68.91	74.09	72.66	71.4	76.03	74.38	76.9	72.66	66.13
Al_2O_3	15.13	15.26	15.48	16.07	15.58	15.2	17.18	16.32	15.6	16.96	16	13.58	13.72	12.5	11.45	14.15
MnO	0.05	0.06	0.06	0.04	0.06	0.02	0.03	0.06	0.01	0.01	0.04	0.03	0.06	0.02	0.04	0.15
FeO	2.33	2.03	1.72	1.71	1.31	1.64	1.43	2	0.31	0.29	1.94	0.96	2.1	0.42	4.46	4.18
Fe_2O_3	1.74	1.88	2.22	1.38	1.52	0.84	0.94	1.34	0.33	0.2	1.01	0.77	1.06	1.28	0.74	1.83
MgO	1.48	1.61	1.65	1.12	1.06	0.94	0.82	1.36	0.15	0.13	0.9	0.3	0.39	0.07	0.64	2.88
CaO	2.79	3.56	3.88	3.43	3.16	2.9	3.47	3.7	1.25	1.97	3.7	1.59	2.09	0.66	0.57	1.32
Na_2O	4.38	4.33	4.24	4.77	3.48	4.73	5.26	4.86	4.94	5.3	4.48	3.82	4.06	3.13	4.33	3.2
K_2O	1.99	1.61	1.76	1.66	2.89	1.89	1.36	1.23	3.96	3.2	1.14	3.23	2.52	4.53	1.11	2.47
TiO_2	0.52	0.49	0.49	0.4	0.36	0.34	0.27	0.41	0.04	0.04	0.33	0.16	0.27	0.09	0.32	0.71
P_2O_5	0.15	0.15	0.15	0.12	0.1	0.1	0.1	0.13	0.02	0.02	0.11	0.04	0.06	0.01	0.02	0.17
LOI	3.24	2.71	1.59	0.7	3.6	3.55	0.46	0.92	0.43	0.28	0.62	0.38	0.75	0.58	3.88	3.19
TOTAL	101.42	101.45	100.98	101.51	101.18	101.32	101.41	101.45	101.17	101.08	101.87	100.98	101.67	100.24	100.73	100.84
Mg#	40	44	44	40	41	41	39	43	31	33	36	24	19	7	18	47
A/CNK	1.05	0.99	0.97	1.01	1.07	1.01	1.05	1.02	1.06	1.08	1.04	1.07	1.04	1.11	1.22	1.37
Li	14	20	18	11	8	12	34	38	4	9	28	23	16	9	2	18
Cs	1.448	1.895	1.361	1.289	3.078	2.424	1.212	1.686	0.75	0.446	0.935	1.15	1.298	1.06	0.25	0.35
Rb	56	41	46	43	103	58	43	41	84	47	31	92	63	75	23	55
Sr	335	548	373	335	138	261	422	432	479	698	244	101	102	61	21	52
Ba	482	384	438	383	311	374	384	373	1179	1105	290	469	600	1581	95	475
Nb	6.6	5.7	6.1	4.3	3.5	3.6	2.8	4.6	1.4	0.6	4.4	5.2	17.2	3.6	32.5	10.9
Zr	157.1	140.3	152	127.2	120.8	129.2	133.6	133.4	57.6	49.9	185.5	160.8	235	120	668	242
Hf	4.1	3.7	4	3.3	3.2	3.4	3.4	3.4	2.1	1.9	4.5	4.8	7.6	3.7	19.2	6.3
Th	4.76	4.23	4.44	3.37	2.94	2.66	1.6	3.25	1.16	0.63	2.87	7.85	6.46	10.7	9.16	4.58
U	0.703	0.895	0.962	0.595	0.798	0.757	0.463	0.615	0.695	0.366	0.224	0.855	1.708	0.84	2.474	1.002
Cr	34	47	44	34	22	27	18	30	13	13	22	2	10	4	2	5
Y	15.21	11.47	9.8	6.14	4.92	4.63	3.32	7.08	2.96	1.35	4.82	15.67	79.62	13.57	155	30.54
La	38.5	28.06	32.96	19.44	16.42	15.94	7.31	25.7	7.21	4.51	19.91	42.69	44.22	57.99	54.39	27.49
Ce	81.55	60.12	66.02	38.95	32.88	31.66	17.72	50.38	13.88	8.17	36.8	86.91	100.46	126.26	129.26	61.64
Pr	9.2	7.03	7.13	4.36	3.74	3.47	1.73	5.59	1.55	0.9	3.9	10.07	12.51	13.845	17.402	7.659
Nd	33.32	25.74	25.11	15.89	13.33	12.27	6.51	20.1	5.93	3.34	13.97	36.02	50.49	49.28	76.12	31.04
Sm	5.17	4.17	3.67	2.58	2.18	2.08	1.34	3.2	0.99	0.56	2.18	6.21	11.03	8.09	19.68	6.54
Eu	1.18	1.05	0.86	0.67	0.53	0.59	0.45	0.86	0.32	0.28	0.63	0.76	1.66	1.04	3.44	1.4
Gd	3.616	2.952	2.527	1.76	1.474	1.451	1.093	2.204	0.711	0.397	1.555	4.584	11.689	5.3	22.75	6.22
Tb	0.501	0.391	0.338	0.229	0.183	0.184	0.15	0.273	0.091	0.046	0.194	0.588	1.978	0.612	4.116	0.969
Dy	2.86	2.196	1.922	1.223	0.987	0.956	0.761	1.432	0.49	0.244	1.026	3.133	13.278	3.01	27.9	5.94
Ho	0.56	0.42	0.36	0.22	0.18	0.17	0.13	0.26	0.09	0.05	0.18	0.57	2.86	0.53	6.04	1.21
Er	1.575	1.187	1.014	0.598	0.487	0.457	0.342	0.687	0.285	0.132	0.475	1.563	8.817	1.49	18.85	3.47
Tm	0.229	0.169	0.147	0.083	0.071	0.065	0.046	0.091	0.045	0.019	0.063	0.207	1.339	0.223	2.849	0.519
Yb	1.52	1.14	0.98	0.57	0.46	0.42	0.28	0.62	0.32	0.14	0.4	1.29	9.04	1.58	18.76	3.46
Lu	0.221	0.169	0.141	0.084	0.069	0.062	0.041	0.087	0.05	0.022	0.059	0.187	1.381	0.255	2.883	0.533
Eu/Eu*	0.79	0.87	0.82	0.91	0.86	0.98	1.09	0.94	1.09	1.71	0.99	0.42	0.44	0.46	0.5	0.66
CeN/YbN	15	15	19	19	20	21	18	23	12	16	26	19	3	22	2	5

Table 3. (continued)

	Groundhog River Batholith		Lake Abitibi batholith		Case batholith			Ramsey-Algoma batholith
	Muskego Tp area							
Sample	7675	7676	7516	7515	7520	7521	7522	7560
SiO_2	56.07	70.81	70.88	67.18	71.96	72.59	73.45	70.41
Al_2O_3	15.49	16.23	16.67	16.9	14.98	16.28	15.11	16.72
MnO	0.12	0.03	0.02	0.08	0.02	0.02	0.02	0.03
FeO	5.15	0.83	1.03	2.26	0.41	0.94	1.05	1.31
Fe_2O_3	2.21	0.48	0.74	1.11	0.8	0.2	0.07	1.1
MgO	5.39	0.54	0.78	1.35	0.31	0.34	0.27	0.94
CaO	6.36	2.77	2.73	3.6	1.2	1.53	1.1	3.17
Na_2O	4.07	5.49	5.68	4.66	4.39	5.1	3.84	5.19
K_2O	1.32	2.09	1.74	1.65	4.68	3.49	5.11	1.38
TiO_2	1.04	0.15	0.25	0.39	0.2	0.16	0.13	0.32
P_2O_5	0.26	0.05	0.08	0.11	0.07	0.06	0.05	0.1
LOI	1.57	0.3	0.58	1.61	0.39	0.64	0.51	0.59
TOTAL	99.61	99.86	101.3	101.15	99.46	101.44	100.84	101.4
Mg#	57	43	45	42	33	35	30	42
A/CNK	0.79	0.99	1.03	1.06	1.04	1.09	1.09	1.06
Li	16.9	27.1	27	28	122	13	36	26
Cs	1.071	1	1.36	0.7	12	0.36	3.6	0.79
Rb	49	56	38	44	199	52	236	42
Sr	481	402	708	433	296	737	145	376
Ba	249	613	630	436	696	1069	518	378
Nb	6.43	3.48	2.2	5.7	5.4	2.2	11.9	2.6
Zr	100	77	87	93	145	83	132	123
Hf	2.9	2.44	2.8	2	4.4	2.7	4.5	3.5
Th	1.57	1.3	2.77	1.69	18.62	3.33	28.14	2.35
U	0.54	0.45	0.635	0.743	2.553	0.542	2.783	0.277
Cr	180	20	15	20	14	11	6	2
Y	14.8	7.9	4.3	7.54	2.53	4.55	10.6	1.87
La	22	6.7	14.91	11.04	38.13	16.36	51.34	13.78
Ce	52.1	13.8	32.55	23.55	72.16	33.82	99.71	26.09
Pr	6.95	1.77	3.978	2.88	6.889	3.534	10.299	2.586
Nd	29.92	7.14	15.76	11.67	21.76	12.6	34.05	8.83
Sm	6.12	1.53	2.76	2.38	2.79	1.98	5.13	1.34
Eu	1.74	0.41	0.72	0.67	0.64	0.52	0.58	0.49
Gd	4.7	1.45	1.85	2	1.36	1.28	2.98	0.85
Tb	0.6	0.22	0.212	0.282	0.138	0.159	0.371	0.092
Dy	3.2	1.4	1.02	1.55	0.6	0.83	1.97	0.44
Ho	0.57	0.26	0.17	0.28	0.09	0.15	0.36	0.07
Er	1.49	0.8	0.42	0.79	0.22	0.4	1.05	0.18
Tm	0.2	0.12	0.055	0.112	0.03	0.056	0.161	0.025
Yb	1.24	0.85	0.34	0.73	0.19	0.35	1.1	0.15
Lu	0.18	0.13	0.045	0.103	0.028	0.05	0.169	0.025
Eu/Eu*	0.95	0.83	0.91	0.91	0.88	0.94	0.42	1.3
CeN/YbN	12	4	27	9	105	27	25	48

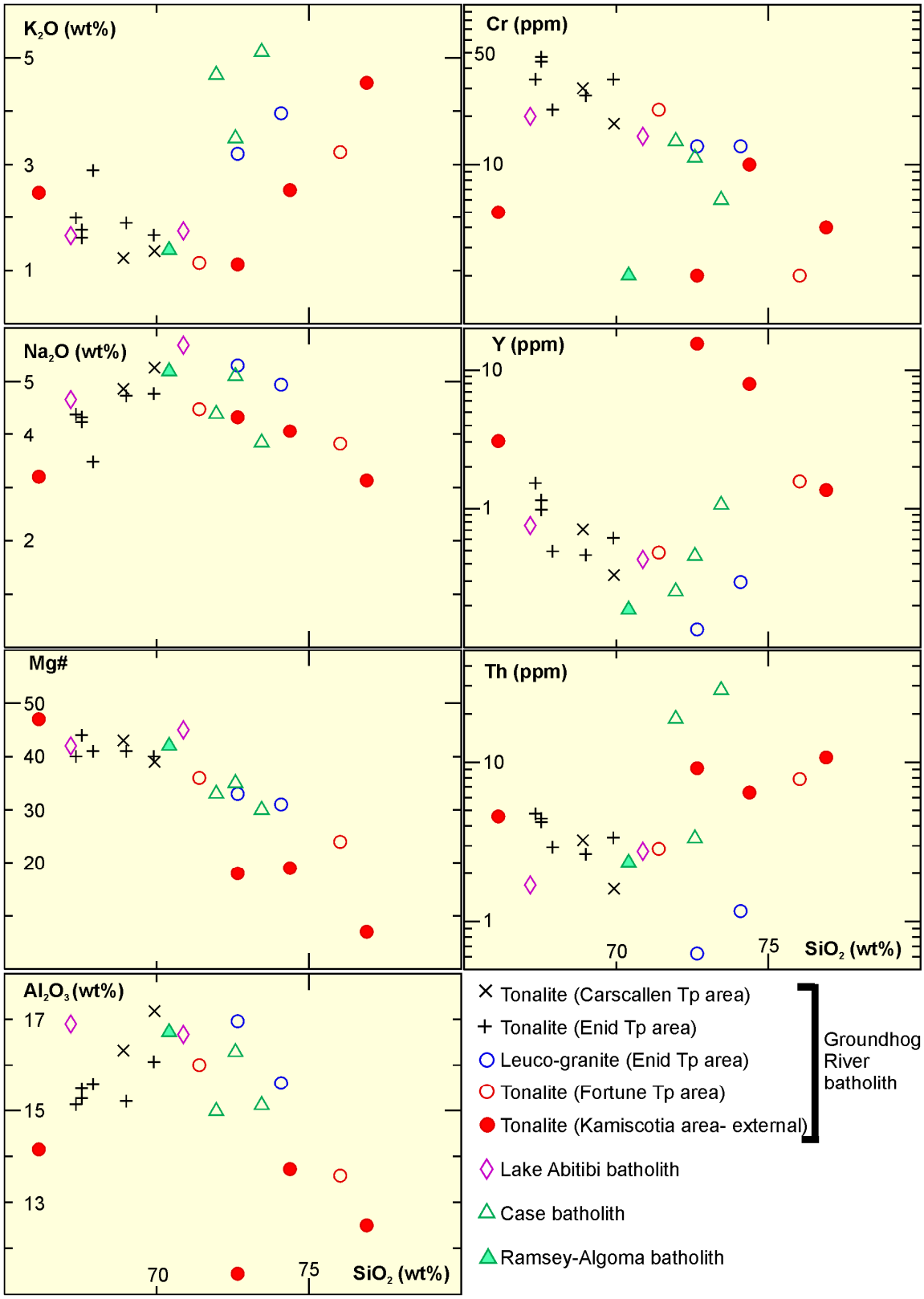

Figure 14. Harker variation diagrams for samples from the Groundhog River, Lake Abitibi, Case and Ramsey–Algoma batholiths.

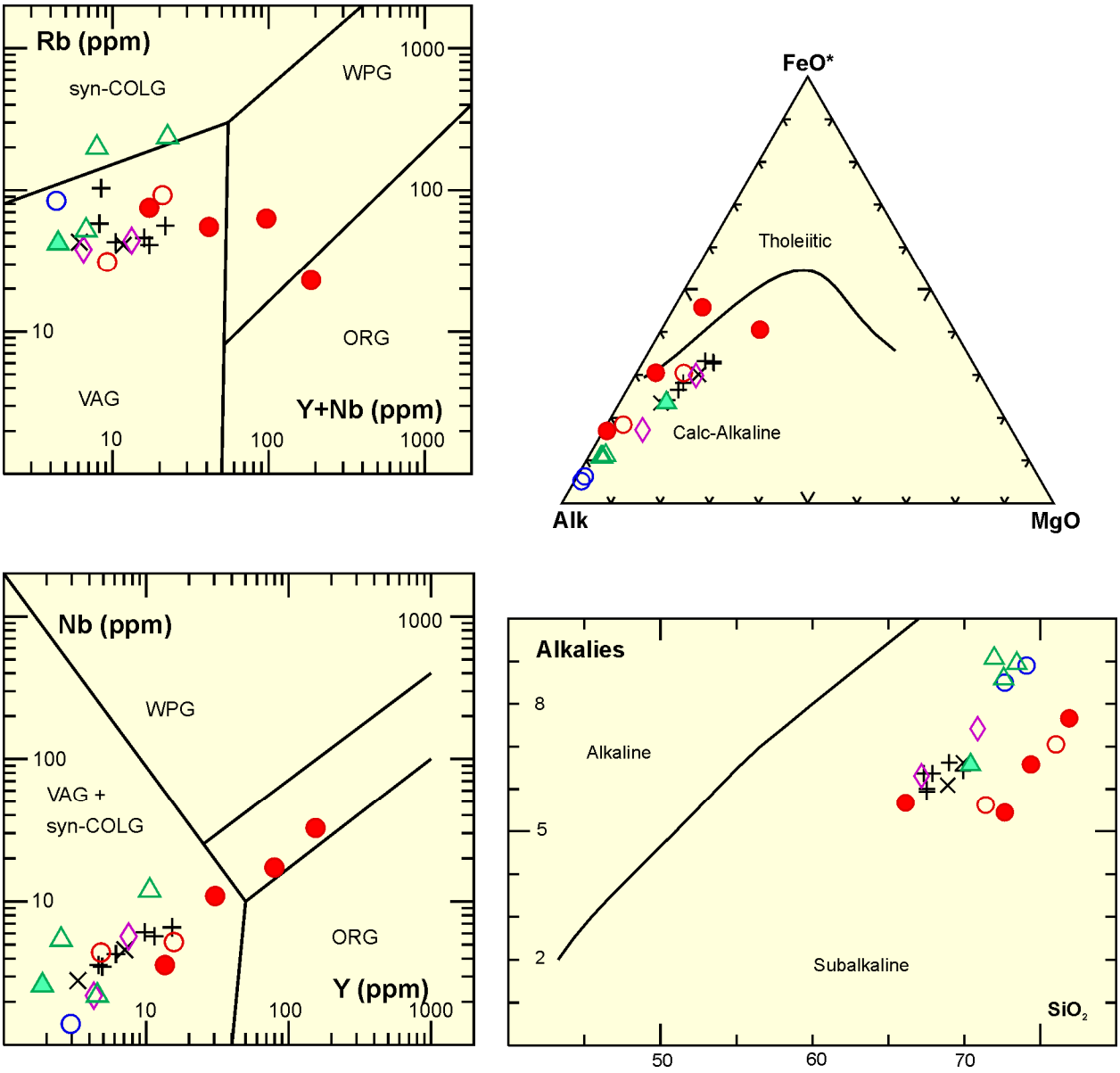

Figure 15. Tectonic discrimination diagrams for samples from the Groundhog River, Lake Abitibi, Case and Ramsey–Algoma batholiths. Rb vs Y+Nb and Nb vs Y plots are after Pearce et al. (1984). AFM and alkalies vs SiO2 plots are after Irvine and Baragar (1971). Symbols same as for Figure 14; abbreviations, Figure 4.

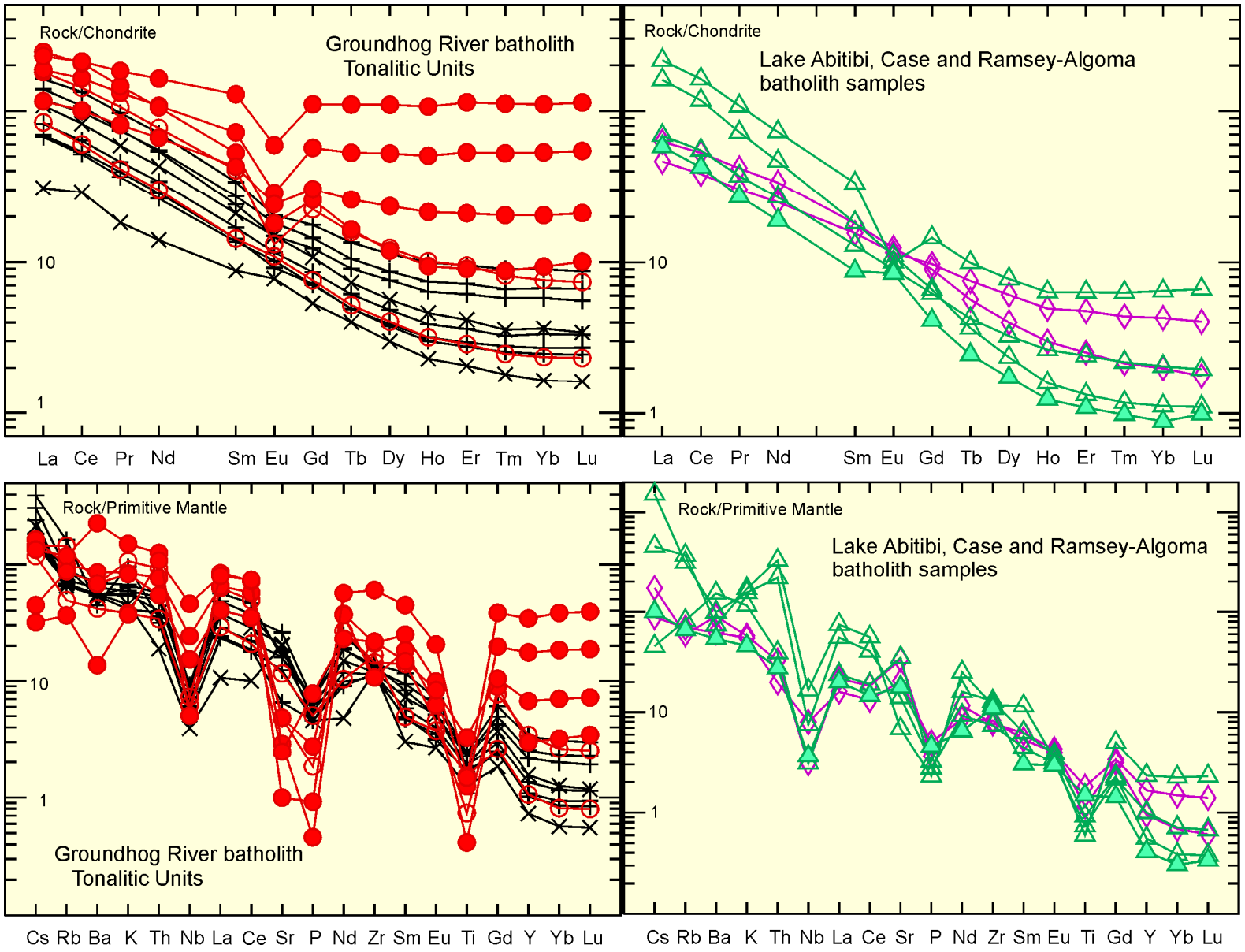

Figure 16. Chondrite and primitive mantle normalized trace element plots for samples from the Groundhog River, Lake Abitibi, Case and Ramsey–Algoma batholiths. Symbols same as for Figure 14.

The bulk composition of both high- and low-Al TTG from the Groundhog River batholith is consistent with derivation by melting of a mafic protolith; however, the distinct differences in Al_2O_3, CaO, Sr and HFSE abundances and Eu/Eu* between the 2 groups are interpreted to indicate melting at a range of pressures. As discussed in previous sections, the fractionated REE with low HREE abundances characterizing the high-Al TTG are attributed to the presence of significant garnet in the residue whereas the high Al_2O_3, CaO and Sr abundances point to low abundance of plagioclase in the residue. In the most extreme (still relatively widespread) cases, positive Eu anomalies and very high Sr/Y are thought to be a signature of melting below the plagioclase stability field with eclogitic residues. In either case (mafic garnet granulite or eclogite residue), these constraints suggest that melting occurred at considerable depth, either near the base of the crust or within the upper mantle. In contrast, the geochemical characteristics of the low-Al TTG suggest that the residue did not contain garnet (unfractionated REE with abundant HREE) or rutile (abundant HFSE) and plagioclase was a significant residual component (low Al_2O_3, CaO and Sr with prominent negative Eu anomalies). Production of a tonalitic melt with these characteristics is interpreted to be a consequence of melting of a mafic protolith at comparatively shallow crustal levels (upper to midcrust) in a high heat flow regime. It is not clear whether these contrasting melting regimes were operating synchronously or successively although it is worthy of note that the Kidd–Munro assemblage contains both calc-alkalic (F1-type felsic components broadly similar to high-Al TTG) and tholeiitic (F3-type felsic components broadly similar to low-Al TTG) volcanic rocks that are similar in age (Berger et al. 2009). Further geochronological investigation of the plutonic rocks would be required to further evaluate this question.

Lake Abitibi Batholith

The Lake Abitibi batholith straddles the Ontario–Quebec provincial border on the north shore of Lake Abitibi. The batholith is not well exposed and was only briefly investigated. A number of earlier investigations (Smith and Sutcliffe 1988; Sutcliffe et al. 1990, 1993) concluded that the batholith is a composite intrusion consisting of earlier, foliated tonalite to granodiorite intruded by later, more massive plutons ranging in composition from diorite to granodiorite. Both samples analyzed for this study (*see* Table 3 and Figures 14 to 16) and most of the analyses reported by Sutcliffe et al. (1990) have characteristics (e.g., high Al_2O_3, CaO and Na_2O, low LILE and compatible trace element abundances, intermediate Mg#'s) typical of high-Al TTG occurring in the Round Lake and Kenogamissi batholiths. One sample (88-37) reported by Sutcliffe et al. (1990) has elevated Mg# and compatible trace element abundances suggesting similarities to dioritic units in the Kenogamissi Batholith.

Two U/Pb zircon ages are reported from the Quebec portion of the batholith (Mortensen 1993). The age of a foliated tonalite (2694.8 ± 1.7 Ma) is just within error of the youngest Blake River assemblage volcanism whereas a megacrystic granodiorite (2689.8 ± 1.2 Ma) representative of one of the youngest phases within the batholith postdates widespread volcanic-dominated assemblages but is similar in age to the Krist volcanics occurring at the base of the Porcupine assemblage.

SUMMARY

Large batholiths bounding the greenstone belt are composite intrusive complexes that structurally underlie the supracrustal rocks. The batholiths are dominated by weakly to well-foliated, locally gneissic, tonalite and granodiorite that was emplaced synchronously with volcanism. These units may be complexly deformed and are interpreted to have been folded along with the overlying greenstone belt. These units are dominantly of high-Al TTG geochemical affinity and are interpreted to originate by partial melting of basaltic crust at lowermost crustal to upper mantle depths. A range of processes, including mantle

interaction, source heterogeneity, crustal interaction and postcrystallization melt and/or fluid introduction, contribute to geochemical diversity within the suite. Low-Al TTG produced by shallower (middle to upper crustal) melting of mafic crust is only known to be present within the Groundhog River batholith.

Several varieties of later, more massive plutons intrude the foliated to gneissic tonalite to granodiorite. Dioritic to quartz monzodioritic plutons crosscut deformational fabrics within the foliated tonalite to granodiorite and, in most cases (exception discussed in subsequent section), have very weak or no superimposed tectonic fabric. The U/Pb age of several such intrusions in the Kenogamissi Batholith (~2680–2685 Ma) is comparable to that of petrologically similar syntectonic plutons occurring within the greenstone belt. These units have geochemical characteristics consistent with derivation from, or extensive interaction with, a variously metasomatized ultramafic (mantle) source and are interpreted to have a sanukitoid geochemical affinity.

Massive granodioritic to granitic plutons are the youngest major constituent of some of the batholiths but their overall abundance is relatively low. The massive character, crosscutting relationships with deformational fabrics in other units and young U/Pb ages (~2675 Ma) suggest the unit is late to posttectonic. These granodioritic to granitic units are interpreted, based on geochemical characteristics, to be products of partial melting of older tonalitic crust similar to the early phases of the batholith.

The petrologic diversity, internal complexity and protracted development of these batholithic complexes reflect and temporally span the evolutionary development of the Abitibi Subprovince. Much of the crust developed between 2750 and 2695 Ma and is distinctly bimodal (basalt – TTG). Although the TTG component is volumetrically predominant in the crust today, only a small proportion (unlikely to be representative) of the mafic crust generated during this interval is preserved within the greenstone belt. This interval of crust formation was followed by regional deformation coupled with a change in the character of magma petrogenesis from TTG-type to sanukitoid and finally intracrustal melting at the latest stage of geodynamic development of the Abitibi Subprovince.

Early Syntectonic Porphyries

High-level quartz ± feldspar porphyries are widespread; however, they are particularly abundant along the Porcupine–Destor fault and especially in the vicinity of Timmins, where they have been extensively investigated because of their strong spatial association with gold mineralization. The characteristics of porphyries associated with the Porcupine–Destor fault have been described by McDonald et al. (2005) to which the reader is referred for more detail. This discussion will focus on investigations of the porphyries in the Timmins area (central and northern trends of McDonald et al. 2005), offer general comparisons with porphyries associated with the Porcupine–Destor fault elsewhere along its length and more regionally within the rest of the main Abitibi greenstone belt and consider the significance of these units for gold mineralization. In a subsequent section, the significance of these units within the magmatic and tectonometamorphic evolution of the Abitibi Subprovince will be considered.

CHARACTERISTICS OF INDIVIDUAL PORPHYRY CLUSTERS

Timmins Area Porphyries

Numerous felsic quartz ± feldspar porphyries occur in the general Timmins area and have been the subject of numerous investigations because of their close spatial association with gold mineralization.

Table 4. Characteristics of selected units associated with early syntectonic magmatism.

	Porphyry Unit	U-Pb age	Relationships and Interpretation
Timmins area			
	Krist Volcanics	2687.5 ± 1.3 Ma[1]	Heterolithic intermediate to felsic lapiili-tuff to tuff-breccia
	Paymaster	2690 ± 2 Ma[2]	Massive to flow-banded and locally autobrecciated quartz-plagioclase porphyry—endogenous dome
	Pearl Lake	2689 ± 1 Ma[2]	Intensely altered and tectonized quartz-plagioclase porphyry
	West		Altered plagioclase-quartz porphyry
	Edwards		Massive quartz-plagioclase porphyry with local mafic "fragments"
	Crown	2688 ± 2 Ma[2]	Massive plagioclase-quartz porphyry—near surface intrusion, possible local fragmental facies
West of Timmins			
	Bristol Lake	2687.7 ± 1.4 Ma[3]	Massive to locally brecciated plagioclase-quartz porphyry—volcanic vs intrusive origin uncertain
Kirkland Lake area			
	Bidgood	2685 ± 3 Ma[4]	Intensely deformed and altered, massive quartz porphyry intrusion
South of Round Lake batholith			
	Britcanna	not available	Massive quartz porphyry intrusion
Blake River syncline			
	Clifford stock	2686.9 ± 1.2 Ma[5]	Medium-grained, equigranular tonalite to granodiorite
	Clarice stock	2689 ± 1 Ma[6]	Medium-grained, equigranular tonalite to quartz diorite

References: 1 – Ayer, Ketchum and Trowell 2002; 2 – Corfu et al. 1989; 3 – Ayer et al. 2003; 4 – Corfu et al. 1991; 5 – MacDonald et al. 2005, 6 – Corfu and Noble 1992.

The most recent summary of this work is that of MacDonald et al. (2005), to which the reader is referred for a more detailed discussion of these units and references to earlier work. Controversies associated with these units have historically included i) whether the units are intrusive versus extrusive, ii) timing relationships with respect to stratigraphy (and especially the Porcupine and Timiskaming assemblages) and iii) the significance of the spatial association between gold and porphyry intrusions, with some workers (e.g., Mason and Melnik 1986) suggesting gold was introduced by magmatic hydrothermal fluids derived from the porphyry magmatic systems and others (e.g., Burrows and Spooner 1989) arguing that gold mineralization significantly postdates the porphyries that served as sites favourable for the development of structures that focused subsequent fluid flow.

Individual porphyries within the Timmins camp that have been examined as part of this study include those exhibiting a general spatial association with large mineralizing systems (Paymaster, West and Edwards porphyries near the Dome Mine and Pearl Lake and Crown porphyries near the Hollinger–McIntire Mine) as well as others occurring more distally from the major deposits but still often associated with mineralization. Characteristics of some of the porphyry units examined within this investigation are summarized in Table 4.

FIELD RELATIONSHIPS

Timmins area porphyries occur primarily within the Tisdale assemblage metavolcanic rocks, which have U/Pb zircon ages in the range 2703 to 2710 Ma (Ayer et al. 2002). The major porphyries are not observed to crosscut Porcupine assemblage metasedimentary rocks but have been interpreted to be genetically related to the basal Krist Formation volcaniclastic rocks of the Porcupine assemblage (Hurst 1936; Pyke 1982). Pyke (1982) further suggested that, although the porphyries may be dominantly shallow-level subvolcanic intrusions, portions of some of the porphyries may represent extrusive rhyolitic domes. Initial U/Pb age determinations initially cast doubt on this correlation (Corfu et al. 1989); however, the age for the Krist Formation metavolcanic rocks was subsequently revised downwards to ages comparable to those characterizing the porphyries (Ayer, Ketchum and Trowell 2002) and is permissive of a genetic link between porphyries and Krist volcanism. The major porphyry units are interpreted to be older than Timiskaming sedimentation based on possible local unconformable relationships and the presence of porphyry fragments in Timiskaming conglomerates as well as U/Pb age determinations that constrain the Timiskaming to being younger than 2679 ± 3 Ma (Corfu et al. 1991), whereas the major porphyry units cluster in the range 2687 to 2690 Ma (MacDonald 2010 and references therein).

Porphyries in the Timmins camp exhibit a wide range in the intensity of development of both deformation and secondary alteration, both of which may obscure field relationships. Where alteration is less intense and late deformation has not intensely overprinted earlier deformational fabrics, the porphyries are interpreted to have a relatively early deformational fabric defined by near-peak metamorphic minerals. A locally present angular unconformity at the base of the Porcupine assemblage (Bateman et al. 2005) suggests that if the porphyries are genetically related to the Krist volcanics, there may be a component of regional deformation that precedes their emplacement.

Many of the major porphyries are lenticular units with their long axes subparallel to stratigraphy in map view and, in many cases, contacts between massive porphyry and volcanic rocks are sharp and relationships are permissive of either intrusive or stratigraphic relationships. However, detailed surface and subsurface mapping (Ferguson 1968) indicates that, in detail, the porphyries at least locally cut stratigraphy and hence are, at least partly, intrusive in character. Locally, however, contacts are characterized by the presence of fragmental textures and structures that may be more consistent with emplacement of the porphyry units at or very near the paleosurface (Figure 17). One such example occurs at the contact between the Paymaster porphyry and mafic metavolcanic rocks near the western termination of the porphyry. At this location, flow banding in the porphyry becomes increasingly prominent near the contact. The contact zone itself consists of a thin (locally up to 5 m) heterolithic zone in which the matrix varies irregularly between being quartzofeldspathic or chloritic and contains clasts of both flow-banded to massive quartz feldspar porphyry and mafic volcanic. The origin of the compositional variation within the matrix of the contact fragmental unit is unclear; it could represent local dominance of matrix sourced from either the porphyry or mafic volcanic unit or it could represent alteration. The sharp truncation of flow banding at the contact and fragment edges indicates that the fragmentation postdates crystallization of the flow-banded porphyry (*see* Figure 17). These relationships are difficult to reconcile with an intrusive contact and are interpreted to have developed as a depositional contact on the paleosurface suggesting that the porphyry at this location is a felsic flow or dome. The depositional environment is not well understood; however, one possible interpretation is that a decrepitating, flow-banded felsic flow or endogenous dome advanced against a fragmented (talus) mafic volcanic rock, with the contact marked by a mixture of matrix and fragments derived from both the pre-existing mafic volcanic and advancing flow. Other examples of fragmental textures possibly indicative of emplacement at or near the paleosurface were noted in association with the Crown and Edwards porphyries (Figure 17e and f).

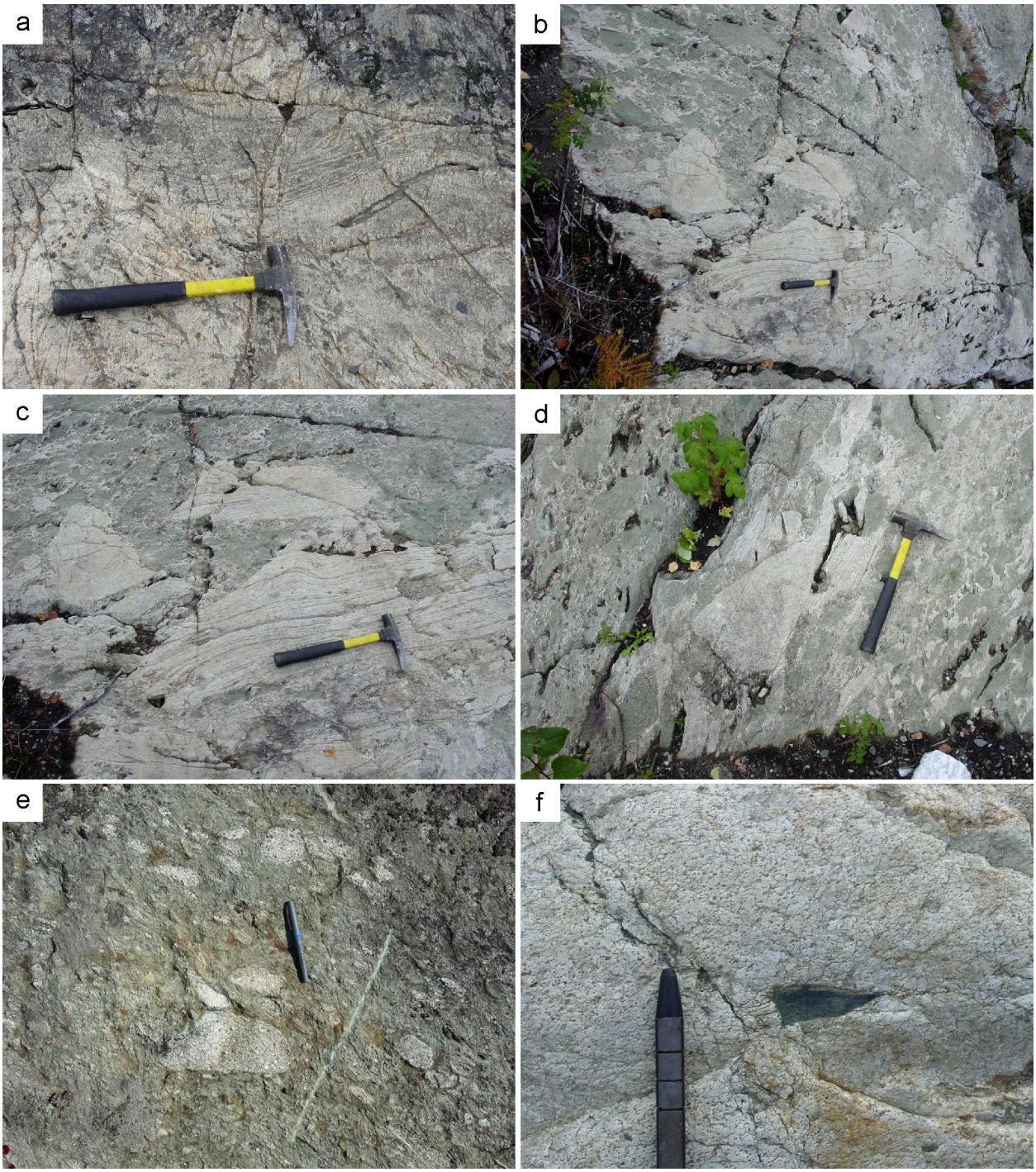

Figure 17. Field characteristics of Timmins area porphyries: a) massive (beneath hammer), flow-banded and brecciated portions of the Paymaster porphyry; b) flow-banded Paymaster porphyry contact with unit characterized by chloritic, mafic matrix containing fragments of porphyry; c) detail of photo b; d) "mixing" of massive to flow-banded Paymaster porphyry with chloritic, mafic unit; e) quartz-plagioclase porphyry fragments within quartz-plagioclase phenoclast-bearing intermediate to felsic matrix near Crown porphyry contact; f) angular mafic fragment within relatively massive Edwards porphyry.

It is concluded, on the basis of the observations and interpretations discussed above, that the Timmins area porphyries are extremely high-level intrusions that locally reached the paleosurface to form endogenous domes or erupt as pyroclastic deposits. The Krist volcanics are a larger scale manifestation of this process.

PETROLOGY

The Timmins area porphyries have fairly consistent mineralogy and porphyritic textures where they have not been modified by secondary alteration and deformation processes. Plagioclase and quartz phenocrysts generally make up 25 to 60% of the rock and are surrounded by a fine-grained quartzofeldspathic matrix. Plagioclase is generally more abundant than quartz (often 2:1 to 4:1); however, the greater susceptibility of feldspar to alteration commonly obscures primary phenocryst proportions. Quartz phenocrysts rarely preserve euhedral crystal outlines, with most phenocrysts being rounded and, in some cases, embayed suggesting they were not in equilibrium with the melt in the final stages of crystallization. Plagioclase phenocrysts are generally subhedral and are partially to completely replaced by white mica along with variable amounts of carbonate and epidote. Chlorite is generally the main mafic mineral present but is rarely present in amounts greater than 5%. In some cases, chlorite forms pseudohexagonal plates suggesting it is replacing biotite; however, the origin of the biotite (primary or metamorphic) is unclear and the primary magmatic mafic mineralogy is uncertain.

Secondary white mica is the most widespread alteration mineral, being present to some degree in all samples, and intense alteration locally produces quartz eye schists within which everything, with the exception of quartz phenocrysts, is replaced by white mica. Carbonate replacement and veining is widespread and locally intense. As described above, primary mafic mineralogy is replaced by chlorite. Other secondary minerals present locally include sulphides, tourmaline and green mica. Mineralization is generally associated either with structurally controlled veins that cut the porphyries or with disseminated sulphides interpreted to be of secondary origin.

GEOCHEMISTRY

The geochemical characteristics of the Timmins area porphyries have been extensively modified by secondary alteration processes as discussed in more detail by McDonald (2010). Modification of major elements is particularly striking for some of the porphyries most closely associated with mineralization (e.g., Pearl Lake and Paymaster) that are depleted in Na_2O and enriched in K_2O (Figure 18). This alteration is attributed to the introduction of potassic aqueous fluids concomitant with feldspar destructive alteration. Local sodium enrichment (6 to 10% Na_2O) may reflect albitization complementary to sodium depletion in other parts of the alteration system. CaO, MgO and $Fe_2O_3^{total}$ show wide dispersion but much of this is associated with secondary introduction of carbonate. Similarly, a very wide range in Mg# (20 to 65) is interpreted to be strongly influenced by the nature of the secondary carbonate mineral species. Lithophile trace elements behave similarly to Na_2O (Sr) and K_2O (Cs, Rb). Trace elements normally thought to be relatively immobile (Zr, Nb, REE) show more limited dispersion and may reflect primary abundances although intense alteration may influence absolute abundances to some degree.

The major element geochemical characteristics of the least-altered porphyries are broadly similar, in most respects, to those of tonalites within the synvolcanic, pretectonic batholithic complexes. The most striking differences are associated with the more altered samples and are likely attributable to feldspar alteration (more erratic Al_2O_3, wide variation in Na_2O/K_2O) or carbonate introduction (CaO abundance, Mg#). HFSE, including the REE, are fairly consistent within porphyry units and display fairly consistent patterns as a group (Figure 19). These units are characterized by moderately fractionated REE (Ce_N/Yb_N

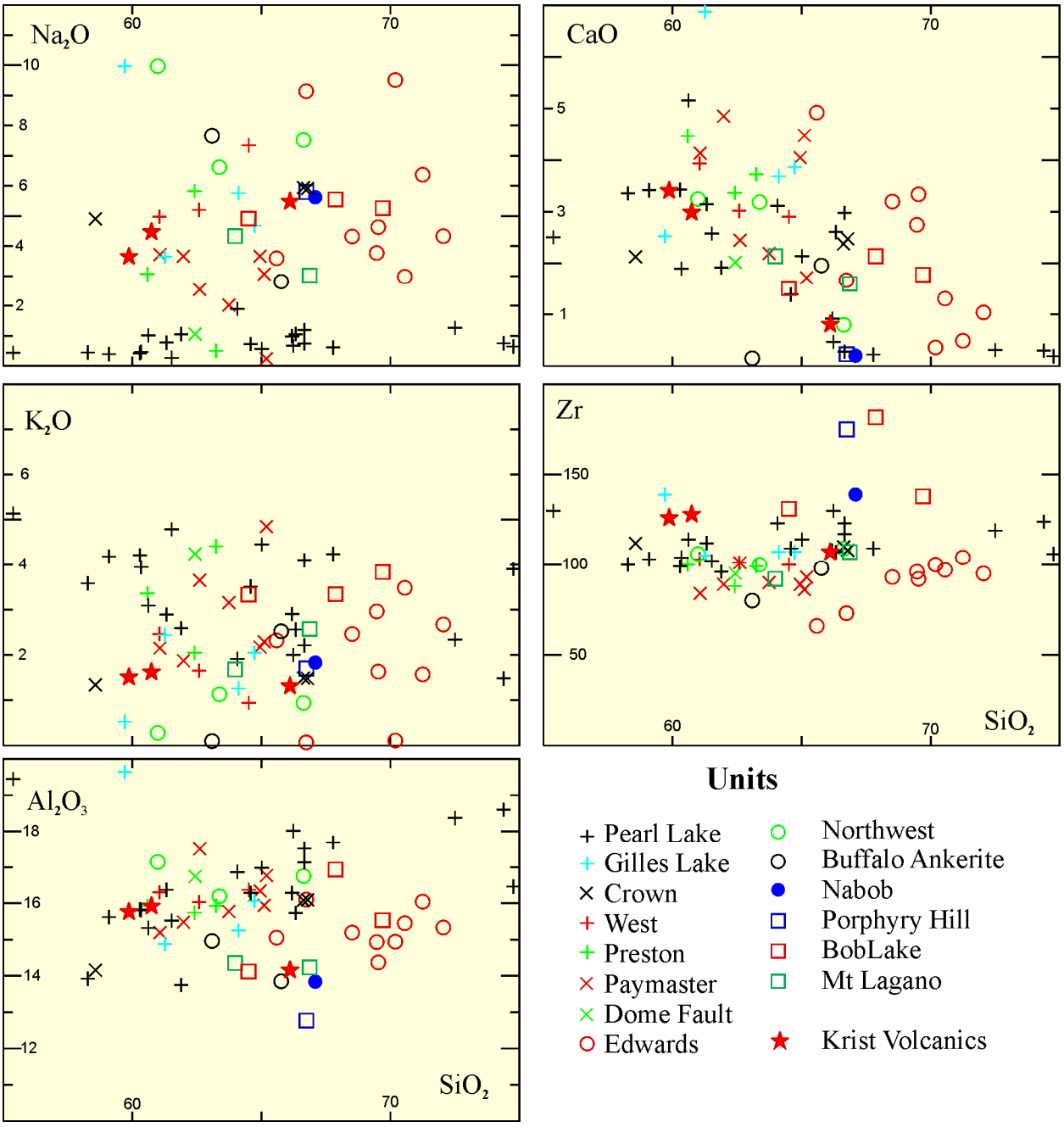

Figure 18. Harker diagrams for porphyry units from the general Timmins area. Data are from this study (Beakhouse 2011, MRD 285) and MacDonald (2010).

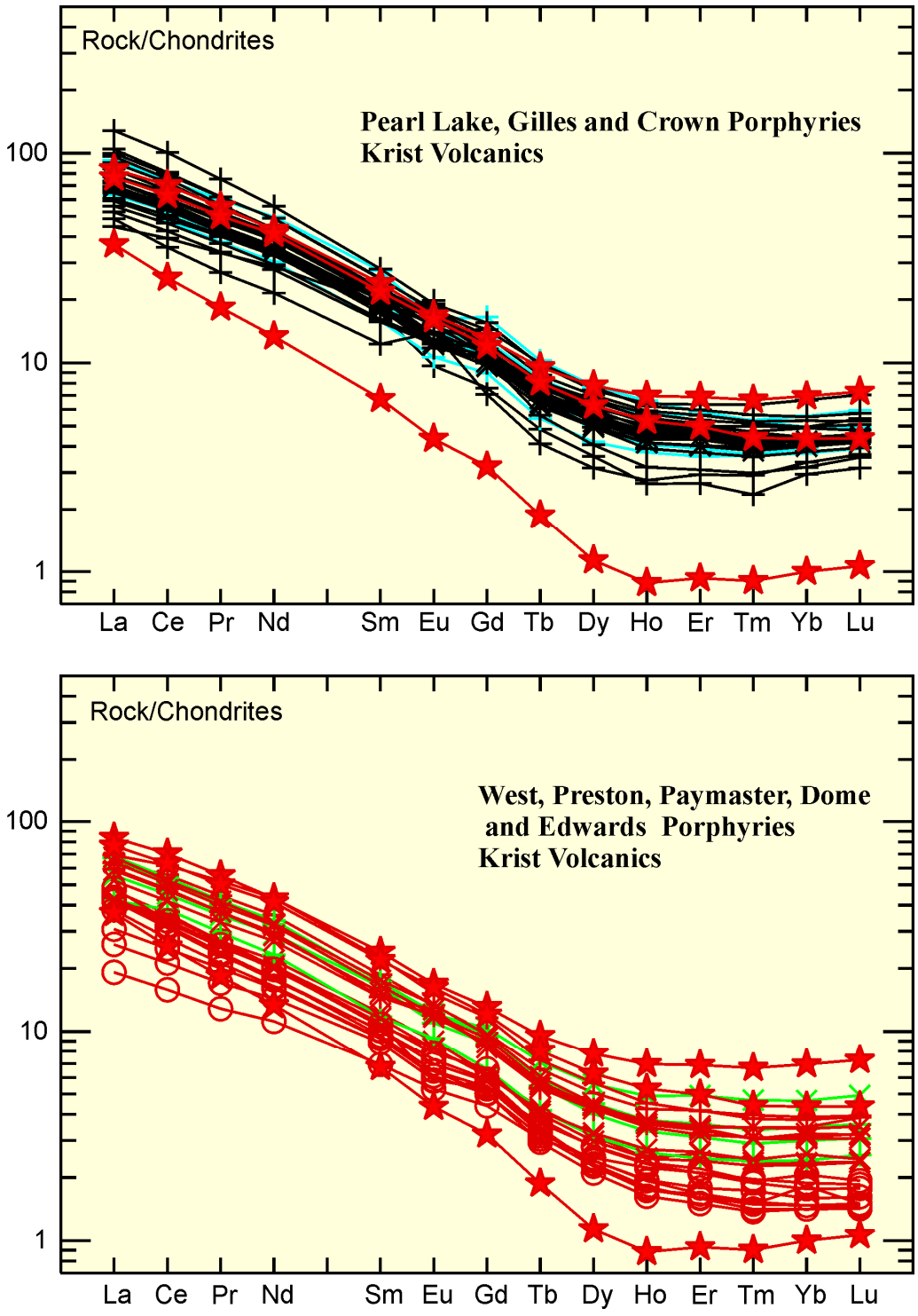

Figure 19. Chondrite normalized REE plots for samples of porphyry units from the general Timmins area. Normalization values from Sun and McDonough (1989), with symbols and data source same as for Figure 18.

~10 to 20) with moderately to strongly depleted HREE (Yb_N ~1 to 7). With the exception of a few samples, Eu anomalies are negligible.

As discussed in more detail elsewhere (McDonald 2010), the geochemical characteristics of the Krist metavolcanic unit in the basal portion of the Porcupine assemblage are closely comparable to those of the porphyries.

PETROGENESIS

The geochemical characteristics discussed above are interpreted to indicate a high-Al TTG geochemical affinity for the Timmins area porphyries although this interpretation is based almost exclusively on the HFSE, and particularly the REE, characteristics. Other geochemical criteria generally considered in this interpretation (relatively low Mg#, elevated Al_2O_3, Sr and Sr/Y ratios, high Na/K) have been extensively modified by secondary alteration processes. MacDonald et al. (2005) also interpreted that a high-Al TTG geochemical affinity predominates but concluded that a subset of samples displayed low-Al TTG characteristics. This later interpretation was based primarily on low Al_2O_3 abundances but is also consistent with the lower Sr abundances (mostly <250 ppm with dispersion to higher values). As discussed above, these geochemical indices have been significantly modified by secondary alteration processes and may not be reliable indicators of primary magmatic characteristics. Furthermore, low-Al TTG affinity is generally associated with high abundances of HFSE and relatively unfractionated REE, and on this basis, Timmins area porphyries with lower Al_2O_3 abundances are regarded as likely representing altered, comparatively deeply sourced, high-Al TTG units. It is difficult to further assess the character of the residue (depth of melting) for these units because the geochemical parameters (Sr, Eu/Eu*) used to distinguish melting depth in relation to the plagioclase stability field (i.e., distinguishing eclogitic from mafic garnet granulitic residue) have been modified to some degree by alteration. However, a mafic garnet granulite (intermediate depth melting) source is provisionally favoured because the least-altered samples generally lack any indication of positive Eu/Eu* and have Sr <400 ppm.

DISCUSSION

The weight of evidence suggests that the Timmins area porphyries are a temporally restricted (2687–2691 Ma) pretectonic to syntectonic, premineralization magmatic event. These units are dominantly high-level intrusions but some probably include an endogenous dome facies. The petrographic, geochemical and temporal similarity to the Krist metavolcanic unit at the base of the Porcupine assemblage suggests a genetic relationship, and consequently the porphyries can be regarded as the subvolcanic and vent facies of the youngest subalkaline volcanic activity within the Abitibi greenstone belt. The Porcupine assemblage is interpreted to slightly predate the earliest (extensional) deformation affecting the Timmins area but was overprinted by much of the regional deformation (Bateman et al. 2005). On this basis, the Timmins area porphyry intrusions are interpreted to be very early syntectonic.

Mineralization within the porphyries is associated with structurally controlled vein systems and secondary disseminated sulphides, suggesting that mineralization postdates emplacement of the porphyries. The long-recognized spatial association of gold mineralization and porphyries is interpreted to reflect the role of the latter in the localization of heterogeneous strain leading to the development of enhanced porosity and permeability which focused the flow of later hydrothermal fluids (*see also* MacDonald et al. (2005) and references cited therein). This interpretation is consistent with recent model Re/Os age estimates for the timing of gold mineralization (2672 ± 7 Ma) at Timmins (Bateman et al. 2005).

The Timmins area porphyry units are interpreted to have a high-Al TTG petrogenetic affinity and these units (~2687–2691 Ma in age) may represent a continuation of protracted high-Al TTG magmatism represented within the synvolcanic phases of the large belt-bounding batholiths discussed in the preceding section. Although the interpretation of petrogenesis is complicated by secondary alteration, one possible difference is the low Sr/Y and the absence of positive Eu anomalies in the least-altered units, suggesting that very deep (eclogitic residue) melting is less likely represented and melting may have occurred primarily in the lowermost crust.

Other Abitibi Subprovince Early Syntectonic Intrusions

Numerous other intrusions that are widely distributed across the Abitibi Subprovince are provisionally interpreted, on the basis of field relationships, composition and/or U/Pb ages, to be potentially related to processes giving rise to the Timmins area porphyries. This section offers brief descriptions and interpretations for a number of these. Geochemical data for units discussed here as well as others are available in the associated MRD 285.

OTHER PORPHYRIES PROXIMAL TO PORCUPINE–DESTOR FAULT

Porphyries exhibiting similarities with those described above in the Timmins area occur elsewhere in a general spatial association with the Porcupine–Destor fault (PDF). A number of these are discussed briefly below.

A number of lenses of fine-grained, felsic, quartz-feldspar porphyry occur within metasedimentary rocks (presumed to be Porcupine assemblage) at or near the contact with Tisdale assemblage metavolcanic rocks in Bristol Township. One of these units has a U/Pb zircon age of 2687.7 ± 1.4 Ma (Ayer et al. 2003). The primary character of these units is obscured by intense alteration and deformation but they are presumed to be high-level intrusions based on the absence of flow banding or fragmentation, massive character and grain size. They are similar to the Timmins area porphyry units petrographically. As with the Timmins area porphyry units, geochemistry has been modified by secondary alteration. Although total REE abundances are relatively low, they are moderately fractionated with near chondritic HREE and negligible to weak positive Eu/Eu* (Figure 20), suggesting a probable high-Al TTG affinity.

A comparatively large area just north of the Porcupine–Destor fault in the central portion of Carr Township is interpreted to be underlain by quartz-feldspar porphyry (Berger 1997). There is no exposure in the area and the characteristics of the unit are inferred from drill core. The unit occurs within a belt of metasedimentary rock interpreted to be Porcupine assemblage. Samples examined as part of this study are predominantly quartz-plagioclase porphyry that is moderately to strongly altered (carbonate and white mica) but preserves primary textural relationships. An original mafic mineral is completely replaced by chlorite. Magnetite is present in some samples but others have little oxide and abundant sulphide minerals (chalcopyrite, pyrite, other sulphide minerals) suggesting possible sulphidation of magnetite. Locally, native gold is associated with sulphide minerals. Whole rock geochemistry is broadly similar to that characterizing Timmins area porphyries, with both primary magmatic processes as well as secondary alteration processes influencing geochemical characteristics. Rare earth elements are moderately fractionated (Ce_N/Yb_N ~7 to 9), primarily because of somewhat elevated HREE abundance (Figure 20), suggesting garnet fractionation is less significant than in other examples, but geochemical characteristics of relatively immobile elements are, in most respects, within ranges typical of high-Al TTG.

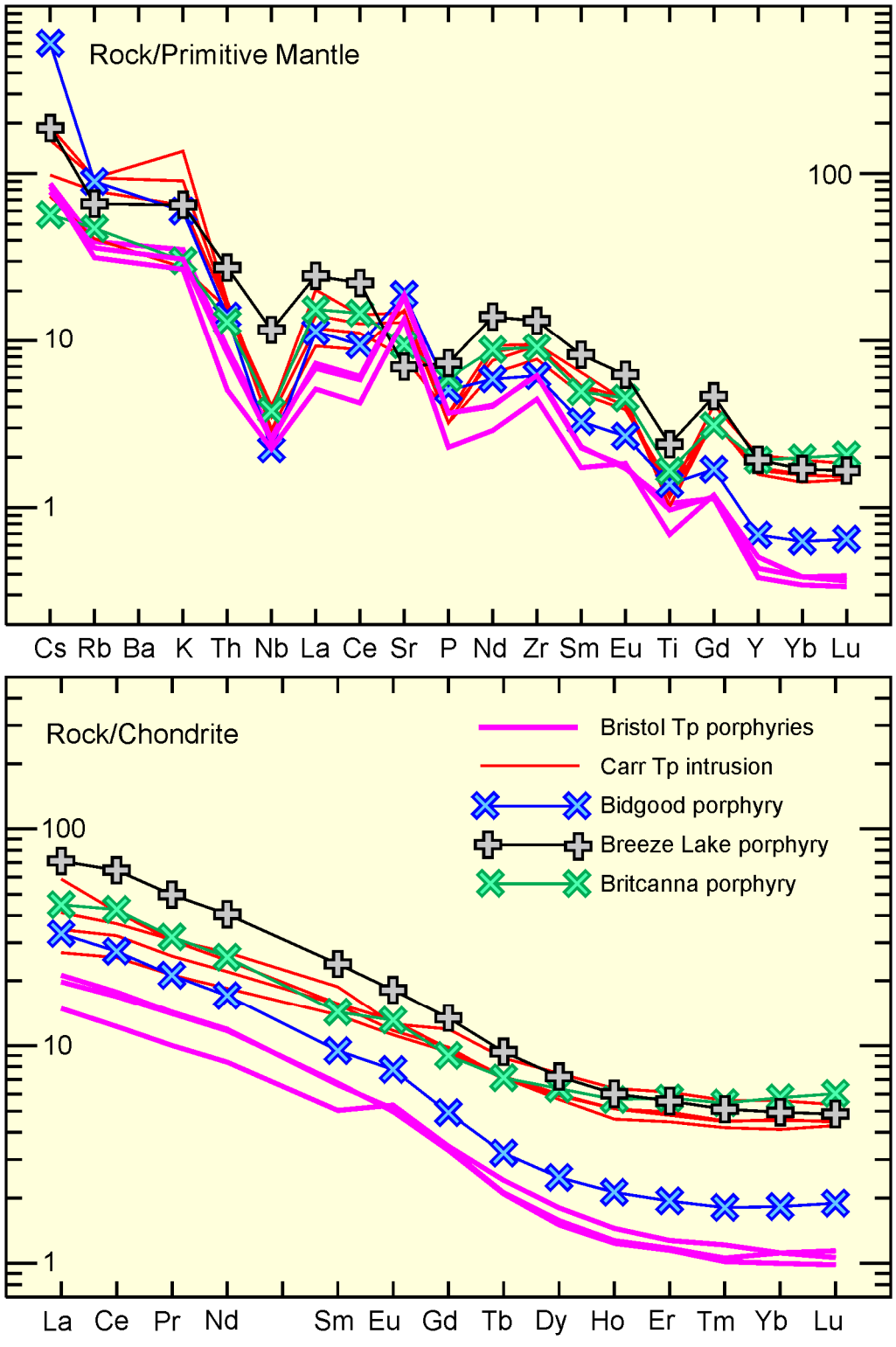

Figure 20. Chondrite and primitive mantle normalized trace element plots for samples of selected porphyry units from the Abitibi Subprovince. Normalization values from Sun and McDonough (1989).

OTHER PORPHYRIES

Broadly similar, fine-grained porphyritic intrusions occur in scattered locations elsewhere in the Abitibi Subprovince. Like those spatially associated with the Destor–Porcupine fault, they often exhibit a spatial association with gold mineralization and possibly with regional faults. Several examples are discussed below.

The Bidgood porphyry, located approximately 7 km east of the town of Kirkland Lake, is a strongly altered and deformed plagioclase-quartz porphyry initially interpreted to lie within a belt of Timiskaming assemblage metasedimentary and metavolcanic rocks just to the north of the Cadillac–Larder Lake fault (Jackson 1995). While acknowledging that contact relationships were modified by deformation and not well-exposed, Corfu et al. (1991) interpreted the unit to be intrusive and suggested that the U/Pb age for the porphyry of 2685 ± 3 Ma point to the hosting units representing an early stage of the Timiskaming assemblage. This interpretation was drawn into question by additional U/Pb geochronology suggesting a maximum age of sedimentation of 2674.3 ± 3.7 Ma (Ayer et al. 2002), which is more in keeping with regionally constrained timing of the Timiskaming assemblage. Assuming this age constraint (based on several samples) on the timing of country rock deposition is correct, then either the U/Pb porphyry age is older than the true age of emplacement or the porphyry is unconformably overlain by the Timiskaming assemblage rather than intrusive into it. In the absence of additional geochronology and detailed field investigations, the age of the Bidgood porphyry is considered here to be unresolved. A single sample from a relatively weakly deformed portion of the porphyry has a well-preserved primary porphyritic texture with predominant euhedral to subhedral plagioclase and subordinate rounded quartz phenocrysts. Alteration of feldspar phenocrysts (white mica) and the fine-grained matrix (white mica and carbonate) is intense. Large-ion lithophile element abundances are relatively high (Figure 20), possibly reflecting secondary hydrothermal alteration. This sample has an unusually high Mg# (56), interpreted to reflect the influence of secondary dolomitic carbonate alteration; the very low Cr abundance (8 ppm) further suggests the high Mg# is unlikely to be a primary characteristic. In all other respects, the geochemical characteristics are broadly similar to those of Timmins area porphyries and high-Al TTG in general.

The Britcanna porphyry intrudes mafic to intermediate metavolcanic rocks south of the Round Lake batholith in Bryce Township (Johns et al. 1985). Gold mineralization associated with carbonatization and quartz veining is reported within and near the porphyry (Johns 1985). The Britcanna porphyry is crudely equant and round in map view but in detail the contacts are irregular, and texturally similar dikes with country rock are likely related. The unit is relatively homogeneous though differentially altered and a single sample examined in detail is a highly altered, intermediate feldspar porphyry. Noteworthy alteration includes carbonatization and quartz veining as well as chloritization (at least in part after an unknown original mafic mineral) and alteration of feldspar to a mixture of white mica, epidote and carbonate. The geochemical characteristics are characteristic of high-Al TTG and very similar in most respects to those of the Carr porphyry discussed above.

The Breeze Lake porphyry is a relatively small, intermediate, feldspar-quartz porphyry intruding metavolcanic rocks and is spatially associated with gold mineralization in Tyrrel Township (Johns 2003). Intensely altered, euhedral to subhedral plagioclase phenocrysts predominate over rounded to irregularly shaped quartz phenocrysts. Carbonatization is generally strongly developed and quartz veining is abundant locally. The presence of quartz phenocrysts indicates a relatively felsic bulk composition and the lower SiO_2 content (~62%) of a single sample in part reflects extensive carbonatization. The relatively low Al_2O_3 (15.2%) and Sr (147 ppm) could reflect relatively shallow melting with residual feldspar; however, the absence of a corresponding negative Eu anomaly suggests that the former may be a consequence of secondary alteration. Modest HREE depletion and REE fractionation (similar to Carr and Britcanna porphyries in Figure 20) suggest garnet may be a less important residual phase than in some of the other porphyry units characterized by more extreme HREE depletion.

OTHER INTRUSIONS

Two units (Clifford stock and Clarice Lake stock) intruding the Blake River assemblage in the central portion of the western Abitibi Subprovince are provisionally assigned to the early syntectonic group based on their ages even though they differ significantly from other intrusions of this group in terms of their coarser grained and relatively equigranular texture. The U/Pb ages for the Clifford stock (2686.9 ± 1.2 Ma, MacDonald et al. 2005) is very similar to that of the Clarice intrusion (2689 ± 2 Ma, Corfu and Noble 1992). On a more regional scale, these ages are very similar to those of the Krist volcanics within the Porcupine assemblage and early synvolcanic porphyries discussed above.

The Clifford stock was the subject of a detailed investigation and literature review by MacDonald et al. (2005) from which much of the following discussion is adapted. The Clifford stock is a medium-grained, equigranular to weakly potassium-feldspar megacrystic, hornblende ± biotite granodiorite to tonalite. Fine- to medium-grained intermediate to felsic dikes, breccia-pipes and stockwork veins containing quartz, pyrite, molybdenite and gold occur in close proximity to the stock and may be genetically related. The geochemical characteristics of the stock indicate the unit is subalkalic and calc-alkalic with an interpreted high-Al TTG affinity (MacDonald et al. 2005).

The Clarice Lake stock is a medium-grained, equigranular, hornblende ± biotite tonalite to quartz diorite. Alteration to white mica, epidote and carbonate (feldspar) and chlorite and/or actinolite (mafic minerals) is variable but locally intense. General geochemical characteristics are similar to those of the Clifford stock (Figure 21) and suggestive of a calc-alkalic, high-Al TTG affinity although high Mg# (57) and Cr abundance (28 to 55) suggest either interaction with the mantle or a cumulate character.

SUMMARY

The units discussed above were emplaced during a brief time interval (2685–2691 Ma) that postdates deposition of volcanic-dominated assemblages and emplacement of synvolcanic intrusions. The emplacement of these units is synchronous with the youngest subalkaline felsic volcanism in the Abitibi Subprovince (Krist volcanics) and the onset of Porcupine assemblage sedimentation. Constraints on both the intrusions discussed above and the Porcupine assemblage suggest both can be regarded as early syntectonic.

The environment and mode of emplacement of the early syntectonic intrusions contrast markedly with that of the earlier, synvolcanic plutons. The latter were primarily emplaced as laterally extensive sheets that underlie the greenstone belt, with a volumetrically subordinate proportion of these magmas being emplaced at high levels or erupting within the greenstone belt. In contrast, the early syntectonic units are apparently dominantly high-level, discordant intrusions, and along with erupted equivalents exhibit a strong tendency to be spatially associated with major east-trending structures such as the Porcupine–Destor fault. Much of the deformation in these east-trending structures postdates the emplacement of early syntectonic intrusions, suggesting that the localization of these intrusions within these is an early manifestation of a protracted crustal-scale zone of weakness that persisted throughout the deformational history of the Abitibi Subprovince. The common association of the early syntectonic intrusions with synemplacement and postemplacement, regional-scale alteration is interpreted to be a further consequence of localization within these zones of weakness that developed enhanced porosity and permeability, focusing the flow of hydrothermal fluids responsible for alteration.

Interpretation of the petrogenetic affinity of the early syntectonic intrusions is complicated by overprinting alteration in many cases; however, a subalkaline, calc-alkalic, high-Al TTG affinity interpreted to reflect relatively deep melting of a mafic source can be inferred for most intrusions. Geochemical signatures of an eclogitic residue (extreme HREE depletion coupled with positive Eu

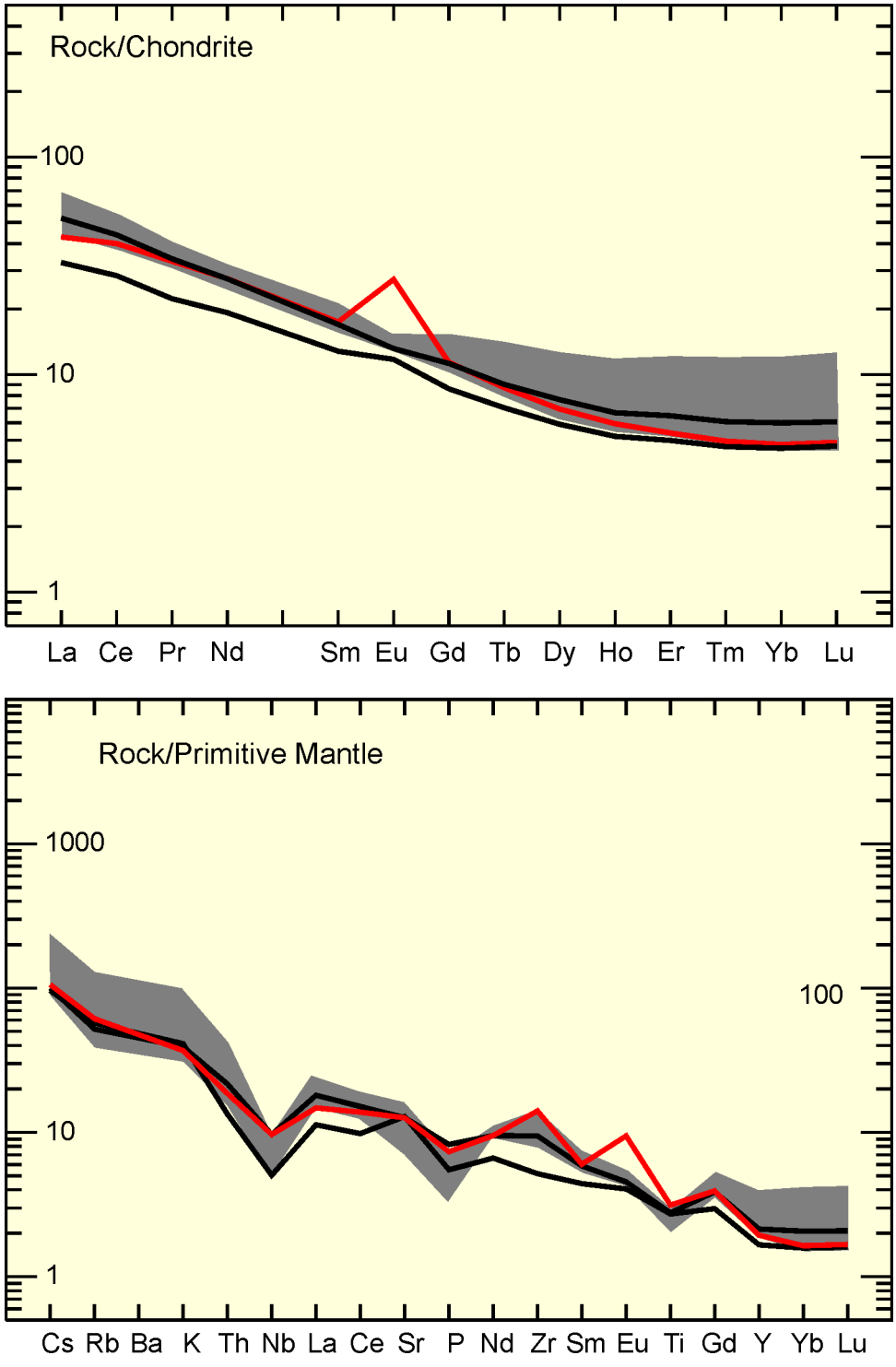

Figure 21. Chondrite and primitive mantle normalized trace element plots for samples from the Clifford (grey shaded area plus atypical analysis in red) and Clarice (black lines) intrusions. Data for the Clifford intrusion is from MacDonald et al. (2005). Normalization values from Sun and McDonough (1989).

anomalies and very high Sr/Y and Sr abundance) is less common than observed for the synvolcanic plutons, suggesting that somewhat shallower melting (mafic garnet granulite residue) may predominate for this younger group of plutons.

Syntectonic Plutons

A number of large- to moderate-sized plutons occurring primarily in the central portion of the Abitibi Subprovince between the Porcupine–Destor and Cadillac–Larder Lake faults are interpreted to represent a distinct group within the Abitibi plutonic record. These plutons include most lobes of the Watabeag Batholith as well as the Blackstock, Fallon, Geikie and Adams plutons. A number of smaller plutons (e.g., Butler Lake, Winnie, Hincks), as well as some of the late, massive plutons occurring within the large batholiths discussed above, may be related to this group. These plutons are discussed separately below, followed by a general comparison and synthesis.

CHARACTERISTICS OF INDIVIDUAL PLUTONS

Watabeag Batholith

FIELD RELATIONSHIPS

The Watabeag Batholith underlies approximately 500 km^2 in the central portion of the western Abitibi Subprovince and consists of numerous discrete "lobes" that likely represent distinct plutons (Figure 22). The area is very poorly exposed and consequently field relationships are not well constrained but, based on the general absence of well-developed, superimposed tectonic fabrics, U/Pb age data (discussed below) and relationships for nearby comparable plutons, the batholith is interpreted to be postvolcanic and syntectonic. The batholith intrudes metavolcanic rocks that have been assigned to the Tisdale and Blake River assemblages in the general vicinity of the poorly constrained contact between the 2 assemblages.

Three U/Pb zircon ages ($2699.0^{+3.5}_{-2.9}$ Ma, $2681.3^{+2.7}_{-2.6}$ Ma and $2676.0^{+2.2}_{-2.1}$ Ma) from different lobes within the Watabeag Batholith (precise locations poorly constrained) have previously been reported (Frarey and Krogh 1986). The oldest of these ages is broadly synvolcanic (Blake River assemblage) and was obtained from a quartz diorite intrusion within Baden Township that has a much more irregular contact than other lobes of the Watabeag Batholith. The age for this unit is interpreted to be unrepresentative of the batholith as a whole; the unit is either significantly older than other components of the batholith (Frarey and Krogh 1986) or the age reflects inheritance. The 2 younger ages are consistent with the absence of imposed tectonic fabrics throughout most of the batholith and are comparable to ages for similar units in the area to the west. These younger ages are thought to be more representative of the components of the batholith examined within this investigation.

A single additional sample (7257; UTM 542904E 5330512N, NAD83) of hornblende-biotite quartz monzodiorite was selected for laser ablation inductively coupled plasma mass spectrometry (LA-ICP-MS) and thermal ionization mass spectrometry (TIMS) U/Pb geochronology as part of this study in order to further evaluate the absolute timing of emplacement. Zircons analyzed by LA-ICP range from highly discordant to modestly reversely discordant. Analyses that are less than 5% discordant have $^{207}Pb/^{206}Pb$ ages mostly in the range 2670 to 2730 Ma suggesting the presence of inheritance. Only 2 of 7 zircon fractions selected for TIMS analysis are less than 5% discordant and these have divergent $^{207}Pb/^{206}Pb$ ages (2765 Ma and 2673 Ma), further suggesting the presence of inheritance. The age of this unit is not well

constrained because of complex Pb loss behavior and the presence of inheritance, but the $^{207}Pb/^{206}Pb$ ages of the youngest least discordant data are broadly consistent with the 2 younger ages reported by Frarey and Krogh 1986.

PETROLOGY

The Watabeag Batholith, despite its large size and multilobate character suggesting it is an amalgam of discrete plutons, is relatively uniform in terms of its mineralogy, texture and internal structure. Granodioritic to, less commonly, quartz monzodioritic compositions predominate. Medium-grained, equigranular textures predominate; however, weakly to moderately microcline megacrystic textures

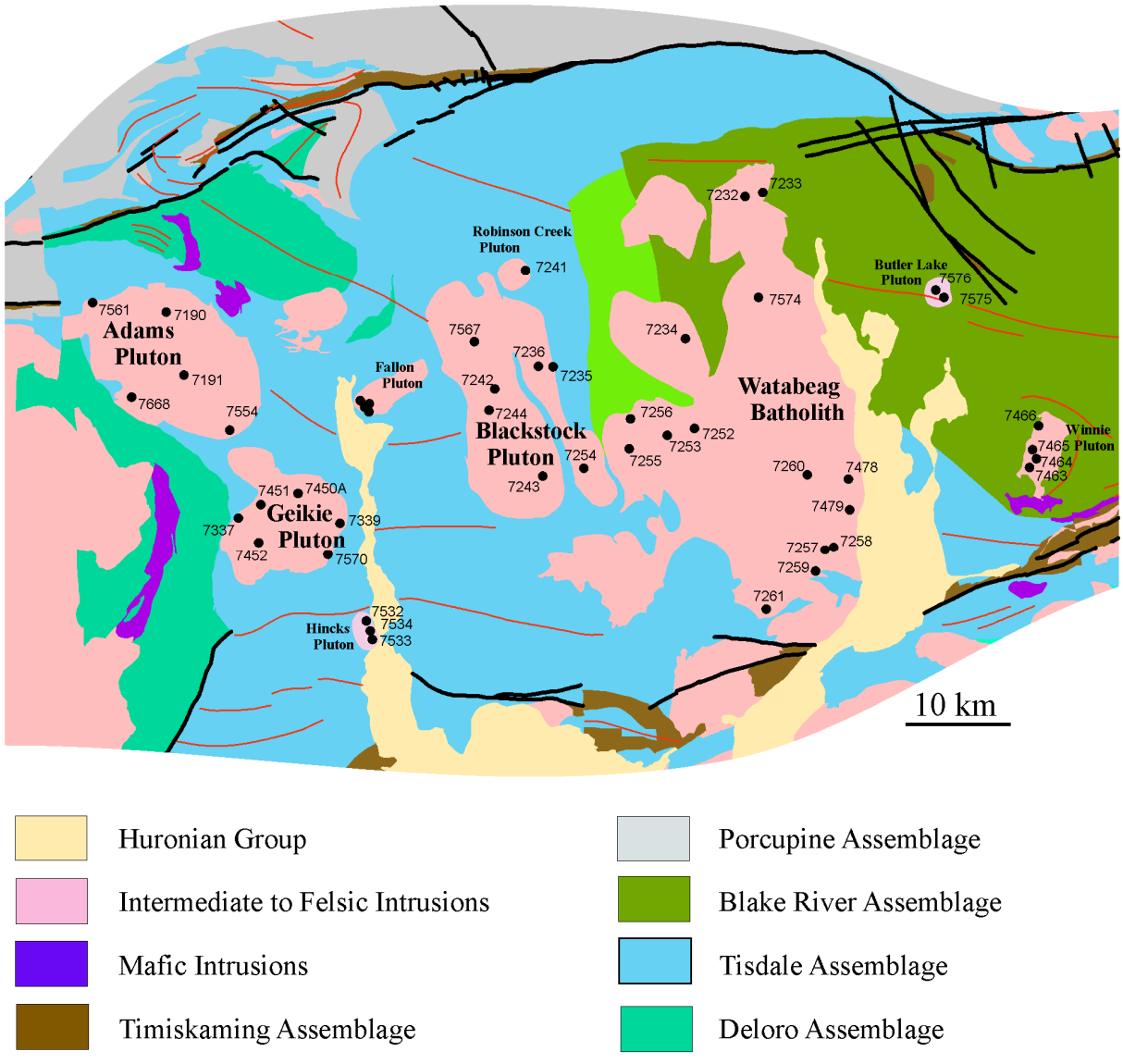

Figure 22. Generalized assemblage map of the central portion of the western Abitibi Subprovince illustrating the location of syntectonic plutons in relation to supracrustal assemblages and regional structures. Locations of selected samples are indicated by numbered dots. Heavy black lines are faults and red lines are regional folds.

(Figure 23) are present locally. Plagioclase is generally uniform to weakly oscillatory zoned and lies in the oligoclase compositional range (sometimes with albitic rims adjacent to microcline). Weak to moderate deuteric alteration to white mica, epidote and carbonate is commonly zone controlled and heterogeneously developed. Microcline occurs as homogeneous, relatively inclusion-free, intergranular crystals and, locally, as incipiently to moderately well-developed megacrysts with irregular margins and abundant inclusions of all other primary mineral phases present. The best developed megacrysts are commonly perthitic. Quartz displays undulatory extinction and, less commonly, weakly developed patchy extinction.

Colour index is characteristically in the range 10 to 15. Subhedral to euhedral hornblende is, almost without exception, the predominant mafic mineral. In each of 6 samples investigated in detail, mineral chemistry confirms the calcic amphibole composition (magnesiohornblende in all cases) of the primary amphibole crystals. Narrow rims of actinolitic amphibole overgrows magnesiohornblende in several of the samples. Biotite is ubiquitous but rarely as abundant as hornblende. In most cases, biotite is extensively chloritized. Clinopyroxene is rarely present as cores within amphibole or within ultramafic clots. Simple magnetite octahedra are always present in trace to low abundance. Ubiquitous, primary accessory minerals include titanite, apatite and zircon, with the former being moderately abundant in some samples.

Dioritic enclaves and ultramafic clots are common and widespread but volumetrically minor (<1%) within the Watabeag Batholith. The dioritic enclaves are more mafic (colour index ~25 to 50) than the host phase. Hornblende, broadly similar in composition to that in the host, is the greatly predominant mafic phase with minor amounts of biotite present in some cases. Plagioclase (oligoclase-andesine) is more calcic than that within the host. Ultramafic clots consist of hornblende ± clinopyroxene ± biotite.

The enclaves, which range up to 1 m in maximum dimension but are more typically 2 to 10 cm long, typically have a weakly to distinctly flattened oblate ellipsoidal form. The contacts between the enclaves and their host are generally sharp but may be gradational (Figure 23f) or marked by a thin hornblendite rim (Figure 23e). Ultramafic clots are smaller (generally <2 cm) but have a similar oblate ellipsoidal form. The long axes of the enclaves and clots are generally aligned parallel to a weak (magmatic?) mineral fabric in the host granodiorite to quartz monzodiorite.

GEOCHEMISTRY

The lithological uniformity of the Watabeag Batholith is reflected in its relatively uniform geochemical characteristics. Most samples lie within a relatively restricted range in SiO_2 (69 to 72%), with a similarly restricted range for most other elements (Figures 24 and 25). The most significant deviations from typical abundances are seen in a single sample (7574) from the interior of the batholith with somewhat higher SiO_2, which is atypical in a number of respects, and 2 samples (7232 and 7233) from the northernmost lobe of the batholith (*see* Figure 22) that are relatively enriched in HFSE. All samples are calc-alkaline and subalkaline (Figure 26), but relative to high-Al TTG units of the large belt-bounding batholiths (cf. Figures 4, 9 and 15), higher alkali element (principally higher K_2O) abundances result in the Watabeag Batholith plotting closer to the alkaline-subalkaline division. Relative to the high-Al TTG units of the belt-bounding batholiths, the Watabeag Batholith also displays a slight tendency to slightly greater abundances of both compatible and incompatible trace elements (Figure 27).

Noteworthy major element characteristics of the Watabeag Batholith include relatively high Al_2O_3 abundance (with the exception of 1 high SiO_2 sample), and relatively high abundances of both Na_2O and K_2O (*see* Figure 24). Mg# exhibits a wide range but the majority of samples have values greater than 50. Among trace elements, high Sr abundance is noteworthy (Figure 25) and both compatable and incompatable trace elements are moderately abundant. REE are moderately fractionated, with HREE ranging from 2 to 7 times chondrite with negligible Eu anomalies (Figure 28).

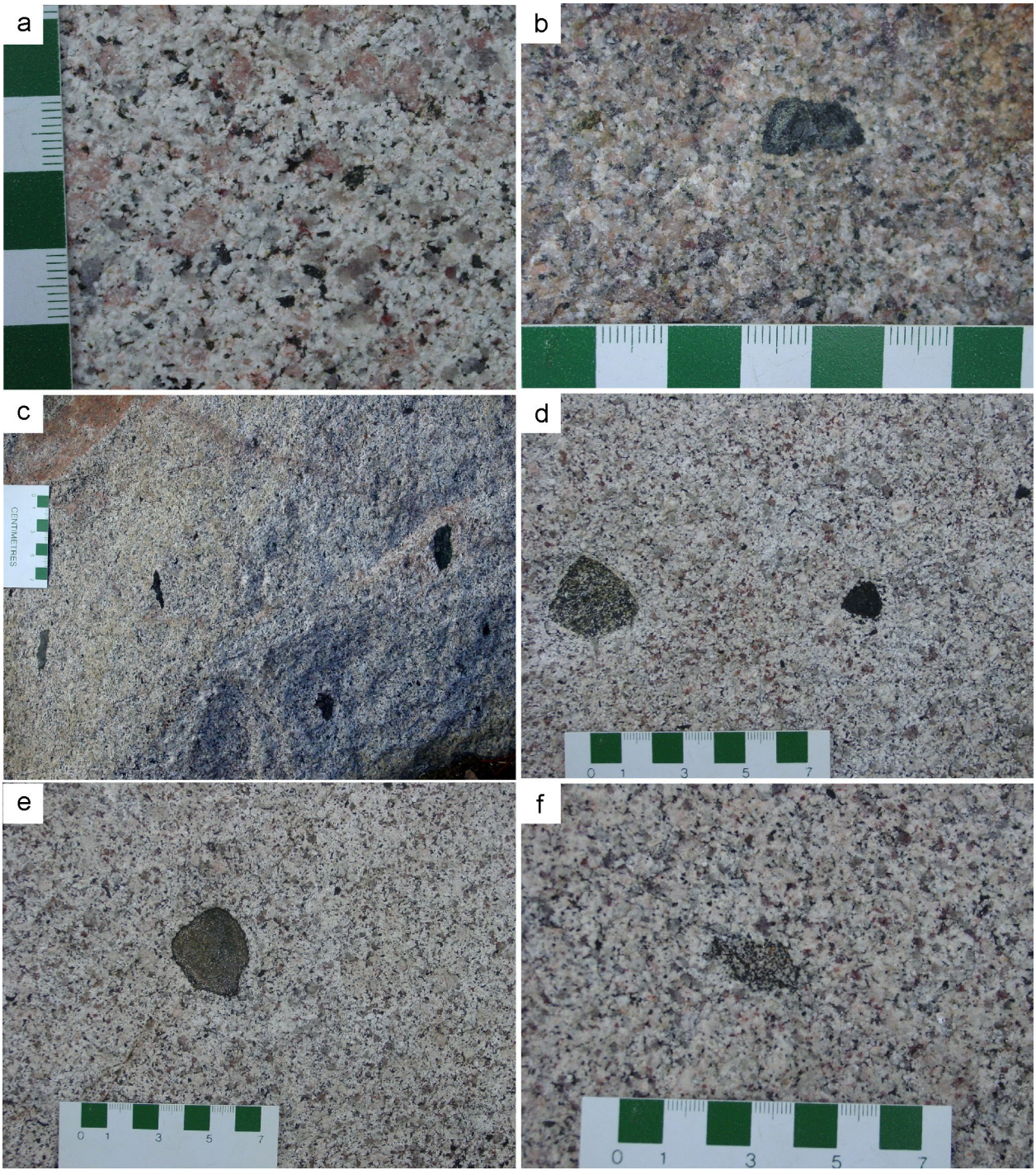

Figure 23. Field photographs illustrating mineralogical and textural characteristics of the Watabeag Batholith. Units are predominantly granodiorite to quartz monzodiorite. Equigranular textures predominate; however, weakly (a) to moderately microcline megacrystic units are widespread. Hornblende generally predominates over biotite (a) and clinopyroxene is rarely present, either as cores within hornblende or within ultramafic clots (b). Dioritic enclaves that are more mafic than the host and ultramafic clots (c and d) are volumetrically minor but common and widespead. Dioritic enclaves may be either sharply bounded (d), rimmed by hornblende (e) or diffusely bounded (f).

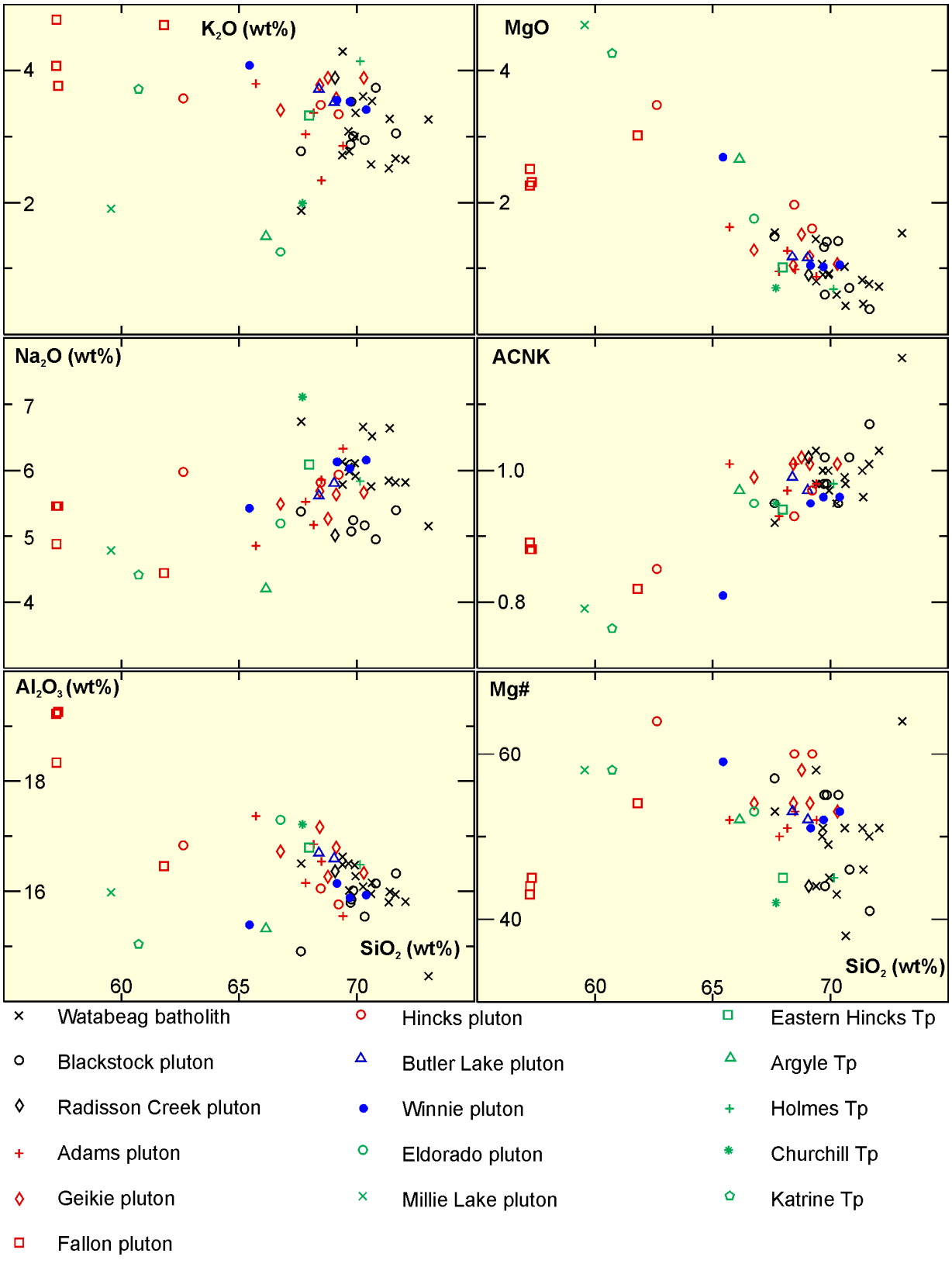

Figure 24. Harker variation diagrams for samples from the syntectonic plutons and possibly correlative minor intrusions.

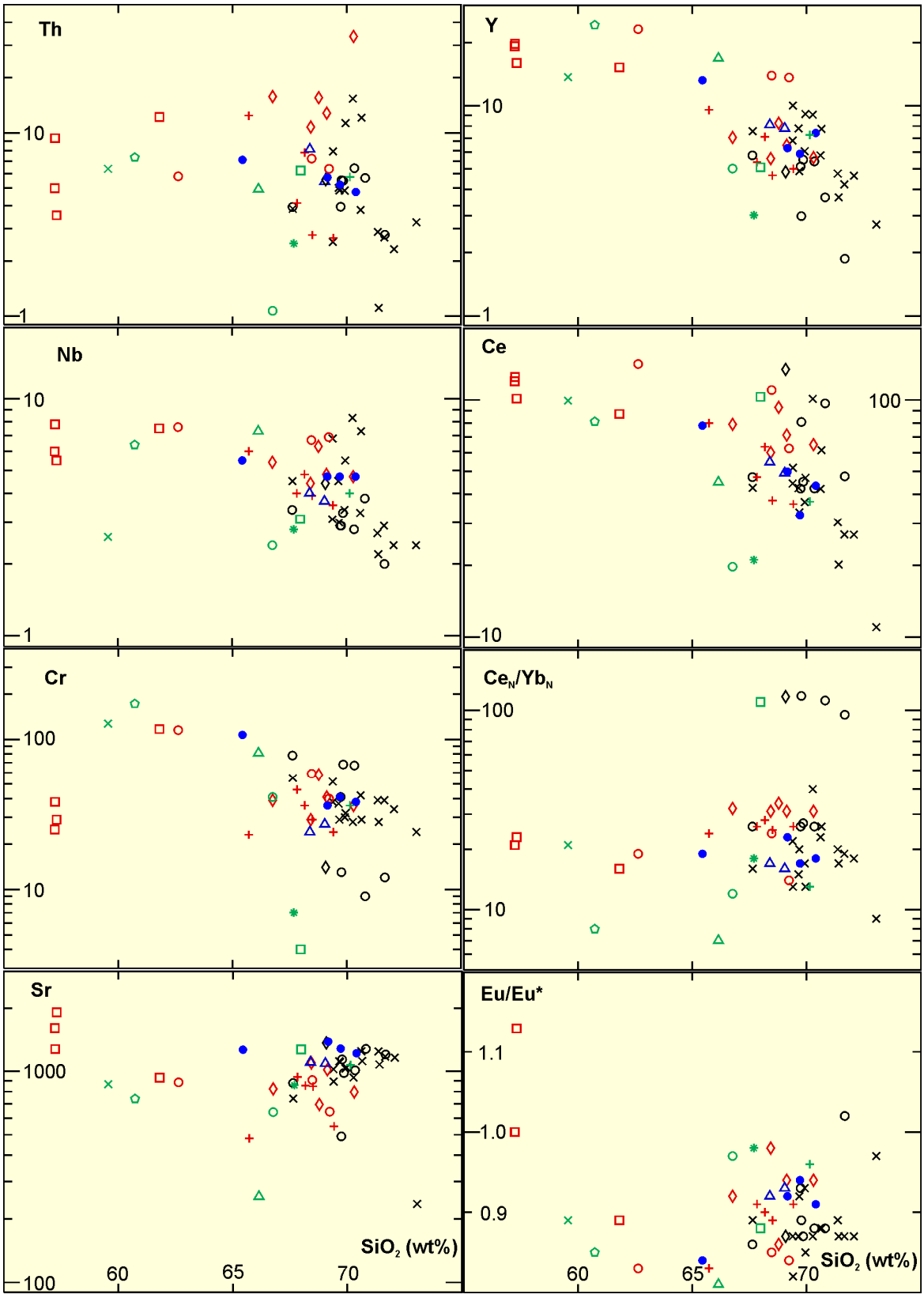

Figure 25. Harker variation diagrams for samples from the syntectonic plutons and possibly correlative minor intrusions. Symbols same as for Figure 24

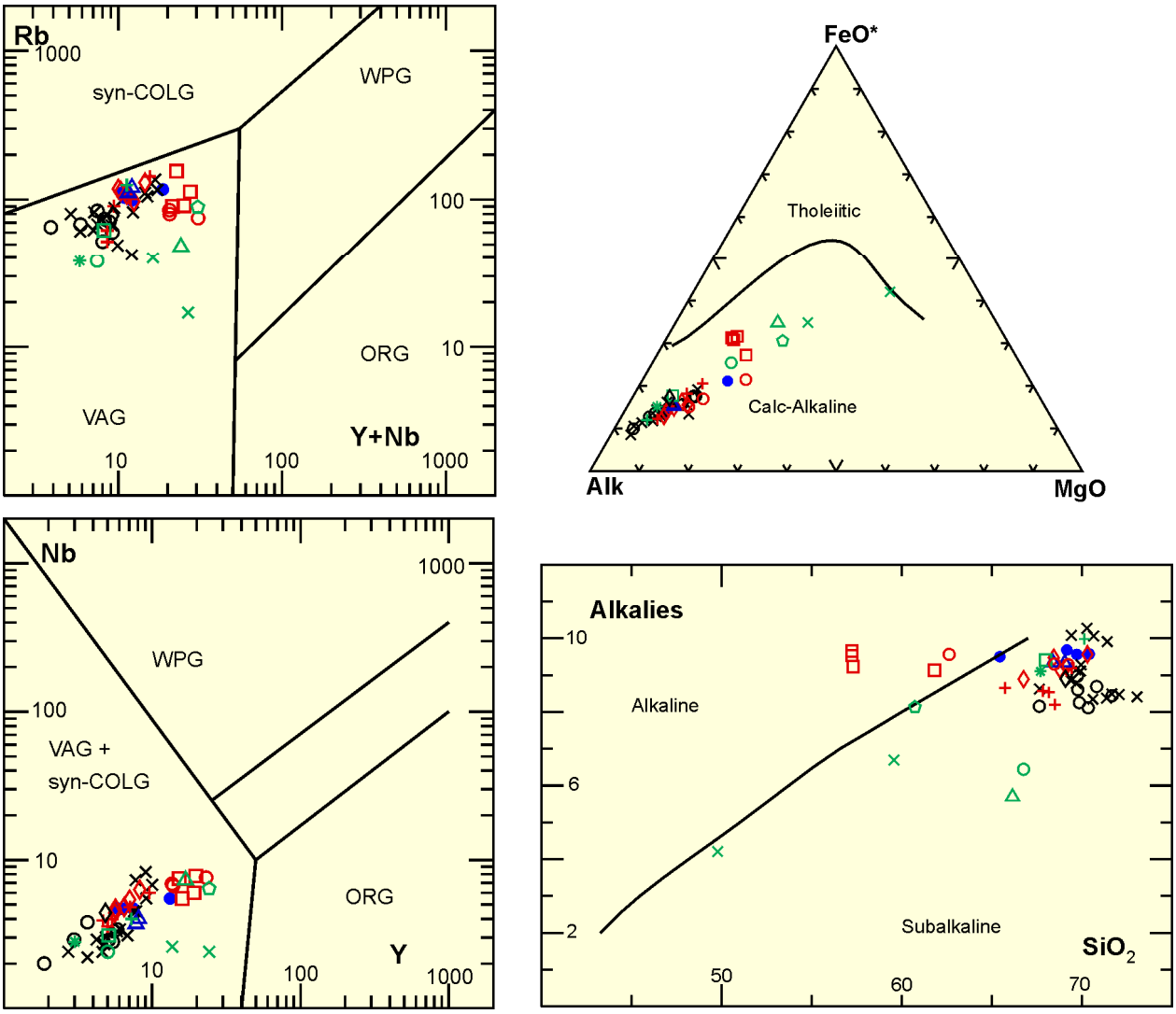

Figure 26. Tectonic discrimination diagrams for samples from the syntectonic plutons. Rb vs Y+Nb and Nb vs Y plots are after Pearce et al. (1984). AFM and alkalies vs SiO_2 plots are after Irvine and Baragar (1971). Symbols same as for Figure 24; abbreviations, Figure 4.

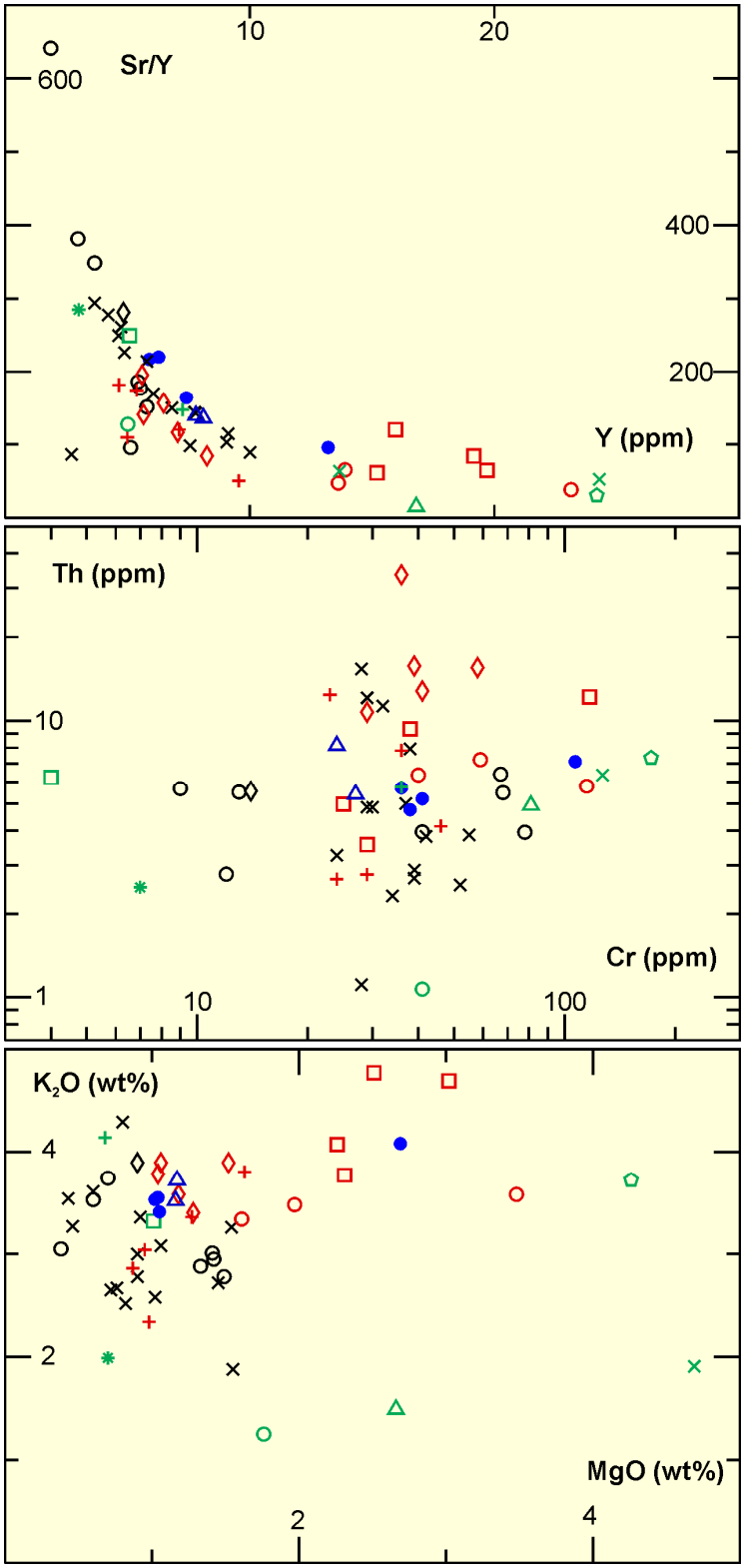

Figure 27. Sr/Y vs Y, Th vs Cr and K_2O vs MgO for samples from syntectonic intrusions. Symbols same as for Figure 24.

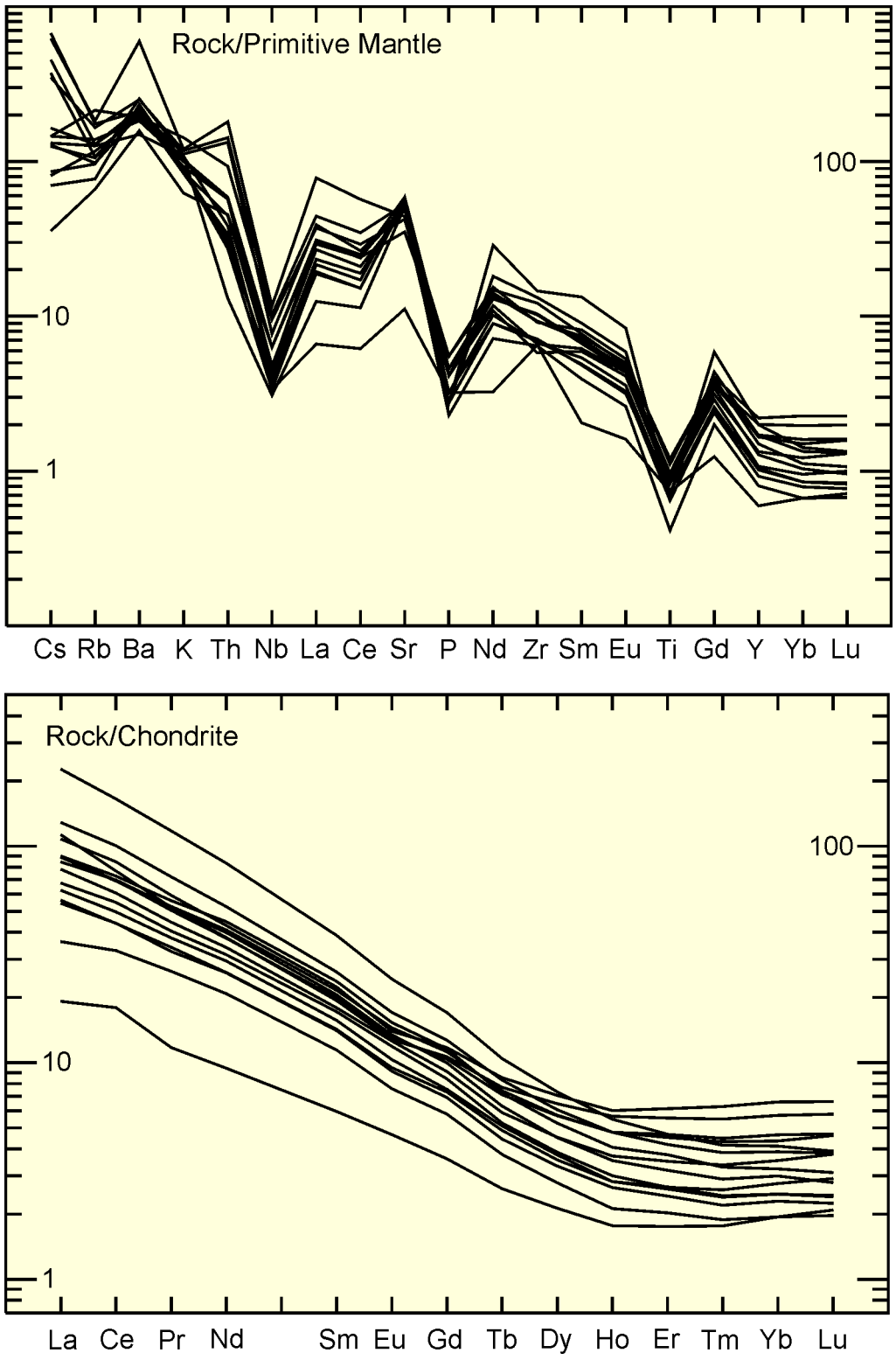

Figure 28. Chondrite and primitive mantle normalized trace element plots for samples from the Watabeag Batholith. Normalization values from Sun and McDonough (1989).

PETROGENESIS

The geochemical characteristics of the Watabeag Batholith place some general constraints on the petrogenesis although the precise detailed petrogenesis is not constrained. Intracrustal melting is unlikely to have generated these magmas because of the moderately high abundance of Al_2O_3 and Sr, which suggests that plagioclase was not a major residual phase, and also because of moderately high abundances of compatable trace elements and relatively high Mg#, which suggests a relatively unevolved source. Partial melting of a mafic (basaltic) source (high-Al TTG model) is consistent with many of the geochemical characteristics; however, the high Mg#'s would require either a mixed mafic or ultramafic source or some interaction of a mafic-derived magma with an ultramafic reservoir. The slight enrichment in both compatible and incompatible elements may also be consistent with partial melting of a metasomatized mantle source (sanukitoid model); however, if this is the case, the magmas must have undergone fractionation (decreasing Mg# and compatible element abundances) such that no primary mantle melt component is preserved. With evidence for some involvement of an ultramafic reservoir but no definitive indication of the nature of the source, the most that can be inferred is that the Watabeag Batholith likely originated by partial melting of a mafic to ultramafic source near the base of the crust or within the upper mantle.

Blackstock Intrusion

FIELD RELATIONSHIPS

The Blackstock pluton underlies approximately 230 km^2, mostly in Blackstock, Faskin, Timmins and Miche townships. A very narrow volcanic septum separates this pluton from the Watabeag Batholith. The pluton is wholly surrounded by metavolcanic rocks interpreted to be correlated with the Tisdale assemblage (*see* Figure 22). In the southern portion of the pluton it is divided into 2 lobes (eastern and western) by a north-northwest trending metavolcanic septum.

Critical exposures along the eastern contact of the pluton (near sample location 7235, *see* Figure 22) permit some constraints on the timing of pluton emplacement in relation to tectonic and metamorphic processes. At this location, the Blackstock pluton and related dikes crosscut a composite D_1-D_2 fabric along the eastern margin of the pluton in Timmins Township (note that D_1 and D_2 are used in a local sense and no regional structural correlation with events recognized elsewhere is implied). The D_1 fabric, which is defined by lower to middle amphibolite grade mineral assemblages (amphibole and garnet), is tightly folded by a second deformational event with attendant development of a second fabric parallel to the axial surface of the folds. Many of the dikes appear to transect the D_2 fabric; however, some dikes emplaced approximately parallel to the axial surface have been boudinaged and rotated (Figure 29c and d). In addition, some dikes oriented at high angles to D_2 axial surfaces are buckled although the amplitude of these folds is less than that of folded foliation surfaces. These relationships suggest that the pluton was emplaced subsequent to the imposition of the D_1 peak metamorphic fabric and was broadly synchronous with D_2 deformation.

A sample (7235; UTM 516485E 5348190N, NAD83) of hornblende-biotite grandiorite was selected for LA-ICP-MS and TIMS U/Pb geochronology as part of this study in an attempt to further constrain the timing of emplacement and contact relationships described above. Zircons analyzed by both LA-ICP-MS and TIMS are mostly highly discordant. The least discordant LA-ICP-MS analyses have $^{207}Pb/^{206}Pb$ ages mostly in the range 2680 to 2755 Ma suggesting the presence of inheritance. The 2 least (~4%) discordant TIMS analyses have slightly different $^{207}Pb/^{206}Pb$ ages (2678 Ma and 2687 Ma) further suggesting the

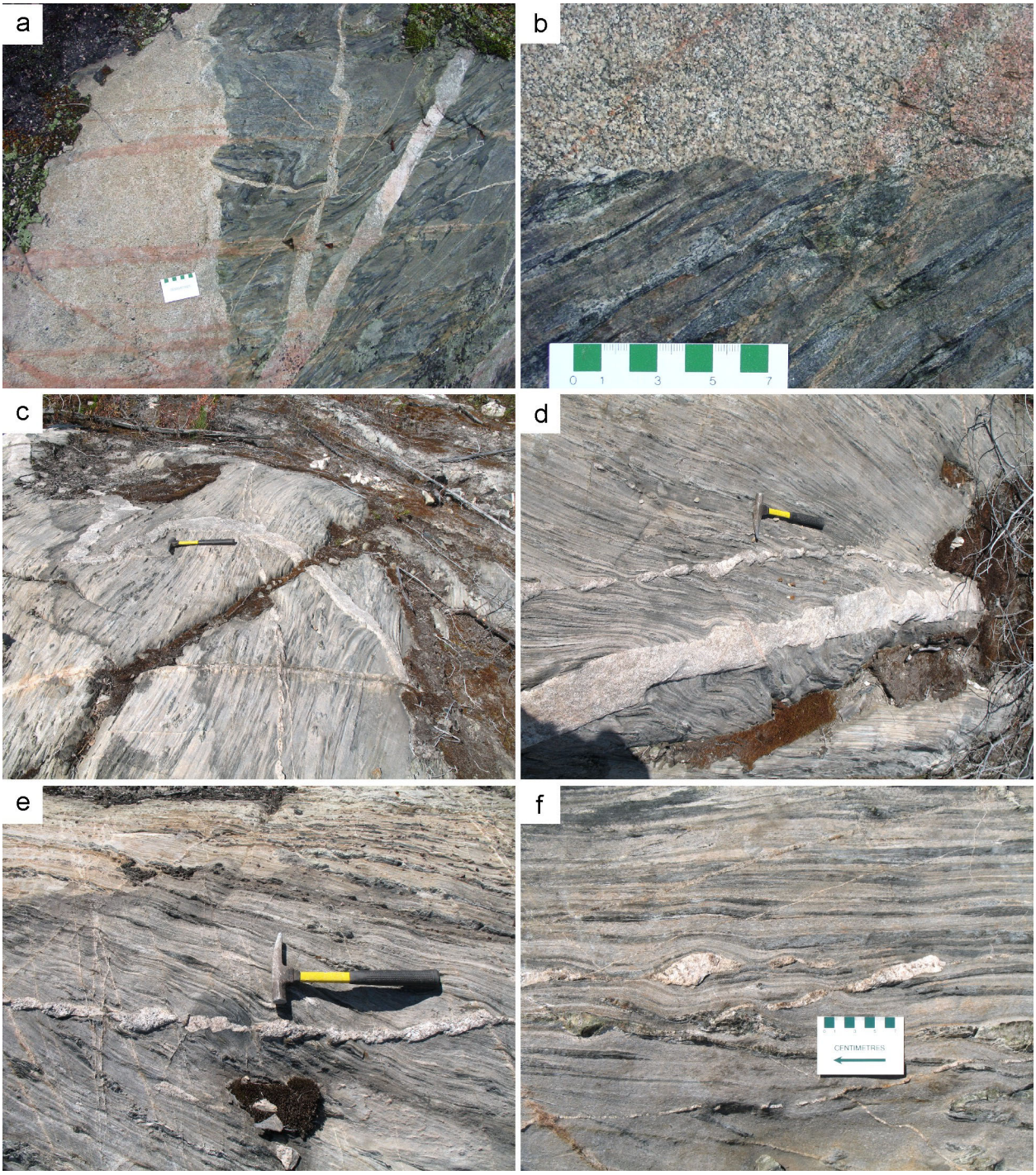

Figure 29. Field photographs illustrating relative timing relationships between the Blackstock pluton and structural and metamorphic elements in adjacent country rocks. Both the plutons and associated dikes are observed to sharply crosscut a well-developed, deformational fabric in the country rock defined by alignment of near-peak metamorphic mineral assemblages (a and b). The fabric is folded by subsequent deformation, which also either folds or boudinages and/or shears dikes depending on their orientation (c-f).

presence of inheritance. The age of this unit is not well constrained because of complex Pb loss behavior and the presence of inheritance but the youngest $^{207}Pb/^{206}Pb$ ages may approximate the maximum age of emplacement.

PETROLOGY

All samples selected from the Blackstock pluton are hornblende-biotite granodiorite; however, the eastern and western lobes are texturally distinct and have minor mineralogical differences (Figure 30). Samples from the western portion of the pluton are medium grained with moderately well-developed microcline megacrysts whereas those from the eastern portion are medium grained and equigranular. The majority of microcline in the former occurs as megacrysts up to 3 cm long that appear subhedral in outcrop but in thin section are observed to have irregular margins, often with marginal myrmykite. The megacrysts are weakly perthitic and contain abundant inclusions of virtually all other primary minerals occurring in the rock, with plagioclase inclusions typically having distinct albitic rims. In contrast to the western lobe, microcline in the eastern lobe occurs as interstitial grains similar in size to associated quartz and plagioclase. These interstitial grains are not perthitic but do contain some inclusions of most other mineral phases occurring in the rock.

A further difference between the 2 lobes is the slightly higher colour index of the western lobe (compare Figure 30a and b). The amphibole (magnesiohornblende with some secondary actinolite) is similar in composition. Primary accessory minerals (titanite, magnetite, apatite, zircon and sometimes epidote) are present in both lobes, with apatite and titanite being moderately abundant in some samples. Secondary minerals include white mica, epidote and carbonate (after plagioclase), chlorite and ilmenite (after biotite) and actinolite (after amphibole).

Both lobes of the pluton are characterized by the presence of volumetrically minor, but widely distributed dioritic to quartz monzodioritic enclaves and ultramafic clots (Figure 30d-f). The enclaves are fine to medium grained with a more melanocratic (CI ~25 to 50) character than the host granodiorite. Margins of enclaves range from sharp to diffuse. Ultramafic clots are less abundant with sharp to diffuse margins.

GEOCHEMISTRY

Whole rock geochemical data for the pluton exhibit broad similarities with those described for the Watabeag Batholith but also suggest that the eastern and western lobes of the pluton differ in certain respects. Three samples from the western lobe (7242, 7243 and 7244) are very similar and a fourth sample (7567), from the northern portion of the pluton, is similar except for distinctly lower Sr and slightly lower LILE abundances. A single sample from the small Radisson Creek pluton, occurring just to the north of the Blackstock pluton, is very similar to the 3 samples (7235, 7236 and 7254) from the eastern lobe of the pluton.

Distinctive characteristics of the western lobe relative to the eastern lobe include higher Mg# (55 to 57 vs 41 to 46) and Cr (67 to 78 ppm vs 9 to 13 ppm) and Ni (26 to 28 ppm vs 5 to 9 ppm) abundances, respectively. The western lobe also has higher abundance of Y and HREE resulting in less fractionated REE patterns (Figure 31). Higher abundance of MgO and $Fe_2O_3^{total}$ in the western lobe is consistent with its more mafic character. The on-average slightly lower Al_2O_3 abundance of the western lobe gives rise to a weakly meta-aluminous character which subtly contrasts with the weakly peraluminous character of the eastern lobe. These differences suggest that either the 2 lobes are discretely sourced plutons or fractionated components of a single magma system. Fractional crystallization involving plagioclase is unlikely given

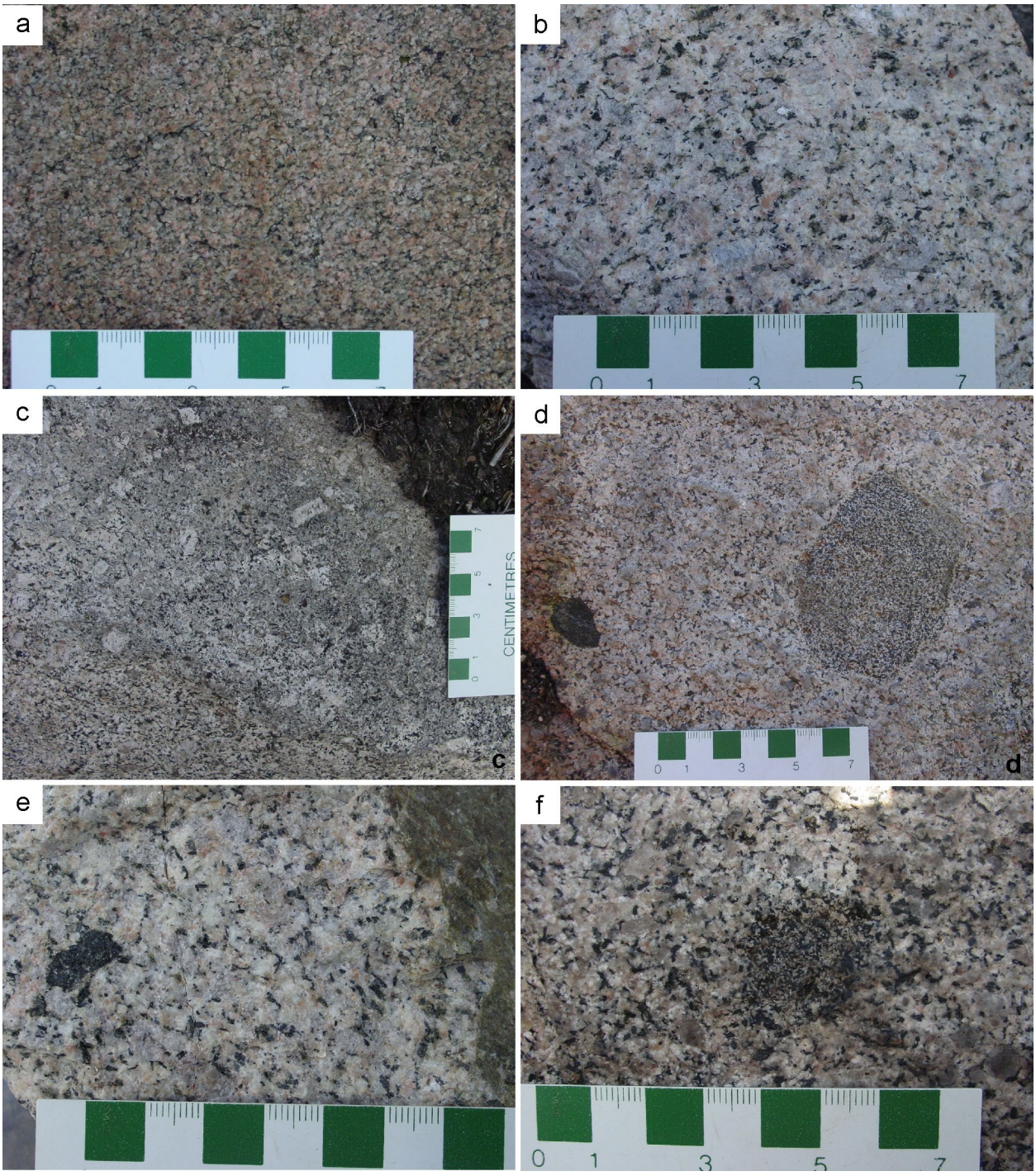

Figure 30. Field photographs illustrating textural and compositional characteristics of the Blackstock pluton. The eastern and western lobes of the pluton have contrasting equigranular (a) and microcline megacrystic (b and c) textures, respectively. Both lobes contain volumetrically minor, widely distributed mafic enclaves and ultramafic clots with sharply to diffusely bounded margins.

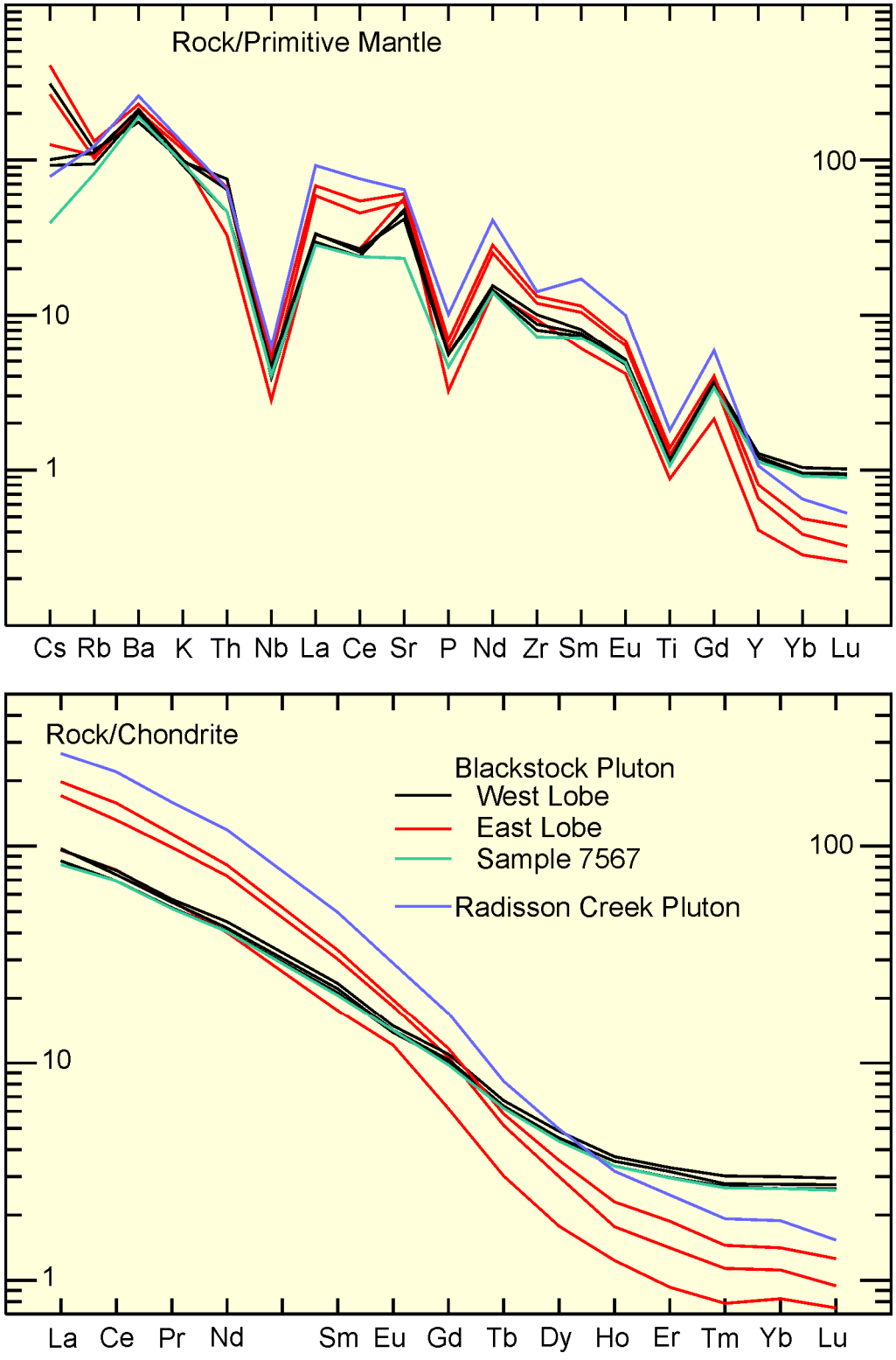

Figure 31. Chondrite and primitive mantle normalized trace element plots for samples from the Blackstock and Radissson Creek plutons. Normalization values from Sun and McDonough (1989).

the consistent absence of Eu anomalies and high abundance of Sr. Crystal fractionation involving hornblende could explain the divergent Mg# and compatible element abundances as well as the HREE depletion and fanning pattern of the REE patterns; however, the consistency of compositions within each lobe and absence of intermediate compositions make discrete sources a more appealing explanation for the contrasting character of the 2 lobes.

PETROGENESIS

As discussed above, the Blackstock pluton may actually represent 2 discretely sourced plutons. The high Mg# and Cr and Ni abundances of the western lobe suggest it was derived from, or extensively interacted with, an ultramafic source. Somewhat elevated LILE abundances suggest that either the ultramafic source was either metasomatically enriched or the magma was contaminated during ascent and emplacement.

The eastern lobe does not retain evidence for involvement of an ultramafic reservoir. Many of the general characteristics, including mildly peraluminous character, high Al_2O_3 and Sr abundance and highly fractionated REE with near chondritic HREE, are comparable to high-Al TTG interpreted to be derived by melting of a garnetiferous mafic source. Slightly elevated LILE suggest either the source must include a subordinate enriched component or the primary magma underwent fractionation and/or assimilation during ascent.

Adams Pluton

FIELD RELATIONSHIPS

The Adams pluton underlies approximately 186 km^2 principally within Adams, McArthur and Price townships (Pyke 1975, 1978, 1982). The pluton is not well exposed; however, most exposures are characterized by a very similar hornblende-biotite granodiorite phase and much of the pluton has a uniform, subdued aeromagnetic expression suggesting that the pluton is relatively uniform.

The pluton intrudes metavolcanic rocks of the Tisdale assemblage, which is interpreted to lie within the age range of 2710 to 2703 Ma (Ayer et al. 2002). Along the western side of the pluton, the contact lies in close proximity to the base of the Tisdale group and the pluton may locally cut the underlying Deloro assemblage (2730 to 2724 Ma), but in a regional sense the pluton lies primarily within the Tisdale assemblage just above the basal contact. The possible significance of this relationship is discussed in a subsequent section of the report.

The contact of the pluton is generally conformable with stratigraphy in the greenstone belt (Pyke 1982). Details of the pluton contact were observed in only 1 location (UTM 471465E 5355102N, NAD83). At this location, the pluton intrudes pillowed mafic volcanic rocks and crosscuts a moderately well-developed tectonic deformational fabric defined by near-peak metamorphic mineral assemblages (Figure 32a and b). The contact here is also a loci for emplacement of late dike phases, which are otherwise rare within the pluton, and the very localized development of a second tectonic fabric within the pluton parallel, and in close proximity, to the contact (Figure 32b). Evidence for the presence of this fabric in adjacent country rocks was not observed. Elsewhere in the pluton a weak fabric is locally developed but is interpreted to be a magmatic flowage fabric rather than a superimposed tectonic deformational fabric (see discussion in following section). These observations suggest that the Adams pluton was emplaced subsequent to the development of the main regional deformational fabric and the initial stages of regional metamorphism. As the pluton crystallized inward, the hot, but largely crystalline, margins were very

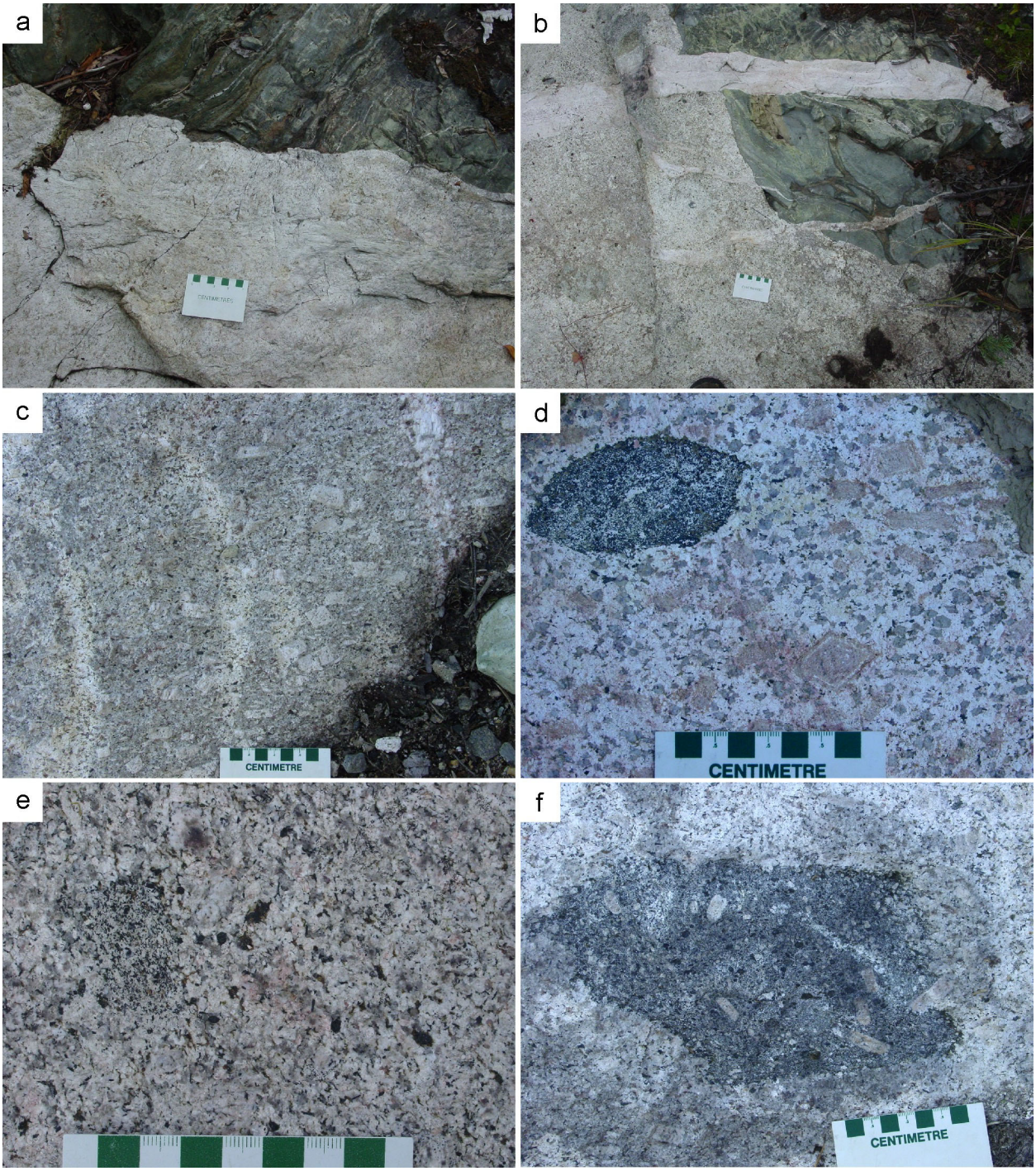

Figure 32. Field photographs illustrating contact relationships and textural and compositional characteristics of the Adams pluton. In an exposure at the northeast contact of the pluton, both the pluton and late dikes crosscut a weakly to moderately well-developed fabric within adjacent pillowed mafic volcanic rocks (a and b). Well- to incipiently developed microcline megacrysts (c-e) occur throughout the pluton. Volumetrically minor mafic enclaves with sharply to diffusely bounded margins (d-f) and rare ultramafic clots are widely distributed within the pluton. Rarely, megacrysts are developed within dioritic enclaves and (on the right side of the enclave in f) transect the enclave-host contact.

locally strained in response to ongoing emplacement. In the early stages, this deformation imposed the second fabric within the pluton margins whereas at later stages it developed brittle fracturing which focused the emplacement of late granitic dikes originating within partially crystallized interior portions of the pluton.

A U/Pb zircon age determination of 2686.4 ± 2.8 Ma for the Adams pluton (Frarey and Krogh 1986) places a minimum age constraint on the near-peak metamorphic development of the main regional deformational fabric in the vicinity of the Adams pluton. Consequently, the development of this fabric either predates or is broadly synchronous with Porcupine Group sedimentation and predates deposition of the Timiskaming assemblage. The significance of this interpretation is discussed in a subsequent section.

PETROLOGY

The Adams pluton is characterized by a predominant granodiorite phase that exhibits relatively limited variation in texture and composition. The predominant phase is a medium-grained, grey to pinkish grey, potassium-feldspar megacrystic, massive to weakly foliated, hornblende-biotite granodiorite. Potassium-feldspar megacrysts are equant to tabular and range in maximum dimension up to 5 cm but are mostly 2 to 3 cm in maximum dimension (Figure 32c-e). In some cases the megacrysts form anhedral masses that may be difficult to distinguish but are most commonly subhedral to approaching euhedral crystals. They are characteristically poikilitic with abundant, small inclusions of virtually all other minerals occurring in the rock. Most abundant are plagioclase inclusions, generally oligoclase but often having albitic rims that are often concentrated within specific zones of the megacrysts. The margins of even the most euhedral megacrysts have, in detail, irregular, optically continuous apophyses extending intergranularly between plagioclase, quartz and other phases surrounding the megacrysts. Although the megacrysts are commonly randomly oriented, they locally are aligned parallel to the alignment of the long axes of enclaves and clots suggesting that they are in some cases aligned by flowage of magma prior to crystallization. These relationships suggest that the megacrysts are not phenocrysts or porphyroblasts but rather grew as poikilitic megacrysts at a relatively late stage of crystallization.

Mafic mineralogy consists of hornblende and biotite, typically in subequal proportions and totalling approximately 10% of the rock by volume. Hornblende is generally quite fresh but may be locally altered to actinolitic amphibole along the margins of crystals or along fractures. Biotite is variously altered to chlorite and minor Fe-Ti oxide. Oxide minerals are predominantly disseminated magnetite octohedra responsible for the moderately elevated magnetic susceptibility (generally 7 to 8 SI units). Primary magmatic accessory minerals include moderately abundant apatite, titanite and epidote as well as trace amounts of zircon and rutile.

Secondary mineralogy is generally weakly developed and attributable to deuteric alteration and consists of partial replacement of plagioclase by a mixture of white mica, epidote and carbonate, chlorite ± Fe-Ti oxide after biotite and actinolite and, rarely, chlorite + magnetite after hornblende.

Small (less that 30 cm and typically less than 10 cm in longest dimension), oblate enclaves composed of fine- to medium-grained diorite to quartz monzodiorite with color index ranging from 25 to 50 are widely distributed in the granodiorite but are volumetrically minor, comprising less that 1% of all outcrops. Generally the margins of the diorite enclaves are quite sharp; however, locally the contact with the host granodiorite is gradational (Figure 32d-f). Mineralogy is dominated by plagioclase and hornblende along with varying proportions of quartz, potassium feldspar and biotite as well as trace amounts of epidote, titanite and apatite. In some cases, potassium feldspar is present as megacrysts, similar to those in the host granodiorite and rarely observed to crosscut the margins of the enclave (Figure 32f). This not

only provides further evidence for the late stage (as opposed to early phenocrystic) growth of megacrysts but also suggests that the granodiorite and diorite coexisted as magmas.

In addition to enclaves, very minor ultramafic clots occur locally in the granodiorite. They are composed predominantly of hornblende along with subordinate biotite that is compositionally similar to the same phases in the host granodiorite. These clots are interpreted to be cognate inclusions composed of agglomerated early crystallizing mafic phases.

GEOCHEMISTRY

The Adams pluton has fairly uniform geochemical characteristics that are broadly similar to those of other syntectonic plutons (*see* Figures 24 to 27). Moderately elevated Mg# (50 to 53) and Cr (23 to 46 ppm) and Sr (500 to 940 ppm) abundances are noteworthy. Abundance of incompatible elements are somewhat erratic but elevated compared to typical Archean TTG. Total REE abundance varies somewhat between samples (Figure 33) but all display similar fractionation (Ce_N/Yb_N ~24 to 28) with very weak negative Eu anomalies.

PETROGENESIS

Certain characteristics of the Adams pluton (moderately high Al_2O_3 and Sr abundances and HREE depleted, moderately fractionated REE) are comparable to typical high-Al TTG. However, other characteristics, notably elevated Mg# and moderate enrichment in both compatible and incompatible elements, are transitional between values typical of high-Al TTG and sanukitoid suite plutons and difficult to reconcile with the former model.

The relationships discussed above are not diagnostic of a particular petrogenetic model; however, the consistently elevated Mg# suggests that the magma was derived from or extensively interacted with an ultramafic (mantle) reservoir. The most probable petrogenetic scenarios that could explain the data include a primary, silica-saturated, metasomatized mantle melt (sanukitoid) modified by fractionation and/or assimilation during ascent or interaction of a deeply sourced mafic melt (high-Al TTG) with a metasomatized mantle reservoir.

Geikie Pluton

FIELD RELATIONSHIPS

The Geikie Pluton underlies approximately 103 km^2 primarily within Geikie and Douglas townships. No outcrops were examined within the small, northern lobe of the pluton which has a somewhat lower total magnetic field intensity, suggesting it may be somewhat different than the main portion of the pluton to which the ensuing discussion pertains. The predominant phase throughout the pluton is a granodiorite very similar to that occurring in the Adams pluton and exhibiting limited variability. The total magnetic field for the main lobe is generally uniform and comparable in intensity to that characterizing the Adams pluton; however, the intensity of the total field locally increases somewhat near the contact. This may indicate a weak zonation with a more melanocratic margin; however, there is insufficient exposure to evaluate this possibility.

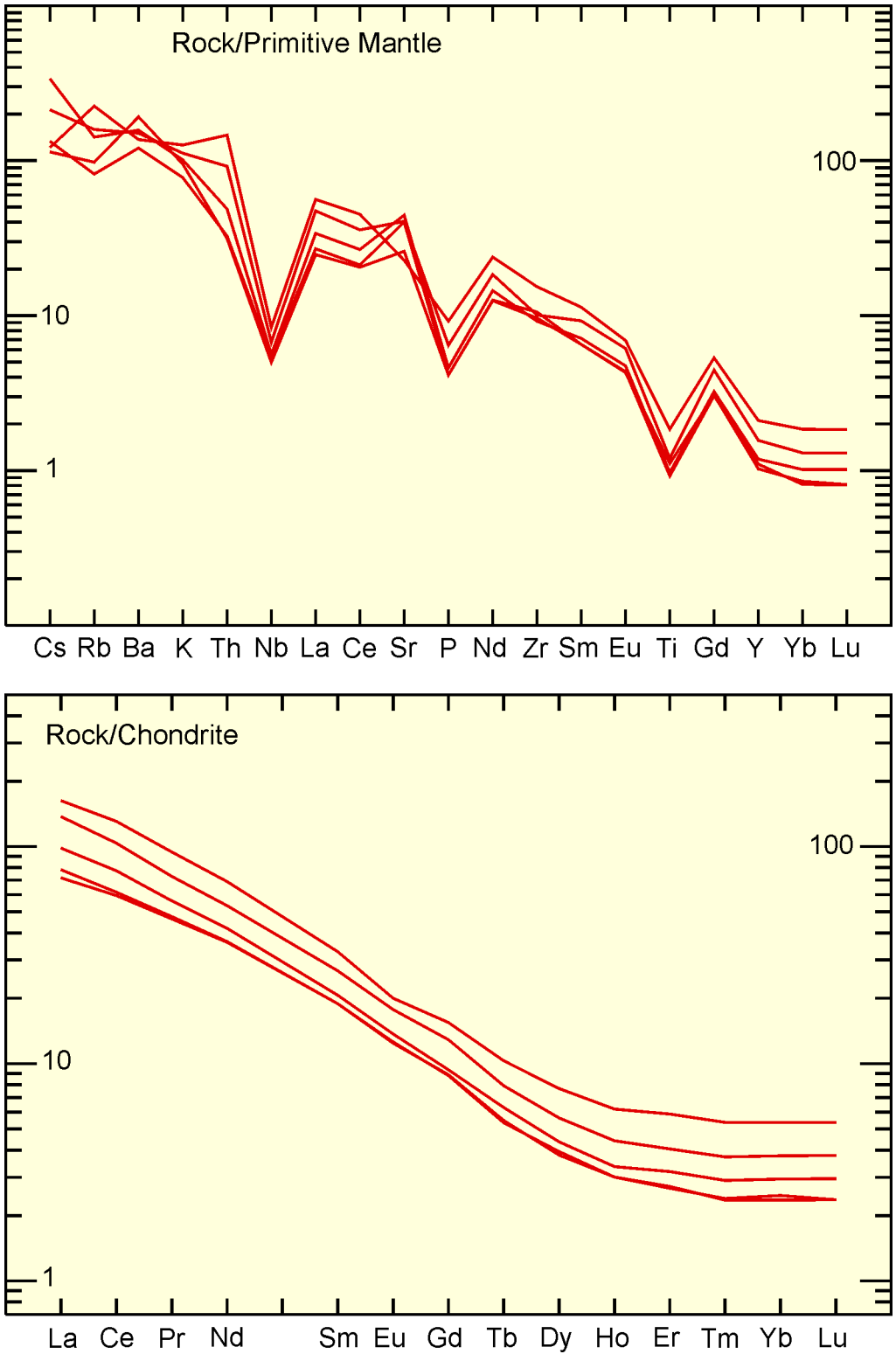

Figure 33. Chondrite and primitive mantle normalized trace element plots for samples from the Adams pluton. Normalization values from Sun and McDonough (1989).

The contact of the pluton was not observed; however, in one exposure near the southwestern contact of the pluton, inclusions of country rock in the pluton provide some constraint on relative timing of pluton emplacement. Here, well-foliated country rock inclusions are incorporated in the pluton (Figure 34). The fabric in the inclusions is sharply truncated by the pluton and this, together with the random orientation of the fabric in adjacent inclusions, demonstrates that the fabric was imposed on the country rock prior to emplacement of the pluton. In addition, some granitic veins within the inclusions are variously buckled and boudinaged, suggesting they were emplaced either during the final stages of fabric formation or during subsequent folding of the fabric.

A sample (7452; UTM 487741E 5331074N, NAD83) of hornblende granodiorite was selected for LA-ICP-MS and TIMS U/Pb zircon geochronology as part of this study in an attempt to further constrain the timing of emplacement. LA-ICP-MS analyses display a wide range in discordance, with some analyses characterized by very high common Pb. $^{207}Pb/^{206}Pb$ ages for the least (>5%) discordant analyses display a wide range (2610–2720 Ma) and average approximately 2680 Ma. Three of 4 zircon fractions analyzed by TIMS are moderately discordant, with the fourth fraction lying just slightly above concordia. One of the discordant analyses (containing higher common Pb) lies just to the left of a discordia line defined by the other 3 analyses suggesting an upper intercept age of 2681.8 ± 4.2 Ma. This is interpreted to be a reasonable estimate of the time of emplacement of the pluton.

PETROLOGY

A limited number of samples from the Geikie Pluton exhibit a very limited range in mineralogy and texture. All samples are medium-grained, microcline megacrystic hornblende-biotite granodiorite. Plagioclase is oligoclase, locally with albitic rims, and commonly has zone-controlled alteration to a mixture of white mica, epidote and carbonate. Microcline occurs largely as subhedral to anhedral, weakly perthitic megacrysts up to 3 cm in diameter and, less abundantly, as small, homogeneous interstitial grains. Megacrysts are poikilitic with inclusions of virtually all other mineral phases occurring in the rock and are interpreted to be formed at a late stage of crystallization.

Colour index is approximately 10 to 15 with amphibole invariably being more abundant than biotite. Amphibole (magnesiohornblende) is generally relatively fresh with actinolitic rims being present locally. Biotite is generally strongly chloritized. Other primary magmatic minerals present in trace amounts include magnetite, titanite, epidote, apatite and zircon. Of these, titanite is relatively abundant in a number of samples.

Dioritic to quartz monzodioritic enclaves and rarer ultramafic clots as described for the Adams pluton are a volumetrically minor but widely distributed component within the pluton. As for the Adams pluton, examples of microcline megacrysts developing within both host and enclave are observed in the Geikie Pluton (*see* Figure 34f).

GEOCHEMISTRY

Five samples selected from the pluton have very similar whole rock geochemical characteristics and these are closely comparable to those of other syntectonic plutons (*see* Figures 24 to 27). The Geikie Pluton has relatively high abundance of Al_2O_3 (16.2 to 17.2 wt%) and Sr (700 to 1100 ppm) as well as relatively high Mg# (53 to 58). Incompatible element abundances (e.g., Rb ~97 to 130 ppm and Th ~10 to 33 ppm) are distinctly elevated compared to typical high-Al TTG and slightly higher compared to other syntectonic plutons. Relatively strongly fractionated REE (Ce_N/Yb_N ~31 to 34) with very weak negative Eu anomalies are broadly comparable to other syntectonic plutons (Figure 35).

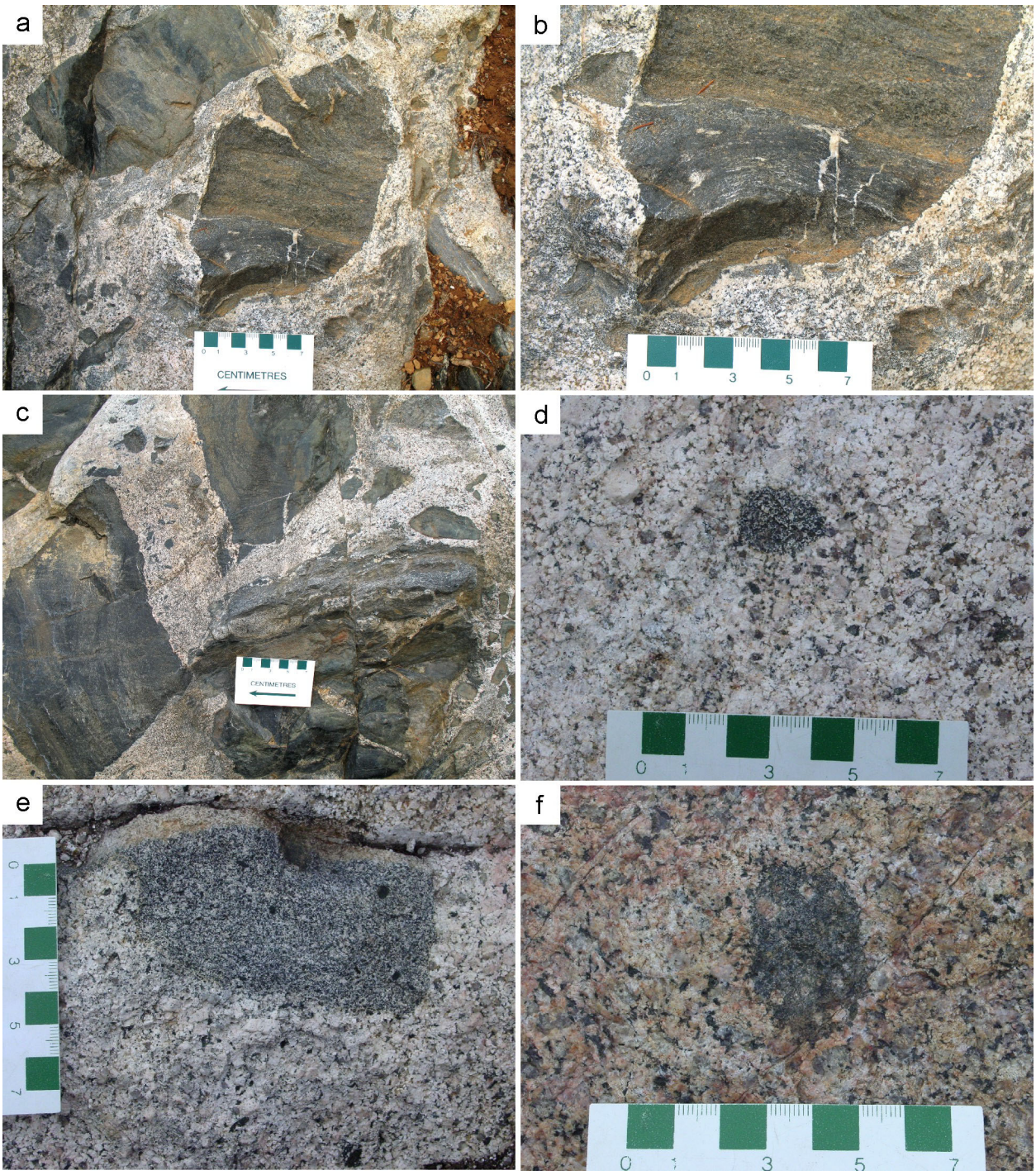

Figure 34. Field photographs illustrating contact relationships and textural and compositional characteristics of the Geikie Pluton. In an exposure near the southwest contact, the granodiorite contains inclusions characterized by a well-developed fabric defined by near-peak metamorphic mineral assemblages and locally cut by discordant veins that were subsequently buckled (a, enlarged in b). The granodiorite cuts the fabric in a number of randomly oriented inclusions (c). Variously developed microcline megacrysts and volumetrically minor but widely distributed diorite enclaves are ubiquitous (d-f). Locally, megacryst development is also observed in enclaves (f).

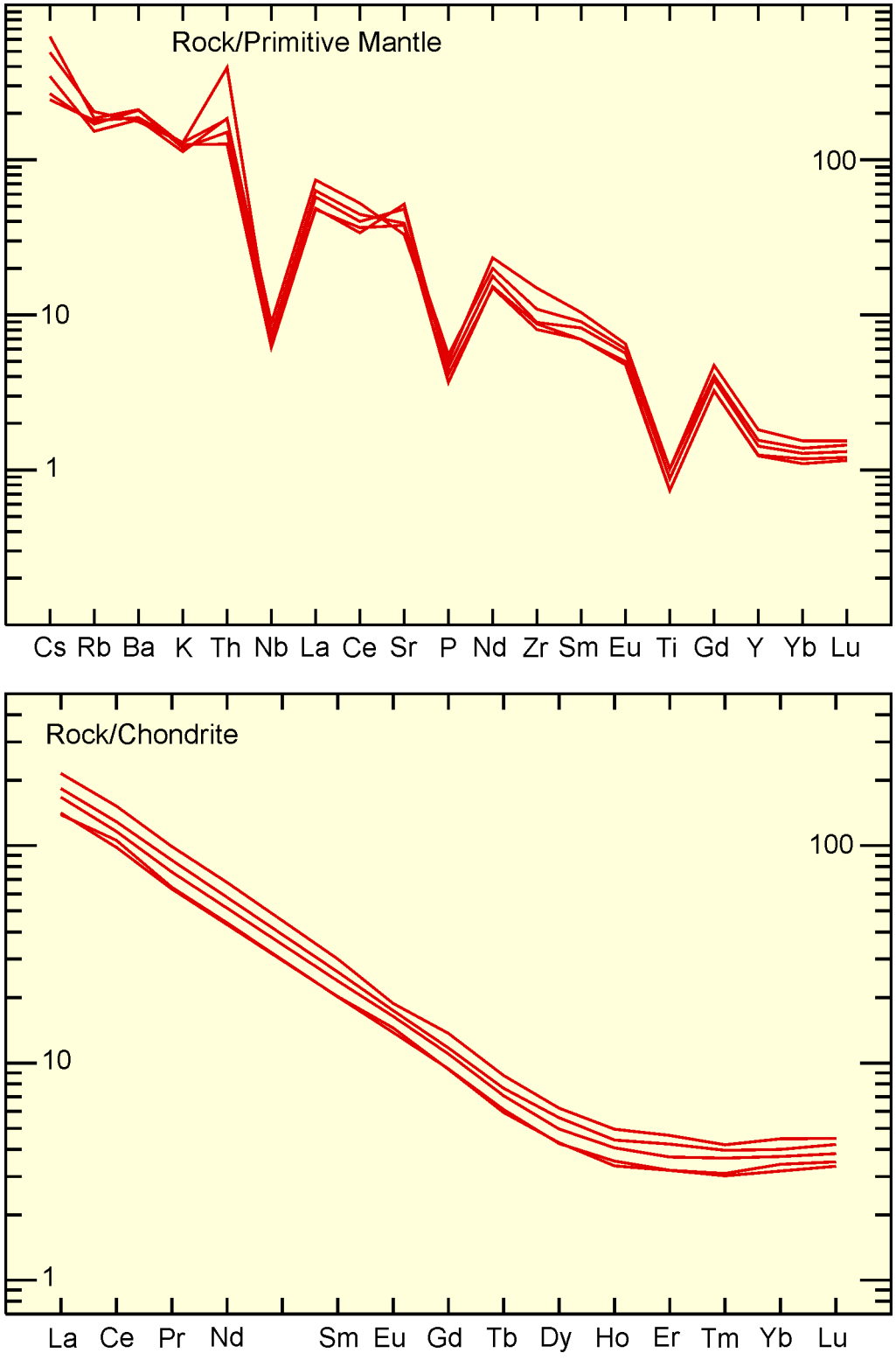

Figure 35. Chondrite and primitive mantle normalized trace element plots for samples from the Geikie pluton. Normalization values from Sun and McDonough (1989).

PETROGENESIS

The dual primitive (high Mg# and Cr abundance) and evolved (incompatible element enrichment) is similar to that described for the Adams pluton although both tendencies are somewhat more pronounced in the Geikie Pluton. The consistent elevated Mg# points to the involvement of a mantle reservoir in the generation of the Geikie Pluton.

Other Plutons

This section briefly describes a number of plutons that are tentatively assigned to the syntectonic group based on limited data.

FALLON PLUTON

Fallon pluton underlies approximately 19 km^2 in Fallon and Langmuir townships. The pluton is surrounded by metavolcanic rocks of the Tisdale assemblages but exposures of contacts or entrained country rock inclusions permitting assessment of contact relationships were not observed. Previous mapping (Pyke 1970, 1973) identified considerable compositional heterogeneity which was attributed to wall rock contamination. Consequently, the small number of samples from a number of closely spaced outcrops in the western portion of the pluton examined as part of this study may not be fully representative of the pluton as a whole.

Penetrative deformational fabrics were not observed within the pluton, although many outcrops have a preferred alignment of mafic minerals and feldspar phenocrysts that is interpreted to be a primary magmatic flowage fabric (Figure 36a). In one exposure, well-developed compositional layering, interpreted to be magmatic layering (Figure 36b), is present locally.

A sample (7568; UTM 4977301E 5344216N, NAD83) of flow-foliated, plagioclase-porphyritic hornblende quartz diorite was selected for LA-ICP-MS and TIMS U/Pb zircon geochronology. The LA-ICP-MS analyses are mostly less than 5% discordant but have moderately high common Pb. $^{207}Pb/^{206}Pb$ ages display a wide range (2650–2710 Ma) and average 2677 ± 20 Ma. The scatter may largely reflect analytical error associated with the common Pb correction as well as possible inheritance and Pb loss. The TIMS data is similarly mildly to moderately discordant, with the least discordant analyses having a range of $^{207}Pb/^{206}Pb$ ages from 2661 to 2688 Ma but not defining a discordia. These data cannot be used to rigorously constrain an age for the pluton but suggest it is relatively young (probably ~2680 Ma) and may contain some inheritance.

Predominant phases within exposures examined as part of this study are relatively mafic (CI ~20 to 35) hornblende monzodiorite to monzonite. Quartz is present in all thin sections examined; however, it is not abundant (<2%) and occurs as small interstitial grains. Variously altered (white mica, epidote, carbonate) plagioclase is invariably the predominant mineral. Cores of plagioclase are oligoclase; however, many grains have less altered rims that are albitic. Well-developed tabular phenocrysts (*see* Figure 36a) are present in many samples; however, most of the plagioclase occurs as grains in the medium-grained hypidiomorphic granular framework. Microcline occurs as fine- to medium-sized grains and, more rarely, as large tabular megacrysts. The fine- to medium-grained framework microcline is homogeneous whereas the rarer large crystals are perthitic and contain inclusions of plagioclase (always with albitic rims), hornblende and biotite. The margins of the megacrysts are irregular in detail and likely

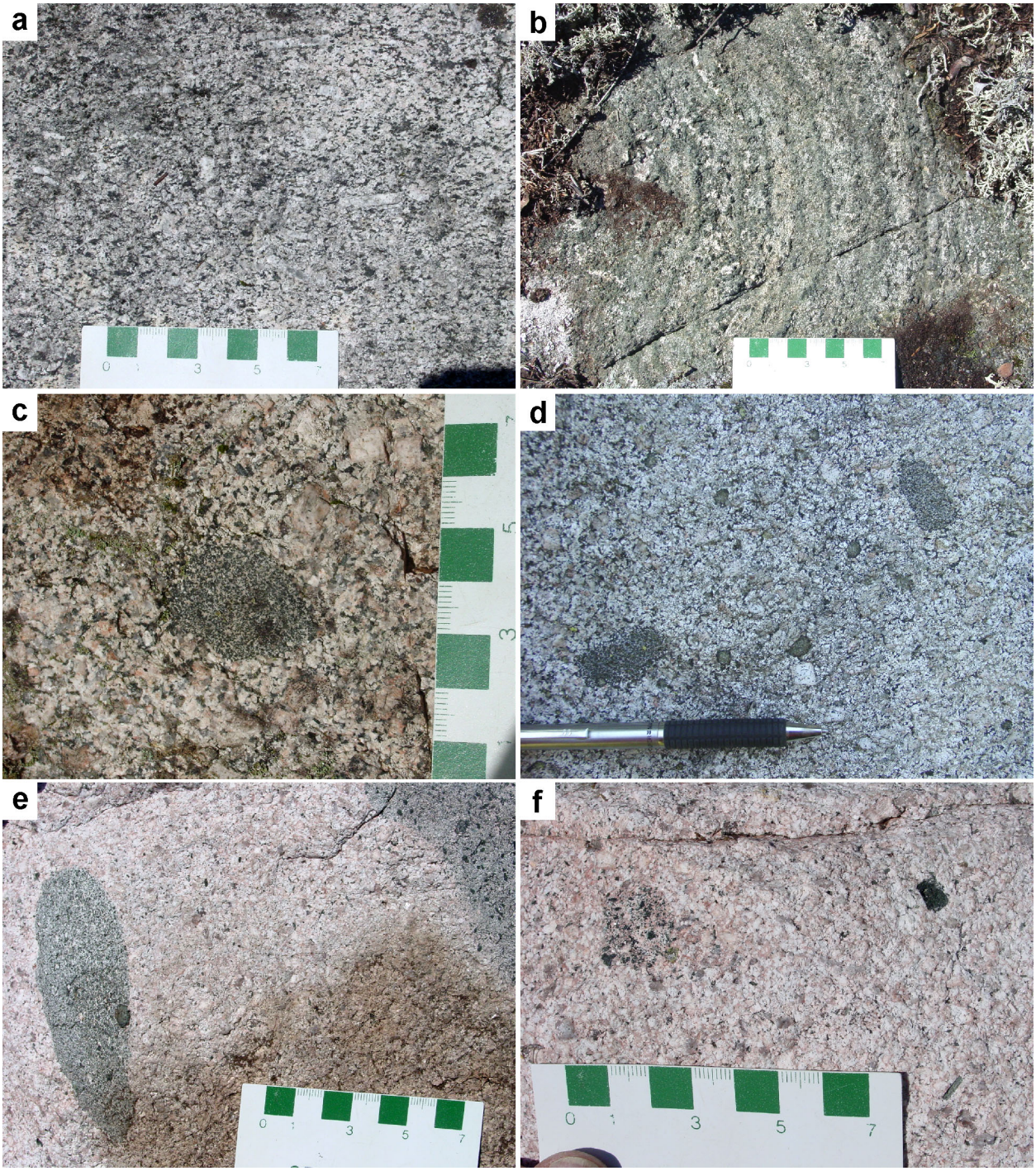

Figure 36. Field photographs illustrating textural and compositional characteristics of several syntectonic plutons: a) oriented feldspar phenocrysts in the Fallon pluton, b) probable magmatic layering within the Fallon pluton, c) and d) texture and enclaves within Hincks pluton, and e) and f) texture and enclaves within the Winnie pluton.

represent late magmatic megacrysts as in many other syntectonic plutons, but their distinctive tabular form is atypical.

Hornblende is always the predominant mafic mineral and occurs as subhedral to euhedral crystals and, less abundantly, as polycrystalline aggregates. Clinopyroxene is present in some samples and usually occurs as cores within hornblende. Biotite is present in some samples. Other primary magmatic minerals include magnetite, titanite, epidote, apatite and zircon. In many of the samples examined, titanite and apatite are unusually abundant accessory minerals.

Dioritic enclaves, which are finer grained and more mafic than the host phase, are a widespread but volumetrically minor component within the pluton. Ultramafic clots are minor; however, in one exposure, they are a component within well-developed layering (*see* Figure 36b) that is interpreted to be primary magmatic layering.

The geochemical characteristics of the Fallon pluton are distinctive in a number of respects compared to other plutons assigned to the syntectonic group. In part, these differences are a reflection of the quartz-poor, melanocratic character of the intrusion which results in lower SiO_2 and high Al_2O_3 and MgO (*see* Figure 24). The abundance of Na_2O and, in particular, K_2O is high for rocks containing 57 to 62% SiO_2 and imparts a distinctly alkalic character that is not as evident in other syntectonic plutons (*see* Figure 25). Elevated abundance of accessory minerals may explain the relatively high abundance of TiO_2 and P_2O_5 as well as a number of trace elements (Nb, Zr, Hf). Other noteworthy geochemical characteristics of the Fallon pluton include relatively high (especially viewed in the context of their relatively low SiO_2) abundance of Sr, Rb, Th and U, moderately fractionated REE (Figure 37) and enrichment in both MgO and K_2O relative to most syntectonic plutons (*see* Figure 27).

HINCKS PLUTON

The exposed surface area of the Hincks pluton is only 5 km^2; however, the central portion of the pluton is overlain by Proterozoic sedimentary rocks which probably conceal a comparable surface area at the Archean–Proterozoic unconformity. No country rock contacts or entrained inclusions were observed but the pluton is interpreted to be syntectonic based on the absence of superimposed tectonic fabrics and similarity to other syntectonic units.

A sample (7532; UTM 498202E 5323385N, NAD83) of weakly microcline-megacrystic, hornblende granodiorite was selected for LA-ICP-MS and TIMS U/Pb zircon geochronology. The LA-ICP-MS analyses are mostly highly discordant, with only 23 of 70 analyses being within 5% of concordia and with many analyses having relatively high common Pb. These least discordant analyses have a very large range of $^{207}Pb/^{206}Pb$ ages, from improbably young (<2450 Ma, with most of these "younger" zircons having large analytical errors, which suggests problems with the analysis) to relatively old (>2731 Ma, suggesting the possible presence of an inherited component). Only 2 zircon fractions were analyzed by TIMS and both of these are highly discordant. The age of this unit cannot be constrained at this time because of analytical problems, extreme Pb loss and possible inheritance.

All exposures examined are hornblende-biotite quartz monzodiorite to granodiorite and display a limited range in composition and texture. Textural variation is limited to differential development of microcline megacrysts, which are present in all exposures examined but range from indistinct, anhedral, highly poikilitic crystals to well-formed, subhedral megacrysts with less abundant inclusions. Dioritic enclaves are volumetrically minor but widely distributed (Figure 36c and d).

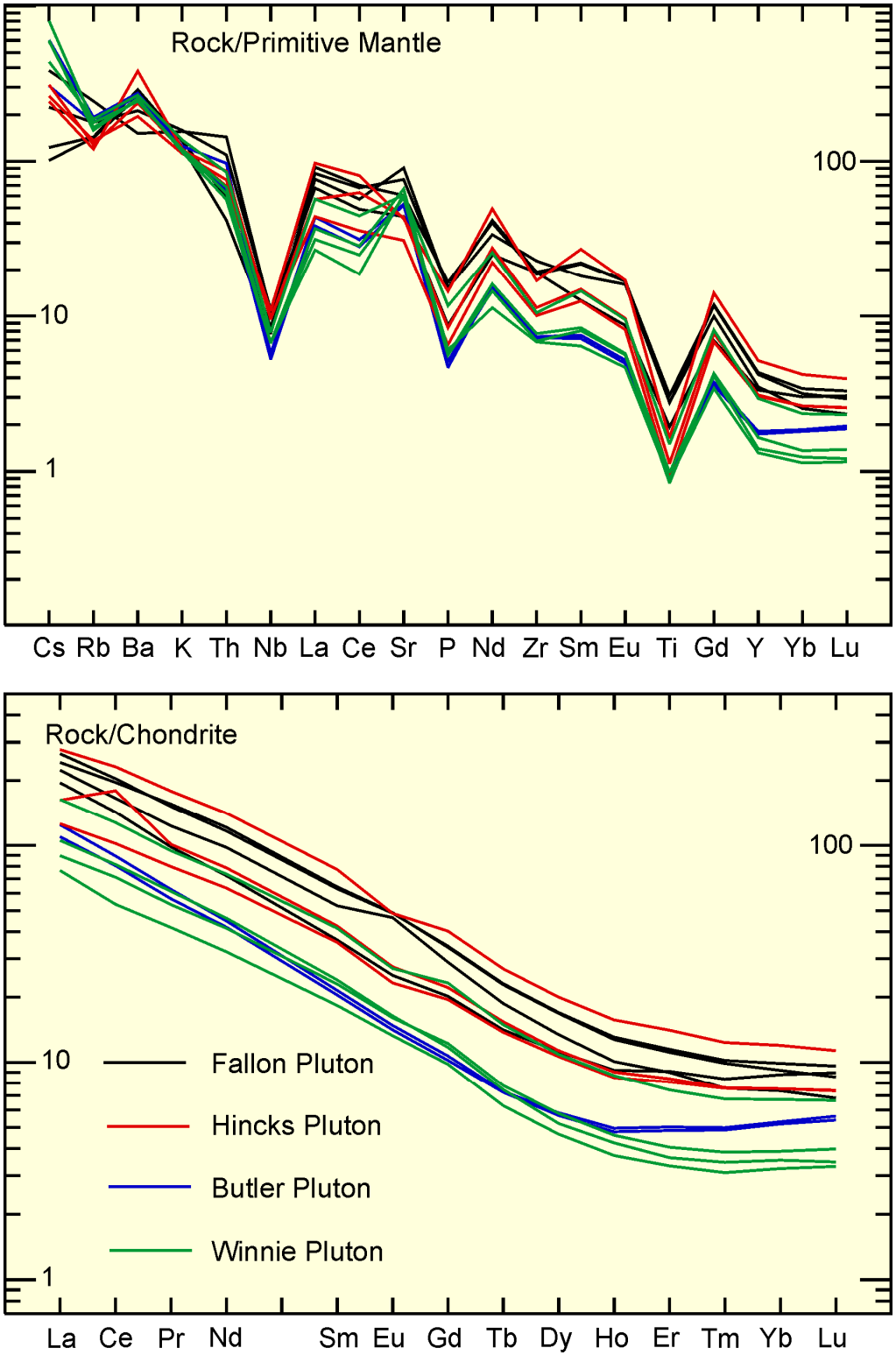

Figure 37. Chondrite and primitive mantle normalized trace element plots for samples from the Fallon, Hincks, Butler and Winnie plutons. Normalization values from Sun and McDonough (1989).

Plagioclase occurs as subhedral to euhedral crystals with zone-controlled alteration to white mica, epidote and carbonate. Sodic oligoclase (~An_{10} to An_{15}) compositions predominate with narrow albitic rims being common, especially in contact with microcline. Microcline occurs both as small, homogeneous interstitial grains and, more abundantly, as anhedral to subhedral, poikilitic, perthitic megacrysts. Quartz occurs as interstitial anhedral crystals.

Colour index is fairly uniform in the range of 12 to 18. Hornblende is the greatly predominant mafic phase and occurs as subhedral to euhedral magnesiohornblende crystals with only minor and local secondary alteration at crystal edges to actinolite. Biotite is present as tabular crystals that are extensively chloritized and constitute only 1 to 2% of the rock. Other primary magmatic minerals present in minor to trace amounts include magnetite, titanite, apatite and zircon.

Three samples exhibit fairly consistent geochemical characteristics. All samples are meta-aluminous and have relatively high abundance of LILE, Na_2O and Al_2O_3 (*see* Figures 24 to 25) although one of these has lower SiO_2 and consequently plots in the alkaline field (*see* Figure 26). A distinctive characteristic is high Mg# (60 to 64) and Cr abundance (40 to 115 ppm). HFSE, including REE abundances, are relatively high compared to other syntectonic plutons. Rare earth element fractionation (Ce_N/Yb_N ~14 to 24) and subtle negative Eu anomalies are typical of other syntectonic plutons.

Although limited data are available, the relatively high abundance of incompatible elements coupled with high compatible element abundance and high Mg# strongly implicates significant involvement of an enriched mantle reservoir in the petrogenesis of the Hincks pluton, suggesting affinity with the sanukitoid suite.

BUTLER LAKE PLUTON

The Butler Lake pluton is poorly exposed but is interpreted to underly approximately 5 km^2 with a small area at the southern end of the intrusion likely concealed beneath Proterozoic sedimentary rocks. The pluton intrudes metavolcanic rocks assigned to the Blake River assemblage. No superimposed tectonic fabrics were observed and the pluton is lithologically similar to other syntectonic plutons leading to its tentative assignment to this group.

A sample (7575; UTM 554316E 5355001N, NAD83) of weakly microcline-megacrystic, hornblende granodiorite was selected for LA-ICP-MS and TIMS U/Pb zircon geochronology. The LA-ICP-MS analyses are mostly moderately discordant, with only 18 of 48 analyses being within 5% of concordia. These least discordant analyses have a range of $^{207}Pb/^{206}Pb$ ages from 2648 to 2708 with a mean age of 2686 ± 16 Ma. TIMS analysis of 4 zircon fractions are moderately to slightly discordant (2.7 to 13%) but are relatively collinear (0.29 probability of fit) and define an upper concordia intercept age of 2681.0 ± 2.7 Ma which is interpreted to be a reliable estimate of the age of emplacement of the pluton.

Two samples investigated in detail are texturally and compositionally uniform medium-grained, weakly megacrystic hornblende granodiorite. Dioritic enclaves and ultramafic clots, common in other syntectonic plutons, were not observed in the Butler Lake pluton. Plagioclase is sodic oligoclase to albite (An_{12} to An_4) occurring as subhedral to euhedral crystals with zone-controlled alteration to white mica, epidote and carbonate. Microcline occurs as 5 to 30 mm diameter anhedral, poikilitic crystals with extremely irregular contacts with enclosing plagioclase, quartz and hornblende. Quartz is interstitial to plagioclase and hornblende.

Amphibole (magnesiohornblende to edenite with local actinolitic alteration) comprises approximately 10% of the rock and is the dominant dark-coloured mineral. Traces of chloritized biotite occur locally. Other primary magmatic minerals include magnetite, titanite, epidote, apatite and zircon.

The geochemical characteristics of 2 samples are virtually identical and very similar to those characterizing the nearby Watabeag Batholith.

WINNIE PLUTON

The Winnie pluton underlies approximately 22 km^2 within metavolcanic rocks interpreted to be related to the Blake River assemblage. The pluton is tentatively assigned to the syntectonic group based on absence of superimposed tectonic fabrics and lithologic similarity to other syntectonic units. Only the western portion of the pluton was examined as part of this investigation.

Exposures examined range from relatively leucocratic (CI ~10), hornblende granodiorite to somewhat more melanocratic (CI ~20), hornblende quartz monzodiorite. No sharp contacts were observed between these 2 varieties and they are thought to be transitional into one another. The more mafic units were observed near the margins of the pluton suggesting it may be compositionally zoned; however, more detailed mapping would be required to confirm this relationship. The pluton is dominated by a medium-grained, equigranular texture; however, both subtly quartz porphyritic and very weakly megacrystic (microcline) textural variants were observed in many outcrops.

Plagioclase (sodic oligoclase to albite) occurs as subhedral to euhedral crystals displaying zone-controlled alteration to white mica, epidote and carbonate. Microcline occurs dominantly as homogeneous, interstitial grains and secondarily as larger, anhedral, poikilitic, weakly perthitic crystals with very irregular margins. Quartz occurs as interstitial crystals and locally as larger, rounded phenocrysts.

Amphibole (magnesiohornblende with local, minor alteration to actinolite) is the sole or dominant mafic mineral. Traces of biotite (generally strongly chloritized) are present locally and minor clinopyroxene was noted in one thin section. Magnetite, titanite, apatite and zircon are other primary magmatic minerals occurring in minor to trace amounts.

Three of 4 samples exhibit similar geochemical characteristics (and closely resemble other syntectonic plutons) whereas a fourth sample, representative of the more mafic rim, is broadly similar in most respects but differs in being characterized by higher Mg# (59 vs 51 to 53) and Cr abundance (107 ppm vs 36 to 41 ppm). This more primitive character of the mafic rim can either be due to it representing a discrete magma or it being, in part, a cumulate phase. The latter is considered less likely because this sample is also slightly enriched in LILE relative to the more leucocratic units.

DISCUSSION

Plutons grouped in the syntectonic category are massive to very weakly foliated hornblende ± biotite (± rare clinopyroxene) granodiorite to quartz monzodiorites. Individual plutons tend to be fairly uniform compositionally and texturally; however, different plutons may be mineralogically distinct because of differences in color index, relative proportions of hornblende and biotite, magnetite content and accessory mineral assemblages.

The geochemical characteristics of these plutons rarely point definitively to a specific petrogenetic model; however, concomitant enrichment in both compatible and incompatible elements are interpreted to reflect an important role for a metasomatized mantle reservoir. Components of some plutons may also be consistent with derivation of some component of these magmas from partial melting of a mafic source. The implications of these conclusions will be discussed in a subsequent section dealing with the overall secular evolution observed within the Abitibi plutonic record.

Several of the plutons display contact relationships indicating that their emplacement postdates development of a deformational fabric defined by near-peak metamorphic mineral assemblages. The synfolding emplacement of dikes related to the Blackstock pluton and the location of some of these plutons (e.g., Adams, Geikie) in regional fold hinges further suggests that the plutons were emplaced synchronously with regional folding. Viewed in a regional sense, most of the syntectonic plutons are emplaced into the Tisdale assemblage, which is characterized by much shorter wavelength regional folds than other assemblages in the area. For example, the folding of stratigraphy within the Deloro and Tisdale assemblages in the vicinity of the Adams and Geikie plutons is markedly different and may be relevant to their emplacement. The Deloro assemblage is deformed into a single, relatively open, steeply plunging fold with a northwest-trending northern limb and a north-trending southern limb suggesting the unit has experienced limited north-south shortening. The Tisdale assemblage, in contrast, is characterized by a series of east-trending synclines and anticlines with map-patterns (Pyke 1978; Bright 1974a; Bright 1974b) suggesting this unit has undergone considerable north-south shortening. The fold axial surfaces on these maps are portrayed as terminating as the contact with the Deloro assemblage is approached. The Geikie Pluton appears to lie within the culmination of one of the major anticlinal folds. Relationships for the Adams pluton are less clear but it is at least in part associated with a synclinal fold structure. A possible explanation for the location of these plutons in fold structures just above the Deloro–Tisdale contact is that this contact has acted as a detachment surface above which disharmonic folds developed within the Tisdale assemblage into which the plutons were emplaced during folding.

To the east, several plutons (eastern contact of Watabeag Batholith, Winnie pluton, Butler pluton) intrude metavolcanic rocks correlated with the Blake River assemblage (the distribution of assemblages is not well constrained in this area) although in a regional context, syntectonic plutons are not widespread within the Blake River assemblage which is characterized by longer wavelength folding. Thus, the spatial association of syntectonic plutons within folded Tisdale assemblage units may not be fortuitous and differential deformation within tectonically bounded lithostratigraphic assemblages may have served to focus syntectonic plutonism.

Late-Tectonic Plutons

This section describes numerous small to moderately large plutons distinguished by their strongly alkalic character and interpreted to be emplaced at a late stage in the tectonic evolution of the Abitibi Subprovince. Most are concentrated in the vicinity of the Cadillac–Larder Lake (CLLF) and Porcupine–Destor (PDF) faults although small intrusions occur in the area between the 2 faults (e.g., Iris, Swan Lake) and well to the south in the New Liskeard area (Casey Mountain syenite). Because, in part, of the close spatial association of many of these plutons with gold mineralization, a number of studies have focused on different aspects of these intrusions (Ben Othman et al. 1990; Rowins et al. 1991; Rowins et al. 1993; Lesvesque et al. 1991; Lesvesque 1994; Hattori et al. 1996; Wilkinson et al. 1999; Pigeon 2003) and these units will not be described in comparable detail as those discussed above.

CHARACTERISTICS OF INDIVIDUAL PLUTONS

Otto Stock

The Otto Stock underlies approximately 90 km^2 centred in Otto Township (Figure 38). This unit has been discussed as part of a number of previous investigations (Smith and Sutcliffe 1988; Sutcliffe et al. 1990; Ben Othman et al. 1990; Hattori et al. 1996). An initial U/Pb age determination for the Otto Stock (Corfu et al. 1989) was subsequently revised (Corfu and Noble 1992) to an age of 2679 ± 1 Ma.

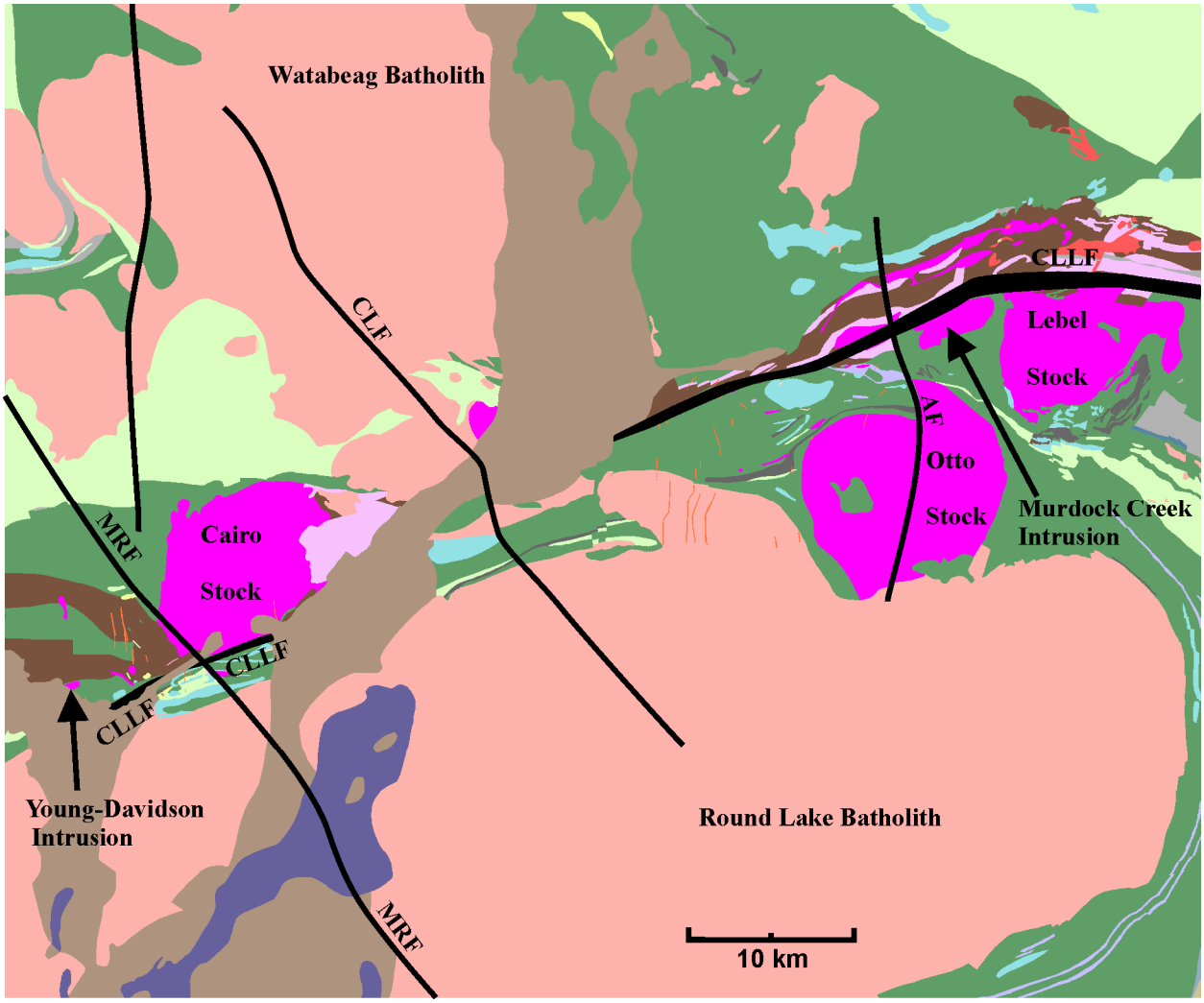

Figure 38. Generalized geological map illustrating the setting of late-tectonic alkalic plutons (e.g., Lebel, Murdock Creek, Otto, Cairo, Young–Davidson) in the Kirkland Lake–Matachewan area. Abbreviations: CLLF = Cadillac–Larder Lake fault, AF = Amikougami fault, CLF = Cross Lake fault, MRF = Montreal River fault.

FIELD RELATIONSHIPS

The stock lies just to the south of the CLLF and intrudes metavolcanic rocks assigned to the Pacaud, Stoughton–Roquemaure and Tisdale assemblages and the Round Lake batholith. The contact of the pluton was observed at only 1 location, on Highway 11, along the northern margin of the stock. Here, both country rock and some components of the pluton are highly strained although syenitic dike phases exhibit a range of relationships to this deformation ranging from moderately deformed to undeformed (Figure 39a-d). All other fabrics within the pluton are not penetrative and are attributed to either igneous layering or flow (Figure 39e and f).

It is difficult to access the significance of the intense deformation at the northern contact location because of uncertainty in its timing. Proximity to the CLLF, which is interpreted to have a long-lived, complex deformational history, is also problematic. For example, Isoplatov et al. (2005) concluded that 3 fabric-forming events postdate an nonfabric-forming event, the maximum age of which is constrained to be younger than 2677.7 ± 3.1 Ma (maximum age of Timiskaming metasedimentary rocks). More regionally, early fabric-forming events precede deposition of Timiskaming-type sequences and the emplacement of the Otto Stock, so it is considered probable here that deformation observed at the contact is a manifestation of a regionally later deformation, perhaps linked to the CLLF. The lack of penetrative deformational fabrics throughout the main body of the stock is consistent with this interpretation.

PETROLOGY

The Otto Stock exhibits considerable lithologic heterogeneity arising from a wide range of textures and a mineralogical continuum from felsic to ultramafic compositions. For the purposes of this discussion, components of the stock are broadly characterized as syenite, quartz syenite and melasyenite to ultramafic.

Medium- to very coarse-grained syenite is the predominant rock type within the stock. Coarsely porphyritic textures with large (up to 5 cm long) potassium-feldspar phenocrysts predominate; however, this texture locally grades into more subtly porphyritic to equigranular varieties (Figure 40a and b). Both hypersolvus (single alkali feldspar) and subsolvus (discrete sodic plagioclase and potassium feldspar) feldspar mineralogy are abundantly represented. Within subsolvus and exsolved hypersolvus varieties, potassium feldspar is always more abundant than plagioclase. Mafic mineralogy is quite complex with 2 types of amphibole, biotite and, more rarely, clinopyroxene being present. Amphibole is generally the most abundant mafic mineral phase and consists of both an olive green to brown amphibole (broadly calcic amphibole or hornblende) and a bluish amphibole (broadly sodic amphibole or riebeckite) (Figure 41a-d). Hornblende occurs as subhedral to euhedral discrete crystals whereas riebeckite occurs in a variety of habits, including i) discrete subhedral to euhedral grains (Figure 41a and b), ii) overgrowths on (Figure 41a) or replacement of (Figure 41c), hornblende and iii) large radiating masses of acicular crystals (Figure 41d). Magnetite is relatively abundant and locally is concentrated in wispy layers thought to reflect magmatic layering (*see* Figure 40f). Titanite is moderately to extremely (1 to 2% by volume) abundant. Apatite is also moderately abundant with zircon occurring in trace amounts.

Quartz syenite is similar to syenite in most respects except for the presence of up to 10% quartz and the absence of clinopyroxene. No sharp contacts were observed and syenite to quartz syenite are interpreted to be part of a compositional continuum.

With increasing colour index, syenite grades into melasyenite and ultramafic compositions. Contacts between more mafic units may either be gradational (Figure 40d) or sharp. Textures are highly variable;

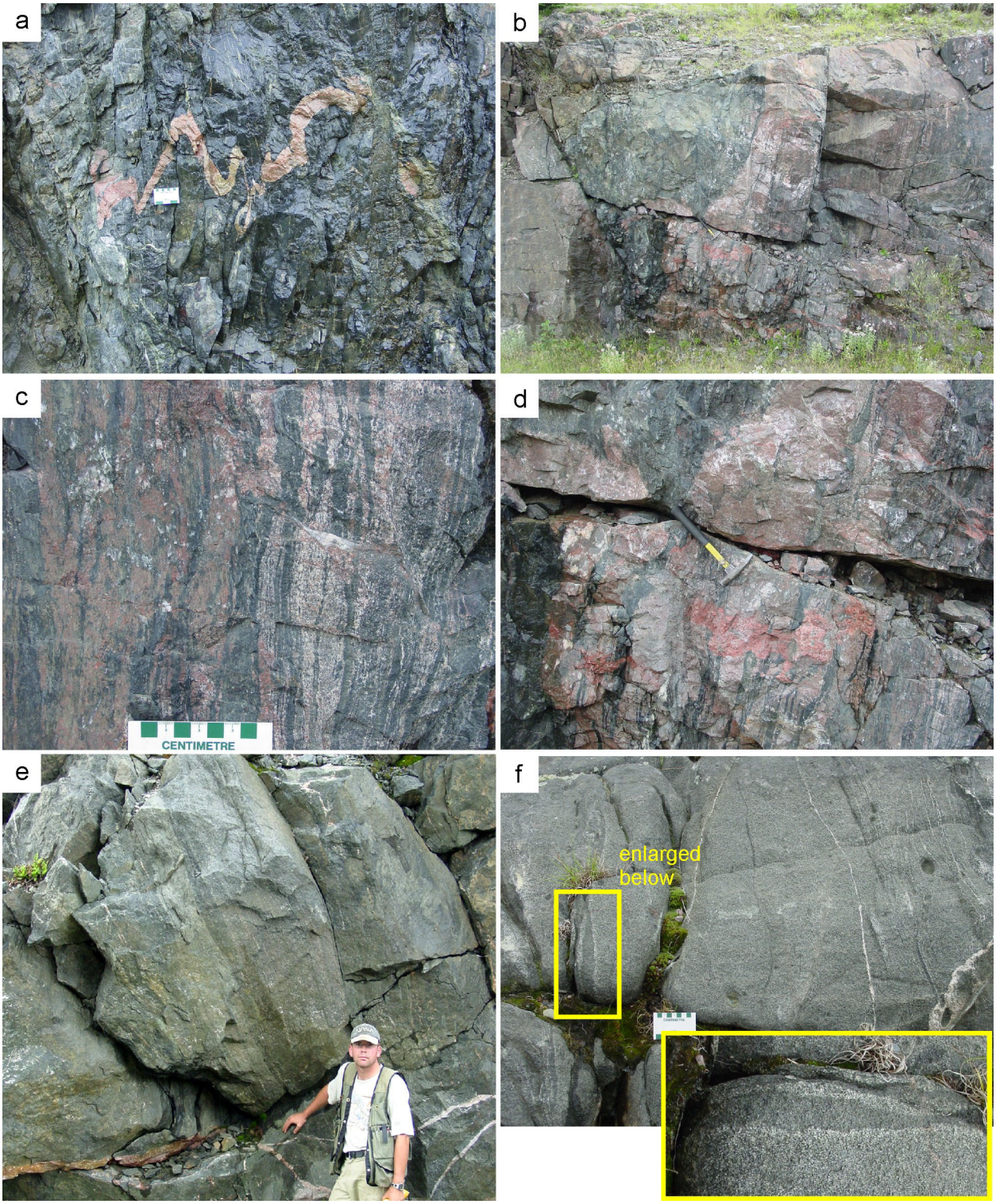

Figure 39. Field photographs illustrating contact relationships at the northern margin and compositional layering within the Otto Stock. Strongly deformed country rock contains variously deformed syenite dikes (a). Both country rock and syenite are strongly deformed at the contact (b and c) although late syenitic phases within this zone may be weakly deformed (d). Well-developed igneous layering (e and f) is recognized locally within weakly deformed units that characterize most of the interior of the stock.

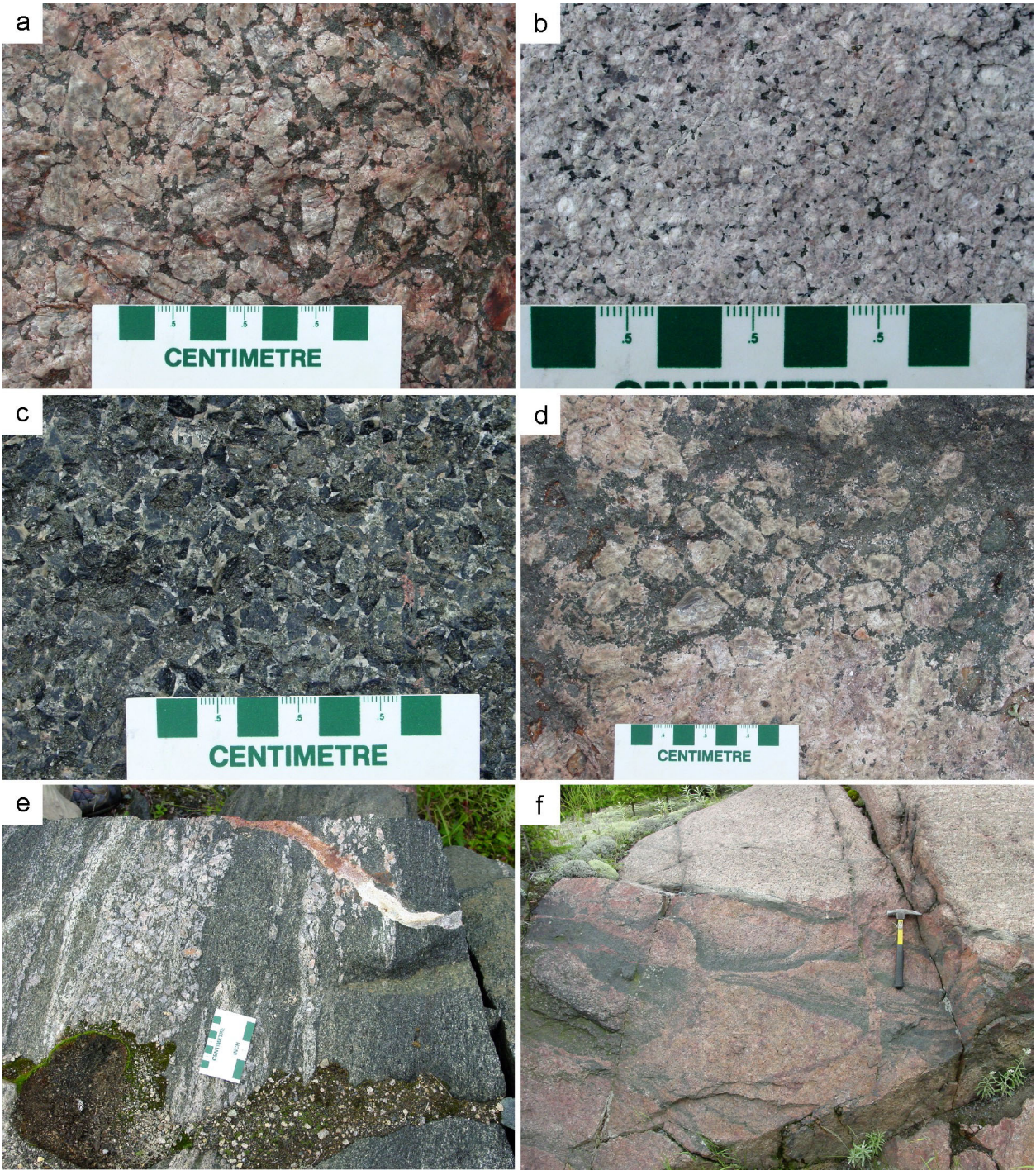

Figure 40. Field photographs illustrating textural and compositional characteristics of the Otto Stock. Much of the stock is underlain by coarsely porphyritic syenite (a). Less distinctly porphyritic and quartz-bearing units (b) are abundant in the interior of the stock. Ultramafic to mafic phases (c) are widespread and locally abundant and characteristically are intimately associated and may have gradational contacts with syenitic phases (d and e). Magnetite is generally relatively abundant within the intrusion and locally forms discontinuous, wispy compositional layering (f).

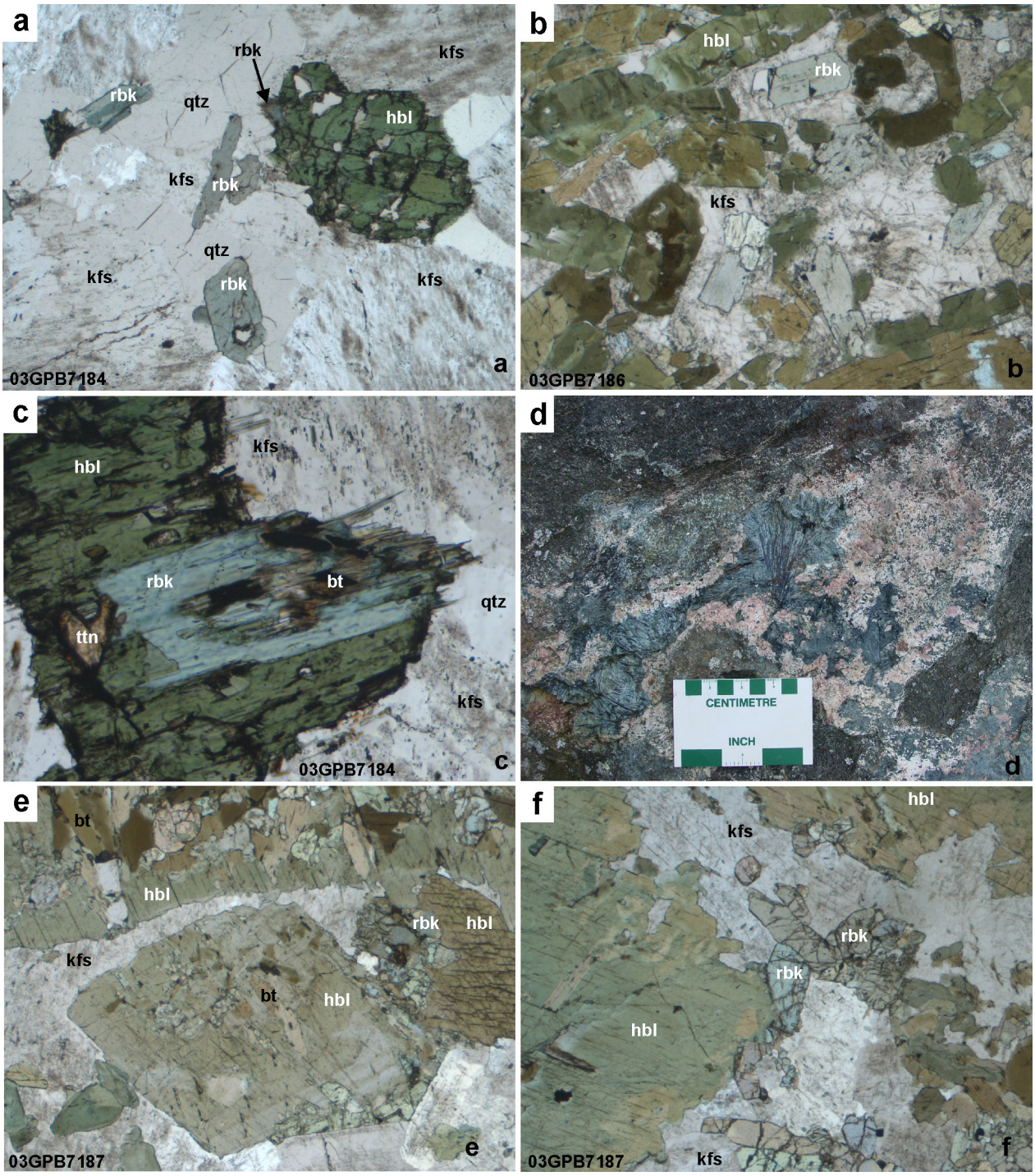

Figure 41. Photomicrographs and field photograph illustrating mineralogical and textural characteristics of the Otto Stock. Riebeckite (blue) and hornblende (olive green to brown) may coexist as discrete grains (a and b) or riebeckite may replace hornblende (c) or form large irregular radiating masses (d). Melasyenites contain large, subhedral to euhedral hornblende (often containing inclusions of biotite and, more rarely, clinopyroxene) surrounded by very large, optically continuous potassium feldspar within which most of the discrete riebeckite crystals occur (e and f). Abbreviations: bt = biotite, hbl = hornblende, kfs = potassium feldspar, qtz = quartz, rbk = riebeckite, ttn = titanite.

however, cumulate-type textures (Figure 40c) with feldspar-dominated intercumulus filling (Figure 41e and f) are common. Mafic minerals, in order of generally decreasing abundance, include hornblende, biotite, clinopyroxene and riebeckite. In general, there is a single alkali feldspar phase that characteristically forms large optically continuous grains enveloping ferromagnesian silicate phases. Other primary magmatic phases include magnetite, titanite and apatite.

GEOCHEMISTRY

Whole rock geochemical data for the Otto Stock indicate a broad range in bulk composition that reflects the diverse mineralogy. The apparent bimodality (melasyenite compositions with 45 to 52% SiO_2 and more leucocratic syenite to quartz syenite compositions with 60 to 70% SiO_2; Figures 42 to 44) in part reflects sampling methodology which avoided heterogeneous rocks with intermediate colour index that may be mixtures of the 2 components.

Despite the diverse geochemical characteristics, a number of general geochemical characteristics are present throughout the compositional spectrum. All samples have very high abundances of alkali elements for their respective SiO_2 abundances which imparts a strongly alkalic signature (Figure 45). All units have prominent negative Nb, P and Ti anomalies on extended trace element plots (Figure 46). Melasyenite units are particularly enriched in HFSE and Cr and have high Mg# whereas syenite and quartz syenite have more erratic abundances of these elements. Syenites have relatively abundant and moderately fractionated REE (Ce_N/Yb_N ~18 to 35) (*see* Figure 46). Mafic units have higher abundance of HREE but more weakly fractionated REE (Ce_N/Yb_N ~7 to 10) with the exception of one sample that contains very high abundances of all REE. Quartz syenites are less fractionated (Ce_N/Yb_N ~10 to 12) than the syenites and have lower overall REE abundances. All units are characterized by weak negative Eu anomalies.

PETROGENESIS

Results reported herein are consistent with those of a number of previous studies of the Otto Stock (Ben Othman et al. 1990; Sutcliffe et al. 1990). As discussed by Sutcliffe et al. (1990), the bulk composition and, in particular, elevated Mg# and Ni and Cr abundance points to equilibration with an ultramafic (mantle) reservoir; however, the abundance of LILE and LREE requires that this source be enriched. Sr and Nd isotopic characteristics are inconsistent with the enrichment being related to involvement of significantly older continental crust (Ben Othman et al. 1990; Hattori et al. 1996) and consequently mantle metasomatism is interpreted to be responsible for observed enrichment in LILE and LREE.

The origin of the exceptional compositional diversity displayed by components of the Otto Stock are likely complex. Sutcliffe et al. (1990) attributed some of the variation to amphibole ± feldspar fractionation. Amphibole fractionation may explain variation in REE fractionation; however, large variation in TiO_2, P_2O_5 and some high field strength elements suggests a role for accessory mineral fractionation which is consistent with unusually high abundance of titanite and apatite observed in many samples. It is also possible that some of the compositional diversity arises from different degrees of melting of the metasomatized mantle source.

Lebel Stock

The Lebel Stock underlies approximately 45 km^2, primarily within Lebel and Boston townships. Only a limited number of exposures were examined within the northern and western portions of the stock as a part of this investigation.

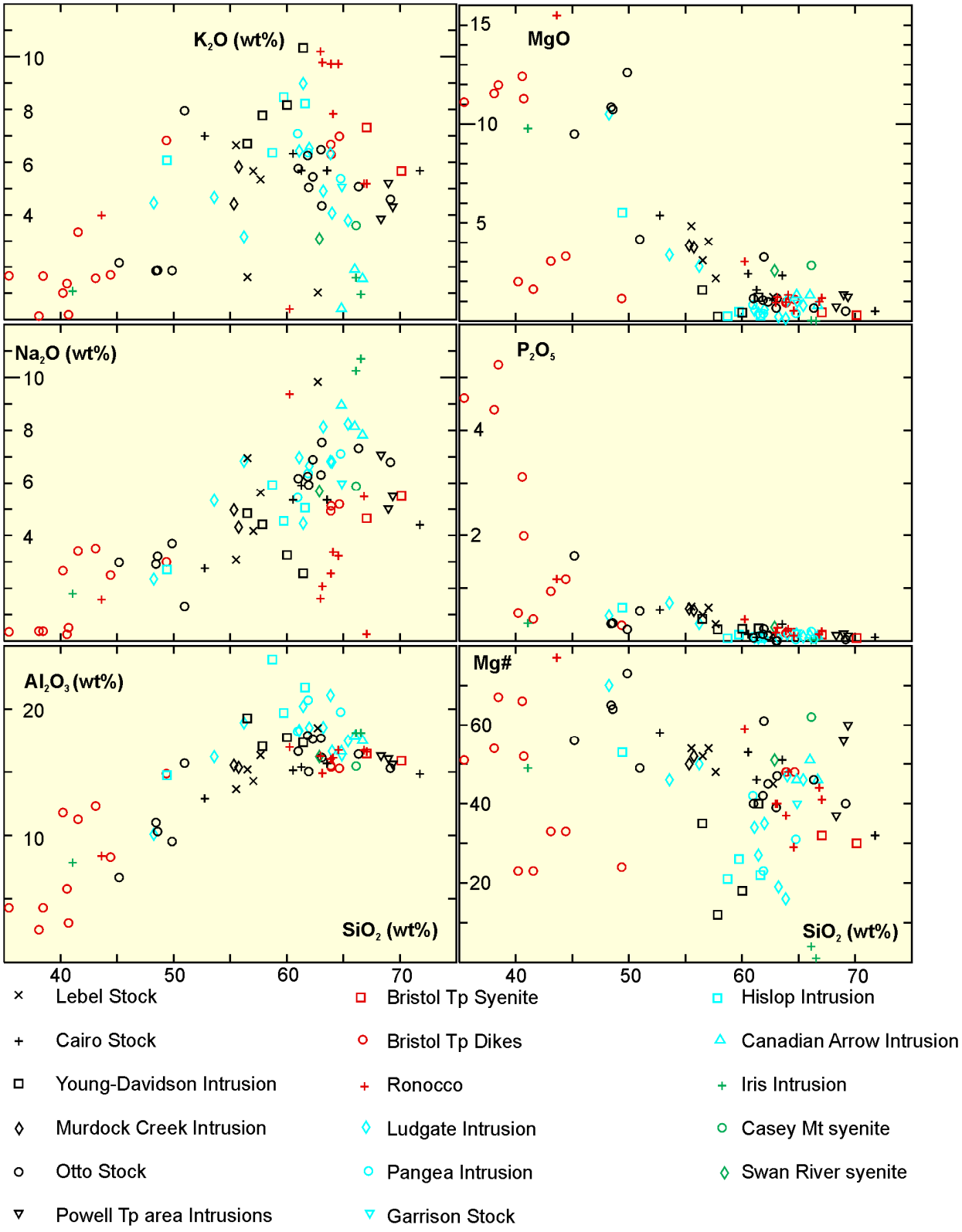

Figure 42. Harker variation diagrams for samples from the late-tectonic plutons and possibly correlative minor intrusions.

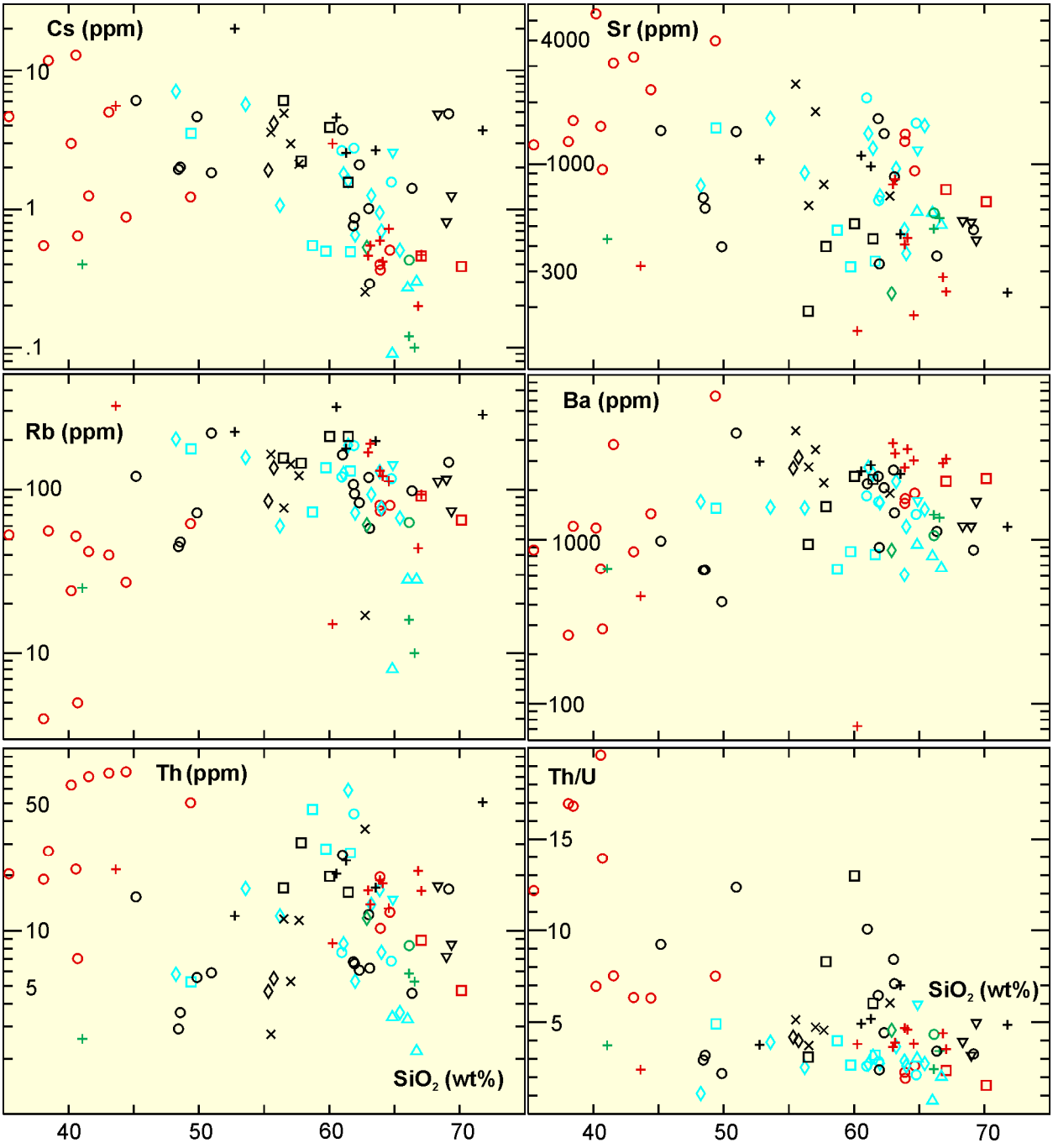

Figure 43. Harker variation diagrams for samples from the late-tectonic plutons and possibly correlative minor intrusions. Symbols same as for Figure 42.

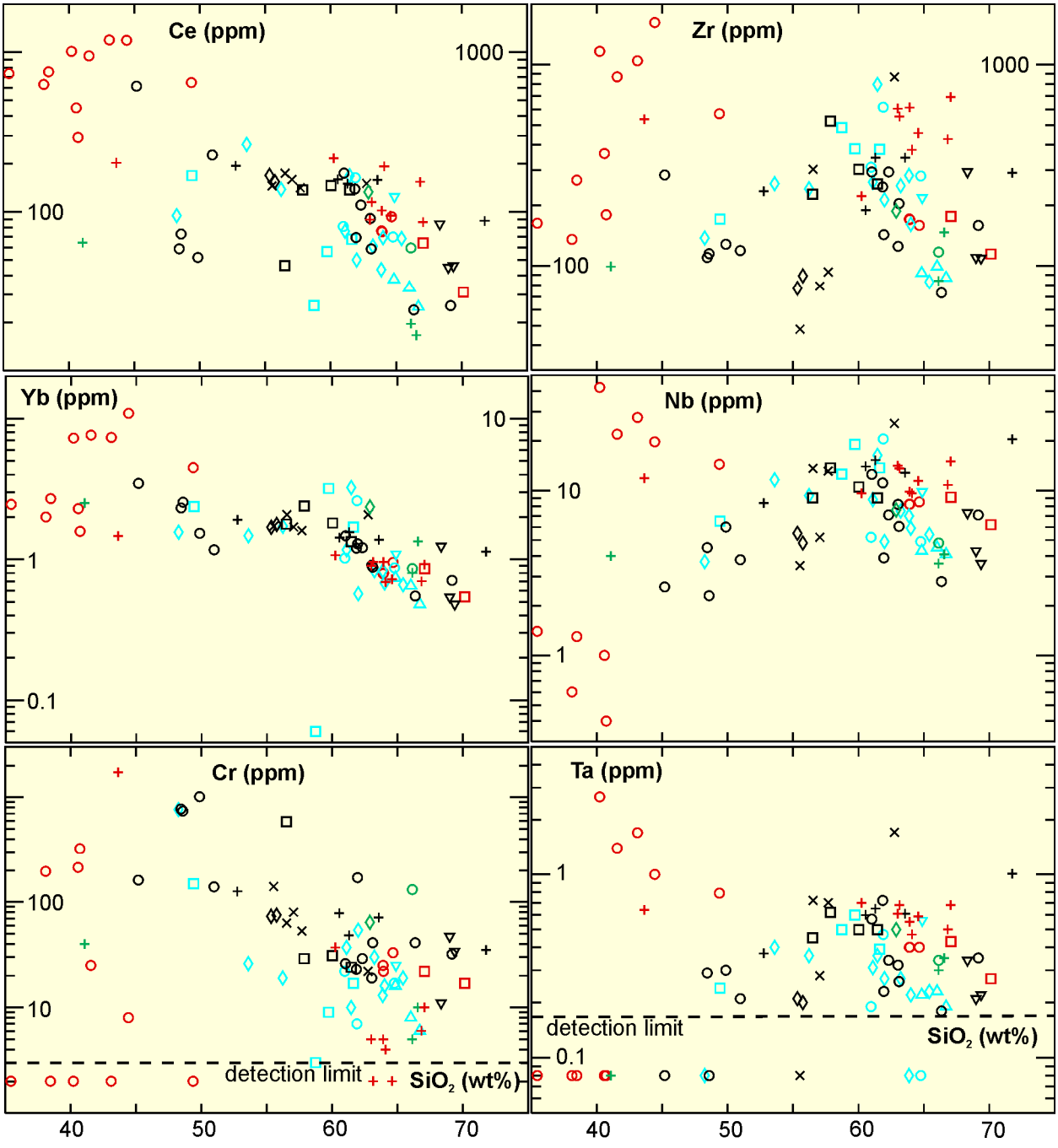

Figure 44. Harker variation diagrams for samples from the late-tectonic plutons and possibly correlative minor intrusions. Symbols same as for Figure 42.

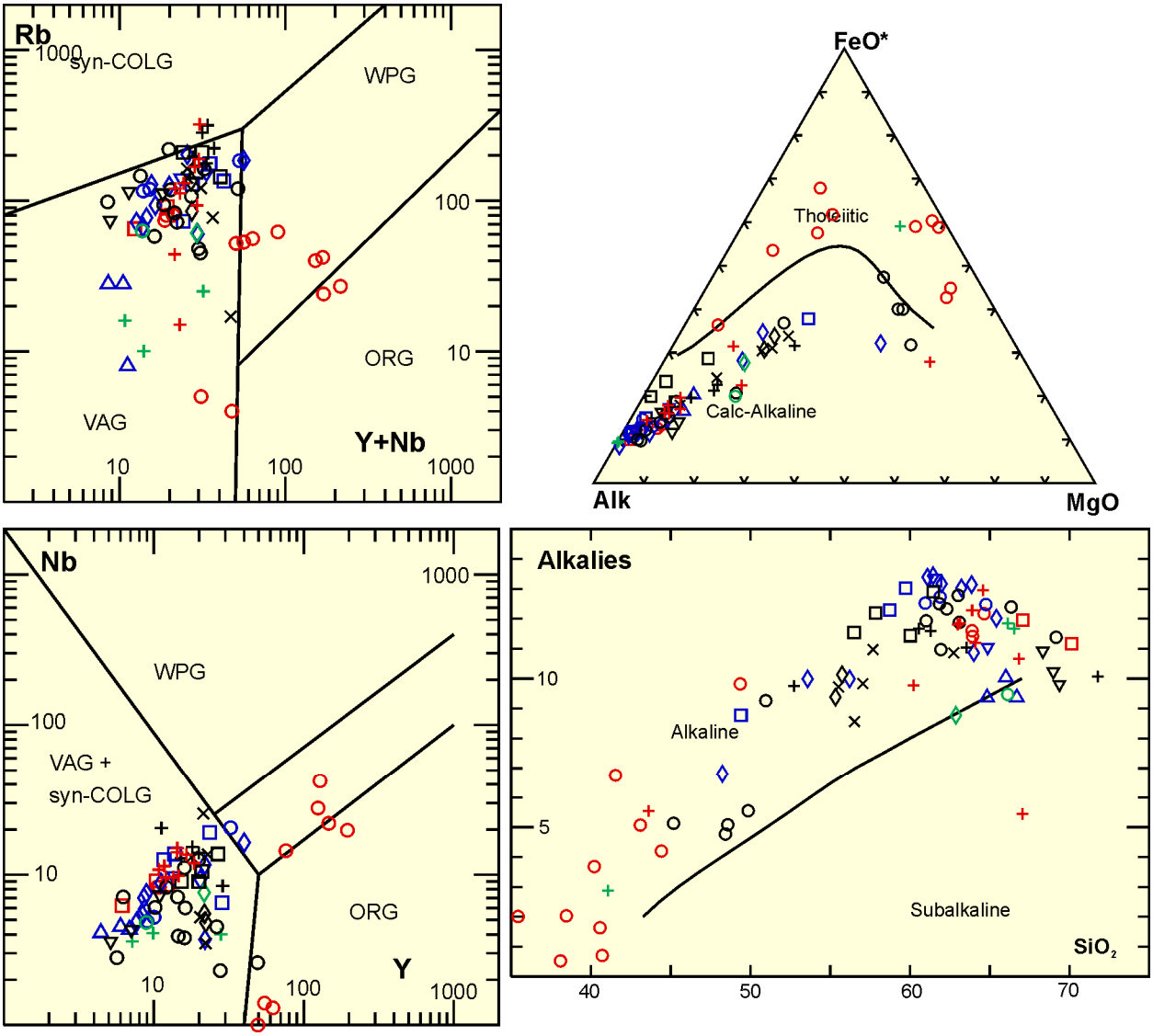

Figure 45. Tectonic discrimination diagrams for samples from the late-tectonic plutons. Rb vs Y+Nb and Nb vs Y plots are after Pearce et al. (1984). AFM and alkalies vs SiO_2 plots are after Irvine and Baragar (1971). Symbols same as for Figure 42.

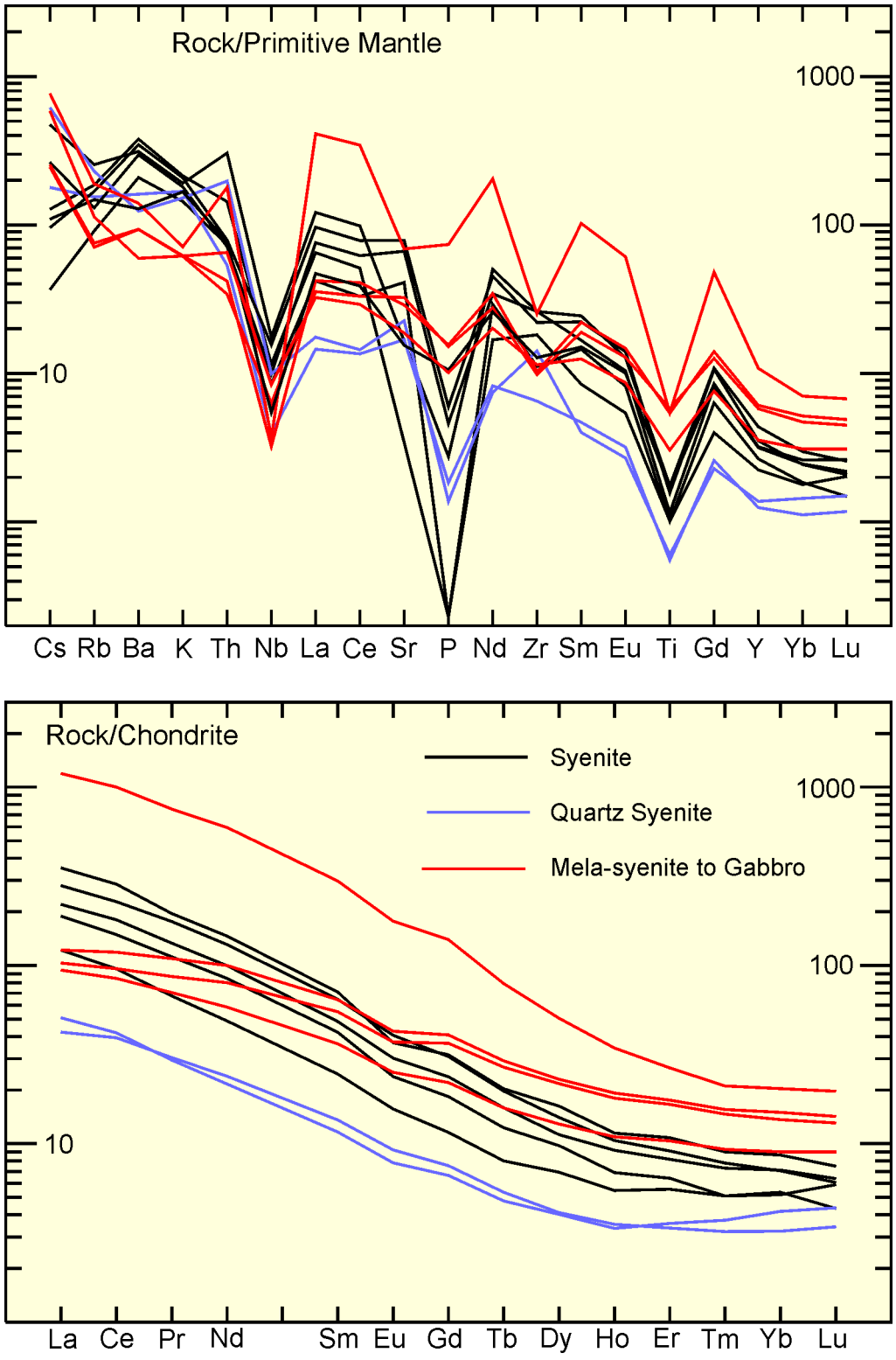

Figure 46. Chondrite and primitive mantle normalized trace element plots for samples from the Otto Stock. Normalization values from Sun and McDonough (1989).

Different aspects of the geology of the stock have been investigated previously, including petrology (Levesque 1994; Levesque et al. 1991), emplacement mechanism (Cruden and Launeau 1994; Launeau and Cruden 1998) and timing of plutonism and deformation (Wilkinson et al. 1999). The latter study reports a U/Pb age for zircon and titanite of 2673 ± 2 Ma. The single zircon fraction incorporated in this age estimate is very nearly concordant and has a $^{207}Pb/^{206}Pb$ age of 2675 ± 2.2 Ma.

FIELD RELATIONSHIPS

Because of generally poor exposure, particularly in the southern and eastern portions, the map pattern of the Lebel Stock is poorly constrained but is crudely semicircular. The western contact of the pluton is concordant to stratigraphy on a regional scale but in detail is locally discordant whereas the northern margin of the pluton is truncated by the CLLF (Cruden and Launeau 1994; *see* Figure 38). A fabric widely developed within the pluton defined by planar alignment of feldspar phenocrysts is attributed to magmatic flowage. Cruden and Launeau (1994) interpreted the Lebel Stock to be a southward propagating thin sheet with a source in the present location of the faulted northern contact.

Penetrative deformational fabrics were only observed in the northern part of the stock and are interpreted to be related to late deformation along the CLLF. These areas where penetrative fabrics are observed are also characterized by moderately intense carbonatization.

PETROLOGY

The dominant lithology within the Lebel Stock is syenite (Figures 47a and b). The principle variation within these units is a range in colour index from approximately 10 to 35. As noted previously (Levesque 1994), the highest colour index is generally associated with the immediate contact zone of the stock.

The dominant mineral in all exposures examined is a single, perthitic alkali feldspar that commonly displays a preferred alignment interpreted to be a consequence of magmatic flow. The feldspar generally includes phenocrysts that are up to 1 to 2 cm in longest dimension. Very minor quartz is present in some samples and always occurs as small grains interstitial to feldspar. Mafic mineralogy includes amphibole (dominant in widespread more leucocratic varieties), clinopyroxene (dominant in more melanocratic units near the contact) and biotite. Primary amphibole is generally dark olive green in colour and presumed to be a calcic amphibole with subordinate blue amphibole, presumed to be a more sodic amphibole, present locally. Minor actinolitic amphibole occurs as a secondary replacement of pyroxene and other amphiboles locally. Biotite forms large, platy crystals that are interpreted to be primary. Magnetite is the dominant oxide, with hematite being observed in some samples; however, it is not clear if it is a primary or secondary phase. Apatite and titanite are widespread and locally abundant whereas zircon is relatively rare.

Much of the pluton is characterized by relatively fresh, unaltered primary mineral assemblages; however, along the northern edge of the stock, in proximity to deformation associated with the CLLF, secondary minerals are abundant. In the most extreme cases, mafic minerals have been largely replaced by carbonate which also occurs as veins.

GEOCHEMISTRY

Most samples from the Lebel Stock are characterized by high abundance of Na_2O and K_2O as well as geochemically analogous trace elements (Figures 42 and 43), imparting a strongly alkalic character (*see*

Figure 45). The exception to this generalization (sample 7543) is subalkaline and differs in a number of other respects including higher SiO_2 (63% vs 55 to 58%) and unusual abundance of a number of minor and trace elements (Figure 48). The sample is from an area of fairly intense alteration near the northern contact and it is not clear if the unusual characteristics of this sample is a reflection of primary and/or secondary processes. Subsequent discussion focuses on characteristics of the more typical components of the stock.

In addition to its LILE enrichment and strongly alkalic character, the Lebel Stock is further distinguished by high abundances of a wide range of HFSE relative to other Archean plutonic rock types although still characterized by negative Nb anomalies on extended trace element plots (*see* Figure 48) because of the extreme enrichment in incompatible elements. REE are abundant (Ce abundance ~230 to 280 times chondrite) and moderately fractionated (Ce_N/Yb_N ~23 to 26) with very weak negative Eu anomalies (*see* Figure 48). A strongly meta-aluminous character with moderately high Mg# (48 to 54) and high Cr abundance (53 to 140 ppm) are also noteworthy.

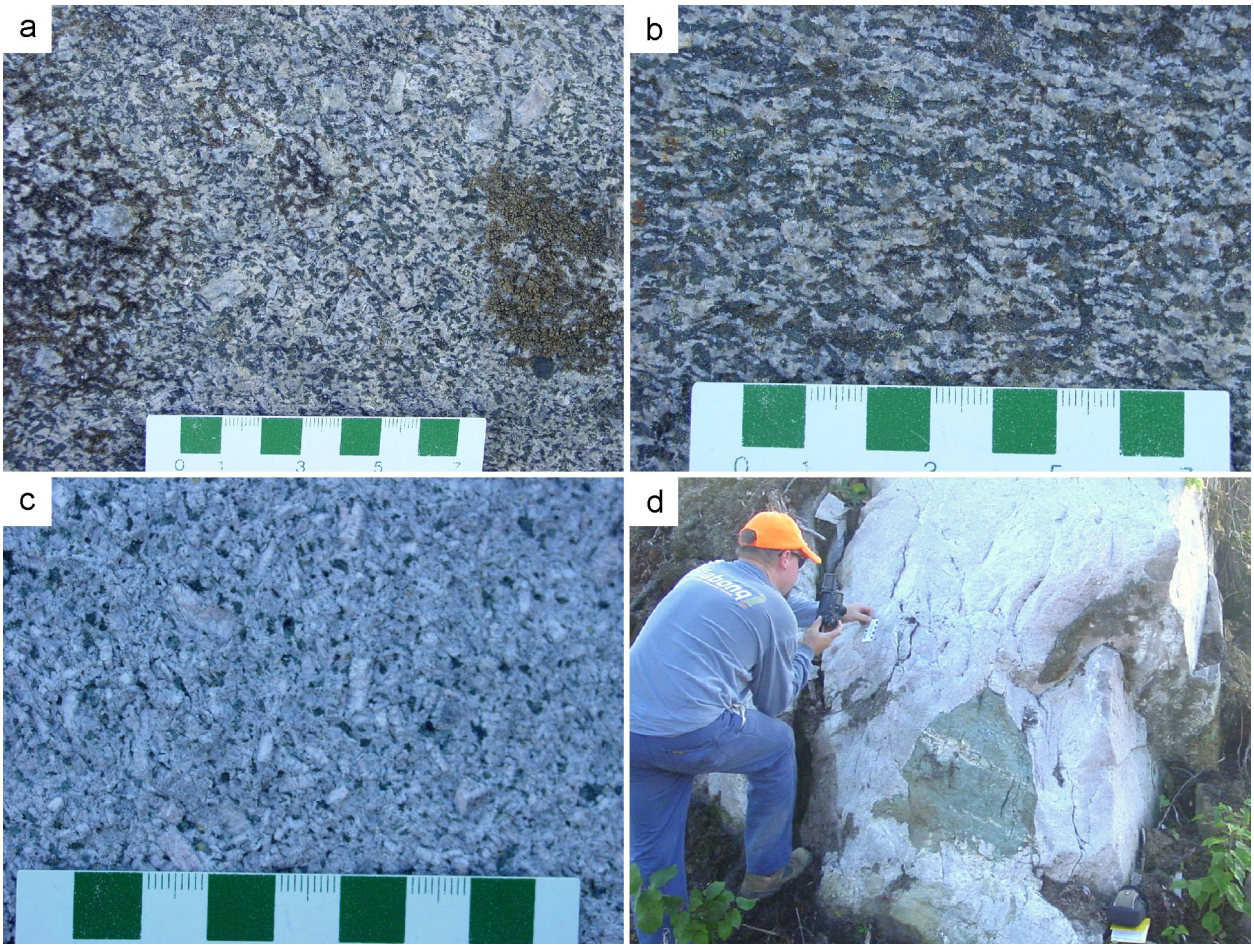

Figure 47. Field photographs illustrating characteristics of the Lebel and Cairo stocks. The northern portion of the Lebel Stock is predominantly syenite with coarse feldspar phenocrysts locally displaying flow alignment (a and b). The Cairo stock consists predominantly of syenite with subordinate quartz syenite and melasyenite, all of which are characterized by coarse feldspar phenocrysts accompanied by both blueish (sodic?) and dark green to black (calcic?) amphibole (c). The Cairo stock locally contains inclusions of foliated country rock (d).

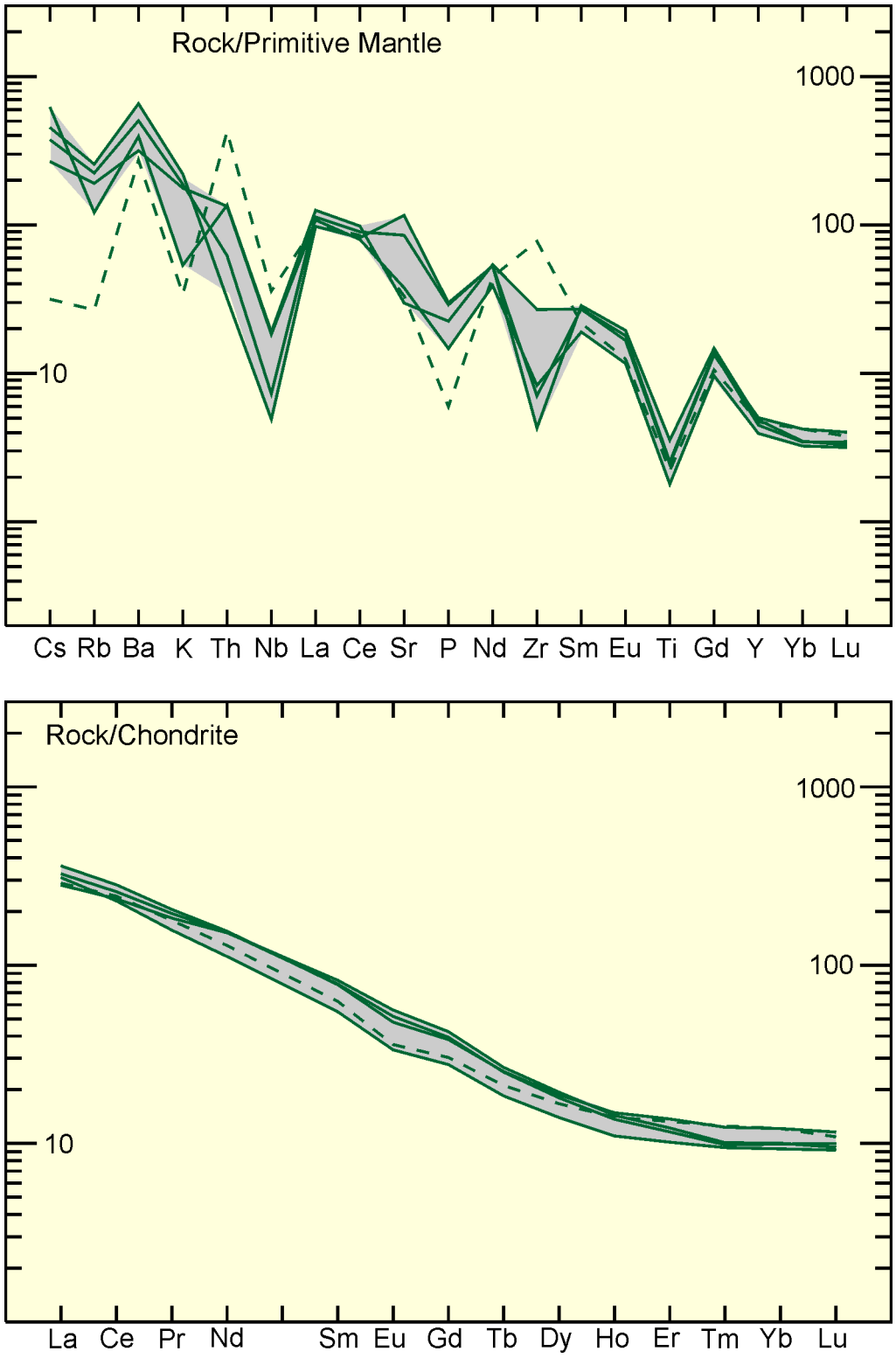

Figure 48. Chondrite and primitive mantle normalized trace element plots for samples from the Lebel Stock. Normalization values from Sun and McDonough (1989). The grey shaded area, encompassing the range for all samples except for one (7543), which is unusual in some respects, is reproduced in some subsequent figures to facilitate comparison.

PETROGENESIS

The Lebel Stock has a dual primitive and evolved character with elevated Mg# and Cr abundance suggesting derivation from, or equilibration with, an ultramafic (mantle) source; however, the very high abundances of incompatible elements require either major crustal contamination or the presence of an enriched component in the source. Crustal contamination is unlikely because the composition of the syenites is more extreme than any potential volumetrically significant crustal contaminants and for such a process to act on a significant scale, it would be unlikely that the ultramafic compatible element signature and strongly meta-aluminous, alkalic character would be preserved. The most probable origin of the enriched component is mantle metasomatism as proposed specifically for alkalic rocks from the Kirkland Lake area (Levesque 1994; Blichert-Toft et al. 1996; Hattori et al. 1996) and more generally (Menzies and Murthy 1980; Peccerillo et al. 1984, Rogers et al. 1985).

Murdock Creek Intrusion

Murdock Creek intrusion underlies approximately 6 km^2 in the southeastern portion of Teck Township. The intrusion lies within a few kilometres of major gold accumulation constituting part of the Kirkland Lake camp and a number of smaller occurrences are present along the contact and with the intrusion itself.

The intrusion has been the subject of a detailed investigation (Rowins 1990; Rowins et al. 1991; Rowins et al. 1993). A limited number of outcrops that are not representative of the full diversity of the stock, as described in the publications listed above, were examined as part of this investigation. Wilkinson et al. (1999) report a U/Pb titanite age of 2672 ± 2 Ma that they interpret to reflect timing of emplacement of the Murdock Creek intrusion.

FIELD RELATIONSHIPS

The Murdock Creek intrusion is emplaced into mafic metavolcanic rocks although the contact is modified by postemplacement faulting in a number of areas, and in particular along the northern contact where the intrusion is cut by the CLLF. Like the Lebel Stock, the intrusion is characterized by a thin mafic rim (Rowins et al. 1993) with a volumetrically dominant, more leucocratic syenite underlying much of the interior of the intrusion.

PETROLOGY

The mafic rim was not examined during the course of this investigation and the following description is from Rowins et al. (1993). The rim is composed of clinopyroxenite grading into meladiorite to melasyenite. Mafic and accessory mineralogy in all components consists of diopside (locally altered to aegerine-augite), biotite, magnetite, apatite and titanite. Compositional variation arises primarily from differing proportions of interstitial feldspars.

The volumetrically predominant, interior syenite phase is characterized by the presence of large, perthitic alkali feldspar crystals with mafic mineralogy being broadly similar to that characterizing the more mafic rim (Rowins et al. 1993). A dark green amphibole (presumed to be calcic amphibole) was noted in one thin section and minor amounts of a fibrous, secondary blue amphibole (sodic amphibole?) occurs locally. Carbonate is generally abundant and although much of it is clearly secondary alteration, in some cases it forms interstitial crystals and may be a primary magmatic phase.

A further noteworthy characteristic of the Murdock Creek intrusion is the abundance of magnetite, which together with the Mg-rich character of ferromagnesian silicate minerals (Rowins et al. 1991), points to the magma being highly oxidized.

GEOCHEMISTRY

Two samples collected as part of this investigation are similar to the alkali feldspar syenite unit described elsewhere (Rowins et al. 1993) as part of the broad compositional spectrum recognized within the Murdock Creek intrusion. Throughout the full compositional spectrum of the intrusion, alkali element abundances are sufficiently high to impart a shoshonitic to ultrapotassic alkalic signature (Rowins et al. 1993). Other noteworthy characteristics include high Mg# and Cr and LILE abundance. Syenite units exhibit Nb–Ti–P anomalies on extended trace element plots and have abundant, moderately highly fractionated REE abundances with weak negative Eu anomalies (Figure 49).

The geochemical characteristics of the Murdock Creek intrusion are very similar to those of mineralogically similar units from the Lebel Stock.

PETROGENESIS

The dual primitive (high Mg# and Cr abundance) and evolved (high LILE) character of the pluton suggests an origin via melting of metasomatized mantle as discussed for the Lebel Stock. More detailed investigations of the intrusion (Rowins et al. 1993) are consistent with this interpretation and further suggest that the intrusion evolved in a two-stage process with partial melting of metasomatized mantle to produce a primitive mafic alkaline melt which subsequently underwent clinopyroxene-dominated fractional crystallization which generated the observed compositional diversity.

Cairo Stock

The Cairo stock underlies approximately 65 km^2 northeast of the village of Matachewan. Distribution of outcrop in the stock is patchy and much of it is of relatively poor quality at the time of this investigation.

A U/Pb zircon age of 2676.3 ± 1.4 Ma is reported (J.A. Ayer, unpublished data) for a foliated syenite from near the southern contact of the stock.

FIELD RELATIONSHIPS

The stock has an approximately semicircular outline in plan view (Berger et al. 2006), intruding metavolcanic rocks of poorly constrained age to the north and south of the stock and Timiskaming metavolcanic and metasedimentary rocks near the eastern and western ends of the exposed area of the stock. The northern, western and eastern margins of the pluton define a crudely convex to the north-northwest curviplanar surface. The southern contact of the stock is more planar and oriented approximately east-northeast although small portions of the stock in this area are unconformably overlain by Proterozoic sedimentary units which conceals the precise geometry. The southern contact coincides with a zone of strong east-northeast-oriented shearing interpreted to be part of the CLLF system and consequently the semicircular form of the stock is interpreted to be a consequence of dislocation of the southern portion of the stock along a fault (*see* Figure 38).

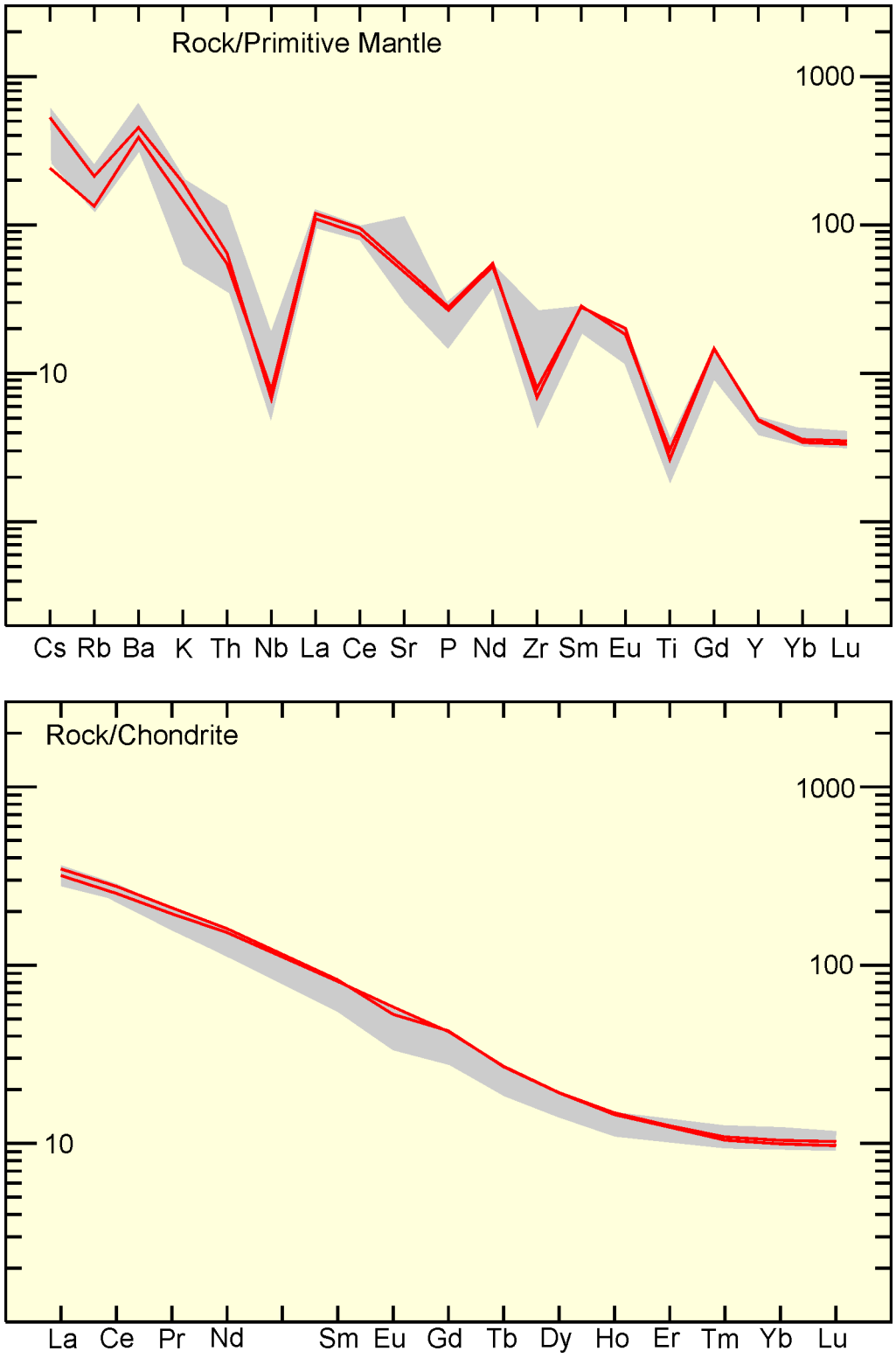

Figure 49. Chondrite and primitive mantle normalized trace element plots for 2 samples from the Murdock Creek intrusion central syenite unit. Normalization values from Sun and McDonough (1989). The grey shaded area is the field for syenites from the Lebel Stock, as discussed in Figure 48.

Contact relationships were not observed other than along the sheared southern contact of the stock. With the exception of the southern contact zone and in the vicinity of a second fault further to the north (Galer Lake fault, Berger et al. 2006) penetrative deformational fabrics were not observed. Many outcrops display a preferred alignment of feldspar phenocrysts that is interpreted to be a primary magmatic flowage fabric. In several locations near the contact, inclusions of penetratively deformed country rock were noted (*see* Figure 47d). Consequently, the stock is interpreted to postdate development of a regional penetrative deformational fabric defined by alignment of near-peak metamorphic mineral assemblages and predate some component of deformation localized within east-northeast-trending faults.

A number of auriferous sulphide mineral occurrences lie within the pluton. Most of these are spatially associated with zones of east-northeast-trending deformation associated with late faults (Berger et al. 2006).

PETROLOGY

The Cairo stock consists predominantly of feldspar porphyritic syenite and quartz syenite (*see* Figure 47c). Colour index varies widely but compositions approaching ultramafic, as observed in the Otto Stock, were not encountered during this investigation. In most locations, the predominant phase is a single alkali feldspar displaying patchy exsolution of albitic feldspar. Quartz, where present, is always intergranular with respect to feldspar. Ferromagnesian silicates observed include a blue-coloured amphibole thought to be riebeckite, a greener amphibole thought to be a more calcic amphibole, erratically distributed clinopyroxene and biotite. Magnetite is abundant except within some of the sheared rocks where it appears to be replaced by sulphides. Apatite and titanite are relatively abundant accessory minerals occurring along with zircon. Carbonate is present in many areas and is mostly clearly a late secondary alteration although in some cases is intergranular, and in these cases its relative timing is not always clear.

GEOCHEMISTRY

With one exception (discussed below), all samples of the Cairo stock are characterized by high abundance of LILE relative to their SiO_2 content which imparts a strong alkalic character (*see* Figure 45). The samples are also characterized by high Mg# (46-58) and Cr abundance (48-126 ppm) (*see* Figures 42 and 44), which together with the LILE enrichment imparts the dual primitive – evolved character observed in other late-tectonic plutons discussed above. Like other plutons of this type, they have high (relative to TTG) abundance of a range of HFSE and REE, although still being characterized by negative Nb–P–Ti anomalies on extended trace element plots (Figure 50). REE abundance correlates inversely with SiO_2 (*see* Figure 44) and are moderately highly fractionated with very weakly negative Eu anomalies (*see* Figure 50).

The single exception to these generalizations (sample 7263) is a hololeucocratic quartz syenite that despite having significantly higher SiO_2 has lower LILE abundance and is subalkalic. This sample is also unusual in a number of other respects (low Mg# and lower abundance of Cr, HFSE and REE) and is interpreted to be a product of extreme fractionation within the stock.

PETROGENESIS

The geochemical characteristics of the Cairo stock are closely comparable to those of the Lebel Stock. Based on arguments discussed in the section pertaining to the comparable intrusion, an origin involving partial melting of metasomatically enriched depleted mantle is favoured for the Cairo stock.

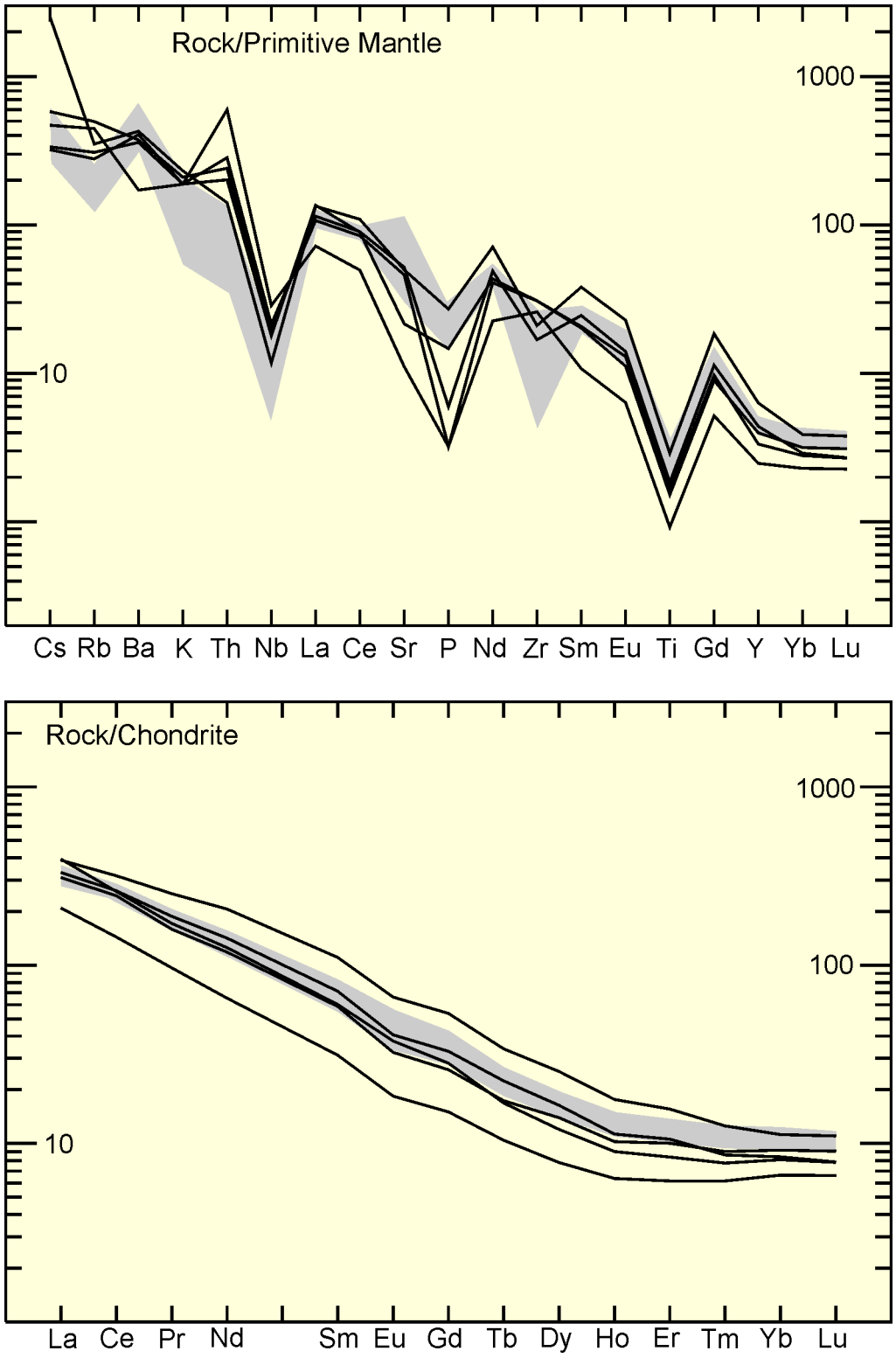

Figure 50. Chondrite and primitive mantle normalized trace element plots for samples from the Cairo stock. Normalization values from Sun and McDonough (1989). The grey shaded area is the field for syenites from the Lebel stock, as discussed in Figure 48.

Young–Davidson Intrusion

A syenite intrusion, informally referred to hereafter as the Young–Davidson intrusion, is situated several kilometres west of the community of Matachewan. The intrusion is relatively small; however, it is locally overlain by Proterozoic sedimentary rocks and consequently the geometry and size of the intrusion is not well constrained.

The Young–Davidson intrusion hosts significant gold mineralization, with combined historical production from 2 mines (Young–Davidson and Consolidated Matachewan) totaling 957 000 ounces Au and 266 000 ounces Ag (Berger and Prefontaine 2005). A decision to renew production was recently (2009) announced by Northgate Minerals Corporation.

FIELD RELATIONSHIPS

As discussed above, Proterozoic sedimentary rocks overly a portion of the intrusion and partially obscure the regional setting; however, the intrusion is thought to be relatively small and lie to the north of, and in very close proximity too, the CLLF. The intrusion lies along the contact between mafic metavolcanics of uncertain age and presumed Timiskaming metasedimentary rocks.

PETROLOGY

All of the samples examined as part of this study are intensely altered and, in some cases, mineralized, which obscures the primary character of the unit. The unit is dominated by very leucocratic syenite consisting largely of perthitic alkali feldspar. Ferromagnesisan silicates are either not present or very low in abundance and extensively altered such that their original composition is not evident. Magnetite and hematite are present in some samples whereas others are dominated by sulphides. Carbonate is abundant in some samples and is dominantly clearly of secondary origin although in some cases carbonate forms crystals interstitial to alkali feldspar and could conceivably be a primary igneous phase. Accessory mineral phases include apatite and titanite but are less abundant than in other syenite units discussed above.

GEOCHEMISTRY

Young–Davidson syenites are not strongly enriched in Na_2O but are extremely enriched in K_2O, which imparts a strongly alkalic character (*see* Figure 42 and 45). Erratic and very low Mg# (12 to 40) is a consequence of the extremely leucocratic nature of these rocks and secondary iron enrichment associated with the introduction of sulphide and carbonate mineral species. Consequently, these low Mg#'s are not deemed to be petrogenetically significant. Most samples have abundant, moderately highly fractionated REE abundances similar to other syenitic intrusions occurring along the CLLF (Figure 51). Extremely erratic abundances of a range of trace elements is interpreted to arise both from intense secondary alteration and accessory mineral control attendant with extreme fractionation evidenced by the extremely leucocratic character of these rocks.

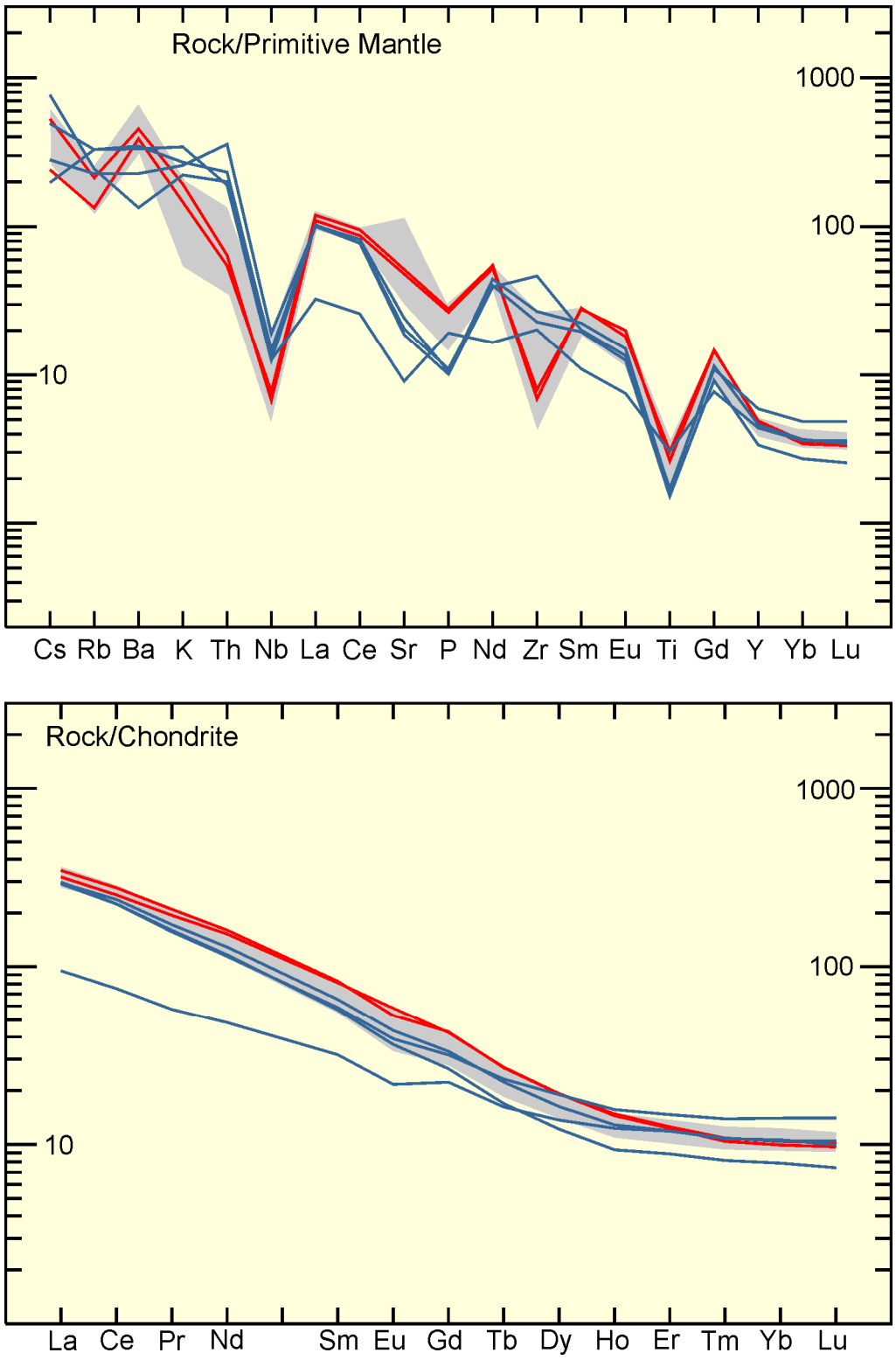

Figure 51. Chondrite and primitive mantle normalized trace element plots for samples from the Young–Davidson intrusion (blue lines). The grey shaded area is the field for syenites from the Lebel Stock, as discussed in Figure 48, and the red lines are syenites from the Murdock Creek intrusion. Normalization values from Sun and McDonough (1989).

PETROGENESIS

The significant modification by secondary alteration and mineralization processes limits inferences that can be drawn pertaining to petrogenesis of this unit. If interpretations advanced for broadly similar units above are extended to this intrusion, there is a further requirement that these units are products of extreme fractionation and are extensively modified by secondary processes.

Bristol Township Alkalic Complex

This section describes characteristics and relationships of a series of alkalic rocks occurring in the southwestern portion of Bristol Township, approximately 15 km southwest of the city of Timmins. Although several of these units form small, mappable intrusions, many of the units constituting this group are minor, dike-like intrusions and all of these units together are referred to informally here as the Bristol Township alkalic complex (BTAC).

The BTAC underlies an area just to the north of the PDF, with many of the components localized near the contact between Porcupine assemblage metasedimentary rocks and Tisdale assemblage metavolcanic rocks (Figures 52 and 53). The BTAC exhibits a close spatial relationship with gold mineralization that is currently being developed at the Timmins Mine by Lake Shore Gold Corporation.

A U/Pb age for andradite garnet of 2687 ± 3 Ma has previously been reported from one of the dikes associated with the BTAC (Barrie 1990). The application of the U/Pb system to andradite garnet is not well understood and 2 observations suggest that the age of the unit might be somewhat younger. Firstly, all other alkalic units in the western Abitibi Subprovince are 8 to 16 million years younger than the andradite age. Secondly, the reported age is very similar to that of early syntectonic porphyries in the Timmins area that have a significantly different petrogenesis and are emplaced at an earlier stage in the tectonic development than the late-tectonic BTAC.

A sample (7644) of syenite was selected from drill core for LA-ICP-MS and TIMS U/Pb zircon geochronology in order to further evaluate the age of the BTAC. The core is from the 236 to 238.9 m interval in diamond-drill hole TC-04-13 (collared at UTM 458500E 5357930N, NAD83). The LA-ICP-MS analyses are mostly highly to moderately discordant with only 27 of 60 analyses being within 5% of concordia and some of these analyses being highly imprecise due to large common Pb corrections. These least discordant analyses have a wide range (2594–2782 Ma) of $^{207}Pb/^{206}Pb$ ages with a mean age of 2698 ± 49 Ma. Two TIMS analyses are both 12 to 15% discordant with unreasonably young $^{207}Pb/^{206}Pb$ ages (~2580 Ma) suggesting older Pb loss. Consequently, neither the LA-ICP-MS or TIMS data allow for useful constraints on the age of the syenite.

FIELD RELATIONSHIPS

The BTAC consists of a cluster of numerous, compositionally diverse minor intrusions localized near a major volcanic-sediment contact. Metavolcanic rocks lying to the north of the contact are correlated with the Tisdale assemblage (2704–2710 Ma, Ayer et al. 2005) with metasedimentary rocks south of the contact assigned to the Porcupine assemblage (2685–2690 Ma, Ayer et al. 2005); however, the ages of the units in the immediate vicinity of the BTAC are not constrained. The area lies just to the north of the PDF and is heterogeneously deformed. The BTAC is interpreted to be emplaced relatively late in the sequence of deformational events based on the generally weakly to nonfoliated character of the units; however, deformation is locally imposed on BTAC units suggesting either the emplacement of the complex

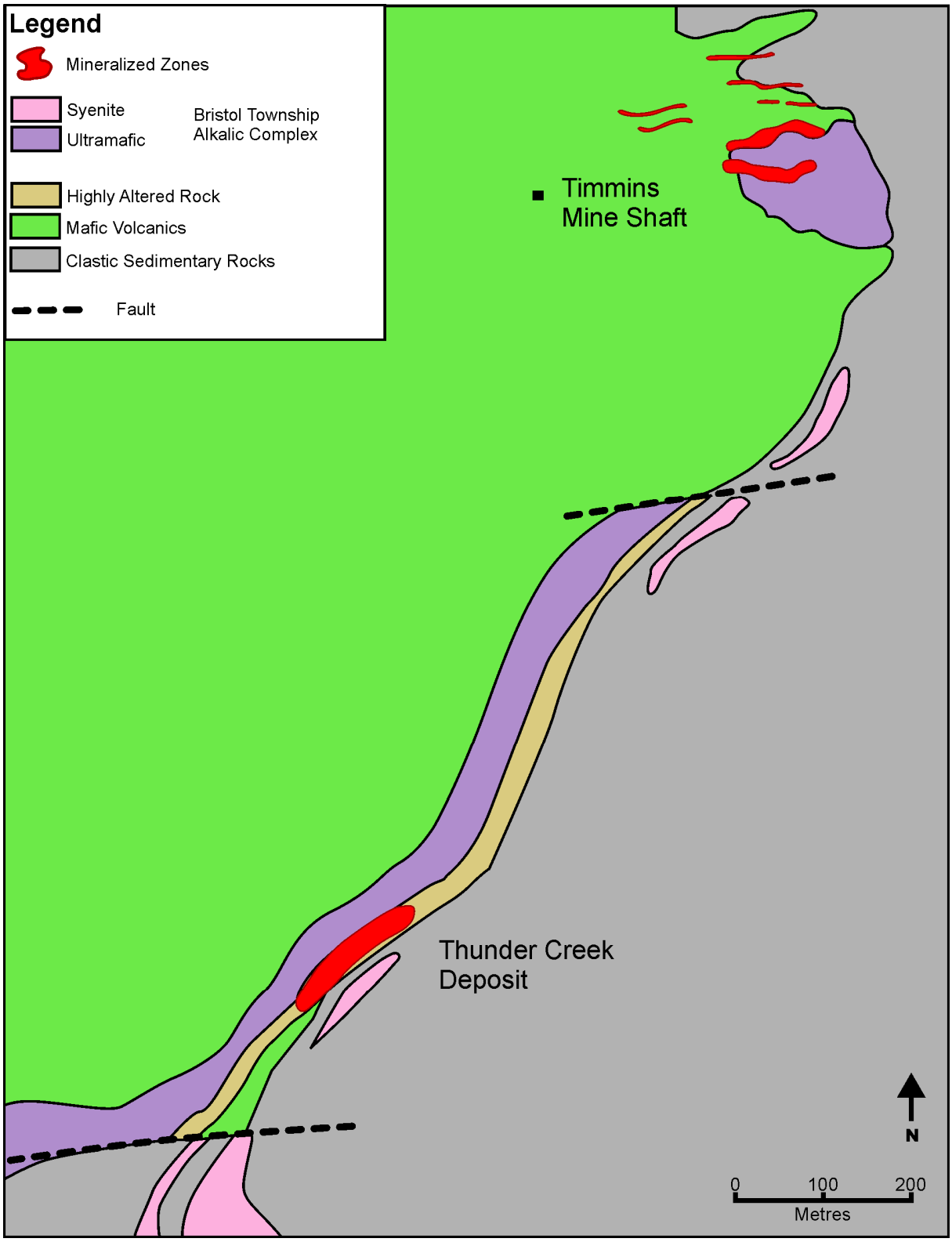

Figure 52. Generalized geological map illustrating the close spatial relationship between the Bristol Township alkalic complex (pink and purple), volcanic-sedimentary (green-grey) contact and gold mineralization (red). The figure is simplified from information presented on the Lake Shore Gold Corporation website (www.lsgold.com/, accessed October 4, 2010).

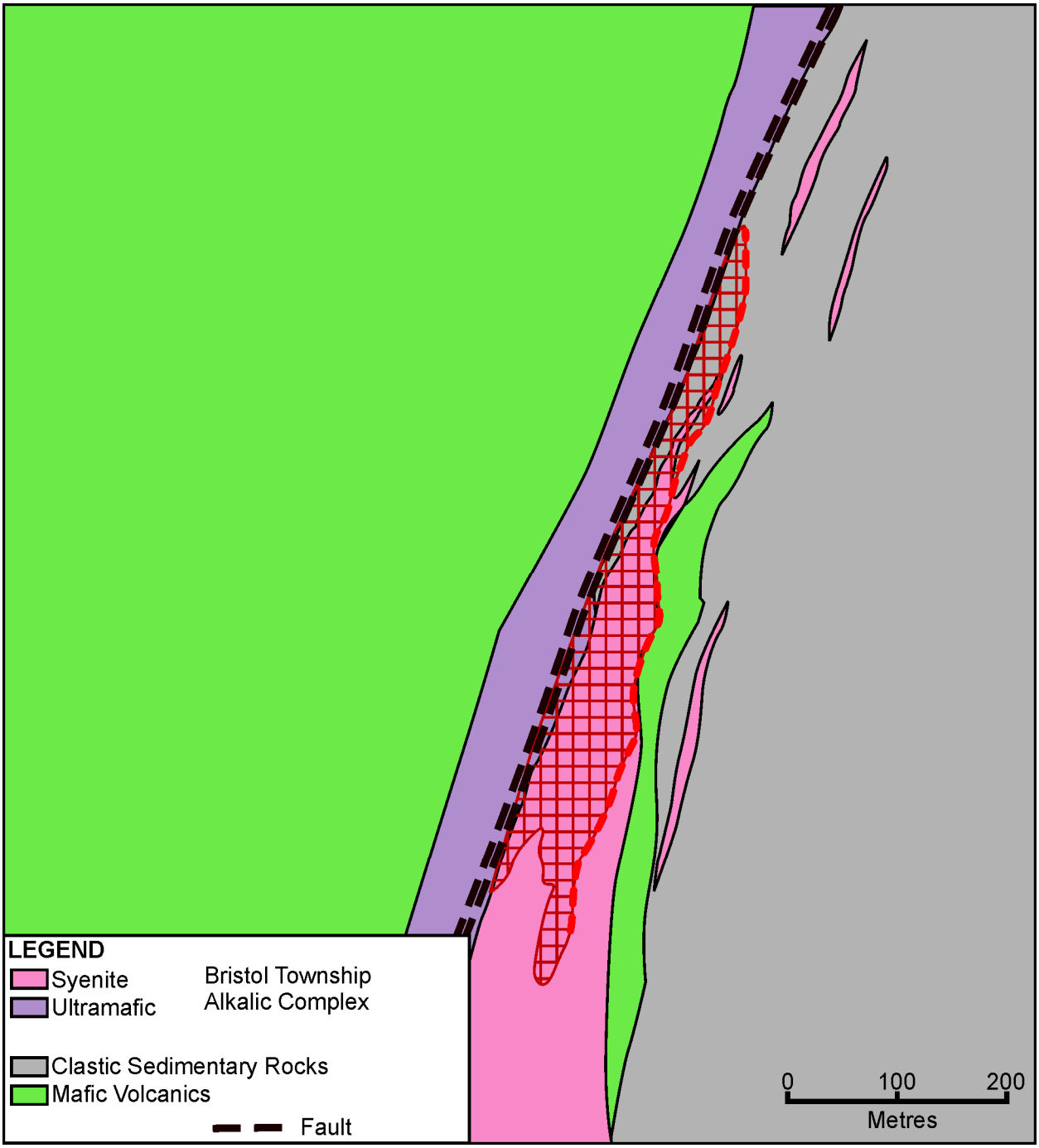

Figure 53. Composite cross-section looking northeast in the vicinity of the Thunder Creek deposit, illustrating the close spatial relationship between the Bristol Township alkalic complex (pink and purple), volcanic-sedimentary (green-grey) contact and gold mineralization (red hatched area). The figure is simplified from information presented on the Lake Shore Gold Corporation website (www.lsgold.com/, accessed October 4, 2010).

occurred over an interval of time straddling the timing of late deformation or late (post-BTAC) deformation was very localized.

Individual intrusions comprising the BTAC are compositionally diverse (Figure 54) and may be relatively homogeneous, but, in many cases, they are intimately admixed with different compositional varieties. Examples of heterogeneity include "patches" of leucocratic syenite within pyroxenite (Figure 55a) and gradations in colour index between syenite and melasyenite (Figure 55b).

PETROLOGY

The compositions of numerous minor intrusions constituting the BTAC are extremely diverse, ranging from ultramafic to hololeucocratic, with some units being characterized by relatively unusual, exotic mineralogy. A complete characterization of units is beyond the scope of this study and the description of rock types below is intended to give a sense of the diversity represented within the BTAC. The units are interpreted to be genetically related, despite the remarkable diversity, based on i) spatial proximity, ii) broadly similar field relationships, iii) local gradational contacts and iv) shared, broad compositional characteristics (e.g., shared exotic mineralogy, alkalic character, HFSE enrichment).

The numerous discrete intrusions and dikes constituting the BTAC may be thought of as consisting of mixtures of 3 end-member components. Two of these (ultramafic and syenitic components) occur as discrete intrusions representing near end member compositions as well as within mixtures of one or more other components. These 2 components may be mixed on either a lithological (discrete "patches" of one in the other, e.g., Figure 55a) or on a more intimate mineralogical (mineral phases mixed in various proportions resulting in a compositional continuum between ultramafic and syenitic compositions) scale. The third component is imperfectly defined and understood and is referred to informally here as the exotic calcic component. This component is recognized primarily as a component mixed with ultramafic and syenitic units and may or may not exist as a discrete end-member component.

The magmatic mineralogy of rocks interpreted to be representative of the near-end-member ultramafic component consists predominantly of clinopyroxene. Biotite (var. phlogopite) is a ubiquitous minor (2 to 10%) component. Magnetite is invariably present and in some cases is abundant, constituting up to 5% of the rock. Apatite is generally present and in some cases is exceptionally abundant, constituting up to 15% of the rock and resulting in P_2O_5 concentrations of up to 5 weight percent (Table 5). It is not clear if high apatite abundance is a characteristic of the ultramafic component or if it is associated in some way with an admixed exotic calcic component (see discussion below).

End-member syenitic units have magmatic mineralogy that consists predominantly of feldspar. In some cases, the feldspar is a single, perthitic hypersolvus alkali feldspar although a subsolvus feldspar assemblage consisting of albite and barium-enriched potassium feldspar is present locally. Grain size is highly variable and, in some cases, hypersolvus alkali feldspars or potassium feldspars form large phenocrysts or megacrysts that poikilitically enclose other primary mineral phases. Magnetite is generally present but extreme variation in magnetic susceptibility reflects extreme heterogeneity in its distribution. Minor amounts of quartz, occurring as interstitial grains, are commonly present. Mafic minerals present in low abundance (generally less than 5%) include blue-green amphibole (riebeckite?) and biotite. Trace amounts of apatite and zircon are present in all samples.

The exotic calcic component is an informal term used to refer to a mineral assemblage dominated by unusual calcium-rich minerals that is recognized locally within mixed ultramafic-syenitic units. The exotic calcic component may not exist as a discrete end-member composition, although it is possible that some carbonate-rich veins (Figure 55d-f) may have such an affinity. The main mineralogical phases

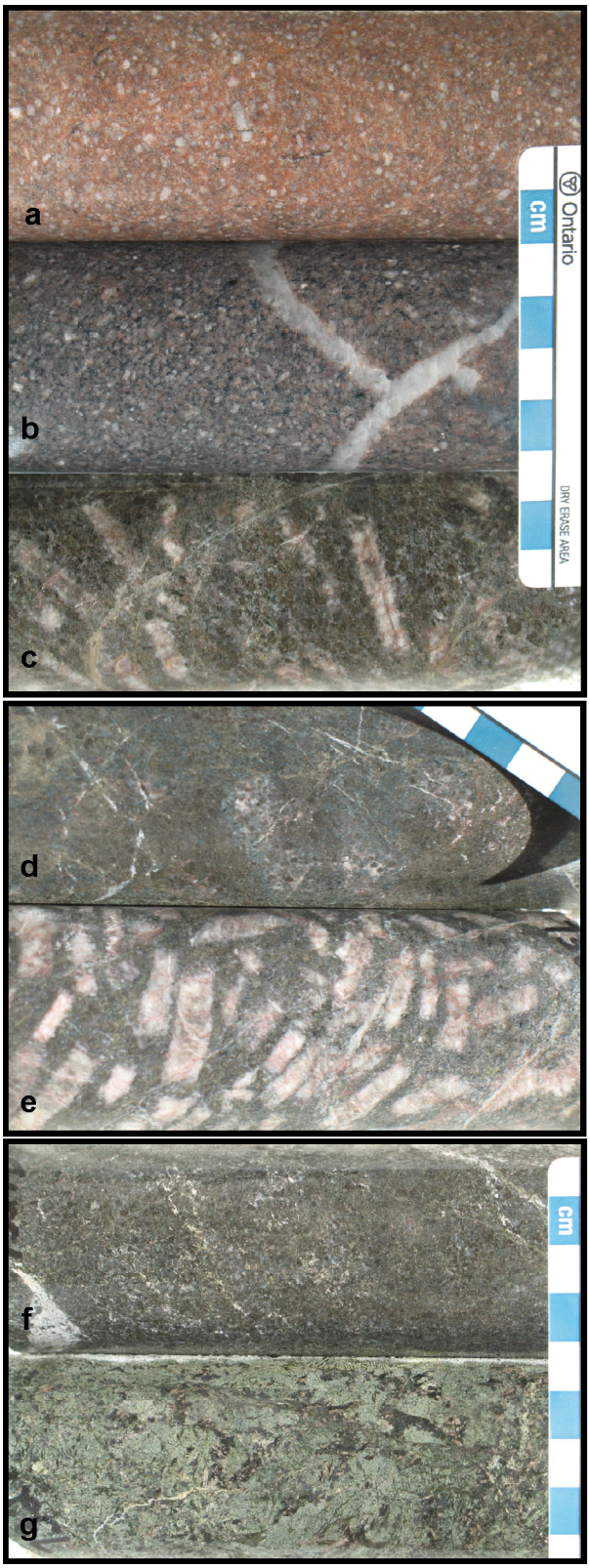

a) Weakly porphyritic leucosyenite with larger, perthitic, subhedral to euhedal alkali feldspar crystals surrounded by a mixture of finer grained alkali feldspar, quartz, magnetite, carbonate and chlorite.

b) Syenite similar to above but more melanocratic with approximately 20% blue amphibole plus minor clinopyroxene and trace andradite.

c) Melasyenite with large, perthitic alkali feldspar crystals partially enclosing clinopyroxene and andradite with a finer grained matrix consisting of alkali feldspar, fibrous blue to green amphibole, carbonate, magnetite, titanite and apatite.

d) Melasyenite consisting of large optically continuous alkali feldspar crystals surrounding euhedral andradite crystals. Other minerals present include fibrous blue to green amphibole, clinopyroxene, magnetite, titanite and apatite.

e) Relatively melanocratic, coarsely porphyritic syenite with large alkali feldspar phenocrysts and smaller subhedral to euhedral andradite crystals surrounded by a finer grained mixture of alkali feldspar, clinopyroxene, fibrous blue to green amphibole, magnetite, titanite and apatite.

f) Garnet melasyenite with large, optically continuous alkali feldspar crystals enclosing euhedral andradite crystals. Other minerals present include green biotite, carbonate, epidote, magnetite, titanite and apatite.

g) Ultramafic rock composed of clinopyroxene, andradite, magnetite and unusually abundant apatite along with subordinate amounts of alkali feldspar, carbonate and titanite.

Figure 54. Photographs of drill core illustrating diversity of alkalic dikes associated with the Bristol Township alkalic complex. Description of rock types to the right of the image.

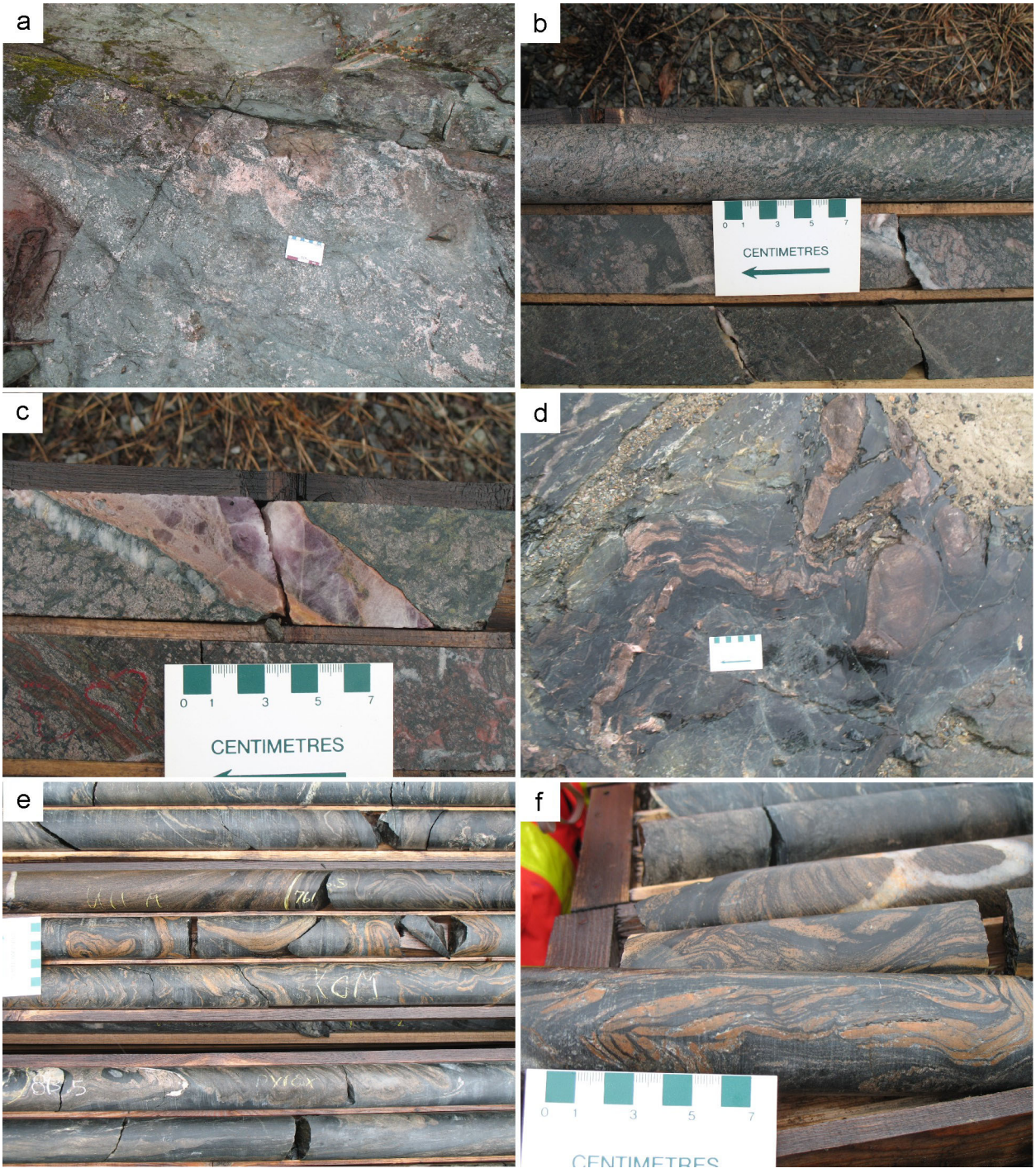

Figure 55. Characteristics of the Bristol Township alkalic complex: a) syenite "patches" within pyroxenite, b) gradational contact between syenite and melasyenite, c) fluorite vein within syenite, d-f) folded veins of possible carbonatitic affinity.

Table 5. Tabulation of whole rock geochemistry and magmatic mineralogy (major minerals bolded) for the Bristol Township alkalic complex.

Sample	05GPB7238	05GPB7239	05GPB7327A	05GPB7327B	05GPB7327C	05GPB7327D	05GPB7328A	05GPB7328B
SiO_2	70.13	67.06	35.44	40.71	40.21	43.1	38.09	38.46
Al_2O_3	15.88	16.45	4.29	3.1	11.8	12.31	2.56	4.29
MnO	0.03	0.04	0.18	0.21	0.35	0.36	0.14	0.16
FeO	0.29	0.4	8.16	7.31	1.66	2.06	7.34	5.87
Fe_2O_3	1.09	1.42	11.9	12.13	11.45	9.91	10.99	5.04
MgO	0.3	0.44	11.1	11.28	1.99	3.03	11.54	11.97
CaO	0.91	1.24	20.08	21.26	22.1	18.44	22.52	22.32
Na_2O	5.5	4.65	0.35	0.51	2.67	3.5	0.38	0.38
K_2O	5.66	7.31	1.66	0.19	1.01	1.57	0.14	1.65
TiO_2	0.13	0.19	1.35	1.46	1.63	1.45	1.38	1.07
P_2O_5	0.06	0.12	4.61	1.99	0.53	0.94	4.39	5.24
LOI	1.09	1.47	0.94	0.58	4.15	3.31	1	3.74
TOTAL	101.1	100.84	100.97	101.54	99.73	100.21	101.29	100.83
Mg#	30	32	51	52	23	33	54	67
A/CNK	0.94	0.92	0.11	0.08	0.26	0.3	0.06	0.1
S	0.01	0.01	0.03	0.02	0.07	0.04	0.04	0.06
CO_2	0.81	1.25	0.51	0.63	3.41	2.41	0.72	2.88
H_2O-	0.07	0.13	0.09	0.05	0.07	0.07	0.05	0.07
H_2O+	0.07	0.2	1.13	0.43	0.82	0.88	0.9	1.31
Cs	0.39	0.46	4.64	0.64	2.98	5.00	0.55	11.76
Rb	65	91	53	5	24	40	4	56
Sr	656	752	1241	940	5381	3308	1286	1627
Ba	2354	2264	868	285	1179	846	261	1208
Nb	6.2	9.1	1.4	0.4	42.1	27.7	0.6	1.3
Zr	115	176	163	180	1165	1046	136	267
Hf	3.6	5.1	5.8	6.3	20.5	19.9	4.8	10.0
Th	4.70	8.84	20.41	7.04	62.94	73.16	19.06	27.33
U	3.04	3.75	1.68	0.51	9.06	11.55	1.12	1.63
Sc	1.9	2.9	33.3	37.3	3.0	4.8	42.2	41.5
V	20	32	116	153	356	318	102	92
Cr	17	22	<4	324	<4	<4	195	<4
Ni	10	13	41	58	17	22	58	42
Co	5	6	51	52	29	20	48	42
Cu	<3	<3	<3	<3	250	55	<3	<3
Zn	30	53	140	138	107	171	119	100
Pb	18	14	8	5	70	36	5	5
Au	55.6	13.0	<6	<6	6.1	<6	<6	<6
Y	6.2	10.4	54.8	30.6	128.4	124.4	47.1	62.3
La	11.36	22.22	298.1	110.7	426.0	522.2	246.5	297.6
Ce	31.09	63.71	734.9	292.9	1010.7	1192.1	628.2	754.3
Pr	4.20	8.62	99.12	42.19	136.2	146.2	85.27	103.5
Nd	17.13	35.58	432.1	192.9	601.3	584.7	377.9	461.5
Sm	3.30	6.40	75.11	36.47	114.3	99.84	66.86	83.68
Eu	0.86	1.62	16.96	8.59	27.74	24.07	14.91	19.27
Gd	2.20	4.19	46.04	23.24	66.01	60.01	40.89	52.23
Tb	0.26	0.48	4.20	2.25	6.73	6.49	3.73	4.83
Dy	1.28	2.26	15.97	8.99	27.87	27.90	14.13	18.36
Ho	0.22	0.37	2.08	1.21	3.93	4.11	1.81	2.37
Er	0.54	0.90	3.94	2.41	8.80	9.41	3.39	4.50
Tm	0.08	0.13	0.39	0.25	1.08	1.14	0.32	0.43
Yb	0.54	0.86	2.46	1.58	7.27	7.34	2.00	2.70
Lu	0.08	0.13	0.26	0.19	0.94	0.94	0.19	0.27
Eu/Eu*	0.92	0.90	0.82	0.84	0.90	0.88	0.81	0.83
Ce^N/Yb^N	16	21	83	51	39	45	87	78
Major	**alkali feld**	**alkali feld**	**cpx**	**cpx**	**and**	**alkali feld**	**cpx**	**cpx**
Magmatic	mt	mt	**biot**	**mt**	**alkali feld**	**and**	**mt**	**ap**
Mineralogy	qz	qz	**ap**	**ap**	**cpx**	**biot**	**ap**	**?**
	b-g amph	b-g amph	**mt**	**biot**	**carb**	cpx	**biot**	
				alkali eld		carb		

Table 5. (continued)

Sample	05GPB7328C	05GPB7329A	05GPB7329B	07-GPB-7642	07-GPB-7643	07-GPB-7644	07-GPB-7645
SiO_2	40.57	49.36	44.42	41.55	63.92	63.89	64.65
Al_2O_3	5.78	14.87	8.28	11.27	15.38	15.49	15.28
MnO	0.19	0.22	0.35	0.35	0.05	0.06	0.05
FeO	5.89	1.5	2.07	2.92	1.31	1.17	0.81
Fe_2O_3	6.13	5.29	11.13	7.45	0.65	0.7	1.41
MgO	12.41	1.14	3.28	1.61	0.97	0.92	1.09
CaO	19.04	10.81	21.09	16.72	2.29	2.44	2.03
Na_2O	0.26	3	2.5	3.41	5.12	4.93	5.19
K_2O	1.37	6.82	1.7	3.34	6.29	6.67	6.98
TiO_2	1.24	0.75	1.56	1.29	0.22	0.22	0.22
P_2O_5	3.12	0.3	1.17	0.42	0.15	0.15	0.16
LOI	4.18	5.72	2.52	8.47	3.59	3.5	2.01
TOTAL	100.84	99.94	100.32	99.13	100.09	100.26	99.96
Mg#	66	24	33	23	48	48	48
A/CNK	0.16	0.47	0.19	0.28	0.79	0.78	0.77
S	0.03	0.02	0.08	0.05	0.07	0.08	0.05
CO_2	2.86	5.16	2.1	7.58	3.25	3.42	1.79
H_2O-	0.04	0.08	0.05	0.2	0.22	0.2	0.2
H_2O+	1.86	0.33	0.53	0.67	0.39	0.37	0.46
Cs	12.88	1.23	0.88	1.25	0.37	0.40	0.51
Rb	52	62	27	42	74	80	80
Sr	1525	3972	2297	3096	1398	1287	927
Ba	665	7433	1438	3782	1779	1666	1919
Nb	1.0	14.4	19.7	21.9	8.2	8.3	8.5
Zr	362	570	1619	870	170	171	159
Hf	13.7	12.2	34.4	19.9	4.9	5.0	4.9
Th	21.67	50.35	74.33	70.00	10.29	19.65	12.58
U	1.11	6.71	11.79	9.31	5.34	8.69	4.82
Sc	52.0	4.1	11.6	7.6	4.0	4.2	4.6
V	88	189	373	381	40	40	59
Cr	213	<4	8	25	22	25	33
Ni	53	19	32	18	12	13	16
Co	39	10	17	16	5	5	6
Cu	<3	<3	<3	12	4	4	2
Zn	113	100	157	157	47	35	98
Pb	9	25	25	26	12	13	13
Au	35.1	<6	77.4	<6	<6	17.0	14.0
Y	49.5	76.0	195.8	146.7	10.5	10.9	12.6
La	168.0	265.5	453.2	377.0	28.70	29.67	34.18
Ce	448.1	646.0	1187.5	949.0	75.00	76.10	93.20
Pr	63.23	83.80	165.2	133.0	9.75	9.85	12.46
Nd	291.8	357.5	740.3	590.9	38.59	39.26	48.85
Sm	55.52	63.21	149.9	114.5	6.83	6.76	8.54
Eu	13.13	15.26	37.46	27.87	1.61	1.63	2.05
Gd	36.94	37.57	97.61	68.85	4.29	4.31	5.29
Tb	3.60	3.91	10.51	7.14	0.48	0.47	0.58
Dy	14.34	16.66	45.64	30.90	2.20	2.30	2.70
Ho	1.92	2.45	6.69	4.57	0.36	0.37	0.44
Er	3.72	5.62	14.72	10.52	0.91	0.95	1.07
Tm	0.37	0.68	1.74	1.31	0.13	0.12	0.14
Yb	2.29	4.48	10.90	7.63	0.80	0.79	0.95
Lu	0.25	0.57	1.35	1.06	0.12	0.12	0.14
Eu/Eu*	0.83	0.88	0.89	0.89	0.85	0.86	0.87
Ce^N/Yb^N	54	40	30	35	26	27	27
Major	**cpx**	**alkali feld**	**alkali feld**	**alkali feld**	**alkali feld**	**alkali feld**	**alkali feld**
Magmatic	**mt**	**and**	**and**	**and**	qz	qz	**b-g amph**
Mineralogy	**ap**	**mt**	**b-g amph**	**b-g amph**	mt	?	qz
	biot	b-g amph	apatite	**carb**			biot
	?	carb?	carb?				

constituting the exotic calcic component are andradite (var. melanite) and calcite. Andradite occurs as euhedral to subhedral crystals (Figure 56) that are commonly zoned and locally comprises up to 70% of the rock. Andradite generally has associated interstitial grains of carbonate that are interpreted to be of primary magmatic origin. Carbonate having similar habit also occurs independent of the presence of andradite and is likely of magmatic origin; however, clearly secondary carbonate is also widespread and in many cases it is problematic to ascribe a magmatic or secondary origin. Minor phases commonly present along with andradite and carbonate include apatite and epidote, both of which are REE-enriched relative to that occurring where the calcic mineral phases are not present as well as allanite and titanite. Sulphates, including barite and celestine are also commonly associated with andradite and magmatic carbonate. The presence of magmatic carbonate in association with andradite, REE-enriched phosphates and sulphates may indicate that the exotic calcic component has carbonatitic affinities. An association of syenitic and carbonatitic affinity units has been noted elsewhere in the Abitibi Subprovince (Bedard and Chown 1992) as well as in other Archean cratons (e.g., Jupiter gold deposit, Blewett and Czarnota 2007).

Much of the BTAC is relatively fresh and unaltered; however, secondary alteration is heterogeneously developed and locally intense. The most commonly observed types of alteration include fibrous amphibole after clinopyroxene, chlorite after biotite and introduction of disseminated carbonate and carbonate ± quartz veins. Sulphide minerals (pyrite, chalcopyrite and, less commonly galena and sphalerite) and gold occur within a range of rock types; however, diagnostic features indicative of primary versus secondary origin are not always obvious.

GEOCHEMISTRY

Whole rock geochemical data (*see* Table 5) reflects the broad lithological diversity and exotic mineralogy of the BTAC. The apparently bimodal compositional spectrum (SiO_2 = 35 to 50% and 63 to 70%, *see* Figure 42) reflects the effort during sampling to, as much as possible, collect samples representative of end-member compositions and it is probable that random sampling would result in some intermediate bulk compositions. Extreme variation related to exceptional abundances of some minor and trace elements (*see* Figures 42 to 44, e.g., P_2O_5, Sr, Ba, Zr and Nb) is related to the presence of the exotic calcic component of possible carbonatitic affinity in some of the samples.

Samples exhibit a moderately to strongly alkaline character across the full compositional spectrum of the BTAC (*see* Figure 45). Geochemical parameters generally useful to differentiate a primitive mantle or evolved crustal signature (e.g., Mg#, Cr abundance) are of limited use in this case because they exhibit an extreme range that is interpreted to reflect a range of second and third order processes (e.g., mixing with exotic calcic component, carbonate alteration, heterogeneous oxide mineral distribution).

A striking characteristic, particularly in the ultramafic portion of the compositional spectrum, is the very high abundance of a range of HFSE including both heavy and light REE (Figure 57). The abundance of these elements is correlated, to some extent, with the presence of the exotic calcic component; however, samples not obviously incorporating this component are also relatively enriched.

PETROGENESIS

Alkalic rocks in Bristol Township span a broad compositional spectrum and include units with highly unusual mineralogical and geochemical characteristics. The alkalic character, presence of a mafic to ultramafic component and the relatively quartz-poor felsic component point to a mantle source and are difficult to reconcile with significant involvement of crustal reservoirs. The moderate to extreme

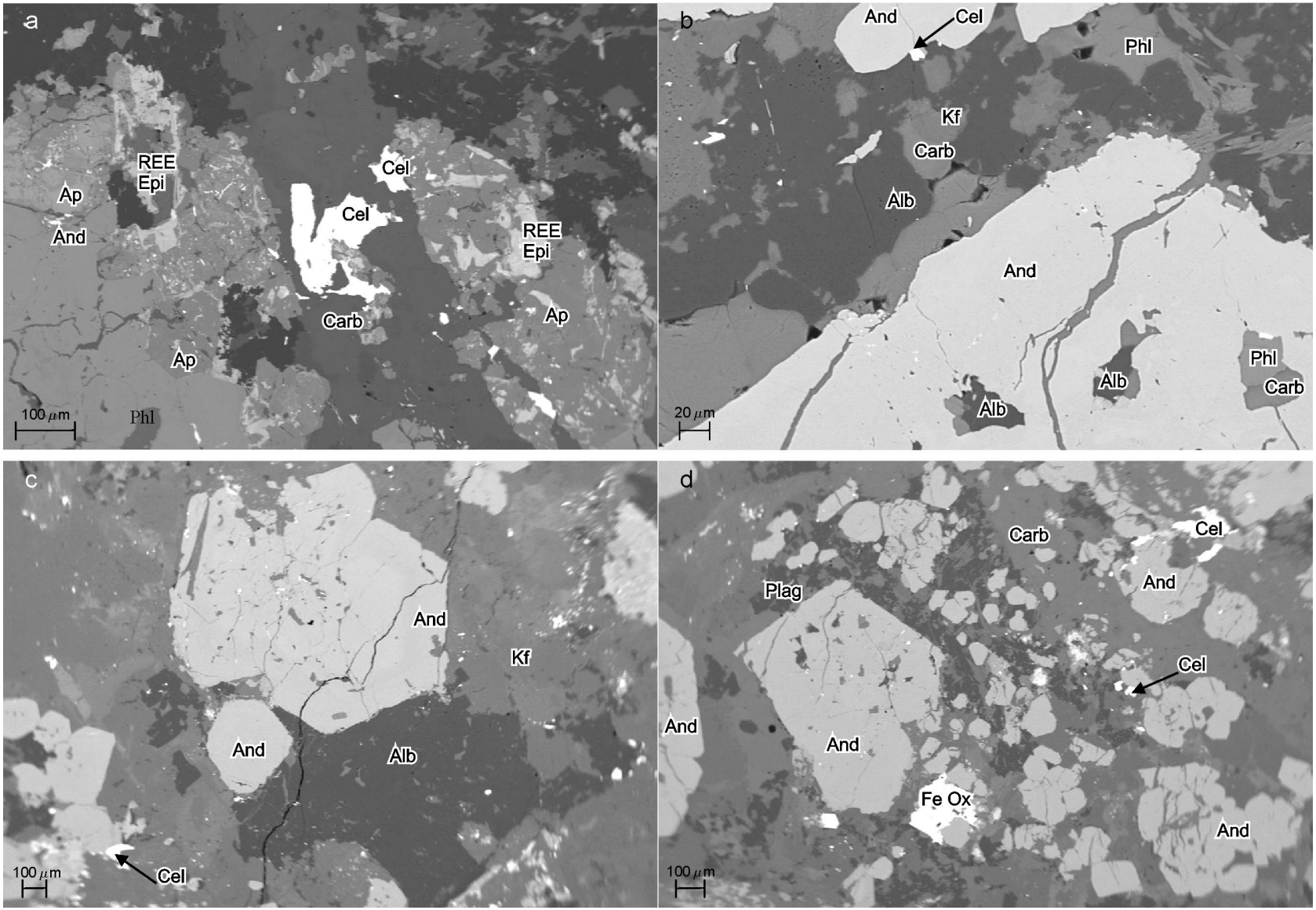

Figure 56. Scanning electron microscope backscatter images of texture and mineralogy in a minor intrusion with exotic calcic component mineralogy from southwest Bristol Township. Exotic mineralogy recognized in this sample includes abundant andradite garnet (And) as well as phlogopite (Phl), albite (Alb), barium-enriched potassium feldspar (Kf), magmatic carbonate (Carb), iron oxides (Fe Ox) and apatite (Ap) that includes both "normal" and REE-enriched varieties. Relatively abundant accessory minerals include REE-enriched epidote (REE Epi) and celestine (Cel) as well as barite, zircon, sphalerite, galena, cobalt-enriched pyrite and gold.

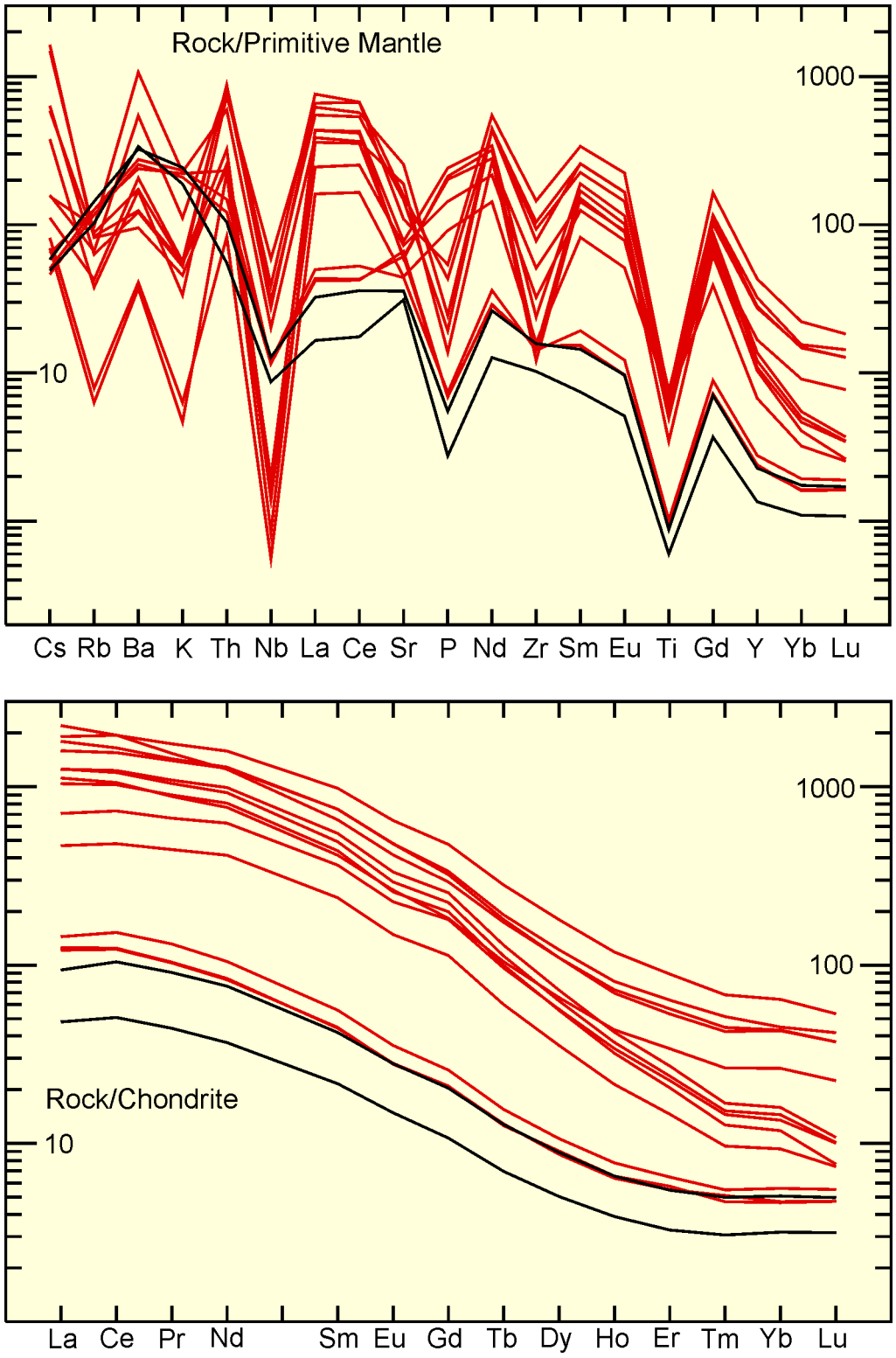

Figure 57. Chondrite and primitive mantle normalized trace element plots for samples from the Bristol Township alkalic complex (red lines), including the southwest Bristol Township syenite (black lines). Normalization values from Sun and McDonough (1989).

abundances of a wide range of trace elements are much higher than the composition of any potential volumetrically significant crustal contaminant and are most reasonably ascribed to metasomatic enrichment in the mantle source. The extreme nature of the enrichment is likely due to some combination of extreme metasomatism, very low degrees of melting and extreme crystal fractionation.

Distinctive characteristics of the exotic calcic component include the presence of magmatic carbonate, abundance of andradite and apatite, unusually high abundances of CaO, P_2O_5 and a wide range of trace elements including REE. These characteristics strongly suggest a carbonatitic affinity, and the intimate mixing of this component with alkalic magmatic units is interpreted to reflect CO_2-dominated melting of a metasomatically enriched mantle source.

Eastern Porcupine–Destor Fault Area Plutons

A number of poorly exposed, alkalic plutons (including Hislop, Pangea, Emons, Ludgate and Garrison intrusions) interpreted to be part of the late-tectonic group occur near the Porcupine–Destor fault (PDF) in Hislop, Guibord, Michuad, Garrison and Harker townships. Many of these intrusions exhibit a close spatial association with gold mineralization. The regional setting and characteristics of these intrusions have been investigated in some detail (Berger 2002; Pigeon 2003), and these intrusions are discussed as a group largely based on these studies augmented by observations made during the course of this investigation.

U/Pb zircon ages for units assigned to this group of intrusions include 2678 ± 2 Ma for the Garrison stock (Corfu 1993) and 2671 ± 1.5 Ma for an alkalic, intermineral dike from the Holloway Mine (Luinstra and Benn 2001).

FIELD RELATIONSHIPS

These units occur in areas where the plutons are juxtaposed against metavolcanic and metasedimentary rocks assigned to the Kidd–Munro, Tisdale and Blake River volcanic-dominated assemblages and Porcupine metasedimentary-dominated assemblage; however, the contacts are not well exposed and, in some cases, the contacts may be tectonic rather than intrusive. These units also exhibit a general spatial association with the Timiskaming assemblage supracrustal rocks, which, as at Kirkland Lake, include alkalic metavolcanics rocks that may be genetically associated with the intrusions (Berger 2002).

In most areas, the intrusions are massive and do not contain a penetrative deformational fabric. Locally, in proximity to deformation zones associated with the PDF, the intrusive units are intensely deformed and mylonitized. These characteristics, together with the relatively young U/Pb ages, suggest that like similar intrusions associated with the CLLF, these units are likely late tectonic in a regional sense but predate late deformation occurring within regional, east-trending faults.

PETROLOGY

The eastern PDF area plutons display considerable overlap in their mineralogy and petrology; however, each of the plutons has its own unique spectrum of compositions. The Pangea intrusion displays a broad continuous range in composition from ultramafic, through melasyenite to syenite with colour index of approximately 15 to 20. The ultramafic end of this spectrum is represented by clinopyroxene- and biotite-bearing hornblendite that contains significant amounts of apatite, magnetite and titanite. This rock type grades into melasyenite and syenite with increasing proportion of perthitic alkali feldspar diluting a similar mafic and accessory mineral assemblage. Minor amounts of andradite are present in some samples.

The Emens intrusion is somewhat similar to the Pangea intrusion except it does not extend to extreme ultramafic compositions and it also contains a distinctly more leucocratic (CI <10) syenite component. The mafic mineralogy is broadly similar to that of the Pangea intrusion, but the proportion of biotite within the mafic assemblage is higher. As in the Pangea intrusion, perthitic alkali feldspar generally forms large, conspicuous crystals. Accessory minerals (apatite, magnetite, titanite and andradite) are relatively abundant.

The Ludgate intrusion has a much more restricted compositional range, being composed almost entirely of a fairly leucocratic quartz syenite. Large, subhedral to euhedral, tabular, perthitic to antiperthitic alkali feldspar crystals that commonly display flowage alignment typically comprise approximately 90% of the rock. Minor quartz and albite is interstitial to these alkali-feldspar megacrysts. Mafic mineralogy includes sodic clinopyroxene and amphibole (aegirine-augite and magnesoriebeckite, Pigeon 2003) but rarely comprises more that 5% of the rock. One sample studied in detail contains an exotic accessory mineral assemblage that includes andradite, phlogopite, REE-enriched epidote, REE-enriched apatite, carbonate, allanite, barite and ancylite (LREE-enriched, hydrated Sr carbonate).

The quartz monzonitic Garrison pluton is unique among the eastern PDF area intrusions in being predominantly medium grained and equigranular as well as containing a subsolvus feldspar assemblage of perthitic alkali feldspar and albite. Minor quartz is interstitial to feldspar. Pigeon (2003) reports mafic mineral assemblages consisting of 3 amphiboles (magnesiohornblende, rickterite and magnesioriebeckite) and rare clinopyroxene. Magnetite, titanite and apatite are relatively abundant accessory minerals.

GEOCHEMISTRY

All of the plutons comprising the eastern PDF area intrusions are strongly alkalic although they exhibit a wide range of Na_2O/K_2O ratios (*see* Figure 42 and 45 and Pigeon 2003). The compositional range for individual plutons correlates with their mineralogical characteristics with the Emens intrusion ranging from 38 to 62% SiO_2 with a compositional gap between 53 and 60% SiO_2, whereas the Pangea intrusion displays a compositional continuum from 42 to 57 % SiO_2 and the more leucocratic Garrison and Ludgate intrusions, with relatively uniform mineralogy, display a more restricted, uniform compositional range (Pigeon 2003).

In addition to the strongly alkalic character, the other especially noteworthy general characteristic of all of these intrusions is enrichment in a wide range of LILE and HFSE while still preserving negative Nb–Ta–Ti anomalies on extended trace element normalized plots (Pigeon 2003). As in the case of the BTAC, extreme fractionation involving unusual minerals, heterogeneous distribution of oxide and sulphide minerals and secondary alteration render some of the standard geochemical monitors of mantle-crustal affinity (e.g., Mg#, Ni, Cr) of limited use.

PETROGENESIS

Characteristics identified during this investigation are consistent with those of a more detailed study that arrived at the conclusion that the eastern PDF area intrusions were derived by partial melting of a metasomatized mantle source (Pigeon 2003). The strongly alkalic character and extreme trace element characteristics are difficult to reconcile with significant involvement of a crustal reservoir.

Pigeon (2003) considered there to be 2 possible origins for the diverse Na_2O/K_2O ratios characterizing various units. He considered that some of the more sodic units could be a consequence of secondary alteration related to late magmatic or postmagmatic albitization. He also advanced an

alternative hypothesis that these rocks could be derived from distinct potassium-rich and sodium-rich metasomatized mantle sources. Both of these hypothesis are interpreted here to be unlikely explanations for the diversity in Na_2O/K_2O ratios. The distinct source hypothesis is considered to be unlikely because of the intimate admixture of sodic and potassic components without evidence for contacts between discrete phases, which requires that the 2 discrete magmas be mixed prior to emplacement (i.e., during melting or ascent). Such mixtures in small batches of magma would be expected to be quickly homogenized. An alteration origin is considered unlikely because sodic and potassic bulk compositions commonly coexist with no textural evidence for secondary replacement of one by the other. Indeed, sodic and potassic alkali feldspars may coexist within individual crystals as discrete zones, indicating that the compositions were attained during crystal growth. An alternative hypothesis to explain the segregation of sodic and potassic phases is equilibration of feldspar with both residual magma and exsolved aqueous magmatitic hydrothermal fluids. Such a process may separate potassium (partitioned into hydrothermal fluid) from sodium which becomes enriched in the residual magmatic phase. Within this hypothesis, the intimate admixture of sodic and potassic phases arises from the crystallization of feldspars in parts of the system where magmas and fluids coexisted. Although this latter hypothesis is interpreted to be most consistent with observations made during this investigation, further study is required in order to understand the origin of the potassic-sodic segregation.

Other Late-Tectonic Intrusions

In addition to the late-tectonic plutons discussed above, a number of other units (Iris, Hislop, Swan River area syenite dikes, Canadian Arrow, a number of small intrusions in Powell Township area, Hare Lake intrusion and Casey Mountain syenite intrusion) examined in various detail are thought to be representative of the same suite. Many of these intrusions exhibit a close spatial association with gold mineralization.

A sample of the Casey Mountain syenite (7523, UTM 605732E 5273257N, NAD83) was selected for LA-ICP-MS and TIMS U/Pb zircon geochronology in order to evaluate the age of one of the "off-break" syenites. The sample is a medium-grained, flow-foliated (alignment of feldspar crystals), hornblende syenite. The LA-ICP-MS analyses are mostly moderately discordant with only 22 of 73 analyses being within 5% of concordia. These least discordant analyses have a comparatively narrow range of $^{207}Pb/^{206}Pb$ ages (2654–2699 Ma), with a mean age of 2678 ± 13 Ma. Three of 5 TIMS analyses are approximately 30% discordant. The $^{207}Pb/^{206}Pb$ age of the least (1.7%) discordant fraction is 2681 Ma and is likely a maximum age for the emplacement of the pluton (inheritance cannot be evaluated); consequently, the mean LA-ICP-MS age may provide a poorly constrained, approximate estimate of the timing of emplacement.

SUMMARY

Intrusions grouped in the late-tectonic category are characterized by distinctive lithologic associations, mineralogy and geochemical characteristics. They range in size from moderately large intrusions (<90 km^2) to small, minor intrusions. All of the large, and many of the small, intrusions comprising this group are emplaced in close proximity to the Porcupine–Destor fault or Cadillac–Larder Lake fault. Many of these intrusions exhibit a close spatial association with gold mineralization.

Although emplaced late within the overall sequence of deformational events, they may be intensely deformed within these late fault zones. Absolute age determinations discussed above for the Otto Stock (2679 ± 1 Ma), Lebel Stock (2673 ± 2 Ma), Murdock Creek intrusion (2672 ± 2 Ma), Cairo stock (2676.3 ± 1.4 Ma), Garrison stock (2678 ± 2 Ma) and a Holloway mine alkalic dike (2671 ± 1.5 Ma) confirm the

comparatively late timing of these units and establish the age range for late tectonic magmatism as being approximately 2671 to 2679 Ma.

Comparatively leucocratic syenites typically predominate; however, mafic to ultramafic phases occur within some of the plutons. Minor amounts of quartz are present in many of the intrusions. Mafic mineralogy includes calcic to sodic amphiboles, clinopyroxene and biotite; in some cases the primary mineralogy is strongly altered to mineral assemblages containing various combinations of fibrous amphiboles, chlorite, carbonate and magnetite. Primary magnetite is typically abundant and units are commonly characterized by high magnetic susceptibility. Magmatic accessory minerals including titanite, apatite and epidote are relatively abundant and are, in some cases, characterized by extreme REE enrichment. Magmatic carbonate, andradite, barite and celestine are present locally and, together with the presence of REE-enriched apatite, may reflect the involvement of a volumetrically minor carbonatitic component.

A consistent geochemical characteristic across the broad spectrum of rock types comprising late-tectonic intrusions is a strongly alkalic character arising from extreme enrichment in LILE. These characteristics, together with the presence of mafic to ultramafic bulk compositions and enrichment in a range of HFSE including moderately to highly fractionated REE, suggest that these rocks were generated by partial melting of a metasomatized mantle source. Extreme enrichment of HFSE and P_2O_5 observed in a number of these intrusions further supports the possible involvement of a carbonatitic component.

Minor Intrusions

Diverse minor intrusions are heterogeneously distributed within the Abitibi Subprovince. As used here, the term minor intrusions refers to small (generally less than 20 m across) intrusive units that commonly have dike or vein forms and are not portrayed on regional geological maps. In many cases, they are thought to simply be smaller scale manifestations of the major plutonic events discussed above, although in many cases it is not possible to unequivocally demonstrate this to be the case.

The regional distribution and abundance of minor intrusions is inherently difficult to constrain because it is in part related to the outcrop density and quality and to the scale of mapping. These limitations not withstanding, some generalizations are possible based on the regional investigations carried out as part of this study. Minor intrusions are most abundant within deformation zones associated with the major east-trending faults, near the contacts of plutons and within portions of the synvolcanic, plutonic infrastructure batholiths. Within the interior of syntectonic to late-tectonic plutons and within the less deformed portions of the greenstone belt away from pluton contacts and deformation zones, minor intrusions are present sporadically but are rarely abundant. Two exceptions to this latter generalization are the Shaw Dome and Maisonville Township, where minor intrusions are somewhat more abundant than is typical of otherwise similar areas. In both cases it is possible that the minor intrusions are manifestations of unexposed plutons at depth.

Minor intrusions occurring within synvolcanic batholithic complexes are generally most abundant in those well-foliated portions of the batholith, and especially where the foliated tonalites contain screens of amphibolite. The dikes are mostly leucogranite (pegmatitic and aplitic textures are extremely common) with subordinate amounts of diorite to quartz monzodiorites and minor, localized intermediate to mafic dikes. The dikes generally have very simple mineralogy. The dikes are variously deformed and even dikes of similar composition in a single outcrop may range from being undeformed to strongly transposed into the plane of the foliation. The concentration of dikes in these zones is interpreted to be a consequence of localization of structures appropriate for hosting dikes within zones of heterogeneous

strain associated with lithological (and hence rheological) diversity synchronous with the emplacement of the later more massive plutons.

Minor intrusions are locally more abundant near the contacts of syntectonic to late-tectonic plutons. The minor intrusions may occur in both the adjacent country rocks as well as marginal portions of the pluton. Along steeply dipping pluton contacts, the concentration of dikes is typically limited to zones within 100 to 200 m of the contact. This effect may be more widespread above plutons in areas where the pluton contact is more shallowly dipping, as may be the case, for example, in the previously discussed Shaw Dome and Maisonville Township areas.

Minor intrusions are also concentrated within deformation zones associated with the Porcupine–Destor and Cadillac–Larder Lake faults. It is possible that the greatest intensity of diking may be associated with mineralized areas within these zones although it is difficult to discount the possibility that the greater numbers of dikes recognized in these areas is a function of the detail of work carried out in these zones. In some areas the minor intrusions associated with these zones have distinctive compositions suggesting they are genetically related to nearby plutons (e.g., alkalic dikes near the Lebel and Murdock Creek intrusions in the Kirkland Lake area, andradite-bearing dikes near a small, syenitic pluton in the southern portion of Bristol Township). Some early, quartz ± feldspar porphyritic felsic dikes in the Timmins area are probably related to the larger, early syntectonic porphyries although rare examples of otherwise similar dikes cutting Timiskaming metasedimentary rocks demonstrate that multiple ages of megascopically similar dikes occur in this area. In many cases the dikes cannot be unambiguously correlated with the major intrusive associations.

Tectonic Significance of Abitibi Subprovince Plutonic Record

The Abitibi Subprovince plutonic record developed over at least an 80 million year period of time and is the only component of the rock record that spans the full development of the subprovince from initial magma production to essentially its final tectonometamorphic configuration. Observations relating to intermediate to felsic intrusive rocks, including their petrology and petrogenesis, absolute ages, relative ages with respect to various tectonic and metamorphic elements and depth of emplacement, have important implications for the tectonic evolution of the Abitibi Subprovince. This section discusses each of these data sets individually, linkages with other aspects of the geological evolution and concludes with a partially new geodynamic model for the evolution of the Abitibi Subprovince. The data and observations used to develop this synthesis are primarily those discussed in the preceding detailed discussion of individual plutons and pluton groupings.

For the purpose of this discussion, intermediate to felsic intrusive rocks are subdivided into 5 groups that are interpreted to have different relative age relationships with respect to the stratigraphic and tectonometamorphic development of the Abitibi Subprovince. U/Pb absolute age constraints are broadly consistent with this subdivision, although in some cases there is partial overlap. The ensuing discussion focuses on the absolute and relative timing of these 5 groups, referred to here as i) synvolcanic, pretectonic plutons, ii) early syntectonic plutons, iii) syntectonic plutons, iv) late-tectonic plutons and v) posttectonic plutons. The posttectonic category was not discussed separately within the preceding discussion because the only volumetrically significant unit assigned to this category (Somme pluton) is an integral component of the Kenogamissi Batholith.

The adoption of this subdivision is problematic in a number of respects, including the i) inability to reliably correlate specific elements of the tectonic evolution across the region, ii) possible transitional

character and diachroneity of deformational "events" and iii) domainal character of some elements of the deformational history. This results in relationships that may be difficult to interpret, such as large, homogeneous pretectonic plutons being very weakly foliated because of their inherent rigidity whereas late-tectonic plutons emplaced in fault zones, into which the latest increments of regional strain are partitioned, may be intensely foliated. Although it is not generally possible to regionally correlate late fabric-forming deformational events, it is proposed here that a relatively early fabric defined by near-peak metamorphic mineral assemblages can be broadly correlated across the western Abitibi Subprovince. The same problems described above also may apply to this correlation; however, because the late fabrics are commonly associated with retrograde, post-peak metamorphic mineral assemblages, it can be inferred that peak metamorphic conditions, and co-temporal fabric development, probably persisted for a maximum of approximately 5 million years. In many cases, it is possible to distinguish early peak metamorphic mineral fabrics from subsequent post-peak metamorphic fabrics although there may be cases associated with development of multiple late fabrics where this distinction is not possible. Although it is probable that this basis for subdivision results in incorrect classification of some units (particularly pretectonic versus syntectonic units), the overall coherence of the data discussed below suggests that this approach can be applied moderately successfully.

ABSOLUTE AND RELATIVE TIMING OF INTERMEDIATE TO FELSIC INTRUSIVE ACTIVITY

This section considers the absolute ages of the various categories of intermediate to felsic intrusions and relative timing with respect to volcanism, sedimentation, deformation and metamorphism. The absolute ages utilized in this discussion are summarized in Table 6 and Figure 58.

Absolute ages of intermediate to felsic intrusive units are broadly consistent with relative ages inferred from field relationships. Plutons assigned to the pretectonic category are characterized by the presence of a weakly to very well developed deformational fabric. Within the interior of large batholithic complexes such as the Kenogamissi Batholith, these fabrics are folded with dips ranging from vertical to subhorizontal whereas near the contacts of these large complexes, the fabrics generally have moderate to steep dips and are parallel to the contact and a deformational fabric defined by near-peak metamorphic mineral assemblages in the metavolcanic country rock. On this basis, these fabrics are interpreted to be correlative with those occurring within the metavolcanic rocks and are regionally folded along with these fabrics and the greenstone belt stratigraphy. Absolute age determinations are consistent with this interpretation, as the pretectonic plutons are the oldest plutons and are emplaced over an interval of time that is essentially identical to that of deposition of the volcanic-dominated assemblages of the greenstone belt (Figure 58).

Plutons regarded to be early syntectonic are emplaced over a narrow time interval, between approximately 2691 Ma and 2685 Ma (Table 6 and Figure 58). Many intrusions of this type are emplaced in proximity to major regional faults and are overprinted by moderately intense late deformation and hydrothermal alteration. As a consequence, it is not always clear whether fabrics that are commonly present within these units are, at least in part, representative of relatively early fabrics developed during peak metamorphism. The timing of emplacement of the early syntectonic intrusions is identical to that of volcanic units occurring near the base of the Porcupine assemblage (e.g., Krist volcanic unit) and consistent with general constraints on the timing of metasedimentary units comprising the Porcupine assemblage. The Porcupine assemblage generally is characterized by a fabric defined by near-peak metamorphic mineral assemblages and has been folded along with the underlying metavolcanic-dominated assemblages; however, its base has been interpreted locally to represent an unconformity or disconformity, with some of the earliest deformation of the underlying volcanic sequences preceding its

Table 6. Summary of U/Pb ages used for relationships discussed in the text.

Sample	Age	Error -	Error +	Reference	Rock Type	Assemblage / Unit	Batholith / Pluton	Relative Relationship Volcanism	Relative Relationship Tectonism	Interpreted Petrogenesis
1,PTF-1	2747.0	2.0	2.0	Mortensen 1993	Felsic volcanic	Pacaud				
98JAA-020	2741.3	9.8	9.8	Ayer et al. 2002	Felsic lapilli tuff	Pacaud				
99JAA-050	2727.9	2.2	2.2	Ayer et al. 2002	Felsic flow	Deloro				
N-77-18	2727.4	1.0	1.0	Corfu and Noble 1992	Dacite tuff	Deloro				
96JAA-0106	2726.0	1.3	1.3	Ayer et al. 2002	Felsic flow	Deloro				
96JAA-089	2724.8	1.0	1.0	Ayer et al. 2002	Felsic flow	Deloro				
DU2, C88-17	2724.6	0.8	0.8	Corfu and Noble 1992	Felsic volcanic	Deloro				
04PCT-0062	2724.1	3.7	3.7	Ayer et al. 2005	Feldspar-phyric lapilli-tuff	Deloro				
96TB099	2723.4	1.7	1.7	Barrie and Corfu 1999	Dacite	Deloro				
96JAA-037	2723.1	1.2	1.2	Ayer et al. 2002	Felsic lapilli tuff	Deloro				
96TB-099	2723.1	1.3	1.3	Barrie & Corfu 1999; Ayer et al. 2005	Felsic volcs	Deloro				
98TB018	2723.0	1.6	1.6	Barrie 1999	Dacite lapilli tuff	Stoughton-Roquemaure				
97TB026	2721.6	1.6	1.6	Barrie 1999	Dacite tuff	Stoughton-Roquemaure				
96TB091	2721.0	2.0	2.0	Barrie 1999	Dacite tuff	Stoughton-Roquemaure				
96TB050	2721.0	2.0	2.0	Barrie 1999	Rhyolite fragmental	Stoughton-Roquemaure				
96JAA-083	2719.5	1.7	1.7	Ayer et al. 2002	Dacite tuff	Kidd-Munro				
KCR	2717.0	2.0	2.0	Barrie and Davis 1990	Rhyolite	Kidd-Munro				
77-22	2717.0	2.0	2.0	Bleeker et al. 1999	Felsic lapilli tuff	Kidd-Munro				
96TB021	2717.0	1.2	1.2	Barrie and Corfu 1999	Dacite flow	Kidd-Munro				
98JAA-019	2716.7	1.7	1.7	Ayer et al. 2002	Felsic tuff breccia	Kidd-Munro				
97JAA-102	2716.3	1.5	1.5	Ropchan et al. 2002	Felsic tuff breccia	Kidd-Munro				
97TB090	2716.2	2.0	3.0	Barrie 1999	Rhyolite	Kidd-Munro				
KC.210	2716.0	1.2	1.2	Bleeker et al. 1999	Felsic lapilli tuff	Kidd-Munro				
KCHW.1	2716.0	0.6	0.6	Bleeker et al. 1999	Rhyolite tuff	Kidd-Munro				
PR, P-23	2716.0	4.0	4.0	Barrie and Davis 1990	Rhyolite tuff	Kidd-Munro				
KCFC.1	2714.9	1.1	1.1	Bleeker et al. 1999	Rhyolite tuff	Kidd-Munro				
04BHA-0297	2714.6	1.2	1.2	Ayer et al 2005	Quartz+feldspar phyric felsic flow	Kidd-Munro				
KCC.9	2714.4	0.8	0.8	Bleeker et al. 1999	Rhyolite	Kidd-Munro				
KCCARN.1	2714.2	0.5	0.5	Bleeker et al. 1999	Rhyolite	Kidd-Munro				
SR, 84SM7	2714.0	2.0	2.0	Corfu et al. 1989; Corfu and Noble 1992	Rhyolite flow	Kidd-Munro				
KC.406E	2713.4	1.3	1.3	Bleeker et al. 1999	Rhyolite flow	Kidd-Munro				
96JAA-088	2713.2	1.8	1.8	Ayer et al. 2002	Felsic tuff breccia	Kidd-Munro				
KCC.1	2713.1	1.3	1.3	Bleeker et al. 1999	Felsic tuffite	Kidd-Munro				
HM,N76-3	2713.0	2.0	2.0	Corfu et al. 1989	Felsic volcanic	Kidd-Munro				
96JAA-094	2712.8	1.2	1.2	Ayer et al. 2002	Felsic tuff	Kidd-Munro				
04BHA-0333	2712.3	2.8	2.8	Ayer et al. 2005	Felsic debris flow	Kidd-Munro				
96JAA-0094	2712.2	0.9	0.9	Ayer et al. 2002; Ayer et al. 2005	Felsic volcs	Kidd-Munro				
98JAA-0006	2712.0	4.0	4.0	Ayer et al. 1999	Heterolithic tuff breccia	Tisdale				
KC.102	2711.3	1.5	1.9	Bleeker et al. 1999	Rhyolite	Kidd-Munro				
99JAA-031	2710.5	1.6	1.6	Ayer et al. 2002	Rhyolite flow	Tisdale				
KCS.4B	2710.1	4.4	4.4	Bleeker et al. 1999	Felsic tuff breccia	Kidd-Munro				
97TB091	2710.0	1.5	1.5	Barrie 1999	Rhyolite	Kidd-Munro				
96TB079	2708.1	2.1	2.1	Barrie and Corfu 1999	Dacite	Tisdale				
01JAA-061	2707.8	1.2	1.2	Ayer, Ketchum and Trowell 2002	Heterolithic lapilli tuff	Tisdale				
97JAA-108	2707.4	1.2	1.2	Ayer et al. 2002	Felsic tuff	Tisdale				
96JAA-091	2707.0	3.0	3.0	Ayer et al. 2002	Mafic flow	Tisdale				
Ti-043	2706.2	2.4	2.4	Ayer et al. 1997	Felsic tuff	Tisdale				
MH, N-77-21	2706.0	2.0	2.0	Corfu and Noble 1992	Andesitic crystall tuff	Tisdale				
RR, R-16	2705.7	2.0	2.0	Barrie and Davis 1990	Laminated lapilli tuff	Tisdale				
KR	2705.0	2.0	2.0	Barrie and Davis 1990	Rhyolite flow	Tisdale				

Table 6. (continued)

Sample	Age	Error -	Error +	Reference	Rock Type	Assemblage / Unit	Batholith / Pluton	Relative Relationship Volcanism	Relative Relationship Tectonism	Interpreted Petrogenesis
96TB082	2705.0	1.5	1.5	Barrie 1999	Dacite fragmental	Tisdale				
LL,N77-9	2705.0	2.0	2.0	Corfu et al. 1989; Corfu & Noble 1992	Felsic fragmental	Tisdale				
97JAA-101	2703.7	1.5	1.5	Ayer et al. 2002	Felsic tuff	Tisdale				
03BHA-0047	2703.1	1.2	1.2	Ayer et al. 2005	Felsic lapilli-tuff	Blake River				
96JAA-087	2703.0	1.9	1.9	Ayer et al. 2002	Felsic flow	Tisdale				
N-77-16	2703.0	1.5	1.5	Corfu et al. 1989	Felsic lapilli tuff	Tisdale				
Ti-1257	2702.9	1.3	1.3	Ayer et al. 1997	Felsic volcanic	Tisdale				
96JAA-093	2702.3	1.4	1.4	Ayer et al. 2002	Felsic volcanic	Tisdale				
98JAA-011	2702.0	3.0	3.0	Ayer et al. 2002	Intermediate lapilli tuff	Tisdale				
97JAA-104	2701.7	2.2	2.2	Ropchan et al. 2002	Felsic flow	Blake River				
03-BAH-0384	2701.1	1.4	1.4	Ayer et al. 2005	Felsic lapilli tuff	Blake River				
KJ,C88-8,	2701.0	3.0	3.0	Corfu and Noble 1992	High silica rhyolite horizon	Blake River				
C91-3	2701.0	2.0	3.0	Corfu 1993	Felsic volcanic	Blake River				
SK,83SM1	2701.0	3.0	3.0	Corfu et al. 1991; Corfu & Noble 1992	Felsic volcanic	Blake River				
BR,N77-12	2701.0	2.0	2.0	Corfu and Noble 1992	Rhyolite	Blake River				
03-BAH-0382	2700.0	1.1	1.1	Ayer et al. 2005	Rhyolite	Blake River				
C88-10	2700.0	3.0	3.0	Corfu 1993	Felsic volcanic	Blake River				
03-BAH-0345	2698.6	1.3	1.3	Ayer et al. 2005	Felsic lapilli tuff	Blake River				
03ASP0179.1.1	2696.6	1.3	1.3	Ayer et al. 2005	Massive rhyolite	Blake River				
96JAA-011	2694.1	4.5	4.5	Ayer et al. 2002	Felsic volcanic	Blake River				
Ti-3488	2691.5	1.5	1.5	Ayer et al. 2003	Felsic volcanic	Porcupine				
99JAA-061	2687.5	1.3	1.3	Ayer, Ketchum and Trowell 2002	Felsic tuff	Porcupine				
TK, 83SM-15	2687.3	1.6	1.6	Corfu 1993, Ayer et al. 2003	Felsic fragmental	Porcupine				
02JAA-009	2685.1	1.3	1.3	Ayer et al. 2003	Felsic tuff	Porcupine				
98GWJ-289	2687.9	1.2	1.2	Ayer et al. 2002	Felsic flow	Porcupine				
96JAA-097	2687.0	1.0	1.0	Ayer et al. 2002	Felsic tuff breccia	Porcupine				
01JAA-075	2703.1	1.6	1.6	Ayer, Ketchum and Trowell 2002	Wacke	Porcupine				
96JAA-105	2701.6	1.4	1.4	Ayer et al. 2002	Sandstone	Porcupine				
96JAA-0060	2699.0	2.4	2.4	Ayer et al. 2002	Wacke	Porcupine				
KC.90	2698.5	1.0	1.0	Bleeker et al. 1999	Sandstone	Porcupine				
99JAA-007	2695.0	3.0	3.0	Ayer, Ketchum and Trowell 2002	Heterolithic conglomerate	Porcupine				
KCHW.2	2692.0	7.1	7.1	Bleeker et al. 1999	Sandstone	Porcupine				
KCR-52	2690.9	2.5	2.5	Ayer et al. 2005	Wacke	Porcupine				
98JAA-022	2689.6	6.0	6.0	Ayer et al. 2002	Sandstone	Porcupine				
03RJB18973-1	2688.2	1.9	1.9	Ayer et al. 2005	Arenite	Porcupine				
04JAA-0003	2687.2	1.6	1.6	Ayer et al. 2005	Fine grained wacke	Porcupine				
97JAA-107	2687.0	3.0	3.0	Ayer et al. 2002	Sandstone	Porcupine				
3D-CG	2686.6	1.8	1.8	Ropchan et al. 2002	Heterolithic tuff breccia	Porcupine				
KCR.43	2684.7	6.3	6.3	Bleeker et al. 1999	Sandstone	Porcupine				
TBv,C88-9	2677.0	3.0	3.0	Corfu et al. 1991	Tuff breccia	Timiskaming				
03VOI0422-1	2669.6	1.4	1.4	Ayer et al. 2005	Feldspar-phyric trachyte flow	Timiskaming				
03RJB18972-6	2689.5	1.7	1.7	Ayer et al. 2005	Fine sandstone	Timiskaming				
99JAA-042	2688.5	1.0	1.0	Ayer, Ketchum and Trowell 2002	Sandstone	Timiskaming				
99JAA-056	2685.8	1.5	1.5	Ayer, Ketchum and Trowell 2002	Sandstone	Timiskaming				
04JAA-0004	2684.4	1.7	1.7	Ayer et al. 2005	Conglomerate	Timiskaming				
98BRB-649	2684.3	1.3	1.3	Ropchan et al. 2002	Sandstone	Timiskaming				
TCs, TCc2, TCcl	2680.0	3.0	3.0	Corfu et al. 1991	Ss with qtz-fel porphyry pebbles	Timiskaming				
BNB-01-T-01	2679.0	4.0	4.0	Ayer et al. 2003	Sandstone	Timiskaming				
TTs, C88-18	2679.0	3.0	3.0	Corfu et al. 1991	Sandstone	Timiskaming				
TLs,C88-13	2679.0	3.0	3.0	Corfu et al. 1991	Pebbly sandstone	Timiskaming				
03VOI0570-1	2677.3	3.1	3.1	Ayer et al. 2005	Sandstone	Timiskaming				
99JAA-055	2674.3	3.7	3.7	Ayer, Ketchum and Trowell 2002	Wacke	Timiskaming				
02JAA-017	2673.9	1.8	1.8	Ayer et al. 2003	Conglomerate	Timiskaming				
02JAA-010	2673.0	0.0	0.0	Ayer et al. 2003	Siltstone	Timiskaming				
BNB-01-T-02	2669.0	7.0	7.0	Ayer et al. 2003	Conglomerate	Timiskaming				

Table 6. (continued)

Sample	Age	Error -	Error +	Reference	Rock Type	Assemblage / Unit	Batholith / Pluton	Relative Relationship Volcanism	Relative Relationship Tectonism	Interpreted Petrogenesis
119	2747.3	2.6	2.6	Ketchum et al. 2008	Biotite-hornblende tonalite	Rice Lake tonalite	Kenogamisis Batholth	Synvolcanic	Pretectonic	TTG
01JAA-072	2746.7	1.4	1.4	Ketchum et al. 2008	Biotite-hornblende tonalite	Rice Lake tonalite	Kenogamisis Batholth	Synvolcanic	Pretectonic	TTG
02JAA-006	2743.6	1.0	1.0	Ketchum et al. 2008	Gneissic tonalite	Round Lake batholith	Round Lake Batholith	Synvolcanic	Pretectonic	TTG
92HNB0070a	2740.0	2.0	2.0	Heather 2001	Biotite trondhjemite	Chester trondhjemite	Ramsey-Algoma Batholith	Synvolcanic	Pretectonic	TTG
93HNB0196	2727.0	9.0	11.0	Heather 2001	Biotite tonalite	Arbutus tonalite	Ramsey-Algoma Batholith	Synvolcanic	Pretectonic	TTG
95HNB0274	2723.0	3.0	3.0	Heather 2001	Hornblende-biotite tonalite gneiss	Gogama tonalite	Kenogamisis Batholth	Synvolcanic	Pretectonic	TTG
02JAA-005	2713.5	1.3	1.3	Ketchum et al. 2008	Hornblende-biotite tonalite	Round Lake batholith	Round Lake Batholith	Synvolcanic	Pretectonic	TTG
92HNB0017	2713.0	3.0	2.0	Heather 2001	Hornblende tonalite	Regan tonalite	Kenogamisis Batholth	Synvolcanic	Pretectonic	TTG
02JAA-007	2701.3	1.3	1.3	Ayer, Ketchum and Trowell 2002	Biotite granodiorite	Rice Lake granodiorite	Kenogamisis Batholth	Synvolcanic	Pretectonic	TTG
01JAA-073	2699.9	0.8	0.8	Ketchum et al. 2008	Biotite granodiorite	Rice Lake granodiorite	Kenogamisis Batholth	Synvolcanic	Pretectonic	TTG
03ASP0130.1.2	2699.8	3.6	3.6	Ayer et al. 2005	Quartz-feldspar porphyry	Blake River	Subvolcanic Intrusion	Synvolcanic	Pretectonic	TTG
FC-3-75	2699.0	2.9	3.5	Frarey and Krogh 1986	Quartz diorite	Watabeag Batholith	Watabeag Batholith	Synvolcanic	Pretectonic	TTG
13,RLB-1	2697.6	3.6	4.8	Mortensen 1993	Tonalite	Round Lake batholith	Round Lake Batholith	Synvolcanic	Pretectonic	TTG
14,ICS-1	2697.0	2.0	2.0	Mortensen 1993	Granodiorite	Indian Chute stock	Round Lake Batholith	Synvolcanic	Pretectonic	TTG
92HNB0124a	2696.0	3.0	3.0	Heather 2001	Biotite tonalite	Northrup tonalite	kenogamisis Batholth	Synvolcanic	Pretectonic	TTG
GB	2695.0	1.5	1.5	Barrie and Davis 1990	Tonalite	Cote Stock	Groundhog River Batholith	Synvolcanic	Pretectonic	TTG
GC	2694.0	4.0	4.0	Barrie and Davis 1990	Tonalite	Nat River granitic complex	Groundhog River Batholith	Synvolcanic	Pretectonic	TTG
MiP, 84SM-2	2691.0	3.0	3.0	Corfu et al. 1989	Quartz-feldspar porphyry	Miller porphyry	Miller Porphyry	Synvolcanic	Early Syntectonic	TTG
PaP,KN76-7	2691.0	2.0	2.0	Corfu and Noble 1992	Quartz-feldspar porphyry	Paymaster porphyry	Paymaster Porphyry	Synvolcanic	Early Syntectonic	TTG
PrP, 83SM-32	2690.0	0.0	0.0	Corfu et al. 1989	Quartz-feldspar porphyry	Preston porphyry	Preston Porphyry	Synvolcanic	Early Syntectonic	TTG
Pep, 83SM-23	2689.0	2.0	2.0	Corfu et al. 1989	Quartz-feldspar porphyry	Pearl Lake porphyry	Pearl Lake Porphyry	Synvolcanic	Early Syntectonic	TTG
03-LAH-0627	2689.0	1.4	1.4	Ayer et al. 2005	Quartz porphyry	Porphyry intrusion	Mt Logano Porphyry	Synvolcanic	Early Syntectonic	TTG
CL,N77-13,	2689.0	1.0	1.0	Corfu and Noble 1992	Quartz diorite	Clarice Lake stock	Clarice Lake Stock	Synvolcanic	Early Syntectonic	TTG
03SJP059	2688.5	2.3	2.3	Ayer et al. 2005	Feldspar phyric dyke	Feldspar phyric dyke	Clifford Stock Dyke	Synvolcanic	Early Syntectonic	TTG
Crp, 84SM-4	2688.0	2.0	2.0	Corfu et al. 1989	Quartz-feldspar porphyry	Crown porphyry	Crown Porphyry	Synvolcanic	Early Syntectonic	TTG
	2688.0	2.0	2.0	Gray and Hutchinson 2001	Quartz-feldspar porphyry	Blueberry Hill porphyry	Blueberry Hill Porphyry	Synvolcanic	Early Syntectonic	TTG
02JAA-019	2687.7	1.4	1.4	Ayer et al. 2003	Quartz-feldspar porphyry	Bristol porphyry	Bristol Porphyry	Synvolcanic	Early Syntectonic	TTG
04ED-198	2687.6	2.2	2.2	Ayer et al. 2005	Quartz-phyric felsic unit	Porphyry intrusion	Hoyle Pond Porphyry Sill	Synvolcanic	Early Syntectonic	TTG
03SJP115-1	2686.9	1.2	1.2	Ayer et al. 2005	Monzonite	Clifford stock	Clifford Stock	Synvolcanic	Early Syntectonic	TTG
04MGH-0283	2686.2	1.1	1.1	Ayer et al. 2005	QFP cutting tuff	Porphyry intrusion	Redstone Mine Porphyry	Synvolcanic	Early Syntectonic	TTG
TBp,CN78-2	2685.0	3.0	3.0	Corfu et al. 1991	Quartz porphyry	Bidgood stock	Bidgood Porphyry	Synvolcanic	Early Syntectonic	TTG
03ED-096A	2684.4	1.9	1.9	Ayer et al. 2005	Quartz-feldspar porphyry	Porphyry intrusion	Hoyle Pond Porphyry	Synvolcanic	Early Syntectonic	TTG
#9,FC10-75	2686.4	2.8	3.0	Frarey and Krogh 1986	Granodiorite	Adams stock	Adams Pluton	Postvolcanic	Syntectonic	LMD-sanukitoid / TTG
117/02JAA8	2684.4	1.2	1.2	Ketchum et al. 2008	Hornblende diorite	Rice Lake diorite	Kenogamisis Batholth	Postvolcanic	Syntectonic	LMD-sanukitoid / TTG
92HNB0123a	2682.0	3.0	3.0	Heather 2001	Hornblende granodiorite	Neville pluton	Kenogamisis Batholth	Postvolcanic	Syntectonic	LMD-sanukitoid / TTG
06GPB7452	2681.8	4.2	4.2	Beakhouse, unpublished	Hornblende granodiorite	Giekie Pluton	Giekie Pluton	Postvolcanic	Syntectonic	LMD-sanukitoid / TTG
06GPB7575	2681.0	2.7	2.7	Beakhouse, unpublished	Hornblende granodiorite	Butler Lake pluton	Butler Lake pluton	Postvolcanic	Syntectonic	LMD-sanukitoid / TTG
92HNB0125	2681.0	3.0	3.0	Heather 2001	Hornblende granodiorite	Hillary pluton	Kenogamisis Batholth	Postvolcanic	Syntectonic	LMD-sanukitoid / TTG
#6,FC5-75	2681.0	3.0	3.0	Frarey and Krogh 1986	Quartz monzonite	Watabeag Batholith	Watabeag Batholith	Postvolcanic	Syntectonic	LMD-sanukitoid / TTG
#5,FC7-75	2677.0	3.0	3.0	Frarey and Krogh 1986	Granite	Winnie Lake stock	Winnie Lake Stock	Postvolcanic	Syntectonic	LMD-sanukitoid / TTG
#7, FC9-75	2676.0	2.1	2.2	Frarey and Krogh 1986	Quartz monzonite	Watabeag Batholith	Watabeag Batholith	Postvolcanic	Syntectonic	LMD-sanukitoid / TTG
OT,K762	2679.0	1.0	1.0	Corfu and Noble 1992	Syenite	Otto Stock	Otto Stock	Postvolcanic	Late Tectonic	LMD-alkalic
#4, FC12-75	2678.9	3.6	3.9	Frarey and Krogh 1986	Granodiorite	Garrison stock	Garrison Stock	Postvolcanic	Late Tectonic	LMD-alkalic
02JAA-022	2676.3	1.4	1.4	Ayer unpublished data	Foliated syenite	Cairo stock	Cairo Stock	Postvolcanic	Late Tectonic	LMD-alkalic
L92-5, L92-8	2673.0	2.0	2.0	Wilkinson et al. 1993	Syenite	Lebel Stock	Lebel Stock	Postvolcanic	Late Tectonic	LMD-alkalic
L92-1	2672.0	2.0	2.0	Wilkinson et al. 1999	Syenite	Murdock Creek stock	Murdock Creek Intrusion	Postvolcanic	Late Tectonic	LMD-alkalic
04JAA-0010	2676.5	1.6	1.6	Ayer et al. 2005	Albitite dike	Albitite dike	Albitite dike	Postvolcanic	Late Tectonic	LMD-alkalic
	2674.0	2.0	2.0	Wyman and Kerrich 1989	Lamprophyre	Dike	Lamprophyre	Postvolcanic	Late Tectonic	LMD-alkalic
Ab, SM85-60	2673.0	2.0	6.0	Corfu et al. 1989	Albitite	Albitiite dike	Albitite dike	Postvolcanic	Late Tectonic	LMD-alkalic
SM85-60	2672.8	1.1	1.1	Corfu et al. 1989; Ayer et al. 2005	Albitite	Dike	Albitite dike	Postvolcanic	Late Tectonic	LMD-alkalic
BL-21	2671.5	1.9	1.9	Ropchan et al. 2002	Lampyrophyre	Dike	Lamprophyre	Postvolcanic	Late Tectonic	LMD-alkalic
92HNB0026b	2676.0	4.0	4.0	Heather 2001; Ketchum et al. 2008	Biotite granite	Somme pluton	Kenogamissi Batholith	Postvolcanic	Posttectonic	Crustal-I
02JAA7	2673.0	12.0	12.0	Ketchum et al. 2008	Granodiorite	Late granodiorite dike	Kenogamissi Batholith	Postvolcanic	Posttectonic	Crustal-I

Abbreviations: TTG = tonalite–trondhjemite–granodiorite; LMD = late mantel derived; Crustal-I = crustal I-type; ss = sandstone; fel = feldspar; qtz = quartz; ss = sandstone

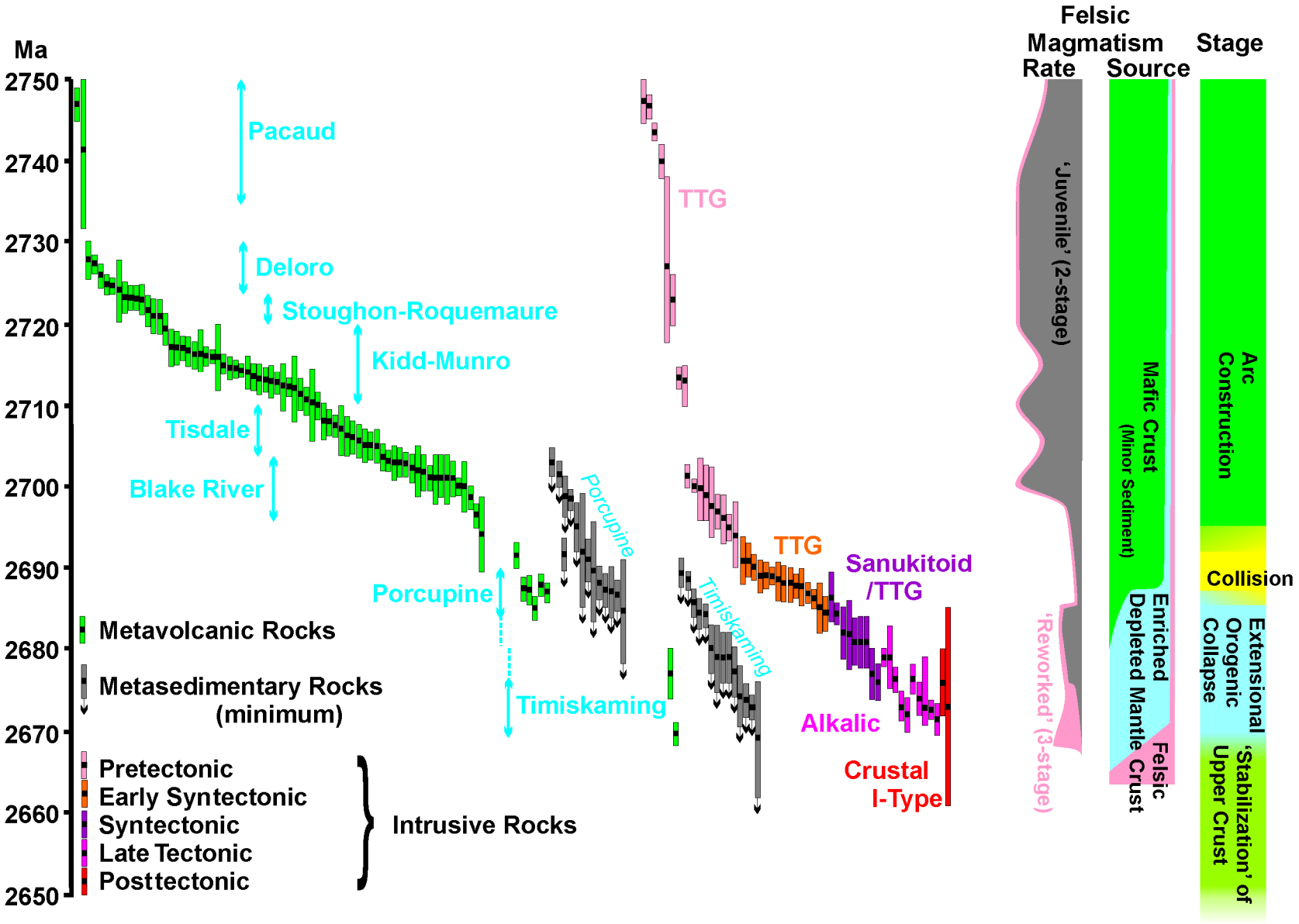

Figure 58. Illustration of timing of volcanism, sedimentation and plutonism and interpreted progression in petrogenesis of intermediate to felsic intrusive units in the western Abitibi Subprovince with reference to a hypothesized tectonic setting. The rate of felsic magma production is not quantified and its portrayal in the diagram is only intended to infer general patterns as discussed in the text. Time, in millions of years before present, is portrayed on the y axis. Geochronological data on which the diagram is based is summarized in Table 6.

deposition (Bleeker et al. 1999; Bateman et al. 2005). On this basis, the Porcupine assemblage, and by inference the coeval porphyry intrusions (2691–2685 Ma), are interpreted to be early syntectonic.

Plutons assigned to the syntectonic group generally lack penetrative deformational fabrics. Mineral foliations, enclave alignment and rare mineral lineations, where present, are interpreted to be generated by magmatic flowage. In all cases where contact relationships are exposed (Blackstock, Adams and Geikie plutons), the plutons crosscut fabrics in the metavolcanic country rocks that are defined by near-peak metamorphic mineral assemblages. Furthermore, as discussed in more detail in a previous section, a number of these plutons were emplaced during folding of the stratigraphy and peak metamorphic deformational fabric and sometimes occupy the axial portions of regional folds. Consequently, these plutons are interpreted to postdate all volcanism as well as imposition of an early fabric defined by near-peak metamorphic mineral assemblages and to be emplaced during regional-scale folding of the greenstone belt. The absolute ages for these plutons range from 2676 Ma to 2686 Ma (Table 6, Figure 58).

Field relationships between plutons regarded here to be late tectonic and fabrics developed near the peak of metamorphism are not well constrained because of late overprinting deformation and alteration. These complexities arise because of the emplacement of many of these plutons within or near major regional faults that are the loci for much of the strain related to this late deformation. As discussed below, these plutons are reasonably grouped together on the basis of their broadly similar and distinctive compositional characteristics. Consequently, although many of these plutons are strongly deformed within the fault zones, the postpeak, metamorphic fabric-development timing of emplacement that can be inferred for a number of intrusions associated with this group can likely be extended to the group as a whole and the deformation and fabric development observed locally in many of these intrusions can be attributed to late deformation localized in the fault systems. The relatively young range in crystallization ages (2672–2679 Ma, Table 6) for these plutons is consistent with this interpretation.

The final grouping considered here is referred to as the posttectonic plutons. These units are only known to occur as a component within the Kenogamissi Batholith although it is possible that minor granitic intrusions in other large batholithic complexes may be comparable. These units do not contain penetrative deformational fabrics, they postdate the development of fabrics in pretectonic units and intrude syntectonic plutons and are therefore interpreted to be emplaced at a relatively late stage. Their timing relative to the late-tectonic plutons and late deformation that is primarily associated with fault zones is unknown because of their setting within batholiths away from these structures. In the absence of relationships with this late deformation, field relationships are permissive of these units being either late tectonic to posttectonic. They are assigned here to a separate grouping based on their distinct compositional characteristics discussed below. Somewhat less precise ages of 2673 and 2676 Ma for 2 units are within the range for late-tectonic plutons, suggesting that the classification adopted cannot be viewed in purely chronological terms.

The field relationships on which the assignment of individual plutons to different groups discussed above are based, together with the absolute ages of these groups, places 3 important constraints on the tectonometamorphic evolution of the Abitibi greenstone belt. Firstly, the presence of a deformational fabric defined by near-peak metamorphic mineral assemblages within all metavolcanic-dominated assemblages, as well as the Porcupine assemblage, constrains the timing of development of this fabric to be post-Porcupine. A minimum age constraint on the timing of this fabric arises from crosscutting relationships recognized at the contacts of syntectonic plutons, including the Adams ($2686.4^{+2.8}_{-3.0}$ Ma), Geikie (2681.8 ± 4.2 Ma) and Blackstock (age unconstrained) plutons. The ages of these crosscutting plutons are within error of, or very slightly younger than, the estimated time of deposition of the Porcupine assemblage (2690–2685 Ma, Ayer et al. 2005). This suggests that the onset of regional deformation and metamorphism progressed very rapidly following deposition of the Porcupine

assemblage. This rapid progression from deposition to the initial stages of the tectonometamorphic phase of greenstone belt development is recognized more generally across the Superior Province (Beakhouse 2007b).

A second constraint arises from the interpretation that regional folding of both the greenstone belt (excluding Timiskaming assemblage) and the early, peak metamorphic deformational fabric was synchronous with emplacement of syntectonic plutons. This interpretation again points to a very rapid progression in the sequence of deformational events. It further suggests that the Abitibi greenstone belt was substantially deformed prior to the deposition of the Timiskaming assemblage.

A final constraint is derived from the observation that late-tectonic plutons are primarily emplaced in proximity to east-trending regional faults but many of these plutons are deformed by transcurrent shearing associated with these fault zones. This suggests that these faults represent zones of weakness that served to localize emplacement of deeply sourced alkalic plutons but that deformation within these zones continued subsequent to emplacement of the late-tectonic plutons.

POSSIBLE SINISTRAL OFFSET ON CLLF

The localization of late-tectonic plutons within major faults allows that these plutons may provide piercing points that may be used to quantify late transcurrent displacement along these fault zones. One possible example is afforded by the occurrence of the Lebel and Murdock Creek plutons on the south side of the Cadillac–Larder Lake fault (CLLF) in the Kirkland Lake area and the Cairo and Young–Davidson plutons on the north side of the CLLF in the Matachewan area. The north contact of both the Lebel and Murdock Creek plutons is cut by the CLLF, and the Lebel pluton, in particular, may have a significant portion of the original pluton faulted-out based on the truncation of the curviplanar, crudely semicircular outline of the southern, eastern and western contact of the pluton (*see* Figure 38). Conversely, the southern contacts of Cairo and Young–Davidson plutons are faulted, with the size and form of the former being consistent with it being the offset northern continuation of the Lebel Stock. Furthermore, the apparent horizontal separation of the Lebel–Murdock Creek and Cairo – Young–Davidson units is very similar (approximately 4 to 5 km). The striking petrological and geochemical similarities of the intrusions, discussed in a previous section of the report, and similar U/Pb ages of the Lebel and Cairo stocks (2673 ± 2 Ma vs 2676.3 ± 1.4 Ma) are consistent with this correlation. If this interpretation is correct, the plutons represent piercing points on the CLLF and indicate approximately 48 km of sinistral offset. A similar conclusion reported elsewhere (Bleeker and van Breemen 2010) is suggested by a number of other interpreted relationships, including offset of Timiskaming units between Larder Lake and Rouyn–Noranda in Quebec, asymmetric attenuation and offset of stratigraphy between Matachewan and the Kenogamissi Batholith and presence of early, sinistral kinematic indicators (W. Bleeker, written communication, 2010).

Detailed investigations in the Kirkland Lake–Larder Lake area (a generally east-trending segment of the CLLF) indicate that post-Timiskaming deformation associated with the CLLF is related to an earlier phase of north-south shortening giving rise to local minor dextral or sinistral offset depending on fault orientation and a later phase of northwest-southeast compression consistent with dextral offset on the fault (Wilkinson et al. 1999; Isoplatov et al. 2008). Isoplatov et al. (2008) further suggest an intermediate stage of east-west shortening. These interpretations suggest that the deformation recognized in this area could not result in sinistral movement on an east-trending fault; however, viewed in a more regional context, the CLLF may have a more east-northeasterly trend, in which case the earlier north-south shortening could generate sinistral offset on the fault. A component of sinistral deformation postdating dextral shearing has been reported in proximity to the Young–Davidson intrusion (Zhang et al. 2009); however, this is interpreted to be a minor deformational event (S. Lin, personal communication, December, 2010). The

apparent absence of evidence for sinistral displacement within the more easterly trending segment of the fault in the Kirkland Lake–Larder Lake area suggests that if such displacement occurred, it must either have occurred on a discrete slip surface without an extensive manifestation in terms of fabric development or the fabrics related to this phase of movement were overprinted by subsequent deformation.

Further work is warranted to evaluate the potential transcurrent offset along the CLLF. Identification of additional piercing points would be desirable although the ductile deformation, transposition and intense alteration of metavolcanic rocks makes it difficult to evaluate offset of stratigraphy across the fault. Further detailed structural investigations, particularly on east-northeasterly trending segments of the fault, may also provide additional insight. Although this interpretation must be regarded as being speculative at this stage, the characteristics of the plutons strongly suggest that the Cairo and Young–Davidson intrusions are the offset equivalents of the Lebel and Murdock Creek intrusions.

TEMPORAL CHANGES IN PLUTON PETROGENESIS

This section discusses the nature and significance of changes in the general character of Abitibi Subprovince plutons with time. For this purpose, a subset of samples, which excludes atypical samples discussed in earlier sections dealing with specific plutons, was considered and are plotted in Figures 59 to 62.

Most pretectonic, synvolcanic intermediate to felsic intrusive rocks are characterized by high Na_2O/K_2O, high Al_2O_3 and Sr and low abundances of LILE. Low abundance of K_2O is largely responsible for imparting a distinctly subalkaline character to these units (*see* Figure 59 and 60). REE are moderately to strongly fractionated, which is indicative of the presence of garnet in the residue. Some units have very high Sr abundances and Sr/Y coupled with weakly positive Eu anomalies suggesting an eclogitic residue, whereas others have more moderate Sr abundance and lower Sr/Y and negligible Eu anomalies suggesting a mafic garnet granulite residue. In all respects these plutons are similar to high-Al TTG intrusions produced by melting of basaltic crust at lower crustal to upper mantle depths that are common in Archean terranes.

One anomalous group of pretectonic, synvolcanic tonalitic plutons occurs on the eastern side of the Groundhog River batholith in the Kamiskotia area. Here, a subset of the tonalitic rocks have characteristics of low-Al TTG including low abundances of Sr, high abundances of HFSE, including REE which are weakly fractionated with prominent negative Eu anomalies. These geochemical characteristics are attributed to melting of a source with a basaltic bulk composition within the plagioclase stability field (explaining low Al_2O_3 and Sr abundances and negative Eu anomalies) without significant residual garnet or amphibole (explaining unfractionated REE) or rutile (explaining elevated HFSE abundances). Low-Al TTG and chemically similar FIII rhyolites are thought to represent high-temperature, shallow-level melting of mafic crust in "thermal corridors" that are highly prospective for volcanogenic massive sulphide deposits (Galley 2003; Hart et al. 2004).

The early syntectonic intrusions have geochemical characteristics that are similar in many respects to the high-Al TTG discussed above; however, many units assigned to this grouping are extensively altered which may mask some of the primary magmatic geochemical characteristics. Positive Eu anomalies, which characterize a subset of pretectonic high-Al TTG samples interpreted to have an eclogitic residue, are not identified in the early syntectonic plutons (*see* Figure 62). Furthermore, Sr abundances are, on average, somewhat lower than those characterizing the pretectonic TTG (*see* Figure 61), further suggesting melting occurred within the plagioclase stability field. This may indicate a general shallowing of the depth of melting with time.

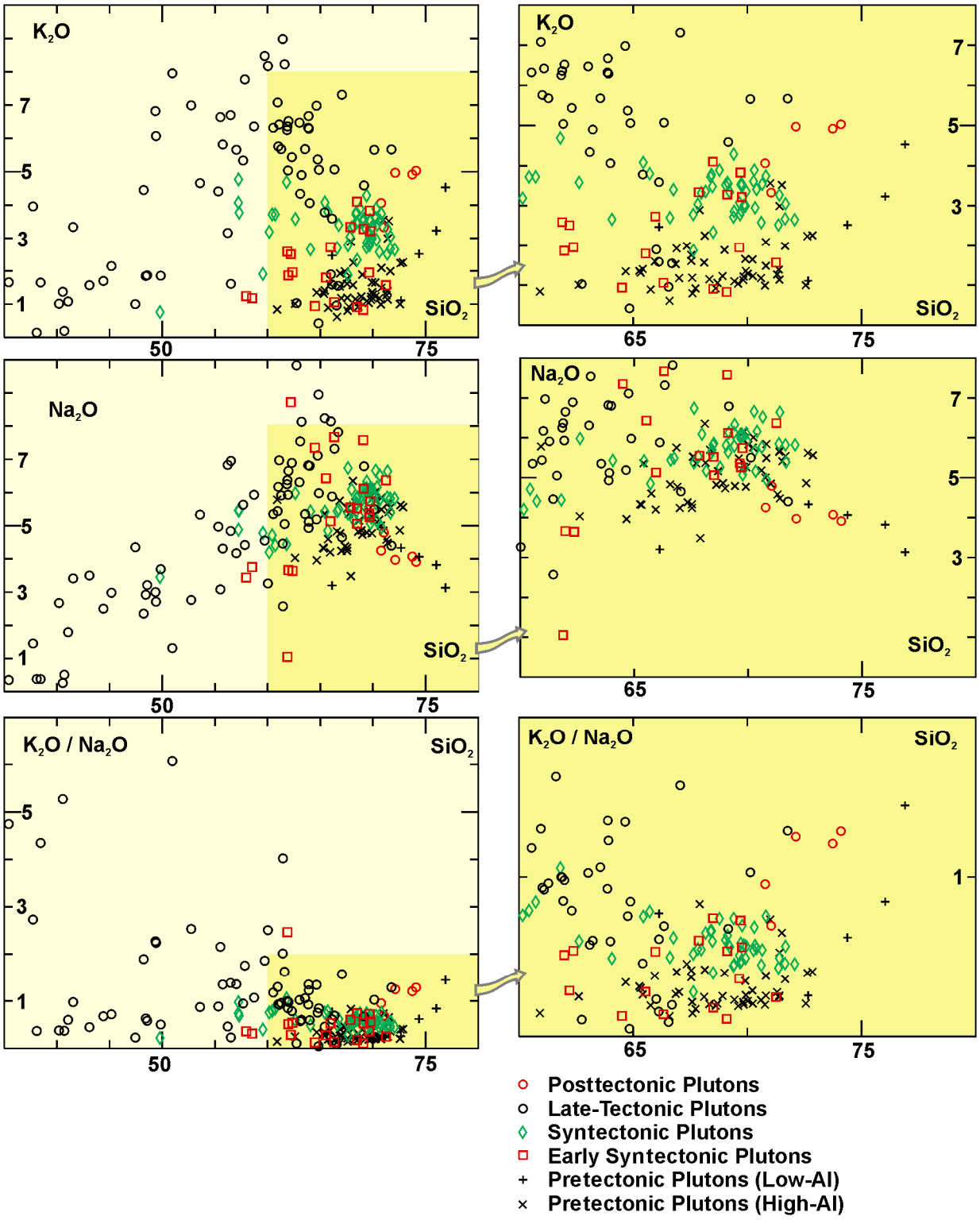

Figure 59. Variation diagrams illustrating the general abundances of alkali elements for major plutonic groups within the western Abitibi Subprovince. The diagrams on the right are enlargements of the dark yellow portions of the diagrams on the left.

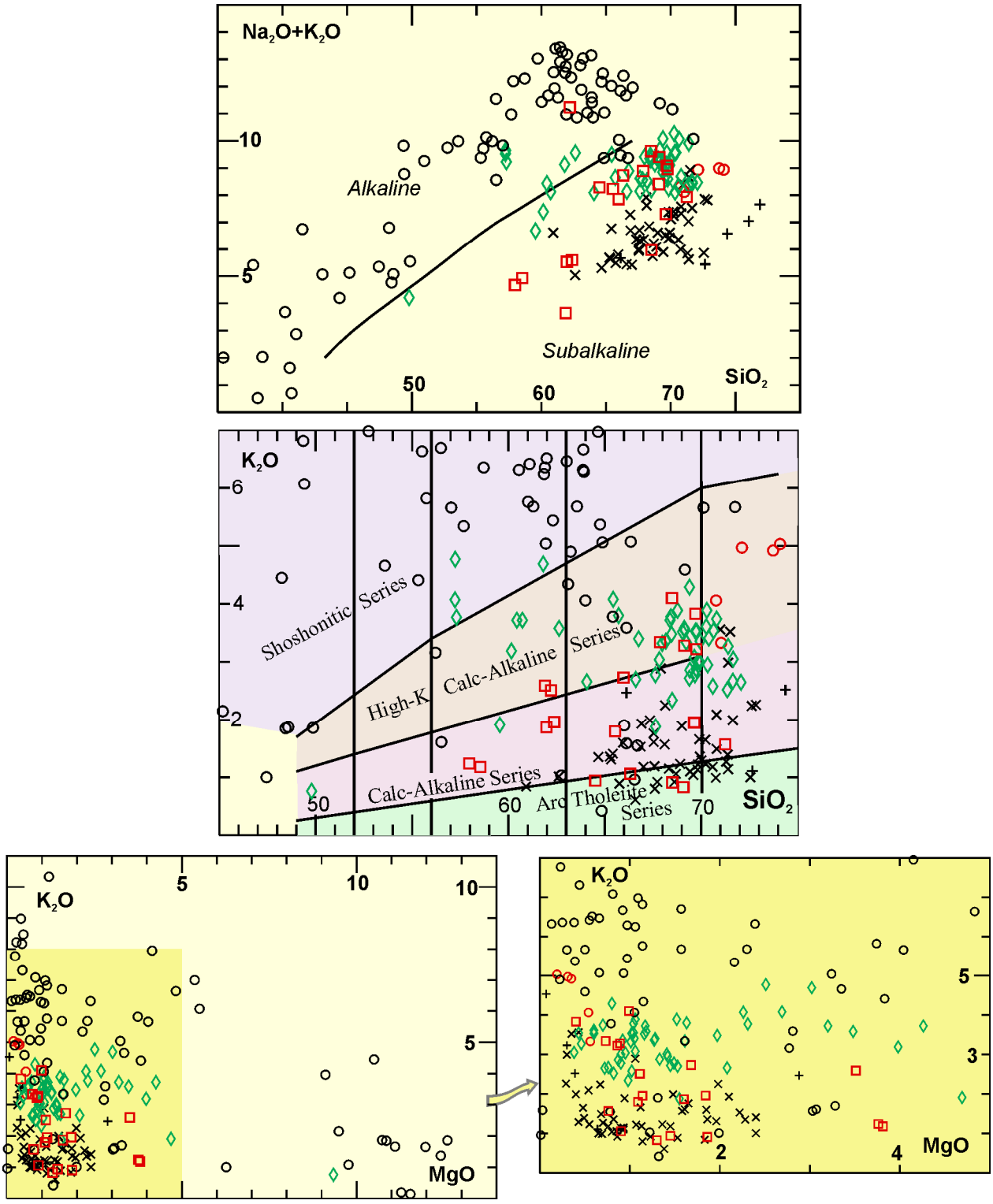

Figure 60. Variation diagrams illustrating the general geochemical characteristics for major plutonic groupings within the western Abitibi Subprovince. The total alkalies vs SiO_2 plot is after Irvine and Baragar (1971) and the K_2O vs SiO_2 plot is after Peccerillo and Taylor (1976). The MgO vs K_2O diagram on the right is an enlargement of the dark yellow portion of the diagram on the left. Symbols are same as for Figure 59.

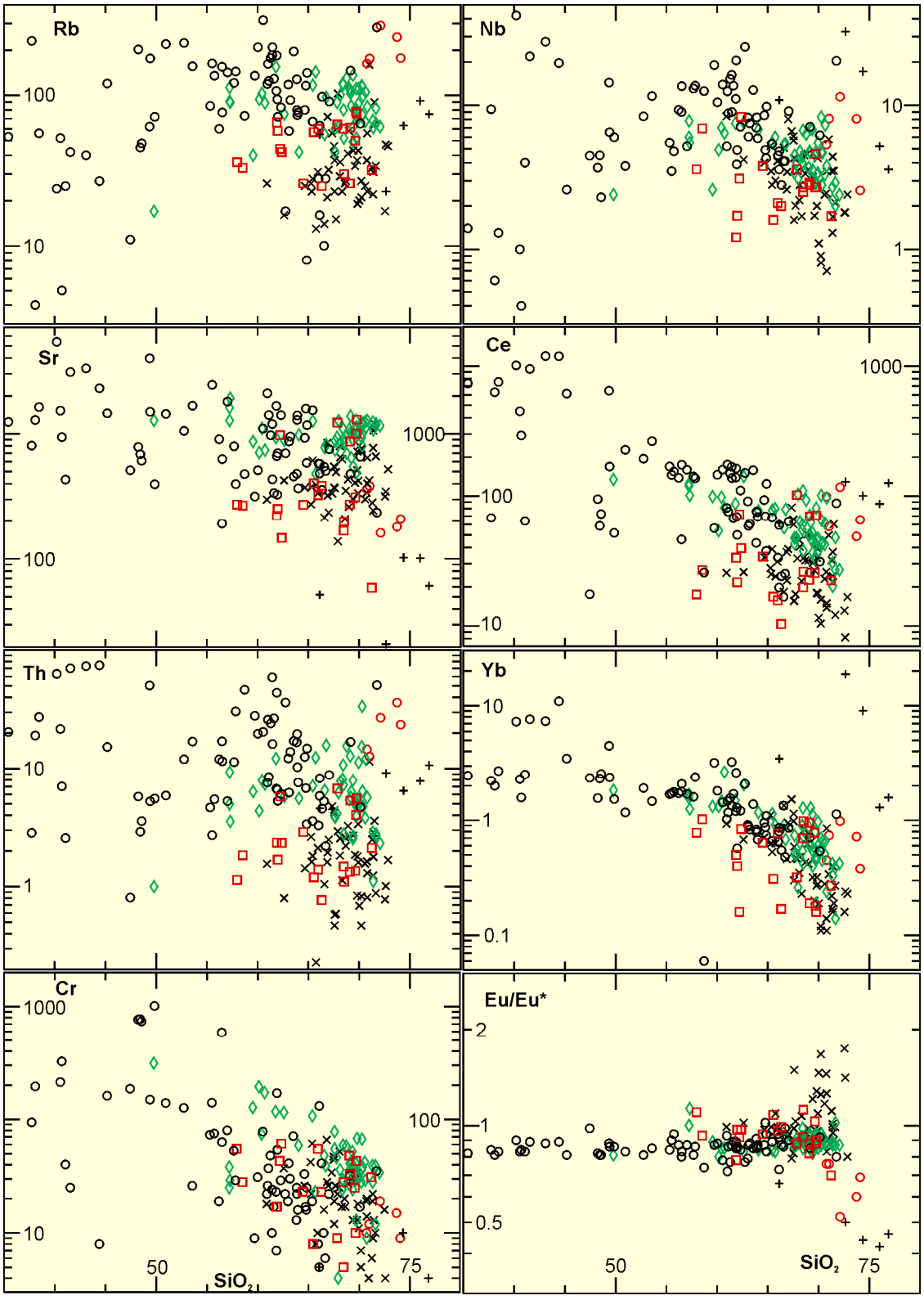

Figure 61. Variation diagrams illustrating the general abundances of selected trace elements for major plutonic groups within the western Abitibi Subprovince. The units for all abundance plots are parts per million (ppm). Symbols as indicated in Figure 59.

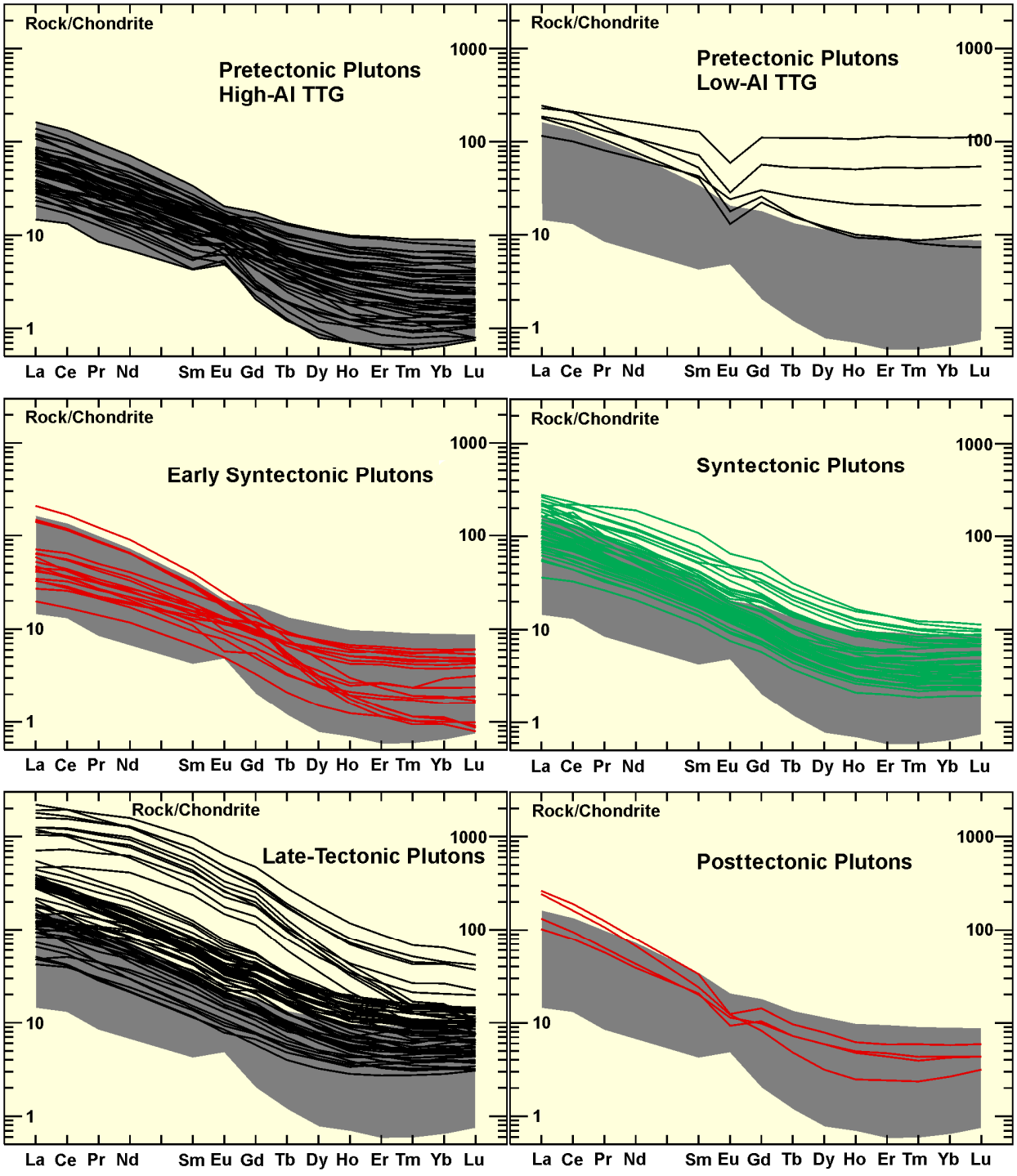

Figure 62. Representative chondrite normalized REE plots for different groupings of plutons within the western Abitibi Subprovince. The grey shaded area in each of the plots is the field for pretectonic, high-Al TTG plutons and is provided to facilitate comparison. Normalization values are from Sun and McDonough (1989).

The geochemical characteristics of the silica-saturated syntectonic plutons are relatively diverse, with individual plutons and individual lobes of irregularly shaped plutons often characterized by relatively uniform compositional characteristics that are distinct from other plutons and/or lobes. As a group they span a broad major element compositional spectrum (SiO2 ~58 to 72%, Mg# ~45 to 60) but tend to have relatively high abundances of K_2O and a wide range of LILE and HFSE, even within the more primitive (low SiO_2 – high Mg#) samples. REE abundance is generally elevated relative to that characterizing high-Al TTG and are moderately fractionated with negligible or weakly negative Eu anomalies. Although elevated LILE could indicate a crustal input, elevated Mg# and Ni and Cr abundances, high Sr abundances and negligible Eu anomalies are inconsistent with significant input from such a source. The geochemical characteristics of these rocks are intermediate between those of high-Al TTG and primitive sanukitoid magmas interpreted to be generated by partial melting of metasomatized, long-term depleted mantle, and these rocks are provisionally interpreted to reflect variously evolved sanukitoid suite plutons or high-Al TTG magmas that have either mixed with sanukitoid magmas or extensively interacted with metasomatized mantle.

Late-tectonic alkalic suite plutons encompass a broad compositional spectrum (SiO_2 ~45 to 70%, Mg# ~20 to 70) that is distinctive by virtue of its high-potassium calc-alkaline to shoshonitic alkalic character (*see* Figure 60). These rocks are generally enriched relative to high-Al TTG in a wide range of LILE and HFSE even in the more primitive members of the suite. REE are abundant and moderately to strongly fractionated with negligible to weakly negative Eu anomalies. Crustal input is limited by similar factors to those discussed above for the syntectonic plutons as well as by long-term depleted mantle isotopic signatures (Ben Othman et al. 1990). The alkalic suite is interpreted to be derived from metasomatized, long-term depleted mantle. Most plutons within this group are associated with areas of extensive carbonate alteration and/or a minor carbonatitic magmatic association.

The posttectonic group plutons are represented by the Somme pluton within the Kenogamissi Batholith and possibly other minor granitic to granodioritic intrusions occurring primarily within the large belt-bounding batholiths. Noteworthy characteristics include elevated LILE abundances with high K_2O/Na_2O, low Mg# and compatible element abundances and low Sr coupled with prominent negative Eu anomalies (*see* Figures 59, 61 and 62). These characteristics suggest an origin via partial melting of evolved felsic crust with residual plagioclase. Pretectonic tonalites in the Kenogamissi Batholith locally preserve textural evidence of *in situ* generation of granitic leucosome, and the composition and mineralogy of these tonalites is consistent with similar rocks at depth being the source for the posttectonic plutons.

The preceding summary of the 5 general groupings of Abitibi Subprovince intermediate to felsic intrusive rocks indicates a temporal evolution in the petrogenesis of these rocks (Figure 63). The production of intermediate to felsic magmas during early stages of development of the Abitibi Subprovince represented by the pretectonic to early syntectonic intrusions is dominated by protracted, deep (base of the crust or mantle depths) melting of mafic crust to generate high-Al TTG. The presence of inherited zircons in many units (plutonic and volcanic) attests to some interaction with more evolved felsic or sedimentary crust; however, the geochemical characteristics of these units suggest that contributions from this evolved crustal component were not volumetrically significant. Based on purely geochemical arguments, subducted oceanic crust and mafic crust emplaced by either magmatic or tectonic processes at the base of the crust are potential source rocks; however, 2 observations suggest that subducted oceanic crust is a major, and perhaps predominant, source. Firstly, although the volcanic stratigraphy of greenstone belts is commonly dominated by mafic metavolcanic rocks, the overall magma-generation processes associated with greenstone belt development are dominated by production of intermediate to felsic magmas when cogenetic plutonic component and derived metasedimentary rocks are considered along with the intermediate to felsic metavolcanic component (see discussion in Beakhouse 2007a). The volume of high-Al TTG magma generated requires a highly efficient mechanism, such as subduction, to cycle large volumes of mafic crust to appropriate pressure and temperature

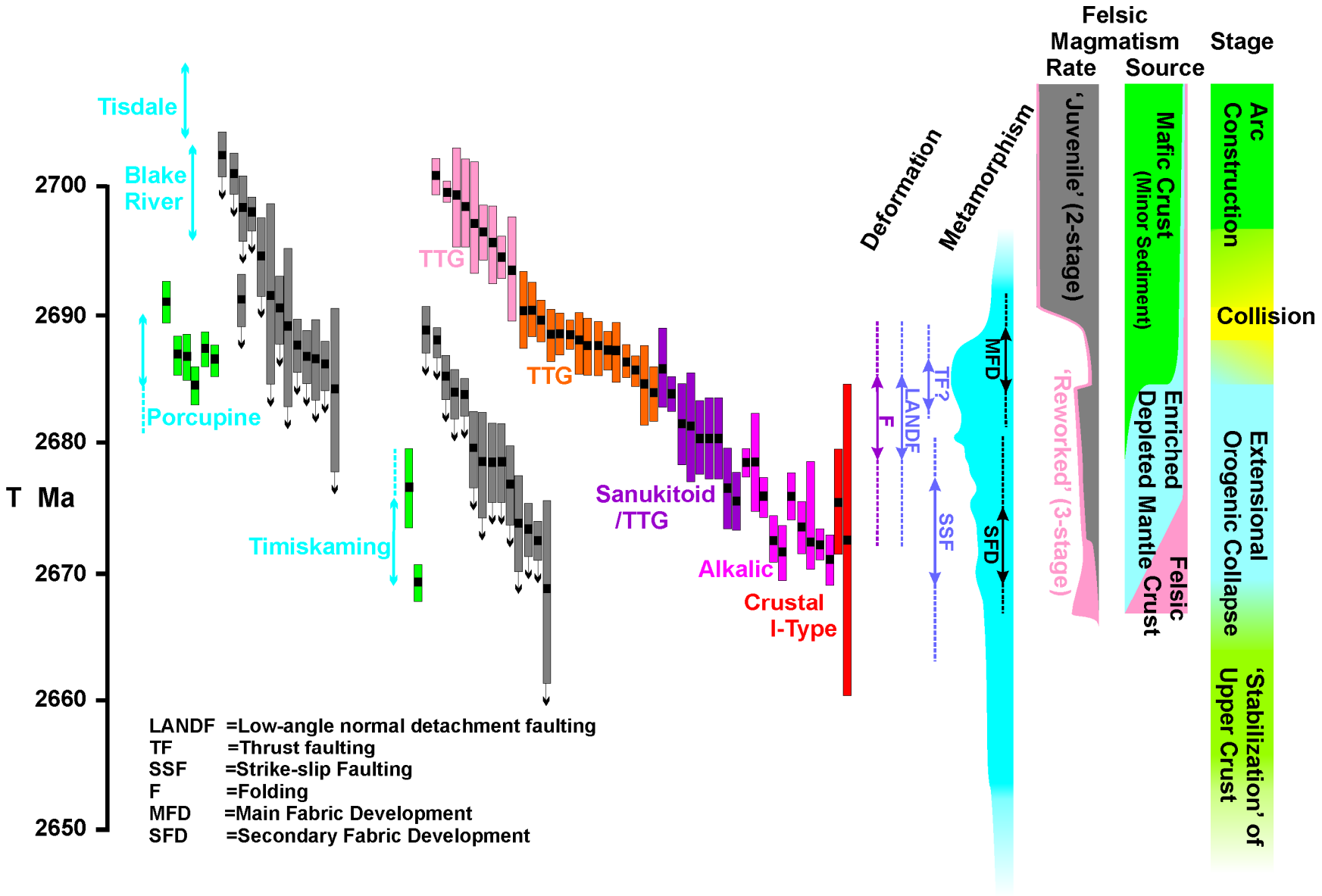

Figure 63. Illustration of timing of volcanism, sedimentation and plutonism elements of the tectonometamorphic evolution and interpreted progression in petrogenesis of intermediate to felsic intrusive units in the western Abitibi Subprovince with reference to a hypothesized tectonic setting. Some of the symbology is after that in Figure 58, with this figure being an enlargement of a portion of that figure, illustrating the portion of the geological evolution of the area that took place after 2700 Ma.

conditions to generate the melts and efficiently remove voluminous residue. It is not clear how purely vertical magmatic processes could generate enormous volumes of mafic magma and remove voluminous residue through a protracted interval of time. Secondly, a metasomatized mantle source generated during the volcanic stage of greenstone belt development is implicated in the generation of syntectonic and late-tectonic plutons (see discussion below). Such a source is generated in Phanerozoic arcs by modification of the mantle wedge above a subduction zone by fluids and low-degree partial melts derived from the slab. This suggests that at least some oceanic crust was subducted at a steep enough angle to emplace it beneath a mantle component that underlay the Abitibi greenstone belt during its volcanic development stage. The predominance of an eclogitic residue signature at early stages of greenstone belt development that diminishes with time and is not recognized during early syntectonic magmatism opens the possibility that the source evolved with time, from early steeply subducted oceanic crust to later shallower subduction and/or melting of basal mafic crust, and that there are multiple sources for intermediate to felsic TTG magmas that are the volumetrically predominant component of the Abitibi Subprovince crust.

Higher level melting of mafic crust to generate low-Al TTG is present very locally, apparently being restricted in the Ontario portion of the Abitibi Subprovince to a portion of the area lying to the north of the Porcupine–Destor fault. The presence of low-Al TTG, and chemically equivalent F3 rhyolites, likely indicates the presence of thinned crust associated with extensional basins with anomalously high heat flow (Galley 2003).

The syntectonic plutons provide the first evidence of involvement of a metasomatized mantle source in the generation of intermediate to felsic magmas, although the geochemical characteristics are compatible with a continued component of a basal mafic crust source component. The late-tectonic plutons do not show evidence for the presence of a mafic crust source component and are interpreted to be generated by the CO_2-dominated melting of a metasomatized mantle source.

A brief interval of production of magma by partial melting of earlier TTG-type crust is among the latest magmatic events in the Abitibi Subprovince. These magmas are not voluminous and occur largely within the large, belt-bounding batholiths.

The pattern of protracted early melting of mafic crust terminating abruptly with an irreversible migration of the melting regime into metasomatized mantle and minor, late onset of melting of evolved crust parallels that observed throughout the Superior Province (Beakhouse and Davis 2005; Beakhouse 2007a). The most distinctive characteristic of the Abitibi plutonic record, relative to that observed more generally, is the very strongly alkalic, CO_2-rich character of the latest phase of metasomatized mantle melt production represented in the late-tectonic plutons.

DEPTH OF EMPLACEMENT AND UPLIFT HISTORY

This section discusses data acquired during the course of this investigation that constrains the depth of emplacement of a number of individual plutons based on the Al-in-hornblende geobarometer. The possibility of utilizing the aluminum content of hornblende as an empirical geobarometer was first proposed by Hammarstrom and Zen (1986) and has been subsequently further refined (Hollister et al. 1987; Schmidt 1992). This technique has been applied here using the revised expression of Anderson and Smith (1995) incorporating the amphibole-plagioclase thermometer of Holland and Blundy (1994). Rocks having the appropriate mineral assemblage (hornblende + biotite + plagioclase + quartz + potassium feldspar + titanite + Fe-Ti oxide) are primarily observed within the pretectonic and syntectonic plutons.

A number of previous investigations have endeavoured to constrain paleopressures within the Ontario portion of the Abitibi Subprovince. Metamorphic mineral assemblages broadly constrain greenstone belt metamorphic conditions to 200 to 350 MPa (Powell, Carmichael and Hodgson 1995; Thompson 2005). Feng and Kerrich (1990) reported Al-in-hornblende pressure estimates for the Round Lake batholith that range between 200 MPa, in a central portion that they interpreted to be a later, more massive quartz monzonite, and 700 MPa, in foliated tonalitic units nearer the margin. These authors also report very low paleopressures of approximately 100 MPa for the Otto Stock; however, based on observations from the present study, it is not clear that this intrusion has appropriate mineral assemblages for the application of the Al-in-hornblende technique. This shallow level of emplacement is consistent with the presence of coeval, chemically similar alkalic metavolcanic rocks in the Kirkland Lake area (Cooke and Moorehouse 1969; Ben Othman et al. 1990). Peshler et al. (2006) present a paleopressures estimate of approximately 700 to 790 MPa for a single garnet-bearing tonalitic unit in the Kenogamissi Batholith.

The paleopressures data obtained as part of this investigation are summarized in Table 7 and Figures 64 and 65. Al-in-hornblende paleopressure data for the Abitibi greenstone belt area indicate that pretectonic tonalitic to granodioritic phases within the Kenogamissi and Round Lake batholith were emplaced at paleopressures of ~500 to 700 MPa, corresponding to midcrustal depths of 14 to 20 km (assuming normal crustal densities). These data confirm and extend the earlier indications summarized above of deep crustal levels being represented within Abitibi batholithic complexes. Syntectonic phases intruding the greenstone belt are characterized by paleopressures (depths) of 250 to 350 MPa (7 to 10 km), which is broadly consistent with maximum paleopressures inferred for regional metamorphism of supracrustal rocks (Powell, Carmichael and Hodgson 1995; Thompson 2005). In contrast, syntectonic phases from within the batholiths are characterized by paleopressures (depths) of 350 to 400 MPa (10 to 12 km), which are intermediate between the deeper crustal levels characterizing the pretectonic units of the large belt-bounding batholiths and shallower crustal levels inferred for greenstone belt metamorphism.

The deep crustal levels (14 to 20 km) represented in the pretectonic phases of the Kenogamissi and Round Lake batholiths contrast sharply with higher crustal levels for the greenstone belt (7 to 10 km) inferred from both Al-in-hornblende barometry for syntectonic, greenstone belt-hosted plutons as well as regional metamorphic studies of the metavolcanic rocks themselves (Powell, Carmichael and Hodgson 1995; Thompson 2005). Locally (e.g., north contact of Round Lake batholith), very deep crustal levels (~18 km) are recorded in close proximity to metavolcanic rocks that have a maximum burial depth of 10 km, requiring that there be a structural discontinuity at the contact. Well-developed ductile deformational (and locally mylonitic) fabrics are locally subhorizontal within the interior of batholiths but steepen and become concordant with respect to both the contact as well as bedding and early deformational fabrics within marginal portions of the greenstone belt. All of the aforementioned planar fabrics are deformed by later upright folds and are interpreted to have initially formed with shallow dips.

The intermediate pressures recorded by syntectonic phases hosted within the batholiths suggest that these units were emplaced during the uplift of the batholiths relative to the greenstone belts and consequently the age of these units corresponds in a general way to the time of uplift. One such unit is the Neville pluton (2682 +3/-2 Ma, van Breemen et al. 2006) which occurs at the south contact of the Kenogamissi Batholith and records a paleopressure of 393 ± 35 MPa.

Batholith contacts having a granite-side-up sense of displacement with tectonic juxtaposition of midcrustal plutonic complexes and upper crustal greenstones are being increasingly recognized within Archean granite-greenstone terranes. One of the first such examples recognized occurs in the Leonora area within the Yilgarn craton of Western Australia. Here, an abrupt transition in metamorphic conditions from approximately 210 MPa in the metavolcanic rocks near the contact to approximately 560 MPa in immediately adjacent portions of the Raeside batholith indicates structural juxtaposition, with granitic rocks

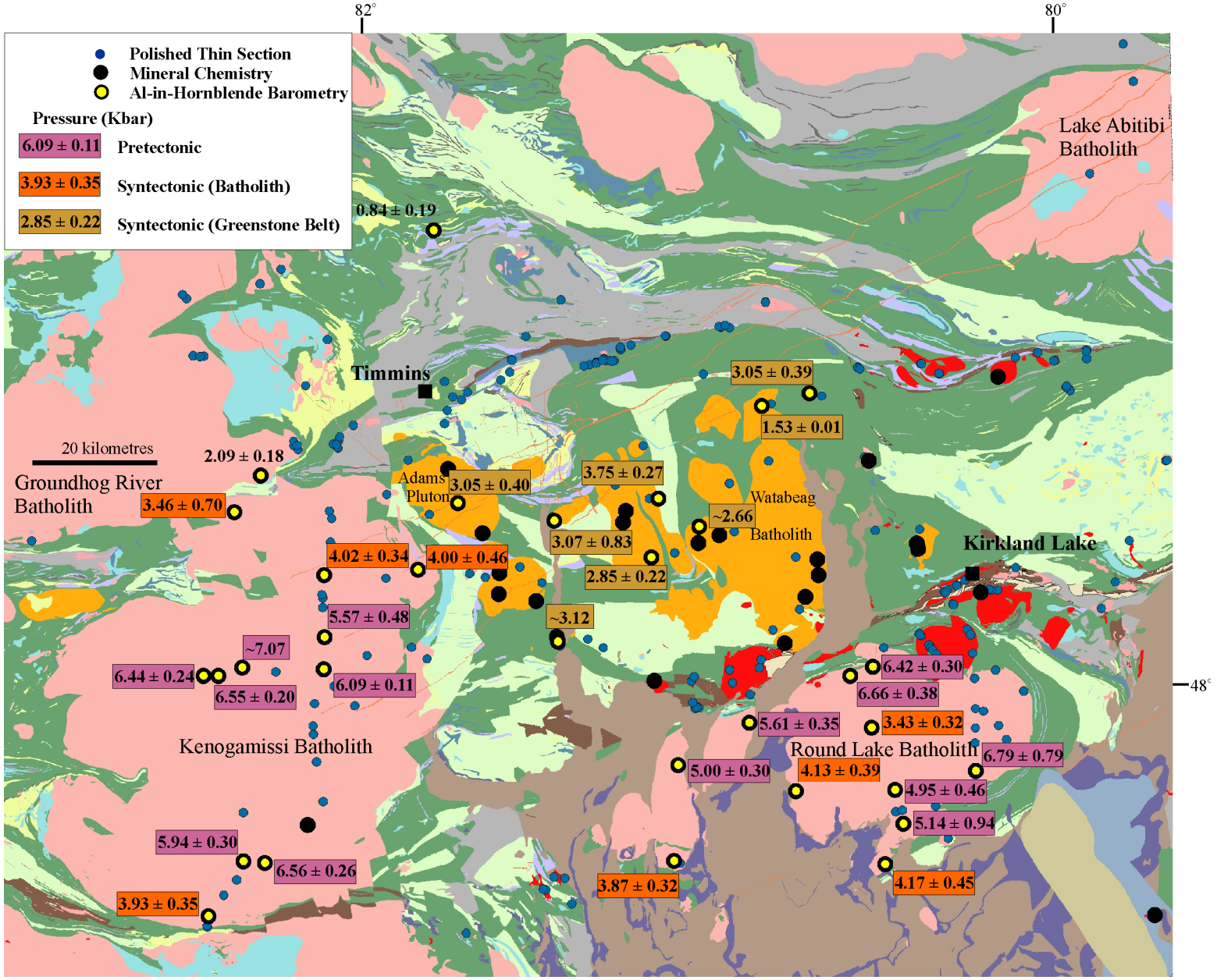

Figure 64. Generalized geological map illustrating the paleopressure determined for different units utilizing the Al-in-hornblende geobarometer.

being uplifted relative to adjacent metavolcanic rocks (Williams and Currie 1993). This pattern of a granite-side up sense of displacement at the margins of greenstone belts is now widely recognized across the Yilgarn craton and interpreted to be extensional detachment faults analogous in certain respects to those developed in metamorphic core complexes (Williams and Whittaker 1993; Swager and Nelson 1997; Blewett and Czarnota 2007).

An additional example exhibiting many similarities to the above is recognized on the north flank of the Barberton greenstone belt in South Africa. Here, the Stentor pluton has been displaced upwards relative to the flanking greenstone belt along an extensional detachment fault associated with the base of the greenstone belt (Dziggel et al. 2006). A Superior Province example is afforded by the Pukaskwa batholith which was magmatically emplaced in the midcrust and subsequently displaced upwards relative to flanking greenstone belts (Beakhouse et al. 2011). In this case, the driving force for tectonic emplacement is density inversion acting on denser greenstones structurally underlain by more buoyant felsic crust, with the timing of uplift controlled by thermal softening attendant with extensional orogenic collapse.

The relationships described above for the depth of emplacement for Abitibi Subprovince plutons are consistent with many of the relationships described for other areas and suggest that the base of the Abitibi greenstone belt is an extensional detachment fault that has juxtaposed the midcrustal plutonic roots of the greenstone belt with higher crustal levels preserved within the greenstone belt. Furthermore, the intermediate paleopressures characterizing syntectonic plutons intruding the uplifted batholiths constrain the timing of this tectonic emplacement as discussed below.

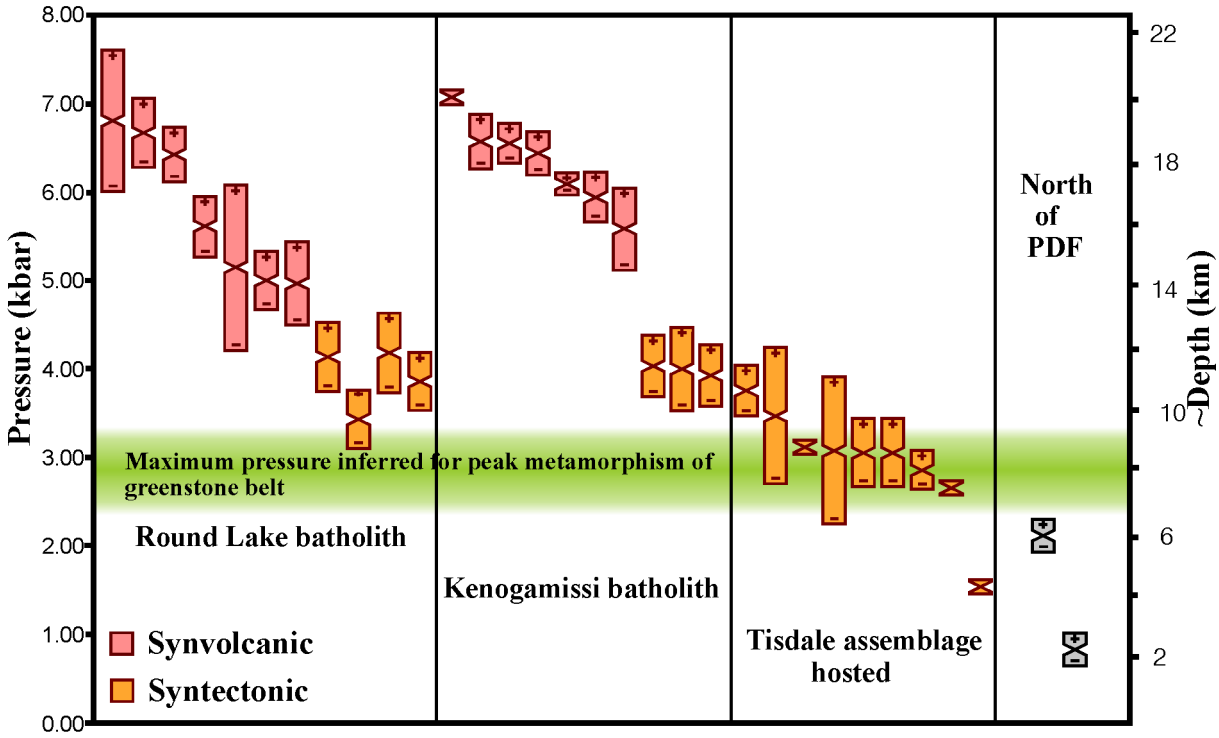

Figure 65. Graph illustrating Al-in-hornblende paleopressure determinations for units from different settings within the western Abitibi Subprovince. The constraint on maximum pressure of greenstone belt metamorphism is based on the interpretations of Powell, Carmichael and Hodgson (1995) and Thompson (2005). PDF = Porcupine–Destor fault.

Absolute and Relative Timing of Detachment Faulting

The intermediate pressures recorded by the syntectonic phases within the Round Lake and Kenogamissi batholiths suggest that components of uplift occurred both before and after emplacement of these units. One of these units, occurring along the southern contact of the Kenogamissi Batholith, is the Neville pluton, having a U/Pb age of 2682 ± 3 Ma (van Breemen et al. 2006). This unit has mineralogical (clinopyroxene) and geochemical (Mg# = 51 to 57; Cr = 48 to 194 ppm) characteristics suggesting affinity with other syntectonic plutons. It cuts a gneissic fabric in the pretectonic tonalites but is itself mylonitized at the contact with the greenstone belt and locally contains shear zones suggesting north (granite)-side up movement (Figure 66). These observations suggest that a significant amount of uplift occurred prior to emplacement of the Neville pluton and continued subsequent to emplacement.

The base of the Porcupine assemblage very locally has evidence for slight angular discordance (Bateman et al. 2005) and no angular unconformities are recognized at the contacts between underlying volcanic-dominated assemblages. This suggests that large-scale folding and/or doming did not commence until approximately 2687 Ma, whereas local high-angle discordance at the base of the Timiskaming assemblage (e.g., Hodgson 1983) suggests that verticalization of the aforementioned assemblages was well-advanced prior to initiation of Timiskaming assemblage deposition (2670 to 2676 Ma, Ayer et al. 2005). These relationships are interpreted to indicate that a major component of regional doming and/or folding occurred within the Abitibi greenstone belt sometime around 2682 ± 5 Ma.

Detachment Faults and Regional Folding

The general concordance of stratigraphy near the base of the greenstone belt and the batholith contacts suggests that large-scale folding of the greenstone belt is linked to the processes that exposed the plutonic substrate in regional structural culminations. However, some aspects of the overall style of deformation in the batholiths (open folding, moderate to subhorizontal dips) and greenstone belt (tight to isoclinal and shorter wavelength folding, moderate to steep dips) are different. In some cases (e.g., Deloro–Tisdale contact east of the Kenogamissi Batholith) the abrupt change in structural style occurs within the lower portions of the greenstone belt stratigraphy, suggesting additional detachment surfaces within the greenstone belt (rooted in the basal detachment?) play a role in this transition. Benn and Peshler (2005) proposed a detachment fold model for the Abitibi greenstone belt that similarly invoked a detachment surface in the lower portions of the volcanic stratigraphy. It is probable that the structural transition from more open folding with shallower dips (observed in batholiths and subgreenstone belt seismic reflections) to shorter wavelength, isoclinal folding and steeper dips in greenstone belts is accommodated by detachment surfaces at the base, and within the lower portions, of the greenstone belt.

Detachment Faults and the Sedimentary Record

The magnitude and time scale of uplift proposed above could be expected to generate significant topographic relief (granitoid-dominated Mount Kenogamissi and Round Mountain) that would almost certainly be emergent and subject to erosion. The Porcupine assemblage of the Timmins area of the Abitibi Subprovince consists predominantly of turbiditic wacke and siltstone and/or argillite, with subordinate conglomerate as well as felsic volcanic rocks (Krist formation) occurring locally at the base of the sequence. These units overlie the dominantly volcanic assemblages, contain detrital zircons as young as 2685 Ma and are themselves unconformably overlain by the Timiskaming assemblage (2670 to 2676 Ma, Ayer et al. 2005), suggesting deposition at approximately 2680 ± 5 Ma. Provenance of arenaceous units of the Porcupine assemblage is interpreted to be dominated by a continental (felsic

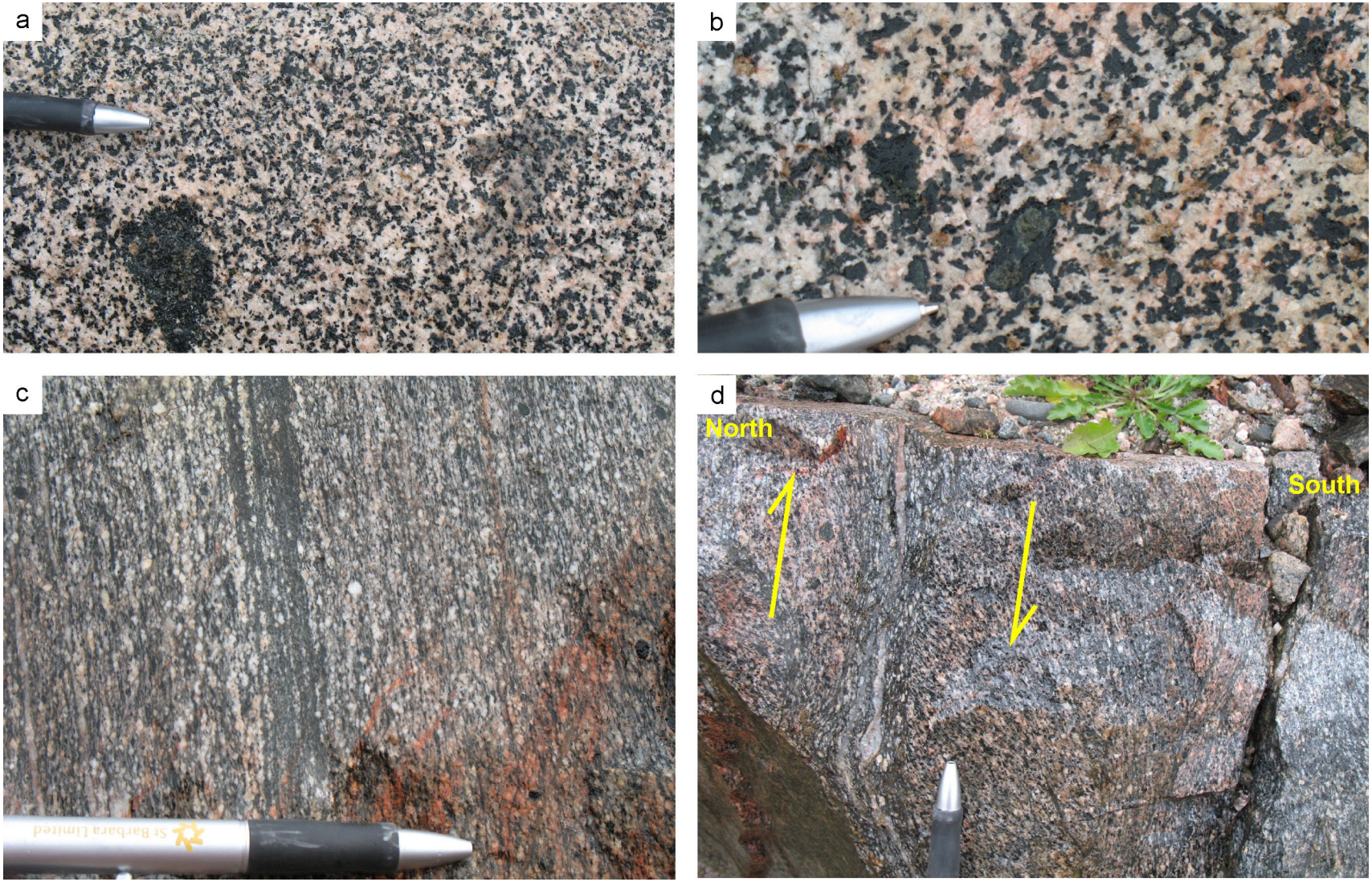

Figure 66. Outcrop photographs illustrating characteristics of the Neville pluton. Much of the pluton is characterized by absence of a deformational fabric and the presence of meladiorite enclaves (a), and clinopyroxene cores occur within amphibole locally (b). Along the southern contact of the unit with the greenstone belt, the pluton has a mylonitic fabric (c) with local indication of a north (granite)-side-up sense of displacement (d).

plutonic) component interpreted to lie to the south (Born 1995). Regional variations in proportion of argillite, grain size and bedding thickness suggest west to east sediment transport within the basin (Berger 2002). These relationships, and the proposed timing and magnitude of uplift, are consistent with the interpretation that the Kenogamissi Batholith was the dominant source for Porcupine sedimentation in this portion of the Abitibi Subprovince. Although studied in less detail, similar inferences regarding timing of uplift and sedimentation and sedimentary provenance can be made for the Round Lake batholith and Pontiac Subprovince metasedimentary rocks.

TECTONIC MODEL

This section summarizes a working hypothesis that endeavours to reconcile diverse observations relating to the intermediate to felsic plutonic record, including petrogenesis, absolute timing, relative timing with respect to volcanism, sedimentation, deformation and metamorphism, with a general tectonic model for the evolution of the Abitibi Subprovince. The hypothesis incorporates 5 stages that correspond to different stages of intermediate to felsic plutonism or tectonism discussed in preceding sections. Absolute time intervals are identified for each of these stages; however, as discussed above, some of the stages may be transitional into one another and/or diachronous across the subprovince and consequently there is overlap between the age ranges proposed for different stages of development.

The model does not address the role of older crust as there is little indication of involvement of such crust in the generation of intermediate to felsic plutonic rocks examined as part of this investigation. It should be noted that older crust has been identified to the west of the area of this investigation (Ketchum et al. 2008) and it is possible that such crust may have influenced the overall geodynamic setting.

Stage 1 – Volcanism and TTG Plutonism (~2750–2695 Ma)

The observations and interpretations summarized above for the large granitoid batholiths that bound the Abitibi greenstone belt indicate that these batholiths structurally underlie, and were deformed along with, the greenstone belt. F1 felsic volcanic rocks predominate within Archean felsic volcanic sequences, including those in the Abitibi Subprovince, and have geochemical characteristics similar to high-Al TTG that predominate within the batholiths. Furthermore, the range of U/Pb ages for TTG phases of the batholith is similar to that of the felsic volcanics (Corfu 1993; Mortensen 1993; van Breemen et al. 2006), suggesting that the TTG component of the batholiths is the plutonic equivalent of greenstone belt felsic volcanism.

The contemporaneous development of the greenstone belt and TTG-dominated plutonic substrate has important implications for the evolution of the Abitibi greenstone belt. Most attempts to develop a geodynamic model for the Abitibi Subprovince have focused to a large extent on the predominantly mafic greenstone belt; however, the geochemical similarity and contemporaneity of felsic volcanism distributed through the Abitibi volcanic stratigraphy and TTG components of the batholiths suggest that both must be considered in development of geodynamic models. The proportions of different crustal components is difficult to assess; however, general arguments advanced elsewhere (Beakhouse 2007a) that TTG-type magmas (including that reworked by crustal melting and represented as a detrital component within metasedimentary sequences) comprise 50 to 75% of the crust are probably approximately valid for the Abitibi Subprovince. Viewed in this context, the development of the Abitibi Subprovince crust should be considered within the context of a range of magmatic processes leading to the generation of a felsic-dominated, bimodal (tonalite and basalt ± minor komatiite) crust. This style of magmatism persisted over

a protracted interval of time from approximately 2750 Ma to 2696 Ma, during which most of the Abitibi crust was ultimately extracted from the mantle.

The volumetrically dominant TTG magmas generated during this time interval are thought to be products of 10 to 15% melting of mafic crust. These are predominantly high-Al type (equivalent to F1-type felsic volcanic rocks) produced by melting within the garnet stability field and, in some cases, outside the plagioclase stability field. Consequently, the overall process must involve generation of large volumes of basaltic crust buried to lowermost crustal or upper mantle depths appropriate for melting to generate high-Al TTG magmas and mafic garnet granulitic or eclogitic residues. Based on purely geochemical arguments, a range of geodynamic settings could be suitable for generating the required conditions, including melting of subducted or subcreted basaltic crust, melting of basaltic crust underplating relatively thick crust or melting of delaminated mafic crust within the mantle. It is possible that all of these processes may have operated to some extent; however, the volumes and protracted production of TTG magma and enormous volume of residue are more readily reconciled with a dynamic, highly efficient process such as is represented by some form of subduction or subcretion and/or delamination.

A high proportion of TTG magma was emplaced at lower crustal levels, with a smaller proportion being erupted or emplaced at higher crustal levels. The reason for this is not clear but it led to the development of an inversely density-stratified crust with denser, mafic-dominated greenstone belt underlain by a less dense TTG-dominated plutonic substrate. Such density stratification is gravitationally unstable and can only persist if the crust is sufficiently cool and rigid to inhibit overturn which requires low average geothermal gradients. The conformity of greenstone belt stratigraphy and the consistently high paleopressures for crystallization of TTG magmas in the plutonic substrate both indicate that large-scale buckling such as would be generated in gravitational overturn did not occur through the interval of greenstone belt development. Low geothermal gradients required to render the crust sufficiently rigid to inhibit overturn is also consistent with the interpretation that crustal melts were not generated in tonalites emplaced at depths approaching 20 km during this time interval.

Although low geothermal gradients may predominate in a regional sense, minor, localized low-Al TTG and chemically equivalent F2-F3 rhyolites suggest localized higher geothermal gradients to explain high-level melting of mafic crust implicated in the generation of these magmas. These magma systems and spatially related hydrothermal alteration and VMS mineralization are attributed to the development of thermal corridors associated with extensional regimes developed within convergent margin settings (Galley 2003). Consequently, although comparatively low geothermal gradients allowing the stabilization and preservation of relatively thick crust may have predominated regionally, more restricted regions were characterized by anomalously high geothermal gradients. This, together with the diversity of mafic to ultramafic metavolcanic rocks, suggests that although the Abitibi Subprovince may have developed in a convergent margin setting, a range of second-order back-arc extensional regimes akin to those in modern convergent margins (Stern 2002) also play an important role.

Stage 2 – Early Syntectonic Stage (~2693–2685 Ma)

A brief interval of early syntectonic magmatic activity marks the termination of both intermediate to felsic TTG-type and mafic-ultramafic magmatic activity, a transition to sedimentary-dominated supracrustal units and the initial stages of regional tectonometamorphism. Most of the syntectonic magmatic activity occurs within a very narrow time interval from approximately 2691 Ma to 2687 Ma. These magmatic products comprise both volcanic and high-level intrusive facies, and together with immediately overlying metasedimentary rocks constitute the Porcupine assemblage.

Magmatic activity associated with the early syntectonic stage is high-Al TTG; however, these units do not have the very high Sr/Y and conspicuous positive Eu anomalies that characterize a subset of the stage 1 high-Al TTG units. This suggests that melting generating these units produced mafic garnet granulitic, as opposed to eclogitic, residues which may indicate that the melting regime may be, on average, at somewhat shallower levels (i.e., within the lower crust) compared to the stage 1 TTG magmas. The absence of coeval mafic magmatic activity is a further difference with the older TTG magmatic activity and also suggests that melting at mantle depths does not characterize the early syntectonic stage. A final difference between stage 1 and 2 magmatic products is the comparatively trivial volumes of magma generated during the early syntectonic stage.

The termination of early syntectonic magmatic activity corresponds with the initiation of Porcupine assemblage sedimentation, and the volcanic–sedimentary transition is interpreted here to be generally associated with the transition into the syntectonic stage.

The local evidence for slight angular discordance at the base of the Porcupine assemblage (Bateman et al. 2005) is interpreted here to indicate that the initial tilting of the underlying, dominantly volcanic assemblages occurred at approximately 2690 to 2695 Ma. The driving force for this earliest manifestation of regional deformation is unclear.

Stage 3 – Syntectonic Stage (~2686–2676 Ma)

Syntectonic magmatic activity is interpreted to be temporally associated with Porcupine assemblage sedimentation and a major phase of regional deformation that imparted the fundamental elements of the observed crustal architecture. The syntectonic magmatism also marks a fundamental change in the petrogenetic character of the Abitibi magmatic record.

The petrogenesis of the syntectonic plutons marks a turning point in the Abitibi plutonic record. Earlier pretectonic and early syntectonic plutons have a TTG affinity reflecting partial melting of a basaltic source with minimal mantle or felsic crustal input. Syntectonic plutons have elevated Mg# and compatible trace element abundances relative to typical TTG, which is interpreted to reflect derivation from, or interaction with, an ultramafic (mantle) reservoir. The slight enrichment in LILE characterizing these plutons could reflect the involvement of a metasomatized mantle source as proposed for the sanukitoid suite (Shirey and Hanson 1984) although none of the plutons would qualify as primary sanukitoid magmas. The transitional sanukitoid–TTG character of these plutons could reflect either a mixed basaltic–metasomatized mantle source or extensive fractionation of primary sanukitoid magmas. In either case, the character of these units is interpreted to reflect increased involvement of a metasomatized mantle source component in the petrogenesis of intermediate to felsic plutonic rocks.

Syntectonic plutons occur as discrete plutons within the greenstone belt and as a component of large belt-bounding batholiths. The former are especially concentrated within the extensively folded Tisdale assemblage in the central portion of the Abitibi greenstone belt where they have simple semicircular to elliptical to multilobate map outlines. Many of the plutons appear to be localized within the hinge zones of regional folds. A number of these plutons display crosscutting relationships indicating that their emplacement postdates the imposition of a regional penetrative deformational fabric that is defined by near-peak metamorphic mineral assemblages. These crosscutting relationships with respect to near-peak metamorphic deformational fabrics, which are interpreted to have developed shortly before emplacement of these plutons, point to a very rapid progression of tectonometamorphism that may be characteristic of Archean granite–greenstone terranes (Beakhouse 2007b). These plutons have Al-in-hornblende paleopressures that are compatible with the peak metamorphic conditions (Powell, Carmichael and Hodgson 1995; Thompson 2002) interpreted for the metavolcanic rocks that they intrude. Syntectonic

plutons intruding pretectonic tonalites within the large belt-bounding batholiths have paleopressures intermediate between those of the tonalites and greenstone belt regional metamorphism. In one case (Neville pluton), the pluton intrudes along the contact of the Kenogamissi Batholith and has been displaced upwards relative to adjacent supracrustal rocks. These relationships indicate that the emplacement of the Neville pluton at 2682 +3/-2 Ma occurred during uplift of the deep crustal levels (500 to 700 MPa) represented by the pretectonic tonalites to tectonically juxtapose these rocks against greenstone belt units metamorphosed at higher levels (~250 to 350 MPa) in the crust. These observations and interpretations suggest that a major detachment fault at the base of the greenstone belt, and subsidiary detachment surfaces within the basal portions of the greenstone belt stratigraphy were synchronous with, and facilitated, long- and intermediate-wavelength folding that defines the architecture of the Abitibi greenstone belt. It is possible that these originally shallowly dipping detachment surfaces within the greenstone stratigraphy include both reverse (thrust) and normal (extensional) faults.

The long wavelength folding and detachment faulting that tectonically emplaced pretectonic TTG batholiths (midcrustal magmatic emplacement) to higher crustal levels involves as much as 10 km of vertical displacement. This is interpreted to have important paleogeographic consequences culminating in the development of major, granite-dominated uplifted regions (Mount Kenogamissi and Round Mountain). As discussed above, such a source is precisely that implicated for the provenance of Porcupine assemblage metasedimentary rocks in the Timmins area (Born 1995). Furthermore, the timing of uplift corresponds well with the timing of sedimentation and provides a linkage between syntectonic plutonism, regional tectonism and Porcupine assemblage sedimentation.

The rapid onset of regional metamorphism alluded to above parallels that interpreted for a number of other areas within the Superior Province (Beakhouse 2007b). Further evidence for a thermal pulse within this time frame arises from clustering of U/Pb titanite ages at approximately 2683 Ma (Ketchum et al. 2008). Very similar U/Pb titanite ages are reported from the Hemlo area (within the probably correlative Wawa Subprovince) and are similarly interpreted to be a manifestation of a major regional thermal event (Beakhouse et al. 2011). A number of processes are invoked to account for the thermal component of regional metamorphism, including internal radiogenic heat production, conduction of heat from the underlying mantle (especially for tectonic settings where the crust is delaminated or convecting asthenospheric mantle is introduced at the base of the crust), convective overturn within the crust and advected heat related to transfer of magmas or fluids to high levels in the crust. It is likely that all of these processes contribute to some degree; however, the rapidity of onset of peak metamorphic conditions suggests that advected heat related to the emplacement of syntectonic plutons plays an important role. Crustal radiogenic heat production and conducted mantle heat would heat the crust more slowly and may be the dominant process associated with the longer-term (~25 Ma) thermal anomaly associated with regional metamorphism. This suggests that the generation of syntectonic magmas is temporally linked to the beginning of a larger scale thermal anomaly linked to regional tectonism.

Stage 4 – Late-Tectonic Stage (~2680–2668 Ma)

Late-tectonic magmatic activity includes strongly alkalic, dominantly syenitic (but compositionally diverse) plutons together with cogenetic volcanic rocks that are spatially and temporally associated with Timiskaming assemblage sedimentation. The aforementioned components exhibit a strong spatial association with major, regional-scale fault systems such as the Porcupine–Destor (PDF) and Cadillac–Larder Lake (CLLF) faults although there are minor occurrences outside of these zones. In some cases, their occurrence in areas of generally poor exposure of Archean crust may indicate the unrecognized presence of such structures. One such example is that of the Casey Mountain syenite which occurs in close proximity to the classical Timiskaming series units exposed at the north end of Lake Timiskaming (Miller 1913).

The compositionally diverse, strongly alkalic igneous rocks characterizing the late-tectonic stage are interpreted to be derived by partial melting of enriched, long-term depleted mantle. The isotopic character of these units indicate that mantle enrichment took place shortly before these magmas were generated, with fluids likely originating from dehydration of subducted oceanic crust (Hattori et al. 1996). These data and interpretations are consistent with development of a metasomatized mantle source during stage 1 for which a subduction regime is independently postulated. Late mantle-derived plutons in the Superior Province span a continuum from mildly alkalic sanukitoid suite to very strongly alkalic syenitic plutons, with the late-tectonic plutons of the Abitibi Subprovince being representative of the latter end member. The development of very strongly alkalic, mantle-derived compositions are generally attributed to either lower degree of melting (Green 1976) or high CO_2/H_2O in the zone of melting (Eggler 1978). The association of carbonatitic phases with some of these intrusions also suggests an important role for CO_2. High CO_2/H_2O in the mantle source could arise either from an unusually CO_2-rich metasomatizing agent or multistage melting with H_2O preferentially extracted in the earlier melting stage, with subsequent melting being perhaps both less extensive and more CO_2-dominated.

These plutons together with Timiskaming assemblage supracrustal rocks are interpreted to be late-tectonic because they are emplaced at relatively high crustal levels following much of the folding that imparts the gross architecture of the Abitibi greenstone belt. In spite of this relatively late emplacement, there is a broad range in the state of strain imposed on these rocks and many of these units are complexly deformed. This is interpreted to be a consequence of the preferential emplacement and deposition of these units within fault zones into which much of the late deformation is partitioned. In contrast to earlier deformation, most of the late deformation appears to be related to transcurrent faulting. The emplacement of these plutons, together with complex hydrothermal alteration within these fault zones, is likely responsible for introduction of advected heat which locally perturbs the ongoing, protracted regional metamorphic conditions.

Stage 5 – Late- to Posttectonic Stage (<~2676 Ma)

A petrogenetically distinct group of plutons that are largely restricted to large, belt-bounding batholiths (notably the Kenogamissi Batholith) are interpreted to be late tectonic to posttectonic. The ages obtained for several of these units are less precise than those for most other types of plutons because of a range of factors (van Breemen et al. 2006; Ketchum et al. 2008) and in some cases may represent maximum ages. The ages obtained in these investigations overlap with those of the late-tectonic group.

The plutons assigned to this group are leucocratic, biotite granodiorite to granite. They have distinctive geochemical characteristics including elevated LILE abundances with high K_2O/Na_2O, low Mg# and compatible element abundances and low Sr coupled with prominent negative Eu anomalies. These characteristics suggest an origin via partial melting of evolved felsic crust with residual plagioclase. Pretectonic tonalites in the Kenogamissi Batholith locally preserve textural evidence of *in situ* generation of granitic leucosome, and the composition and mineralogy of these tonalites is consistent with similar rocks at depth being the source for the posttectonic plutons.

The granodiorite to granites crosscut the foliation and gneissosity in older units of the Kenogamissi Batholith and are devoid of penetrative deformational fabrics and in this respect can be regarded as posttectonic. However, the absolute ages for these units overlap with those of the late-tectonic group and their undeformed character may in part reflect their occurrence outside of zones within which much of the late strain is strongly partitioned.

The generation of granitic rocks by partial melting of tonalitic crust implies some linkage with regional metamorphism. The melting to generate these units is not temporally or spatially associated with

emplacement of mantle-derived intrusions, and their generation at least 10 to 15 million years after the onset of regional metamorphism suggests that gradual heating of deep crustal levels due to conduction of mantle heat and/or intracrustal radiogenic heat production may be a viable mechanism for achieving thermal conditions required for melting.

Significance for Gold Mineralization

The Abitibi greenstone belt hosts numerous gold deposits and is one of the most richly endowed greenstone belts in the Superior Province and the world. Poulsen et al. (2000) list 12 "world-class" gold deposits in the Superior Province with 10 of these (representing approximately 80 percent of production from these deposits) occurring within the Abitibi Subprovince. Furthermore, within the Abitibi Subprovince itself, economic gold mineralization tends to be geographically concentrated, with deposits occurring in clusters localized along major faults. These observations lead to a number of questions that have implications for gold exploration both within the Abitibi Subprovince and more generally:

Is the rich endowment of the Abitibi Subprovince real or apparent? The ensuing discussion is predicated on the assumption that the Abitibi greenstone belt contains more economic gold concentration per unit volume than other greenstone belts in the Superior Province; however, it is possible that the long perceived rich endowment of the region has influenced the intensity of exploration (if you look hard enough, you will find it!).

What is responsible for the apparent or real concentration of economic mineralization in proximity to certain segments of faults? The answer to this question has implications for where we should look along faults, whether or not there may be additional highly prospective faults and whether or not there is significant mineralization occurring outside these fault zones, and has implications for gold exploration within the Abitibi Subprovince and more generally.

Are there differences in geological evolution of the Abitibi Subprovince compared to that of other greenstone terranes that can be plausibly linked to the rich gold endowment? This has implications for how gold deposits are formed and possible factors that should be considered within exploration strategies on a variety of scales.

The scope of this investigation does not allow for the full range of variables relative to the above questions to be addressed. The focus of the following discussion will be on the possible role of magmatism and the broad geodynamic environment as a determinant of crustal gold endowment. The approach builds on earlier, more general investigations focused on the interrelationship between gold mineralization and the magmatic and tectonometamorphic development of greenstone belts in the Superior Province (Beakhouse 2007a).

GOLD MINERALIZATION WITHIN THE MAGMATIC AND TECTONOMETAMORPHIC FRAMEWORK FOR THE ABITIBI SUBPROVINCE

Most gold-dominated mineral deposits in the Abitibi Subprovince can be regarded to be broadly structurally controlled hydrothermal deposits. Consequently, constraints on the timing of mineralization can be derived from a number of relationships, including relative and absolute constraints on the timing of minerals paragenetically related to gold, intrusions genetically linked to gold, mineralized host rocks, intrusions postdating mineralization, structures hosting gold and the relationship to regional metamorphism. In practice, the application of these constraints is complicated by a range of factors

including complex field relationships, complex isotope systematics and the rapid, possibly diachronous, progression of various elements of the geological record in the critical time interval.

In addition to gold-dominated mineral deposits, several volcanogenic massive sulphide base metal deposits in Quebec contain sufficient gold to be regarded as world class or significant gold deposits (Horne, LaRonde). The origin of gold in these deposits is controversial, with some workers arguing for syngenetic introduction of gold along with the base metals (Poulsen et al. 2000). Consequently, these deposits may be an example of "early" gold preceding a later "main" gold event. Other workers have argued that these deposits may be volcanogenic massive sulphide base metal deposits with superimposed, temporally distinct (late) gold mineralization (Marquis et al. 1990). The origin of these deposits is outside the scope of this study and they will not be considered further.

Mineralized units associated with the PDF in the Timmins area include a variety of volcanic units, sedimentary rocks, porphyries and albitite dikes (Burrows et al. 1993; Brisbin 1997). Mineralized volcanic units include the Tisdale assemblage (~2703–2710 Ma) and Krist volcanics (~2686–2693 Ma) (*see* Table 6 for individual ages and references). Mineralized metasedimentary units include the Porcupine assemblage (~2675–2685 Ma) and the Timiskaming assemblage (~2670–2676 Ma). The possibility that some Timiskaming assemblage units postdate a component of the gold mineralization cannot be discounted as mineralization in some clasts has been interpreted to predate sedimentation (Gray 1994; Gray and Hutchinson 2001). If correct, this interpretation would imply either multiple gold mineralizing events that both predate and postdate the Timiskaming assemblage or a single, protracted syn-Timiskaming mineralizing event.

Alteration and gold mineralization in the Timmins area is spatially associated with, and superimposed on, porphyries (e.g., Pearl Lake, Crown, Paymaster, Preston) that are interpreted to be high-level intrusive rocks (Brisbin 1997). U/Pb zircon ages for several of these porphyries lie in a narrow age range between 2688 and 2691 Ma (Corfu et al. 1989) and are interpreted here to be associated with the early syntectonic stage. The youngest altered and mineralized intrusive rocks recognized in the Timmins camp are "albitite" dikes (Burrows et al. 1993) for which a U/Pb zircon age of 2673^{+6}_{-2} Ma has been interpreted (Corfu et al. 1989). Although overprinted by mineralization, these albitite dikes have been interpreted to be closely temporally associated with gold mineralization (Burrows et al. 1993; Brisbin 1997). These albitite dikes are interpreted here to be associated with the late-tectonic stage.

Generally, similar constraints are reported from the Holloway Mine along the eastern portion of the Ontario portion of the PDF, where mineralization occurs in Timiskaming assemblage units and is cut by a late intermineral dike with a U/Pb zircon age of 2671.5 ± 1.9 Ma (Ropchan et al. 2002).

Relationships between regional geology and gold mineralization are broadly similar along the Cadillac–Larder Lake fault (CLLF) in the Kirkland Lake area. In the Kirkland Lake–Larder Lake area, rocks predating gold mineralization include metavolcanic rocks of the Tisdale and Blake River assemblages, syntectonic metasedimentary rocks and porphyries (Bidgood porphyry (2685 ± 3 Ma), Corfu et al. 1991). The timing of late-tectonic Timiskaming assemblage supracrustal rocks and alkalic intrusions with respect to mineralization is less clear: although many units of this association are mineralized, intermineral dikes are alkalic (Isoplatov et al. 2005) and likely related to the late-tectonic igneous suite. Furthermore, magmatic hydrothermal fluids exsolved from the alkalic plutons have been proposed as the fluid responsible for mineralization in the Kirkland Lake area (Cameron and Hattori 1987) and elsewhere along the CLLF (Robert 2001). The widespread occurrence of tellurides in many of the Kirkland Lake area deposits is also characteristic of magmatic hydrothermal mineralization associated with alkaline magmas (Jensen and Barton 2000). The foregoing suggests that gold mineralization at Kirkland Lake may be not only spatially but temporally and genetically related to late-tectonic alkaline magmatism.

Relationships in a number of other areas characterized by the presence of gold mineralization in association with late-tectonic faults and alkalic units, including Matachewan, Bristol Township and Shining Tree, are not well understood but broadly consistent with the types of relationships discussed above.

Powell et al. (1995) interpreted regional metamorphism to postdate all supracrustal rocks and bracketed it between 2677 and 2643 Ma. However, results reported within this investigation indicate that deformational fabrics defined by near-peak metamorphic mineral assemblages predate syntectonic plutons, indicating that portions of the greenstone belt were metamorphosed prior to deposition of the Timiskaming assemblage. Numerous studies have identified relatively young metamorphic and/or hydrothermal events along the Porcupine–Destor and, especially, the Cadillac–Larder breaks based on U/Pb (Jemelita et al. 1990; Zweng et al. 1993; Kerrich and King 1993; Kerrich and Kyser, 1994), Nd/Sm (Anglin et al. 1996) and Ar/Ar (Hanes et al. 1992; Feng et al. 1992; Powell et al. 1995) isotopic investigations. Many of these investigations have focused on areas of gold mineralization and, in some cases, these younger ages have been cited as evidence for a younger gold mineralizing event that postdates regional metamorphism and plutonism. The younger U/Pb ages (titanite and rutile generally in the range 2620 to 2630 Ma) have been linked to processes in the lower crust (Jemelita et al. 1990; Zweng et al. 1993) and are approximately 50 million years younger than the latest plutonism and other estimates for gold timing discussed above. However, this interpretation has generated considerable controversy and has led to suggestions that a) the younger ages represent localized late hydrothermal events that remobilize earlier mineralization (Kerrich and King 1993; Kerrich and Kyser 1994), b) gold mineralization postdates plutonism and regional metamorphism (Jemilita et al. 1990) or c) there are 2 regional episodes of gold mineralization (Couture et al. 1994).

The interpretation favoured here is that regional metamorphism should be regarded as a protracted event related to large-scale geodynamic processes that is punctuated by local- to regional-scale thermal perturbations related to introduction of advected heat by magmas and fluids.

It is clear, based on the foregoing discussions, that the detailed relative and absolute timing of gold introduction remains a complex problem requiring additional work. However, a number of generalizations can be made, based on the relationships discussed above, that provide broad constraints and can form the basis of a preferred testable hypothesis for ongoing work:

> *All gold mineralized areas are interpreted to be characterized by a "main stage" gold mineralizing event that broadly correlates with the late-tectonic stage although "early" gold enrichment and "late" remobilization of gold undoubtedly has occurred and may be locally important.*
>
> *"Main stage" gold mineralization postdates most volcanism and sedimentation but may be broadly synchronous with deposition of volumetrically subordinate, younger sequences (the so-called "Timiskaming-type" or late unconformable sequences) that unconformably overlie the dominant "earlier" sequences and their associated plutonic components.*
>
> *Plutons most closely spatially associated with gold mineralization include early syntectonic porphyries and late-tectonic alkalic plutons; other intrusive suites are not spatially and/or temporally associated with gold mineralization. The early syntectonic porphyries predate gold mineralization, and the spatial association is interpreted to arise from i) long-lived zones of weakness that controlled the emplacement of both porphyries and later gold mineralizing fluids and ii) the contribution of porphyries to extreme ductility contrast that localizes the development of heterogeneous strain which leads to*

enhanced porosity and permeability that serves to focus hydrothermal fluid flow. Late-tectonic plutons are temporally and, in some cases, spatially associated with the "main stage" gold mineralizing event and are the most likely source of any auriferous magmatic hydrothermal fluids that may be involved in the generation of gold deposits.

Regional deformation and metamorphism was initiated very shortly following the deposition of the regionally dominant, "earlier" supracrustal sequences and in part overlaps the deposition of the late unconformable sequences. Greenstone belts achieved something close to their final tectonometamorphic configuration by the time of emplacement of the late-tectonic plutons although minor deformation and slow cooling persisted.

Gold mineralization is structurally controlled and hence is synchronous with or postdates the development of the hosting structures. In most cases, these structures postdate an earlier fabric and, though commonly overprinted by minor deformation, are comparatively late in the regional sequence of deformational events.

The timing of "main stage" gold mineralization is similar to that of early stages of regional metamorphism; however, the protracted interval during which regional metamorphism developed contrasts with the more restricted time interval of "main stage" gold mineralization. The role of local, late perturbation of metamorphic and hydrothermal conditions in redistributing or introducing gold is poorly understood.

SOURCE OF AURIFEROUS HYDROTHERMAL FLUIDS

The foregoing working hypothesis advocates formation of Abitibi lode gold deposits during a brief, dynamic, late stage of greenstone belt development but is not diagnostic of a particular origin for the source of the mineralizing fluids. The data and interpretations are permissive of a linkage with several competing hypotheses for the origin of the mineralizing fluids, including 1) devolatilization attendant with regional metamorphism, 2) direct introduction of fluids originating in the mantle and 3) magmatic devolatilization. Recognizing that it is possible (likely?) that any or all of these mechanisms may generate potential mineralizing fluids, the ensuing discussion will focus on the potential role of magmatic hydrothermal fluids and then briefly speculate on the possible interrelationship of other fluid sources.

The results of this study suggest that only the late-tectonic alkalic suite is both temporally and spatially associated with gold mineralization and consequently these plutons are the only plausible source of exsolved magmatic hydrothermal fluids that may contribute to the gold endowment of the Abitibi Subprovince. Several other lines of evidence discussed below suggest that magmatic hydrothermal fluids exsolved from these plutons are a plausible source for some of the mineralization.

Oxidation State

The critical role for oxidation state in the case of mineralization associated with highly oxidized plutons is attributed to its role in determining the stable sulphur species (Burnham and Ohmoto 1980). Under highly oxidizing conditions, sulphate is stabilized and magmas reaching sulphur saturation will precipitate sulphates (primarily anhydrite), whereas under conditions approximately less oxidizing than the Ni-NiO buffer, sulphur saturation will result in the precipitation of sulphides (Carroll and Rutherford 1985). Because of the highly chalcophile character of the ore metals, they will be concentrated in the sulphide mineral phases, thereby reducing the metal and sulphur concentration in the residual magma. Gold will

also tend to be concentrated in sulphides, although its behavior is relatively complex, with copper-iron sulphides being more effective at concentrating gold than iron sulphides (Cygan and Candela 1995; Jugo et al. 1999; Kesler et al. 2002). A consequence of the sequestering of ore metals in sulphides, is that subsequently exsolved magmatic volatile phases that are responsible for mineralization will have less potential to be enriched in sulphur and ore metals.

An association of oxidized intermediate to felsic intrusions has also been proposed for Archean lode gold deposits within the Superior Province (Hattori 1987; Cameron and Hattori 1987; Beakhouse 2007a). These authors proposed a linkage between oxidized hydrothermal fluids involved in the generation of several gold deposits and magnetic felsic intrusions that are spatially associated with these deposits. The abundance of magnetite in these intrusions is attributed to their being highly oxidized (Hattori 1987). The oxidation state of one of the late-tectonic plutons investigated in this study (Murdock Creek pluton), occurring within the Kirkland Lake gold camp, was rigorously evaluated and found to be highly oxidized (Rowins et al. 1991).

The mineralogy of most late-tectonic plutons investigated within this study is suggestive of crystallization under highly oxidizing conditions. The abundance of magnetite in most intrusions results in relatively high magnetic susceptibility which has been proposed as a proxy for fO_2 (Beakhouse 2007a). Application of a similar approach (Figure 67; with diagram modified to a logarithmic scale for $Fe_2O_3^{total}$ to accommodate the felsic to ultramafic compositional range for Abitibi Subprovince plutons) reveals some similarities to the pattern described in the earlier study but there is considerable scatter reflecting a range of processes.

As discussed elsewhere (Beakhouse 2007a), the bulk composition influences the magnetic susceptibility in 2 ways: i) more magnetite will crystallize in the more iron-rich of 2 similarly oxidized magmas and ii) the abundance and type of ferromagnesian silicates controls the paramagnetic mineral contribution to magnetic susceptibility. The oxidation state of the magma influences magnetic susceptibility because at any given Fe content, the amount of magnetite formed will be influenced by the Fe^{3+}/Fe^{2+} ratio in the magma. Under conditions less oxidizing than the quartz + fayalite + magnetite (QFM) buffer, Fe will reside primarily in Fe-Mg silicates and the bulk rock will be characterized by low magnetic susceptibility. Under progressively more oxidizing conditions (up to the magnetite-hematite buffer) magnetite will be stabilized and its abundance will progressively increase and be coupled with progressively higher Mg# in the ferromagnesian silicate minerals. Consequently, at a fixed Fe content, magnetic susceptibility will generally be proportional to fO_2. The 2 lines in Figure 67 are not rigorously constrained but represent an attempt to broadly distinguish strongly oxidized, "normally" oxidized (between the 2 lines) and more reduced systems. The lower of the 2 lines approximates the estimated maximum magnetic susceptibility as a function of $Fe_2O_3^{total}$ for rocks without primary magnetite (i.e., fO_2 at or below QFM) for which magnetic susceptibility is dominated by paramagnetic mineral contribution with some allowance for minimal secondary Fe-Ti oxides. Above this lower line, most samples would be expected to contain some magnetite, with the amount of magnetite being crudely proportional to the magnetic susceptibility. The position of the upper line is arbitrary but was chosen based on observations made during this investigation and in other areas (Hemlo area and western Wabigoon Subprovince) where similar rocks have been investigated such that samples lying above it generally have conspicuously abundant magnetite (>1 and 3 volume % in felsic and mafic end members, respectively). Several units that have been investigated in detail (e.g., Cedar Creek stock, Cameron and Carrigan 1987; Murdock Creel pluton, Rowins et al. 1991) have inferred fO_2 at or above the Ni-NiO buffer and may crudely approximate the oxidation state of this buffer. Although this approach may generally approximate the oxidation state characterizing the magmas from which these rocks crystallized, a number of processes may result in scatter and misclassification, including:

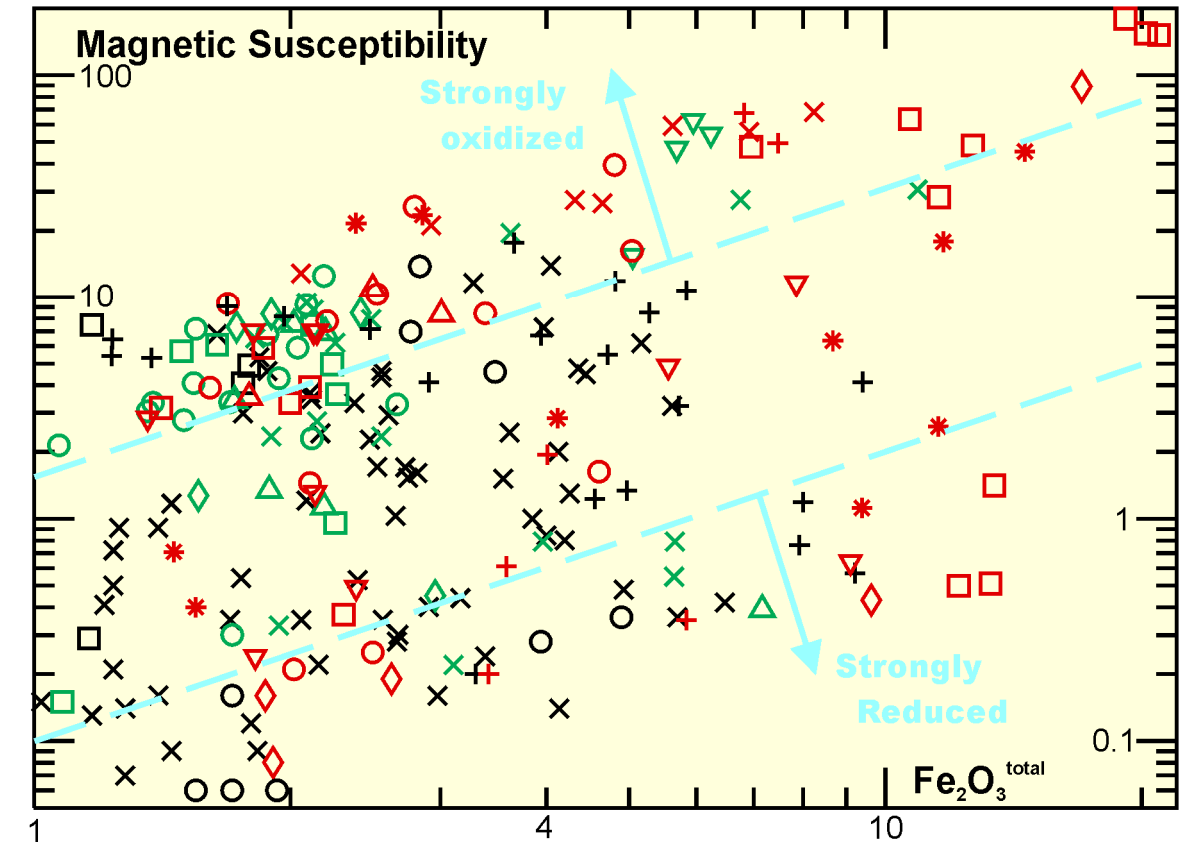

× Pretectonic
\+ Syntectonic
□ Posttectonic

Belt-bounding Batholiths

○ **Early Syntectonic Porphyries**

Syntectonic Plutons

- ○ Watabeag
- □ Blackstock
- ◊ Adams
- △ Geikie
- ▽ Fallon
- × Other

Late-tectonic Plutons

- □ BTAC (Bristol Twp)
- △ Canadian Arrow
- ▽ Ludgate
- ◊ Hislop
- × Lebel, Cairo
- \+ Murdock Creek, Young-Davidson
- ✱ Otto
- ○ Other

Figure 67. Plot of magnetic susceptibility versus weight percent $Fe_2O_3^{total}$ for various plutonic units within the Ontario portion of the Abitibi Subprovince. Note logarithmic scale for both variables. The 2 diagonal lines (control points {MS,$Fe_2O_3^{total}$} are {1,1}, {15,20}, {15,1} and {75,20}) are not rigorously constrained but may approximately delineate strongly oxidized, "normally" oxidized and weakly oxidized (reduced) fields as discussed in text.

- under extremely oxidizing conditions (above magnetite-hematite buffer) iron oxide may crystallize as hematite, in which case the magnetic susceptibility might be quite low and erroneously suggest a strongly reduced system;

- the formation of ferromagnetic minerals other than magnetite (e.g., pyrrhotite);

- physical processes associated with fractionation, such as crystal settling, may result in removal or addition of Fe-oxide minerals;

- secondary alteration of magnetite by oxidizing fluids (producing hematite) or sulphur-bearing fluids (sulphidation of magnetite) may reduce magnetite abundance and hence magnetic susceptibility; and

- secondary alteration of ferromagnesian silicate minerals may lead to the formation of Fe-Ti oxides and more magnesian silicate phases and increase the magnetic susceptibility.

Application of this approach for major Abitibi Subprovince intermediate to felsic intrusions reveals a broad general pattern for different types of intrusions but with considerable scatter in the data (*see* Figure 67). For the most part, pretectonic TTG lie below the strongly oxidized field and most commonly within the normally oxidized field. Early syntectonic porphyries exhibit considerable scatter, which is interpreted to reflect diverse secondary alteration that has largely replaced magmatic mineral assemblages within these units. In particular, the very low magnetic susceptibility characterizing some of these units may be attributed to sulphidation reactions. The majority of the syntectonic units lie near the upper line, with the majority of these samples lying in the strongly oxidized field. Some samples from this group plot near or below the lower line and include samples from some units for which there is limited data (e.g., Eldorado pluton, Gosselin Lake pluton) and may be misclassified whereas others are highly altered samples from plutons that are otherwise characterized by relatively high magnetic susceptibility.

The late-tectonic plutons are characterized by a broader range in bulk composition but are similar to the syntectonic plutons in displaying a predominance of samples plotting in the strongly oxidized field but with dispersion of data across all fields. Some of this dispersion to apparently lower oxidation state can be attributed to processes recognized in a number of these plutons. The low magnetic susceptibility in some samples can be attributed to the presence of hematite rather than magnetite. It is possible in some cases that the hematite may be a primary magmatic phase indicative of extremely oxidizing conditions although in many cases, the hematite appears to be secondary and reflect interaction with late, oxidizing hydrothermal fluids (this study and Ben Berger, personal communication, 2011). Physical depletion and/or concentration of magnetite by crystal fractionation processes such as described for the Otto Stock (*see* Figure 40f) is responsible for variation in magnetic susceptibility locally. Textural evidence of replacement of magnetite by sulphides is observed locally and indicates reduction of magnetic susceptibility due to secondary alteration processes. The weight of evidence suggests that the late mantle-derived plutonic suites, and the late-tectonic alkalic plutons in particular, are dominated by high bulk composition adjusted magnetic susceptibility that is interpreted to reflect crystallization from intrinsically highly oxidized magmas.

Other mineralogical characteristics are consistent with the interpretation that the late-tectonic alkalic plutons crystallized from highly oxidized magmas. Detailed mineralogical investigation of a small number of samples from the late-tectonic alkalic suite revealed the common occurrence of accessory barite and celestite. Barite is also reported to occur in the Emens intrusion (Pigeon 2003), and barite veins spatially associated with the Cairo stock may be both Archean and Proterozoic in age (Berger 2006). Although the occurrence of some of these barium and strontium sulphates in veins clearly indicates that late magmatic hydrothermal or secondary fluids are involved for some of these occurrences, textural

observations, including the occurrence of the sulphates as disseminations enclosed within unaltered magmatic minerals, suggest a primary magmatic origin for others. Although most attention has been focused on the presence of anhydrite as an indicator of oxidizing conditions sufficient to preclude the formation of sulphide phases (Carroll and Rutherford 1985), primary magmatic barite has also been reported and the presence of other sulphates may also be an indicator of highly oxidizing conditions (Marchev 1991). It is not clear why none of the sulphate observed is anhydrite although it is worthy of note that the most notable occurrences of sulphates correlate with the presence of calcium-rich mineral phases (magmatic carbonate and andradite).

The foregoing discussion suggests that intermediate to felsic intrusions generated by partial melting of metasomatized mantle, and in particular the late-tectonic alkalic suite, are characterized by high intrinsic fO_2 that is interpreted to be a consequence of their source. It is proposed that these magmas would not have crystallized early sulphide phases that would have sequestered ore metals, and consequently magmatic hydrothermal fluids exsolved from the magmas at later stages of crystallization would have been ore metal enriched and potential mineralizing fluids. Together with the temporal, and in some cases spatial, association of gold mineralization and late-tectonic alkalic plutons, this suggests that at least one component of gold mineralization is genetically associated with mantle-derived alkalic magmatism.

Ore Mineralogy

The ore mineralogy of Abitibi Subprovince gold deposits is not well constrained, with only a few major deposits having been characterized in detail. A noteworthy characteristic of syenite-associated mineralization at Kirkland Lake is the widespread occurrence of gold tellurides (calaverite and petzite) along with base metal and bismuth tellurides in addition to native gold (Thompson 1950). Robert (2001) describes other syenite-associated gold deposits that are variously enriched in tellurium. Tellurides are also present in several other deposits and, although not widespread (occurring in only 4% of deposits), this may in part reflect the paucity of detailed mineralogical investigations and the difficulty in identifying tellurides (Hodgson 1983). The characteristic of variable enrichment in tellurium is shared by gold deposits related to alkaline magmatism in Phanerozoic systems (Jensen and Barton 2000).

The close spatial association of gold mineralization with a significant telluride component and alkalic intrusions in portions of the Abitibi Subprovince is interpreted here to indicate a genetic linkage. Many gold deposits, notably in the Timmins area, are not characterized by abundant tellurides and genetic linkages to alkaline magmatism are less certain.

Analogy to Phanerozoic Systems

The initial rationale for specifically addressing the role of magmatic hydrothermal fluids in the generation of Archean lode gold deposits in a series of earlier investigations (Beakhouse 2001, 2007a) is derived from the observations that i) broadly uniformitarian geotectonic models are being increasing applied to Archean systems and ii) magmatic hydrothermal fluids are widely interpreted to have played a major role in the generation of gold deposits occurring in Phanerozoic terranes that are proposed analogues for these Archean terranes.

Phanerozoic gold-rich porphyry and high-sulphidation epithermal systems develop in subduction environments at all stages of arc development and magmatic hydrothermal fluids exsolved from intermediate to felsic plutons are widely interpreted to be the principle source of contained metals (Arribas 1995; Sillitoe 1997; Candela and Piccoli 1995, 2005; Seedorff et al. 2005). Fluids involved in the

generation of low-sulphidation epithermal deposits are dominated by meteoric water; however, these deposits also occur in arc environments characterized by the presence of shallow plutons and there is evidence for the widespread presence of a small, but potentially important, magmatic hydrothermal fluid component (Simmons 1995; Christie et al. 2007). Similarly, a range of fluid types are involved in the generation of sediment-hosted (Carlin type) gold deposits, but some contribution of magmatic hydrothermal fluids that may be the critical auriferous fluid component has been proposed (Sillitoe and Bonham 1990; Cline et al. 2005). The foregoing suggests that a diverse range of types of gold deposits develop in Phanerozoic subduction-related geotectonic settings and that magmatic hydrothermal fluids exsolved from intermediate to felsic intrusions are genetically linked to many or most of these deposits.

The tectonic model for the Abitibi Subprovince developed in a preceding section has parallels with that developed previously for the Superior Province more generally (Beakhouse 2007a). This working hypothesis can be regarded as a modified uniformitarian model in that it invokes the principle elements of the plate tectonic paradigm but incorporates some uniquely Archean characteristics. These distinctive features of Archean systems are likely related to differences in the thermal structure of Archean subduction systems. One of the most fundamental differences is the early dominance of high-Al TTG produced by melting of basalt with evidence for extensive interaction with subduction-modified mantle wedge being restricted to the latter stages of the magmatic record. This contrasts with Phanerozoic systems where adakites (geochemically similar, but not identical, to high-Al TTG) are comparatively minor and most magmas at all stages of arc development are either derived from, or have extensively interacted with, the subduction-modified mantle wedge.

The interpretation that the main stage of gold mineralization is temporally associated with a brief interval during the magmatic evolution of Archean greenstone belt crust when plutons display evidence of having been derived from, or extensively interacted with, a metasomatized mantle source may indicate a genetic linkage. As discussed elsewhere (Beakhouse 2007a), if magmas sourced in subduction-modified mantle are genetically linked to gold mineralization, this provides an explanation why Archean gold mineralization develops late in the overall evolution of Archean greenstone belts while Phanerozoic gold deposits develop at all stages of arc development.

Diversity of Hydrothermal Fluids

Much of the preceding discussion focuses on the potential for magmatic hydrothermal fluids to play a major role in formation of lode gold deposits, but it is probable that a range of different fluid types are involved in this process. This is expected to be the case because structurally controlled porosity and permeability will focus the flow of all fluids present and consequently become a zone of fluid mixing. The range of fluids that could potentially be involved includes magmatic hydrothermal fluids, metamorphic fluids generated by devolatilization reactions at deeper crustal levels, mantle fluids generated by devolatilization reactions (without melting) in subducted oceanic crust and/or subduction-modified mantle, formational fluids and downwardly focused sea water or meteoric water. Consequently, zones of enhanced porosity and permeability are likely to be zones of fluid mixing. The generally deeper crustal level characterizing formation of Archean lode gold deposits as compared to Phanerozoic porphyry and epithermal deposits may result in different characteristic fluid assemblages (e.g., dominance of meteoric fluid such as characterizes many shallow epithermal deposits is less probable in deeper level Archean mineralizing systems).

Numerous studies have concluded that a low-salinity, mixed aqueous-carbonic fluid that has fairly uniform compositional characteristics is virtually always present and involved in the generation of lode gold deposits and several other fluid types (carbonic and/or low- to moderate salinity aqueous) are present in some deposits (see review of Ridley and Diamond 2000). There is considerable controversy regarding

the origin and possible interrelationships between the various fluids; however, many studies have concluded that the ubiquitous aqueous carbonic fluid introduced the gold (Ridley and Diamond 2000) whereas a lesser number of studies have concluded gold was introduced by the carbonic fluid phase (Schmidt-Mumm et al. 1997; Chi et al. 2009; Baker et al. 2010). Constraining the origin of the various fluid components has been controversial because of the non-unique compositions of some of the fluid components as well as the tendency for all fluids to interact and equilibrate with wall rocks and hence no longer retain all of their original compositional characteristics (Ridley and Diamond 2000; Evans et al. 2006).

A review of the relative role of the range of different fluids that may be associated with Abitibi Subprovince gold deposits is outside the scope of this study; however, based on these general considerations it is proposed that it is likely that a range of different fluid types are involved in the generation of these deposits. The close association of alkaline magmatism with some of these deposits discussed above strongly suggests that auriferous magmatic hydrothermal fluids exsolved from these plutons have contributed significantly to the overall gold endowment of the region although it remains possible that other types of fluid are the source for some of the gold.

Summary

The results and interpretations discussed above suggest that gold mineralization within the Abitibi Subprovince is temporally and, in some cases, spatially and genetically associated with late-tectonic, mantle-derived alkalic igneous activity. Characteristics of these alkaline magmas (e.g., highly oxidized character, CO_2-enriched character) make it probable that these magmas would have exsolved a metalliferous aqueous-carbonic fluid at some stage during their crystallization and emplacement into the upper crust. A subset of gold deposits have mineralogical characteristics (e.g., presence of tellurides) with some similarities to Phanerozoic gold deposits interpreted to be associated with alkaline magmatic systems. Consequently, it is interpreted here that aqueous-carbonic fluids exsolved from late-tectonic alkaline magmas are auriferous and have contributed to the gold endowment of the Abitibi Subprovince.

Late-tectonic alkaline magmatism and gold mineralization are dominantly, though not exclusively, localized in major, generally east-trending fault or deformation zones (e.g., PDF, CLLF), with gold mineralization generally localized in higher order structures related to these zones. In addition to magmatic hydrothermal fluids, these zones of enhanced porosity and permeability would have served to focus the flow of a range of other types of hydrothermal fluid (crustal metamorphic fluids, mantle fluids not dissolved in magmas, formational fluids and deeply circulating meteoric and/or sea water), some of which may also be auriferous. The presence of multiple fluids opens the possibility that depositional mechanisms for gold mineralization may be related to some combination of fluid mixing, wall-rock interaction and physical processes.

As discussed above, late-tectonic, mantle-derived alkalic plutons are probable major sources for auriferous hydrothermal fluids but these arguments do not rule out the possibility that other fluids may have been auriferous as well. However, based on analogy with Phanerozoic gold deposits, it is proposed here, as a working hypothesis, that these magmatic hydrothermal fluids may be the dominant source of gold in Archean greenstone belt systems. If this working hypothesis is valid, it affords a plausible answer to 2 fundamental questions posed at the beginning of this section:

What is responsible for the apparent or real concentration of economic mineralization in proximity to certain segments of faults? Late-tectonic magmatic activity occurs primarily in association with major east-trending faults, but tend to be most abundant within certain segments of these faults that are also characterized by a significant gold endowment. The most significant anomaly with respect to the inverse

argument (segments of the faults hosting gold mineralization have associated alkaline magmatism) are the major deposits near Timmins, although volumetrically minor albitite dikes are interpreted to be related to the late-tectonic plutonic suite and could be a manifestation of a larger alkalic system at depth. The working hypothesis predicts that zones of structurally controlled, enhanced porosity and permeability proximal to late-tectonic, mantle-derived alkaline magmatism will be favourable sites for gold exploration. Consequently, the non-uniform distribution of gold along faults may be due to large-scale controls on the distribution of alkaline magmatism. Although it seems clear that regional faults have exerted control on the distribution of the alkaline magmatic centres, it is less clear what the relative roles of "crustal architecture" and "mantle-melting heterogeneity" play in controlling spacing of these centres along regional faults. Other remaining questions include the scale over which magmatic hydrothermal fluids may migrate and the possibility that alkalic plutons may serve to indicate the presence of hitherto unrecognized crustal-scale faults. An example of the latter possibility is the occurrence of the Casey Mountain syenite along with the type Timiskaming series near the town of New Liskeard, which may indicate the presence of a major fault largely concealed by overlying Proterozoic and Phanerozoic sedimentary units and possibly correlating with a possible ill-defined "break" in the Shiningtree area that may link to the Rideout fault in the Swayze belt.

Are there differences in geological evolution of the Abitibi Subprovince compared to that of other greenstone terranes that can be plausibly linked to the rich gold endowment? The temporal progression from voluminous, synvolcanic high-Al TTG plutonic activity to postvolcanic, syntectonic to late-tectonic, mantle-derived plutonism in the Abitibi Subprovince parallels that recognized more generally across the Superior Province (Beakhouse 2007a, 2007b; Beakhouse and Davis 2005). However, one anomalous feature of the Abitibi plutonic record is the unusually alkalic character of the late-tectonic plutons that are implicated as the probable source of auriferous, magmatic hydrothermal fluids that have contributed to the gold endowment of the Abitibi Subprovince. An important role for CO_2 in the generation of these plutons is inferred from their strongly alkalic character, association of extensive carbonate alteration with many of the plutons and the presence of a minor carbonatitic-affinity component in association with some of these plutons. An important role for CO_2 in buffering the pH of hydrothermal fluids in a range that optimizes the capability of the fluid to transport gold has been proposed previously (Phillips and Evans 2004). Consequently, the unusually alkaline and CO_2-enriched character of the late-tectonic, mantle-derived magmas that the working hypothesis associates with mineralization may offer an explanation for the exceptional gold endowment of the Abitibi Subprovince. It remains unclear whether this alkalic, CO_2-enriched character is due to the nature of the subduction-modified mantle source or differences in the melting processes that generated these magmas, but this hypothesis ultimately links crustal gold endowment with processes occurring in the mantle and suggests that understanding the character of late, mantle-derived magma generation may have regional-scale mineral exploration implications.

Conclusions

Following is a summary of the major conclusions of this investigation:

Intermediate to felsic intrusive rocks within the Abitibi Subprovince display a broad, secular evolutionary trend as summarized below:

Pretectonic: synvolcanic / 2750 to 2695 Ma / predominantly high-Al TTG affinity with geochemical signature of eclogitic to mafic garnet granulitic residue / minor low-Al TTG affinity restricted to portions of the Groundhog River batholith / most voluminous component of the plutonic record

Early syntectonic: synchronous with "Krist" volcanism and the initiation of Porcupine assemblage sedimentation / 2691 to 2685 Ma / high-Al TTG affinity with geochemical signature of mafic garnet granulitic residue / locally abundant but overall volumetrically minor

Syntectonic: postdate all but Timiskaming assemblage volcanism / 2686 to 2676 Ma / petrogenetic affinity transitional between sanukitoid and high-Al TTG / postdate early penetrative deformational fabrics defined by near-peak metamorphic mineral assemblages and broadly synchronous with a component of regional folding / concentrated in folded Tisdale assemblage and in belt-bounding batholiths / locally abundant but significantly less voluminous than pretectonic component

Late-tectonic: synchronous with Timiskaming assemblage volcanism / 2680 to 2668 Ma / strongly alkalic, locally with associated units having carbonatitic affinity / derived from metasomatized mantle / postdate early deformational fabrics defined by near-peak metamorphic mineral assemblages / concentrated within or proximal to major east-trending fault systems / locally abundant but significantly less voluminous than pretectonic component

Late tectonic to posttectonic: postvolcanic / <2676 Ma (poorly constrained) / crustal I-type affinity with source broadly comparable to pretectonic suite / locally abundant but overall volumetrically minor / largely restricted to belt-bounding batholiths, notably the Kenogamissi Batholith.

The broad secular evolutionary trend described above is comparable to that recognized elsewhere in the Superior Province (cf., Beakhouse and Davis 2005; Beakhouse 2007a, 2007b); however, the late-tectonic suite is unusual both with respect to its abundance and extreme alkalic character. Late plutons across the Superior Province may have compositions within a continuum, from silica-saturated, subalkalic to weakly alkalic plutons to silica-undersaturated, strongly alkalic plutons with both being derived from metasomatized, long-term depleted mantle (Beakhouse 2007a). The more strongly alkalic character of late-tectonic, mantle-derived Abitibi plutons is interpreted to be linked to higher CO_2/H_2O ratio of volatiles associated with melting. This difference in the nature of the Abitibi plutonic record relative to that characterizing the rest of the Superior Province reflects the nature of the metasomatized mantle and/or the controls of melting of this source during the terminal stage of the Abitibi magmatic record.

The evolutionary trend in the petrogenesis of intermediate to felsic plutons within the Abitibi Subprovince is interpreted within a modified uniformitarian working hypothesis. Voluminous, synvolcanic, high-Al TTG magmas are attributed to partial melting of subducted oceanic crust as well as tectonically or magmatically underplated mafic crust. During this interval, the subarc mantle was modified by the introduction of fluids and/or low degree partial melts originating in subducting oceanic crust. The syntectonic suite marks an irreversible transition from magmas sourced from mafic crust to those sourced from the subduction-modified mantle wedge. This cessation of TTG magmatism is attributed to either the termination of subduction or slab roll-back with migration of the melting regime into the subduction-modifed mantle due to introduction of hot asthenospheric mantle following slab break-off or roll-back. Conductive and advective heat transfer into the crust is responsible for regional metamorphism and the generation of late, minor crustal I-type melts.

Much of the Abitibi crust developed during the pretectonic–synvolcanic stage forming an inversely density-stratified crustal configuration with an upper portion dominated by conformable, mafic-dominated volcanic assemblages overlying a less dense, tonalite-dominated plutonic substrate. The conformable nature of volcanic assemblages and consistently high paleopressures (500 to 700 MPa)

of tonalites indicate that this gravitationally unstable crustal configuration persisted thoughout the synvolcanic stage requiring the crust be rigid (low average geothermal gradient). The observed juxtaposition of midcrustal tonalites against low-grade (maximum paleopressures approximately 350 MPa) metavolcanic rocks is interpreted to be a consequence of extensional detachment faulting at the base of the greenstone belt. Disharmonic folding in portions of the greenstone belt (notably isoclinally folded Tisdale assemblage overlying openly folded Deloro assemblage) is interpreted to be due to additional detachment surfaces within lower portions of the greenstone belt that may be related to a master detachment at the base of the greenstone belt.

Detachment faulting and related regional doming or folding which generated the first order architecture of the Abitibi greenstone belt is constrained to have occurred synchronously with the emplacement of syntectonic plutons at approximately 2682 ± 5 Ma. The trigger for this process is interpreted to be introduction of heat which modified rheology of the midcrust leading to density inversion (Rayleigh–Taylor-type instabilities) as described in more detail elsewhere (Beakhouse et al. 2011). The timing of this process is similar to that of initiation of melting of a metasomatized mantle source that is ascribed to introduction of hot asthenospheric mantle.

Regional metamorphism is interpreted to have commenced at approximately the same time as detachment faulting and the transition to intermediate to felsic magmas being at least in part sourced from a metasomatized mantle reservoir. The main long-term source of heat driving this process is attributed to upwelling asthenospheric mantle associated with slab roll-back or detachment (cf., Beakhouse and Davis 2005). The truncation of deformational fabrics defined by near-peak metamorphic mineral assemblages by syntectonic plutons indicates rapid onset of regional metamorphism that is difficult to reconcile with purely conductive heat transfer. This suggests that advective heat transfer (syntectonic plutons and/or deeply-sourced fluids) contributed to the early introduction of heat.

The initiation of Porcupine assemblage sedimentation corresponds closely with that of uplift of the midcrust exposed in the Kenogamissi and Round Lake batholiths, which are interpreted to be major provenance components for these units.

Gold mineralization in the Abitibi Subprovince is primarily associated with major east-trending regional-scale faults and locally exhibits a spatial association with early syntectonic porphyries and/or late-tectonic alkalic plutons. The early syntectonic porphyries are interpreted to predate the introduction of gold and the spatial association is attributed to rheological contrasts between porphyries and host rocks, serving to localize deformation and heterogeneous strain and creating zones of enhanced porosity and permeability which localize hydrothermal fluid flow. The late-tectonic alkalic plutons are interpreted to be approximately coeval with a main stage of gold introduction and are the probable source of any magmatic hydrothermal fluid component contributing to gold mineralization.

In addition to their spatial and temporal association, a variety of characteristics suggest a genetic linkage between late-tectonic alkalic plutons and at least some gold mineralization. Most late-tectonic plutons are interpreted to have crystallized from magmas that are sufficiently intrinsically oxidized to stabilize sulphate thereby inhibiting the removal of ore metals by sulphide crystallization and increasing the potential of exsolved magmatic hydrothermal fluids to be metaliferous. A subset of Abitibi Subprovince gold deposits contains significant tellurides, which are a characteristic of gold deposits genetically associated with alkaline magmatism.

Zones of gold mineralization are likely characterized by the sequential and/or concurrent introduction of multiple fluid types. Acknowledging that more than more than one type of fluid

may be auriferous and additional study is required, a working hypothesis is proposed wherein magmatic hydrothermal fluids exsolved from late-tectonic alkaline magmas are a major or dominant source of gold in Abitibi Subprovince gold deposits. The atypical abundance and extremely alkalic character of the late-tectonic suite contrasts with that observed more generally throughout the Superior Province. These atypical characteristics are attributed to differences in either the nature of the subduction-modified mantle or melting process at the terminal stage of mantle-derived magmatism. The hypothesis implicates a major role for high CO_2/H_2O fluids in both mantle melting and magmatic volatile phase exsolution. CO_2-enrichment may have the potential to optimize the capability of hydrothermal fluid to transport gold (Phillips and Evans 2004) and consequently this hypothesis may provide a viable explanation for the significant gold endowment of this region.

Acknowledgments

This project was initiated as a collaborative research agreement between the Ontario Geological Survey and Placer Dome Inc. (now Goldcorp). The enthusiastic support of Greg Hall in setting up this collaboration is greatly appreciated. Placer Dome Inc. partially supported the participation of Kevin Cassidy (then with Australian Geological Survey Organization) in the initial phase of field work for this project. Many Placer Dome / Goldcorp staff and associated consulting geologists (Erik Barr, Keith Green, Scott Haley, Greg Hall, Bill Macrae, David Rhys, Marcus Willson) provided a variety of logistical support and contributed geological insight. Many other mineral exploration companies and geologists provided access to properties, general information and geological insight. Resident Geologist Program staff (notably Brian Atkinson (Timmins) and Gary Grabowski and Dave Guindon (Kirkland Lake)) visited some field areas with the author and provided a range of practical and technical help. The general concepts discussed in this report benefited from geological discussions with numerous individuals, including Ben Berger, David Bielhartz, Wouter Bleeker, Keith Benn, Richard Blewett, Kevin Cassidy, Karol Czarnota, Greg Hall, Shoufa Lin, Steve Piercey, David Rhys and Denver Stone, as well as numerous others. New preliminary geochronology reported herein is taken from an “in progress” investigation carried out in conjunction with Larry Heaman (University of Alberta). The assistance of Dave Crabtree, Sandra Clarke and John Hechler in completing electron microprobe and scanning electron microscope analyses is greatly appreciated. Editing of this manuscript by Marg Rutka greatly improved its readibility and is much appreciated.

References

Anderson, J.L. and Smith, D.R. 1995. The effects of temperature and fO_2 on the Al-in-hornblende barometer; American Mineralogist, v.80, p.549-559.

Anglin, C.D., Jonasson, I.R. and Franklin, J.M. 1996. Sm-Nd dating of scheelite and tourmaline: Implications for the genesis of Archean gold deposits, Val d'Or, Canada; Economic Geology, v.91, p.1372-1382.

Arribas, A. 1995. Characteristics of high-sulphidation epithermal deposits, and their relation to magmatic fluid; *in* J.F.H. Thompson, ed., Magmas, Fluids and Ore Deposits, Mineralogical Association of Canada, Short Course Notes, v.23, p.419-455.

Ayer, J., Amelin, Y., Corfu, F., Kamo, S., Ketchum, J., Kwok, K. and Trowell, N. 2002. Evolution of the southern Abitibi greenstone belt based on U-Pb geochronology: Autochthonous volcanic construction followed by plutonism, regional deformation and sedimentation; Precambrian Research, v.115, p.63-95.

Ayer, J.A., Barr, E., Bleeker, W., Creaser, R.A., Hall, G., Ketchum, J.W.F., Powers, D., Salier, B., Still, A. and Trowell, N.F. 2003. Discover Abitibi. New geochronological results from the Timmins area: Implications for the timing of late-tectonic stratigraphy, magmatism and gold mineralization; *in* Summary of Field Work and Other Activities 2003, Ontario Geological Survey, Open File Report 6120, p.33-1 to 33-11.

Ayer, J.A., Ketchum, J.W.F. and Trowell, N.F. 2002. New geochronological and neodymium isotopic results from the Abitibi greenstone belt, with emphasis on the timing and the tectonic implications of Neoarchean sedimentation and volcanism; *in* Summary of Field Work and Other Activities 2002, Ontario Geological Survey, Open File Report 6100, p.5-1 to 5-16.

Ayer, J.A., Thurston, P.C., Bateman, R., Gibson, H.L., Hamilton, M.A., Hathway, B., Hocker, S.M., Hudak, G., Lafrance, B., Ispolatov, V.O., MacDonald, P.J., Peloquin, A.S., Piercey, S.J., Reed, L.E., Thompson, P.H. and Izumi, H. 2005. Digital compilation of maps and data from the Greenstone Architecture Project in the Timmins–Kirkland Lake region; Ontario Geological Survey, Miscellaneous Release—Data 155.

Ayer, J.A., Trowell, N.F., Madon, Z. and Corfu, F. 1997. Geological compilation of the Abitibi greenstone belt in Ontario: The correlation of metallogenic potential with stratigraphy; *in* Summary of Field Work and Other Activities 1997, Ontario Geological Survey, Miscellaneous Paper 168, p.3-9.

Ayer, J.A., Trowell, N.F., Madon, Z., Kamo, S., Kwok, Y.Y. and Amelin, Y. 1999. Compilation of the Abitibi greenstone belt in the Timmins–Kirkland Lake area: Revisions to stratigraphy and new geochronological results; *in* Summary of Field Work and Other Activities 1999, Ontario Geological Survey, Open File Reort 6000, p.4-1 to 4-14.

Baker, T., Bertelli, M., Blenkinsop, T., Cleverly, J.S., McLellan, J., Nugus, M. and Gillen, D. 2010. P-T-X conditions of fluids in the Sunrise Dam gold deposit, Western Australia, and implications for the interplay between deformation and fluids; Economic Geology, v.105, p.873-894.

Barrie, C.T. 1990. U-Pb garnet and titanite age for the Bristol Township lamprophyre suite, western Abitibi Subprovince, Canada; Canadian Journal of Earth Sciences, v.27, p.1451-1456.

——— 1999. Kidd–Munro extension project: Year 3 report; unpublished report, 263p.

Bateman, R., Ayer, J.A., Dubé, B. and Hamilton, M.A. 2005. The Timmins–Porcupine gold camp, northern Ontario: The anatomy of an Archaean greenstone belt and its gold mineralization: Discover Abitibi Initiative; Ontario Geological Survey, Open File Report 6158, 90p.

Beakhouse, G.P. 2011. Lithogeochemical data for Abitibi Subprovince intermediate to felsic intrusive rocks; Ontario Geological Survey, Miscellaneous Release—Data 285.

Beakhouse, G.P. 2001. Nature, timing and significance of intermediate to felsic intrusive rocks associated with the Hemlo greenstone belt and implications for the regional geological setting of the Hemlo gold deposit; Ontario Geological Survey, Open File Report 6020, 248p.

——— G.P. 2007a. Structurally controlled, magmatic hydrothermal model for Archean lode gold deposits: A working hypothesis; Ontario Geological Survey, Open File Report 6193, 133p.

——— G.P. 2007b. Gold, granite and Late Archean tectonics: A Superior Province perspective; *in* B.P. Bierlein and C.M. Knox-Robinson, eds., Proceedings of Geoconferences (WA) Inc. Kalgoorlie '07 Conference, Geoscience Australia Record 2007/14, p.191-196.

Beakhouse, G.P. and Davis, D.W. 2005. Evolution and tectonic significance of intermediate to felsic plutonism associated with the Hemlo greenstone belt, Superior Province, Canada; Precambrian Research, v.137, p.61-92.

Beakhouse, G.P., Lin, S. and Kamo, S.L. 2011. Magmatic and tectonic emplacement of the Pukaskwa batholith, Superior Province, Ontario, Canada; Canadian Journal of Earth Sciences, v.48, p.187-204.

Bedard, L.P. and Chown, E.H. 1992. The Dolodau dykes, Canada: An example of an Archean carbonatite; Mineralogy and Petrology, v.46, p.109-121.

Ben Othman, D., Arndt, N.T., White, W.M. and Jochum, K.P. 1990. Geochemistry and age of Timiskaming alkali volcanics and the Otto syenite stock, Abitibi, Ontario; Canadian Journal of Earth Sciences, v.27, p.1304-1311.

Benn, K. and Peshler, A.P. 2005. A detachment fold model for fault zones in the Late Archean Abitibi greenstone belt; Tectononophysics, v.400, p.85-104.

Berger, B.R. 1997. Precambrian geology of the Monteith area; Ontario Geological Survey, Preliminary Map P.3367, scale 1:50 000.

——— 2002. Geological synthesis of the Highway 101 area, east of Matheson, Ontario; Ontario Geological Survey, Open File Report 6091, 124p.

——— 2006. Geological synthesis along Highway 66 from Matachewan to Swastika; Ontario Geological Survey, Open File Report 6177, 125p.

Berger, B.R., Houlé, M.G. and Dinel, E. 2009. Preliminary ideas on the stratigraphy, geochemistry and geochronology of the Kidd–Munro assemblage; *in* Summary of Field Work and Other Activities 2009, Ontario Geological Survey, Open File Report 6240, p.4-1 to 4-8.

Berger, B.R., Pigeon, L. and Leblanc, G. 2006. Precambrian geology, Highway 66 area, Swastika to Matachewan; Ontario Geological Survey, Map 2677, scale 1:50 000.

Berger, B.R. and Prefontaine, S. 2005. General geology of Powell Township, District of Timiskaming; *in* Summary of Field Work and Other Activities 2005, Ontario Geological Survey, Open File Report 6172, p.5-1 to 5-10.

Bleeker, W., Parrish, R.R. and Sager-Kinsman, A. 1999. High-precision U-Pb geochronology of the Late Archean Kidd Creek deposit and Kidd volcanic complex; Economic Geology, Monograph 10, p.43-70.

Bleeker, W. and van Breemen, O. 2010. The fundamental architecture of the south-central Abitibi greenstone belt, Superior craton, Canada, and the localization of world-class Au deposits; abstract *in* Fifth International Archean Symposium, Abstracts, Geological Survey of Western Australia, Record 2010/18, p.153-154.

Blewett, R.S. and Czarnota, K, 2007. Diversity of structurally controlled gold through time and space of the central Eastern Goldfields Superterrane—A field guide; Geological Survey of Western Australia, Record 2007/19, 65p.

Blichert-Toft, J., Arndt, N.T. and Ludden, J.N. 1996. Precambrian alkaline magmatism; Lithos, v.37, p.97-111.

Born, P. 1995. A sedimentary basin analysis of the Abitibi greenstone belt in the Timmins area, northern Ontario, Canada; unpublished PhD thesis, Carleton University, Ottawa, Ontario, 489p.

Bright, E.G. 1974a. English and Zavitz townships, Sudbury District; Ontario Geological Survey, Map 2290, scale 1:31 680.

Bright, E.G. 1974b. Semple and Hutt townships, Sudbury District; Ontario Geological Survey, Map 2291, scale 1:31 680.

Brisbin, D.I. 1997. Geological setting of gold deposits in the Porcupine gold camp, Timmins, Ontario; unpublished PhD thesis, Queen's University, Kingston, Ontario, 523p.

Burnham, C.W. and Ohmoto, H. 1980. Late stage processes of felsic magmatism; Mining Geology Special Issue, no.8, p.1-11.

Burrows, D. R. and Spooner, E.T.C. 1989. Relationship between Archean gold quartz vein – shear zone mineralization and igneous intrusions in the Val d'Or and Timmins areas, Abitibi subprovince, Canada; Economic Geology, Monograph 6, p.424-444.

Burrows, D.R., Spooner, E.T.C., Wood, P.C. and Jemielita, R.A. 1993. Structural controls on formation of the Hollinger–McIntyre Au quartz vein system in the Hollinger shear zone, Timmins, southern Abitibi greenstone belt, Ontario; Economic Geology, v.88, p.1643-1663.

Cameron, E.M. and Carrigan, W.J. 1987. Oxygen fugacity of Archean felsic magmas: Relationship to gold mineralization; *in* Current Research, Part A, Geological Survey of Canada, Paper 87-1A, p.281-298.

Cameron, E.M. and Hattori, K. 1987. Archean gold mineralization and oxidized hydrothermal fluids; Economic Geology, v.82, p.1177-1191.

Candela, P.A. and Piccoli, P.M. 1995. Model ore-metal partitioning from melts into vapor and vapor/brine mixtures. *in* Thompson, J.F.H., ed, Magmas, Fluids and Ore Deposits, Mineralogical Association of Canada, Short Course Notes, v.23, p.101-127.

——— 2005. Magmatic processes in the development of porphyry-type ore systems; Economic Geology, 100th Anniversary Volume, p.25-37.

Carroll, M.R. and Rutherford, M.J. 1985. Sulfide and sulfate saturation in hydrous silicate melts; Journal of Geophysical Research, v.90, p.C601-612.

Chi, G., Liu, Y. and Dube, B. 2009. Relationship between CO_2-dominated fluids, hydrothermal alterations and gold mineralization in the Red Lake greenstone belt, Canada; Applied Geochemistry, v.24, p.504-516.

Chown, E.H., Harrap, R. and Moukhsil, A. 2002. The role of granitic intrusions in the evolution of the Abitibi belt, Canada; Precambrian Research, v.115, p.291-310.

Christie, A.B., Simpson, M.P., Brathwaite, R.L., Mauk, J.L. and Simmons, S.F. 2007. Epithermal Au-Ag and related deposits of the Hauraki goldfield, Coromandel volcanic zone, New Zealand; Economic Geology, v.102, p.785-816.

Cline, J.S., Hofstra, A.H., Muntean, J.L., Tosdal, R.M. and Hickey, K.A. 2005. Carlin-type gold deposits in Nevada: Critical geological characteristics and viable models; Society of Economic Geologists, 100th anniversary volume, p.451-484.

Cooke, D.L. and Moorehouse, W.W. 1969. Timiskaming volcanism in the Kirkland Lake area, Ontario, Canada; Canadian Journal of Earth Sciences, v.6, p.117-132.

Corfu, F. 1993. The evolution of the southern Abitibi greenstone belt in light of precise U-Pb geochronology. Economic Geology, v.88, p.1323-1340.

Corfu, F., Krogh, T.E., Kwok, Y.Y. and Jensen, L.S. 1989. U-Pb geochronology in the southwestern Abitibi greenstone belt, Superior Province; Canadian Journal of Earth Sciences, v.26, p.1747-1763.

Corfu, F and Noble, S.R. 1992. Genesis of the southern Abitibi greenstone belt, Superior Province, Canada: Evidence from zircon Hf isotope analyses using a single filament technique; Geochimica et Cosmochimica Acta, v.56, p.2081-2097.

Corfu, F., Jackson, S.L. and Sutcliffe, R.H. 1991. U-Pb ages and tectonic significance of late Archean alkalic magmatism and non-marine sedimentation: Temiskaming Group, southern Abitibi belt, Ontario; Canadian Journal of Earth Sciences, v.28, p.489-503.

Couture, J.-F., Pilote, P., Machado, N. and Desrochers, J.-P. 1994. Timing of gold mineralization in the Val-d'Or District, southern Abitibi Belt; evidence for two distinct mineralizing events; Economic Geology, v.89, p.1542-1551.

Cruden, A.R. and Launeau, P. 1994. Structure, magnetic fabric and emplacement of the Archean Lebel stock, SW Abitibi greenstone belt; Journal of Structural Geology, v.16, p.677-691.

Cygan, G.L. and Candela, P.A. 1995. Preliminary study of gold partitioning among pyrrhotite, pyrite, magnetite and chalcopyrite in gold-saturated chloride solutions at 600 to 700ºC, 140 Mpa; *in* J.F.H. Thompson, ed., Magmas, Fluids, and Ore Deposits, Mineralogical Association of Canada, Short Course v.23, p.129-138.

Dziggel, A., Kniper, S., Kisters, A.F.M. and Meyer, F.M. 2006. P – T and structural evolution during exhumation of high-T, medium-P basement rocks in the Barberton Mountain Land, South Africa; Journal of Metamorphic Geology, v.24, p.535-551.

Eggler, D.H. 1978. The effect of CO_2 upon partial melting of peridotite in the system Na_2O-CaO-Al_2O_3-MgO-SiO_2-CO_2 to 35 kb, with an analysis of melting in a peridotite-H_2O-CO_2 system; American Journal of Science, v.278, p.305-343.

Evans, K.A., Phillips, G.N. and Powell, R. 2006. Rock-buffering of auriferous fluids in altered rocks associated with the Golden Mile-style mineralization, Kalgoorlie Gold Field, Western Australia; Economic Geology, v.101, p.805-817.

Feng, R. and Kerrich, R. 1990. Geobarometry, differential block movement, and crustal structure of the southwestern Abitibi greenstone belt, Canada; Geology, v.18, p.870-873.

——— 1992a. Geochemical evolution of granitoids from the Archean Abitibi southern volcanic zone and the Pontiac subprovince, Superior Province, Canada: Implications for tectonic history and source regions; Chemical Geology, v.98, p.23-70.

——— 1992b. Geodynamic evolution of the southern Abitibi and Pontiac terranes: Evidence from geochemistry of granitoids magma series (2700–2630 Ma); Canadian Journal of Earth Sciences, v.29, p.2266-2286.

Feng, R., Kerrich, R., McBride, S. and Farrar, E. 1992. $^{40}Ar/^{39}Ar$ age constraints on the thermal history of the Archean Abitibi greenstone belt and the Pontiac Subprovince: Implications for terrane collision, differential uplift and overprinting of gold deposits; Canadian Journal of Earth Sciences, v.29, p.1389-1411.

Ferguson, S.A. 1968. Geology and ore deposits of Tisdale Township, District of Cochrane; Ontario Department of Mines, Geological Report 58, 177p.

Frarey, M.J. and Krogh, T.E. 1986. U-Pb ages of late internal plutons of the Abitibi and eastern Wawa subprovinces, Ontario and Quebec; *in* Current Research, Part A, Geological Survey of Canada, Paper 86-1A, p.43-48.

Galley, A.G. 2003. Composite synvolcanic intrusions associated with Precambrian VMS-related hydrothermal systems; Mineralium Deposita, v.38, p.443-473.

Gray, M.D. 1994. Multiple gold mineralizing events in the Porcupine mining district, Ontario, Canada; unpublished PhD thesis, Colorado School of Mines, Golden, Colorado, 220p.

Gray, M.D. and Hutchinson, R.W. 2001. New evidence for multiple periods of gold emplacement in the Porcupine mining district, Timmins area, Ontario, Canada; Economic Geology, v.96, p.453-475.

Green, D.H. 1976. Experimental testing of "equilibrium" partial melting of peridotite under water-saturated, high-pressure conditions; Canadian Mineralogist, v.14, p.255-268.

Hammarstrom, J.M. and Zen, E-An. 1986. Aluminum in hornblende: An empirical igneous geobarometer; American Mineralogist, v.71, p.1297-1313.

Hanes, J.A., Archibald, D.A. and Hodgson, C.J. 1992. Dating of auriferous quartz vein deposits in the Abitibi greenstone belt, Canada: $^{40}Ar/^{39}Ar$ evidence for a 70- to 100-m.y.-time gap between plutonism-metamorphism and mineralization; Economic Geology, v.87, p.1849-1861.

Hart, T.R., Gibson, H.L. and Lesher, C.M. 2004. Trace element geochemistry and petrogenesis of felsic volcanic rocks associated with volcanogenic massive Cu-Zn-Pb sulfide deposits; Economic Geology, v.99, p.1003-1013.

Hattori, K. 1987. Magnetic felsic intrusions associated with Canadian Archean gold deposits; Geology, v.15, p.1107-1111.

Hattori, K., Hart, S.R. and Shimizu, N. 1996. Melt and source mantle compositions in the Late Archean: A study of strontium and neodymium isotope and trace elements in clinopyroxenes from shoshonitic alkaline rocks; Geochimica Cosmochimica Acta, v.60, p.4551-4562.

Heather, K.B. 2001. The geological evolution of the Archean Swayze greenstone belt, Superior Province, Canada; unpublished PhD thesis, Keele University, Keele, United Kingdom, 370p.

Hodgson, C.J. 1983. Preliminary report on the Timmins–Kirkland Lake area gold deposit file; Ontario Geological Survey, Open File Report 5467, 434p.

Holland, T. and Blundy, J. 1994. Non-ideal interactions in calcic amphiboles and their bearing on amphibole-plagioclase thermometry; Contributions to Mineralogy and Petrology, v.116, p.433-447.

Hollister, L.S., Grissom, G.C., Peters, E.K., Stowell, H.H. and Sisson, V.B. 1987. Confirmation of the empirical correlation of Al in hornblende with pressure of solidification of calc-alkaline plutons; American Mineralogist, v.72, p.231-239.

Hurst, M.E. 1936. Recent studies in the Porcupine area; Transactions of the Canadian Institute of Mining and Metallurgy, v.39, p.448-458.

Irvine, T.N. and Baragar, W.R. 1971. A guide to the chemical classification of the common igneous rocks; Canadian Journal of Earth Sciences, v.8, p.523-548.

Isoplatov, V., LaFrance, B., Dube, B., Creaser, R. and Hamilton, M. 2008. Geologic and structural setting of gold mineralization in the Kirkland Lake–Larder Lake gold belt, Ontario; Economic Geology, v.103, p.1309-1340.

Isoplatov, V., LaFrance, B., Dube, B., Hamilton, M. and Creaser, R. 2005. Geology, structure and gold mineralization, Kirkland Lake and Larder Lake areas (Gauthier and Teck Townships): Discover Abitibi initiative; Ontario Geological Survey, Open File Report 6159, 170p.

Jackson, S.L. 1995. Precambrian geology, Larder Lake area; Ontario Geological Survey, Map 2628, scale 1:50 000.

Jemielita, R.A., Davis, D.W. and Krogh, T.E. 1990. U-Pb evidence for Abitibi gold mineralization postdating greenstone magmatism and metamorphism; Nature, v.346, p.831-834.

Jensen, E.P. and Barton, M.D. 2000. Gold deposits related to alkaline magmatism; Reviews in Economic Geology, v.13, p.279-314.

Johns, G.W. 1985. Geology of the Hill Lake area, District of Timiskaming; Ontario Geological Survey, Report 250, 100p.

Johns, G.W. 2003. Precambrian geology, Shining Tree area; Ontario Geological Survey, Preliminary Map P.3521, scale 1:50 000.

Johns, G.W., Hoyle, W. and Good, D. 1985. Hill Lake; Ontario Geological Survey, Map 2501, scale 1:31 680.

Jugo, P.J., Candela, P.A. and Piccoli, P.M. 1999. Magmatic sulfides and Au:Cu ratios in porphyry deposits: an experimental study of copper and gold partioning at 850 ºC, 100 Mpa in a haplogranite melt – pyrrhotite – intermediate solid solution – gold metal assemblage, at gas saturation; Lithos, v.46, p.573-589.

Kerrich, R. and King, R. 1993. Hydrothermal zircon and baddeleyite in Val-d'Or Archean mesothermal gold deposits: Characteristics, compositions, and fluid-inclusion properties, with implications for timing of primary gold mineralization; Canadian Journal of Earth Sciences, v.30, p.2334-2351.

Kerrich, R. and Kyser, T.K. 1994. 100 Ma timing paradox of Archean gold, Abitibi greenstone belt (Canada): New evidence from U-Pb and Pb-Pb evaporation ages of hydrothermal zircons; Geology, v.22, p.1131-1134.

Kessler, S.E., Chryssoulis, S.L. and Simon, G. 2002. Gold in porphyry copper deposits: Its abundance and fate; Ore Geology Reviews, v.21, p.103-124.

Ketchum, J.W.F., Ayer, J.A., van Breemen, O., Pearson, N.J. and Becker, J.K. 2008. Pericontinental crustal growth of the southwestern Abitibi Subprovince, Canada—U-Pb, Hf and Nd isotope evidence; Economic Geology, v.103, p.1151-1184.

LaFleur, P.J. 1986. The Archean Round Lake batholith, Abitibi greenstone belt; A synthesis; unpublished MSc thesis, University of Ottawa, Ottawa, Canada, 245p.

Lesher, C.M., Goodwin, A.M., Campbell, I.H. and Gorton, M.P. 1986. Trace-element geochemistry of ore-associated and barren felsic metavolcanic rocks in the Superior Province, Canada; Canadian Journal of Earth Sciences, v.23, p.222-237.

Levesque, G. 1994. Duality of magmatism at Kirkland Lake, Ontario, Canada; unpublished MSc thesis, University of Ottawa, Ottawa, Ontario, 217p.

Levesque, G., Cameron, E.M. and Lalonde, A.E. 1991. Duality of magmatism along the Kirkland Lake–Larder Lake fault zone, Ontario*; in* Current Research, Part C, Geological Survey of Canada, Paper 91-1C, p.17-24.

Launeau, P. and Cruden, A.R. 1998. Magmatic fabric acquisition mechanisms in a syenite: Results of a combined anisotropy of magnetic susceptibility and image analysis study; Journal of Geophysical Research, v.103, B3, p.5067-5089.

Luinstra, B. and Benn, K. 2001. Structural geology of the Holloway Mine, Abitibi greenstone belt, Ontario; Ontario Geological Survey, Open File Report 6045, 36p.

MacDonald, P.J. 2010. The geology, lithogeochemistry and petrogenesis of intrusions associated with gold mineralization in the Porcupine gold camp, Timmins, Canada; unpublished MSc thesis, Laurentian University, Sudbury, Ontario, 188p.

MacDonald, P.J., Piercey, S.J. and Hamilton, M.A. 2005. An integrated study of intrusive rocks spatially associated with gold and base metal mineralization in the Abitibi greenstone belt, Timmins area and Clifford Township: Discover Abitibi Initiative; Ontario Geological Survey, Open File Report 6160, 190p.

Marchev, P. 1991. Primary barite in high-K dacite from the Eastern Rhodope, Bulgaria; European Journal of Mineralogy, v.3, p.1005-1008.

Marquis, P., Hubert, C., Brown, A.C. and Rigg, D.M. 1990. Overprinting of early, redistributed Fe and Pb-Zn mineralization by late-stage Au-Ag-Cu deposition at the Dumagami Mine, Bousquet District, Abitibi, Quebec; Canadian Journal of Earth Sciences, v.27, p.1651-1671.

Mason, R., and Melnik, N. 1986. The anatomy of an Archean gold system—The McIntyre–Hollinger Complex at Timmins, Ontario, Canada; *in* Macdonald, A.J., ed., Gold '86, Willowdale, Ontario, Konsult International, p.40-55.

Menzies, M. and Murthy, V.R. 1980. Mantle metasomatism as a precursor to the genesis of alkaline magmas – Isotopic evidence; American Journal of Science, v.280, p.622-638.

Miller, W.G. 1913. The cobalt-nickel arsenides and silver deposits of Timiskaming (Cobalt and adjacent areas), Fourth Edition; Ontario Bureau of Mines, Annual Report, 1910, v.19, pt.2, p.1-132.

Mortensen, J.K. 1993. U-Pb geochronology of the eastern Abitibi Subprovince, Part 2: Noranda–Kirkland Lake area; Canadian Journal of Earth Sciences, v.30, p.29-41.

Pearce, J.A., Harris, N.B.W. and Tindle, A.G. 1984. Trace element discrimination diagrams for the tectonic interpretation of granitic rocks; Journal of Petrology, v.25, p.956-983.

Peccerillo, A., Poli, G. and Tolomeo, L. 1984. Genesis, evolution and tectonic significance of K-rich volcanics from the Alban Hills (Roman comagmatic region) as inferred from trace element geochemistry; Contributions to Mineralogy and Petrology, v.86, p.230-240.

Peccerillo, A. and Taylor, S.R. 1976. Geochemistry of Eocene calc-alkaline volcanic rocks from the Kastamonu area, northern Turkey; Contributions to Mineralogy and Petrology, v.58, p.63-81.

Peschler, A.P., Benn, K. ad Roest, W.R. 2006. Gold-bearing fault zones related to Late Archean orogenic folding of upper and middle crust in the Abitibi granite-greenstone belt, Ontario; Precambrian Research, v.151, p.143-159.

Phillips, G.N. and Evans, K.A. 2004. Role of CO_2 in the formation of gold deposits; Nature, v.429, p.860-863.

Pigeon, L. 2003. Mineralogy, petrology and petrogenesis of syenitic rocks of the Porcupine–Destor fault zone near Matheson, Ontario; unpublished PhD thesis, University of Ottawa, Ottawa, Canada, 285p.

Poulsen, K.H., Robert, F. and Dube, B. 2000. Geological classification of Canadian gold deposits; Geological Survey of Canada, Bulletin 540, 106p.

Powell, W.G., Carmichael, D.M. and Hodgson, C.J. 1995. Conditions and timing of metamorphism in the southern Abitibi greenstone belt, Quebec; Canadian Journal of Earth Sciences, v.32, p.787-805.

Powell, W.G., Hodgson, C.J., Hanes, J.A., Carmichael, D.M., McBride, S. and Farrar, E. 1995. $^{40}Ar/^{39}Ar$ geochronological evidence for multiple postmetamorphic hydrothermal events focussed along faults in the southern Abitibi greenstone belt; Canadian Journal of Earth Sciences, v.32, p.768-786.

Pyke, D.R. 1970. Geology of Langmuir and Blackstock Townships, District of Timiskaming; Ontario Geological Survey, Geological Report 86, 65p.

——— 1973. Geology of Fallon and Fasken Townships, District of Timiskaming; Ontario Geological Survey, Geological Report 104, 31p.

——— 1975. Geology of Adams and Eldorado townships, District of Cochrane; Ontario Geological Survey, Report 121, 51p.

——— 1978. Geology of the Redstone River area, District of Timiskaming; Ontario Geological Survey, Report 161, 75p.

——— 1982. Geology of the Timmins area, District of Cochrane; Ontario Geological Survey, Report 219, 141p.

Ridley, J.R. and Diamond, L.W. 2000. Fluid chemistry of orogenic lode gold deposits and implications for genetic models; Society of Economic Geologists Reviews, v.13, p.141-162.

Rivé, M., Pintson, H. and Ludden, J.N. 1990. Characteristics of late Archean plutonic rocks from the Abitibi and Pontiac subprovinces, Superior Province, Canada; *in* Rive, M., Verpaelst, P., Gagnon, Y., Lulin, J.M., Riverin, G. and Simard, A., eds, The Northwestern Quebec Polymetallic Belt, The Canadian Institute of Mining and Metallurgy, Special Volume 43, p.65-76.

Robert, F. 2001. Syenite-associated disseminated gold deposits in the Abitibi greenstone belt, Canada; Mineralium Deposita, v.36, p.503-516.

Rogers, N.W., Hawkesworth, C.J., Parker, R.J. and Marsh, J.S. 1985. The geochemistry of potassic lavas from Vulsini, central Italy and implications for mantle enrichment processes beneath the Roman region; Contributions to Mineralogy and Petrology, v.90, p.244-257.

Ropchan, J.R., Luinstra, B., Fowler, A.D., Benn, K., Ayer, J., Berger, B., Dahn, R., Labine, R. and Amelin, Y. 2002. Host-rock and structural controls on the nature and timing of gold mineralization at the Holloway Mine, Abitibi Subprovince, Ontario; Economic Geology, v.97, p.291-309.

Rowins, S.M. 1990. Mineralogy and geochemistry of the Murdock Creek intrusion, Kirkland Lake, Ontario; unpublished MSc thesis, Univeristy of Ottawa, Ottawa, Canada, 196p.

Rowins, S.M., Cameron, E.M., LaLonde, A.E. and Ernst, R.E. 1993. Petrogenesis of the late Archean syenitic Murdock Creek pluton, Kirkland Lake, Ontario: Evidence for an extensional tectonic setting; Canadian Mineralogist, v.31, p.219-244.

Rowins, S.M., Lalonde, A.E. and Cameron, E.M. 1991. Magmatic oxidation in the syenitic Murdock Creek intrusion, Kirkland Lake, Ontario: Evidence from the ferromagnesian silicates; Journal of Geology, v.99, p.395-414.

Schmidt, M.W. 1992. Amphibole composition in tonalite as a function of pressure: An experimental calibration of the Al-in-hornblende barometer; Contributions to Mineralogy and Petrology, v.110, p.304-310.

Schmidt-Mumm, A., Oberthur, T., Vetter, U. and Blenkinsop, T.G. 1997. High CO_2 content of fluid inclusions in gold mineralizations in the Ashanti belt, Ghana: A new category of ore forming fluids; Mineralium Deposita, v.32, p.107-118.

Seedorf, E., Dilles, J.H., Proffett, J.M., Einudi, M.T., Zurcher, L., Stavast, W.J.A., Johnson, D.A. and Barton, M.D. 2005. Porphyry deposits: Characteristics and origin of hypogene features; Economic Geology, 100th Anniversary Volume, p.251-298.

Shirey, S.B. and Hanson, G.N. 1984. Mantle-derived Archean monzodiorites and trachyandesites; Nature, v.310, 222-224.

——— 1986. Mantle heterogeneity and crustal recycling in Archean granite-greenstone belts: Evidence from Nd isotopes and trace elements in the Rainy Lake area, Superior Province, Ontario, Canada; Geochemica Cosmochemica Acta, v.50, p.2631-2651.

Sillitoe, R.H., 1997. Characteristics and controls of the largest porphyry copper-gold and epithermal gold deposits in the circum-Pacific region; Australian Journal of Earth Sciences, v.44, p.373-388.

Sillitoe, R.H. and Bonham, H.F. 1990. Sediment-hosted gold deposits: Distal products of magmatic hydrothermal systems; Geology, v.18, p.157-161.

Simmons, S.F. 1995. Magmatic contributions to low-sulphidation epithermal deposits; *in* Thompson, J.F.H. ed., Magmas, Fluids and Ore Deposits, Mineralogical Association of Canada, Short Course Notes, v.23, p.455-477.

Smith, A.R. and Sutcliffe, R.H. 1988. Plutonic rocks of the Abitibi Subprovince; *in* Summary of Field Work and Other Activities 1988, Ontario Geological Survey, Miscellaneous Paper 141, p.188-196.

Smithies, R.H. 2000. The Archaean tonalite-trondhjemite-granodiorite (TTG) series is not an analogue of Cenozoic adakite; Earth and Planetary Science Letters, v.182, p.115-125.

Stern, R.J. 2002. Subduction zones; Reviews of Geophysics, v.40, no.4, p.3-1 to 3-38.

Sun, S.S. and McDonough, W.F. 1989. Chemical and isotopic systematics of oceanic basalts: Implications for mantle composition and processes; *in* Magmatism in the Ocean Basins, Geological Society, Special Publication, v.42, p.169-190.

Sutcliffe, R.H., Barrie, C.T., Burrows, D.R. and G.P. Beakhouse, 1993. Plutonism in the southern Abitibi subprovince: A tectonic and petrogenetic framework; Economic Geology, v.88, p.1359-1375.

Sutcliffe, R.H., Smith, A.R., Doherty, W. and Barnett, R.L. 1990. Mantle derivation of Archean amphibole-bearing granitoid and associated mafic rocks: Evidence from the southern Superior Province; Contributions to Mineralogy and Petrology, v.105, p.255-274.

Swager, C.P. and Nelson, D.R. 1997. Extensional emplacement of a high-grade granite gneiss complex into low-grade greenstones, Eastern Goldfields, Yilgarn craton, Western Australia; Precambrian Research, v.83, p.203-219.

Thompson, J.E. 1950. Geology of Teck Township and the Kenogami Lake area; Ontario Department of Mines, Annual Report for 1948, v.57, pt5.

Thompson, P.H. 2002. Toward a new metamorphic framework for gold exploration in the Timmins area, central Abitibi greenstone belt; Ontario Geological Survey, Open File Report 6101, 51p.

Thompson, P.H. 2005. A new metamorphic framework for gold exploration in the Timmins–Kirkland Lake area, western Abitibi greenstone belt: Discover Abitibi Initiative; Ontario Geological Survey, Open File Report 6162, 104p.

van Breemen, O., Heather, K.B. and Ayer, J.A. 2006. U-Pb geochronology of the Neoarchean Swayze sector of the southern Abitibi greenstone belt; Geological Survey of Canada, Current Research 2006-F1, 32p.

Wilkinson, L., Cruden, A.R. and Krogh, T.E. 1999. Timing and kinematics of post-Timiskaming deformation with the Larder Lake–Cadillac deformation zone, southwest Abitibi greenstone belt, Ontario, Canada; Canadian Journal of Earth Sciences, v.36, p.627-647.

Williams, P.R. and Currie, K.L. 1993. Character and regional implications of a sheared Achaean granite–greenstone contact near Leonora, Western Australia; Precambrian Research, v.62, p.343-365.

Williams, P.R. and Whitaker, A.J. 1993. Gneiss domes and extensional deformation in the highly mineralized Archaean Eastern Goldfields Province, Western Australia; Ore Geology Reviews, v.8, p.141.

Wyman, D.A. and Kerrich, R. 1989. Archean lamprophyre dikes of the Superior Province, Canada: Distribution, petrology and geochemical characteristics; Journal of Geophysical Research, v.94, B4, p.4667-4696.

Zhang, J., Lin, S., Linnen, R., Martin, R. and Berger, B. 2009. Structural controls on syenite-hosted gold mineralization of the Matachewan area, a westernmost exposure of the Cadillac–Larder Lake deformation zone, south Abitibi greenstone belt, Canada; abstract *in* American Geophysical Union–Geological Association of Canada–Mineralogical Association of Canada, Joint Assembly 2009, Toronto, Ontario, Geological Association of Canada, Abstracts, v.34, abstract GA24A-03.

Zweng, P.L., Mortensen, J.K. and Dalrymple, G.B. 1993. Thermochronology of the Camflo gold deposit, Malartic, Quebec; implications for magmatic underplating and the formation of gold-bearing quartz veins; Economic Geology, v.88, p.1700-1721.

Metric Conversion Table

Conversion from SI to Imperial			Conversion from Imperial to SI		
SI Unit	*Multiplied by*	*Gives*	*Imperial Unit*	*Multiplied by*	*Gives*
		LENGTH			
1 mm	0.039 37	inches	1 inch	**25.4**	mm
1 cm	0.393 70	inches	1 inch	**2.54**	cm
1 m	3.280 84	feet	1 foot	**0.304 8**	m
1 m	0.049 709	chains	1 chain	20.116 8	m
1 km	0.621 371	miles (statute)	1 mile (statute)	**1.609 344**	km
		AREA			
1 cm^2	0.155 0	square inches	1 square inch	**6.451 6**	cm^2
1 m^2	10.763 9	square feet	1 square foot	**0.092 903 04**	m^2
1 km^2	0.386 10	square miles	1 square mile	2.589 988	km^2
1 ha	2.471 054	acres	1 acre	0.404 685 6	ha
		VOLUME			
1 cm^3	0.061 023	cubic inches	1 cubic inch	**16.387 064**	cm^3
1 m^3	35.314 7	cubic feet	1 cubic foot	0.028 316 85	m^3
1 m^3	1.307 951	cubic yards	1 cubic yard	0.764 554 86	m^3
		CAPACITY			
1 L	1.759 755	pints	1 pint	0.568 261	L
1 L	0.879 877	quarts	1 quart	1.136 522	L
1 L	0.219 969	gallons	1 gallon	**4.546 090**	L
		MASS			
1 g	0.035 273 962	ounces (avdp)	1 ounce (avdp)	28.349 523	g
1 g	0.032 150 747	ounces (troy)	1 ounce (troy)	**31.103 476 8**	g
1 kg	2.204 622 6	pounds (avdp)	1 pound (avdp)	**0.453 592 37**	kg
1 kg	0.001 102 3	tons (short)	1 ton(short)	**907.184 74**	kg
1 t	1.102 311 3	tons (short)	1 ton (short)	**0.907 184 74**	t
1 kg	0.000 984 21	tons (long)	1 ton (long)	**1016.046 908 8**	kg
1 t	0.984 206 5	tons (long)	1 ton (long)	**1.016 046 9**	t
		CONCENTRATION			
1 g/t	0.029 166 6	ounce (troy) / ton (short)	1 ounce (troy) / ton (short)	34.285 714 2	g/t
1 g/t	0.583 333 33	pennyweights / ton (short)	1 pennyweight / ton (short)	1.714 285 7	g/t

OTHER USEFUL CONVERSION FACTORS

	Multiplied by	
1 ounce (troy) per ton (short)	31.103 477	grams per ton (short)
1 gram per ton (short)	0.032 151	ounces (troy) per ton (short)
1 ounce (troy) per ton (short)	20.0	pennyweights per ton (short)
1 pennyweight per ton (short)	0.05	ounces (troy) per ton (short)

Note: Conversion factors in bold type are exact. The conversion factors have been taken from or have been derived from factors given in the Metric Practice Guide for the Canadian Mining and Metallurgical Industries*, published by the Mining Association of Canada in co-operation with the Coal Association of Canada.*

ISSN 0826-9580 (print)
ISBN 978-1-4435-7404-4 (print)

ISSN 1916-6117 (online)
ISBN 978-1-4435-7405-1 (PDF)